

Robert Richter

*Institut für Rebenzüchtung in Siebeldingen*

Phenotypic key factors,  
genetic regions and genes  
associated to cluster architecture  
in grapevine (*Vitis vinifera*)



Dissertationen aus dem Julius Kühn-Institut

## **Kontakt | Contact:**

Robert Richter  
Julius Kühn-Institut  
Bundesforschungsinstitut für Kulturpflanzen  
Institut für Rebenzüchtung  
Geilweilerhof  
76833 Siebeldingen

Die Schriftenreihe „Dissertationen aus dem Julius Kühn-Institut“ veröffentlicht Doktorarbeiten, die in enger Zusammenarbeit mit Universitäten an Instituten des Julius Kühn-Instituts entstanden sind.

*The publication series „Dissertationen aus dem Julius Kühn-Institut“ publishes doctoral dissertations originating from research doctorates and completed at the Julius Kühn-Institut (JKI) either in close collaboration with universities or as an outstanding independent work in the JKI research fields.*

Der Vertrieb dieser Schriftenreihe erfolgt über den Buchhandel (Nachweis im Verzeichnis lieferbarer Bücher - VLB). Einige der Dissertationen erscheinen außerdem online open access und werden unter einer Creative Commons Namensnennung 4.0 Lizenz (CC-BY 4.0) zur Verfügung gestellt (<https://creativecommons.org/licenses/by/4.0/deed.de>). Die Schriftenreihe ist nachgewiesen in unserem Repository OpenAgrar:  
[https://www.openagrar.de/receive/openagrar\\_mods\\_00005667](https://www.openagrar.de/receive/openagrar_mods_00005667).

*The publication series is distributed through the book trade (listed in German Books in Print - VLB). Some of the dissertations are published online open access under the terms of the Creative Commons Attribution 4.0 International License (<https://creativecommons.org/licenses/by/4.0/deed.en>). The publication series is documented within our repository OpenAgrar:  
[https://www.openagrar.de/receive/openagrar\\_mods\\_00005667](https://www.openagrar.de/receive/openagrar_mods_00005667).*

## **Bibliografische Information der Deutschen Nationalbibliothek**

Die Deutsche Nationalbibliothek verzeichnet diese Publikation in der Deutschen Nationalbibliografie: detaillierte bibliografische Daten sind im Internet über <http://dnb.d-nb.de> abrufbar.

## ***Bibliographic information published by the Deutsche Nationalbibliothek***

*(German National Library)*

*The Deutsche Nationalbibliothek lists this publication in the Deutsche Nationalbibliografie; detailed bibliographic data are available in the Internet at <http://dnb.dnb.de>.*

ISBN 978-3-95547-101-9  
ISSN (elektronisch) 2510-0602  
ISSN (Druck) 2510-0599  
DOI 10.5073/20210622-104529

## **Herausgeber | Editor**

Julius Kühn-Institut, Bundesforschungsinstitut für Kulturpflanzen, Quedlinburg, Deutschland  
Julius Kühn-Institut, Federal Research Centre for Cultivated Plants, Quedlinburg, Germany



© Der Autor/ Die Autorin 2021.

Dieses Werk wird unter den Bedingungen der Creative Commons Namensnennung 4.0 International Lizenz (CC BY 4.0) zur Verfügung gestellt (<https://creativecommons.org/licenses/by/4.0/deed.de>).

© The Author(s) 2021.

This work is distributed under the terms of the Creative Commons Attribution 4.0 International License (<https://creativecommons.org/licenses/by/4.0/deed.en>).

Research Centre for Biosystems, Land Use and Nutrition  
Institute of Plant Breeding and Agronomy I Department  
of Plant Breeding, Justus Liebig University, Giessen

**Phenotypic key factors, genetic regions and genes  
associated to cluster architecture in grapevine  
(*Vitis vinifera*)**

Inaugural Dissertation for a Doctorate Degree in Agricultural Sciences  
in the Faculty of Agricultural Sciences, Nutritional Sciences and  
Environmental Management

Examiners

1. Prof. Dr. Reinhard Töpfer
2. Prof. Dr. Rod Snowdon

Submitted by  
Robert Richter  
from  
Aalen, Germany  
Gießen 2020

Approved by the Faculty Agricultural Sciences,  
Nutritional Sciences and Environmental Management,  
Justus Liebig University, Giessen

**Examining Committee:**

First Reviewer: Prof. Dr. Reinhard Töpfer

Second Reviewer: Prof. Dr. Rod Snowdon

Examiner: Prof. Dr. Joachim Schmid

Examiner: Prof. Dr. Matthias Frisch

Chair of the Examining Committee: Prof. Dr. Gesine Lühken

Date of Defence: May 25th , 2021

## Table of Contents

1 - General Introduction .....	1
1.1 Viticulture and its products in a dynamic world .....	2
1.2 Biology and diversity of grapevine.....	3
1.3 Grapevine breeding .....	8
1.4 Cluster architecture determines the physical resilience to pathogens.....	11
1.5 Aims and Scope .....	16
2 - Identification of co-located QTLs and genomic regions affecting grapevine cluster architecture.....	17
3 - Differential expression of transcription factor- and further growth related genes correlates with contrasting cluster architecture in <i>Vitis vinifera</i> 'Pinot Noir' and <i>Vitis</i> spp. genotypes.....	37
4 - General Discussion.....	62
4.1 Considerations on grapevine cluster architecture as breeding target .....	63
4.2 QTLs related to cluster architecture .....	68
4.3 Proof-of-concept for marker assisted selection of dense cluster architecture.....	71
4.4 Candidate genes derived in the framework of the 'MATA' project .....	72
4.5 Differentially expressed transcription factors and related candidate genes.....	74
4.6 Conclusion and outlook .....	81
5 - Summary .....	82
6 – Zusammenfassung .....	84
7 - References.....	87
8 - Appendices .....	98
Appendix I: Electronic supplementary materials from Chapter 2 Richter et al. (2019) .....	99
Appendix II: Electronic supplementary materials from Chapter 3 Richter et al. (2020) .....	119
Appendix III: Supplementary materials from Chapter 4.....	154
List of Abbreviations.....	164
Declaration .....	167
Acknowledgments.....	168

# 1 - General Introduction

### 1.1 Viticulture and its products in a dynamic world

Cultivated grapevine (*Vitis vinifera* ssp. *vinifera* L.), is one of the most widely grown fruit crops in the world. At global scale, the area cultivated with grapevines, leveled firmly around 7.5 million ha between the years 2014 to 2018. The average annual harvest during these years was around 75.5 million tons. The main commodities resulting from grapevine cultivation are wine grapes (57%), table grapes (36%), and raisins (7%) (OIV 2019). During the seasons 2014 to 2016, the average world gross production value for grapes at farm gate level was above 68.15 billion USD per annum (FAOSTAT 2016). Taken together, these numbers highlight the importance and value of grapevine as commodity.

Although the global area used for viticulture varied only around one percent between 2014 and 2018, at the scale of individual countries, clear dynamics are perceivable. On the one hand, the area under vine declined in the Near East and Central Asia i.e. Turkey (- 64,000 ha), Iran (- 54,000 ha) and Uzbekistan (-1,500 ha). These countries have been recognized as important producers of table grapes and raisins. For wine grapes in the USA (-11,000 ha) and Portugal (-31,000 ha) a decline of area for viticulture can be observed. On the other hand China (+ 62,000 ha) and Italy (+15,000 ha) recorded a clear increase in viticulture area comparing 2014 and 2018. Further indicators for a dynamic development are the increased areas under vine e.g. in Latin American countries: Peru (+26% = 7,000 ha), Mexico (+24% = 7,000 ha) and on the Indian sub-continent (+18% = 23,000 ha) (OIV 2019). These countries may develop to new production centers.

Viticulture is a climate-sensitive agricultural system that can be considered as an indicator of climate change (Mosedale et al. 2016). According to the Intergovernmental Panel on Climate Change (IPCC) report presented in 2013, the average global temperature will rise between 1.5 °C up to 2.0 °C within this century (Stocker et al. 2013) depending on the prediction model. Consequently, traditional wine growing areas are facing changing conditions with impact on yield and quality of vines. Northern European regions may benefit from the wide range of varieties for viticulture under moderate climate conditions (Fraga et al. 2012). Whereas wine growing areas in Southern Europe will need to utilize scion and rootstock varieties more suitable to warmer and dryer climates (Duchêne 2016). Furthermore, recent studies suggest that grapevine yield and quality will respond to elevated CO<sub>2</sub> levels e.g. by promoted photosynthesis levels (Zhao et al. 2019) or altered host pathogen interactions

(Reineke and Selim 2019). Thus, breeding of new varieties, more adapted to future climatic conditions while maintaining key aspects of existing varieties, is regarded to be a major task for grapevine breeders (van Leeuwen et al. 2019).

### **1.2 Biology and diversity of grapevine**

Grapevine is a woody perennial climbing liana that, after a juvenile stage, develops a distinctive growth pattern with leaf-opposed tendrils and inflorescences (Gerrath et al. 2017; Keller 2015).

#### **Grapevine development**

Vines establish reproductive organs after two to three years, supposed that environmental drivers of flower induction, such as light, temperature and nutrient status are sufficient. Initiation and differentiation of the reproductive organs takes two consecutive seasons divided by winter dormancy (Carmona et al. 2008; Keller 2015; Rossmann et al. 2020). The inflorescence induction, followed by the inflorescence initiation, takes place in compound buds, during late spring of the first season (Figure 1a). The induced inflorescence primordia further differentiate inner and outer arm initials until morphological development rests when dormancy commences during autumn of the first season (Figure 1b-c). Before budburst in the second season, the compound bud starts to swell and inflorescence growth and differentiation continues during early spring of the second season. At morphological level, further branching, branch elongation and the formation of (in general) hermaphroditic flowers can be observed (Figure 1e-f). After bud burst (BBCH09 Figure 1d), the growth kinetics of the rachis can be described with two main phases. Initially, early in the season the rachis lengthens swiftly parallel with shoot elongation (BBCH13-19) (Shavrukov et al. 2004; Zyprian et al. 2018) and thickens until mid-flowering stage BBCH65, when it reaches 75% of its final diameter and over 85% of its final length. During 4 weeks after flowering the rachis elongation accounted for 11% of the final rachis length (Coombe 1995; Theiler and Coombe 1985). Berry growth follows a double sigmoid curve for berry volume separated by a lag phase with unaltered volume. The first phase, while the berries are green, is characterized by cell division and differentiation of the fruit itself but also of its seeds. The second growth maximum is reached during the ripening phase of the berry but is mainly based on cell enlargement (Carmona et al. 2008; Houel et al. 2013). The berry number is fixed one or two weeks after berry formation (Bessis

## General Introduction

and Fournioux 1992). All developmental steps interfere with environmental conditions and viticultural practices (Li-Mallet et al. 2016; Tello and Ibáñez 2017). Recent reports suggest an inverse correlation of flower number (later berries) and rachis development (Gourieroux et al. 2017; Gourieroux et al. 2016).

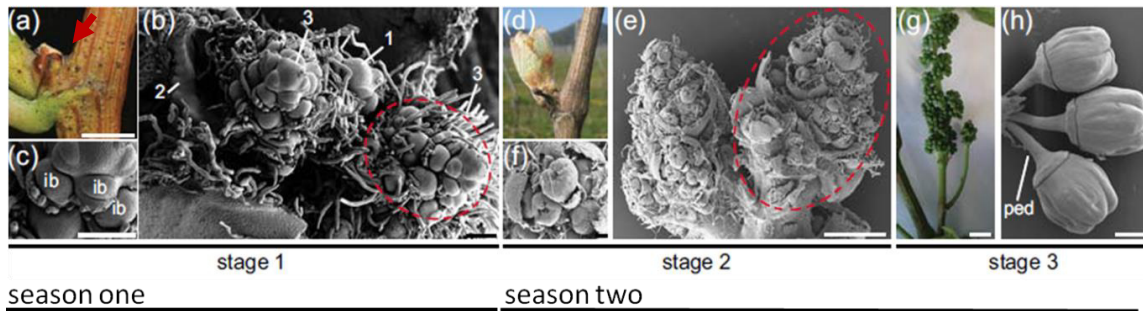


**Figure 1.** Inflorescence development in *Vitis vinifera* (cv. 'Pinot Noir') at three different stages during season one (a-c). (a) Latent bud in a leaf axil prior to bud dormancy. (b) SEM image of a compressed shoot within a (stage 1) compound bud, including shoot apical meristem (1), leaves (2) and immature inflorescences (3). Dashed line marks the premature inflorescence. (c) Close up view of b, showing inflorescence branch meristems (ib). (d) Inflorescence development during season two (d-h). (d) Bud burst (BBCH09). (e, f) Developing inflorescences with flowers (f shows close up of e). Dashed line marks the premature inflorescence. (g) Grapevine inflorescence of (BBCH57) just before flower opening. (h) Detached floral buds characterized by elongated pedicels (ped). Scale bars: 100  $\mu$ m (b, c, f), 1 mm (e, h), 1 cm (a, g). (Stage 1 to stage 3 samples were used in Rossmann et al. 2020 for DNA and RNA sequencing experiments) (Source: Rossmann *et al.* (2020), modified).

### Grapevine taxonomy

Taxonomically, grapevine is a member of the *Vitaceae* family consisting of approximately 900 species from 16 genera (Wen et al. 2018). Within the family of *Vitaceae*, solely the genus *Vitis* produces edible fruits (Adam-Blondon et al. 2016). The genus *Vitis* was recognized to have two subgenera, differing in chromosome number (Patel and Olmo 1955), basic morphological, and anatomical traits (Galet 1979). It comprises the subgenus *Muscadinia* ( $2n = 40$ ) with a recently reported haploid genome size between 300 and 460 Mbp (Cochetel et al. 2020) of and the subgenus *Vitis* ( $2n = 38$ ) with a reference genome size of 475 Mbp (Jaillon et al. 2007). The subgenus *Muscadinia* with two identified species: *V. rotundifolia* Michx. and *V. popenoei* J.H. Fennel, are native in humid, subtropical environment (Hickey et al. 2019). The subgenus *Vitis* consists of ~ 65 species that are found in two diversity hotspots in the northern hemisphere i.e. eastern Asia and North America (Wen et al. 2018). In essence, current global viticulture utilizes almost exclusively *Vitis vinifera* varieties for wine production (OIV 2017). Several other *Vitis* species serve as important resistance donors in grapevine breeding

## General Introduction

(Migicovsky and Myles 2017). *Vitis labrusca* is an important species in table grape breeding e.g. as part of the pedigree of 'Kyoho' (Maul et al. 2019) the world's most cultivated variety (OIV 2017).

### **Grapevine domestication**

Early domestication evidence by means of archaeological, historical and ethno-botanical information dates back to the Near East over 8,000 years ago (McGovern and Mondavi 2003). Hence, grapevine can be regarded as one of the first domesticated perennial fruit crops. The recent wine grape (*Vitis vinifera* ssp. *vinifera*) henceforth referred to as *V. vinifera* is the domesticated descendant form its wild relative *Vitis vinifera* ssp. *sylvestris* henceforth referred to as *V. sylvestris* (Wen et al. 2018). The genetic structure and phenotypic features of cultivated grape varieties are linked to human selection and geographic region (Bacilieri et al. 2013; Migicovsky et al. 2017). Riaz et al. (2018) suggested two geographic centers that contributed to the domestication of *V. sylvestris*. Primarily, Transcaucasian wild grapes were selected in a region between the Caucasus and China and wild grapes of Western Europe were selected in a secondary domestication event. During domestication enormous biological changes occurred. Compared to the *V. sylvestris* wild type, flower sex, fruit size, seed and leaf shape have changed over time. Most important is the flower sex, which changed from dioecious male and female towards hermaphrodite flowers in most cultivated plants conveying more regularly and higher yield. Further domestication and selection steps are interconnected with the cultural development of humankind (Töpfer et al. 2011).

### **Genetic diversity in domesticated varieties**

Probably promoted by the early domestication approximately 6,000 *V. vinifera* varieties are available for viticultural production (OIV 2017). Among them are locally prioritized varieties that are adapted to e.g. dry conditions like the table grape variety 'Yaghooti' (Shiri et al. 2018). Also currently commercially unimportant varieties provide traits that are desirable with respect to global warming. Old varieties like 'Heunisch' and 'Orleons Gelb' may pass on stable acidity and late ripening to the offspring (Schmid J. 2019). These "Old Landraces" could clearly broaden the genetic basis available for cultivar improvement (Gascuel et al. 2017). Facing climatic change, the existing genetic diversity provides the chance for breeders to cope with altered conditions as long they are maintained in an accessible condition i.e. free of virus

## General Introduction

infection and true to type. However, globally only 33 *Vitis vinifera* varieties account for 50% of the total area covered with grapevine (OIV 2017). Due to consumer preference, producers tend to cultivate varieties with high acceptance on the market (Eibach and Töpfer 2015) i.e. 13 “international” varieties account for 33% of the overall viticultural area with a tendency to focus even more (OIV 2017). Hence, on-farm genetic diversity represents only a small fraction of the existing genetic diversity. In order to preserve the genetic variation in grapevine for future breeding programs, several thousand genotypes are maintained in public grapevine germplasm repositories such as the collection with thousands of accessions at the Julius Kühn-Institute, Institute for Grapevine Breeding Geilweilerhof in Germany. Moreover, databases like the ‘Vitis International Variety Catalogue’ [www.vivc.de](http://www.vivc.de) (Maul et al. 2019) make the data for varieties accessible.

### **Relation of grapevine varieties and clones**

Cultivated grapevine (*V. vinifera*) varieties have highly heterozygous genomes. This is inherited from their wild ancestors being dioecious and therefore obligate out-crossers. Thus, to propagate a highly heterozygous cultivar along with preserving its viticultural characteristics, vegetative propagation was the method of choice since ancient times (Carbonell-Bejerano et al. 2019). In terms of genetic diversity, vegetative propagation shows two effects: Propagation of cultivars by cuttings contribute to decrease the diversity in commercial plantings (Carmona et al. 2008). On the other side, vegetative multiplication for centuries, originally intended to avoid the loss of cultivar attributes, conserves somatic mutations in grapevine cultivars due to the lack of meiotic DNA exchange. These mutations may cause phenotypic variation and could be a source for cultivar adaptation under changing environmental conditions (Carbonell-Bejerano et al. 2019). Well studied examples are berry color mutations, which resulted in independent cultivars like ‘Pinot Noir’ as the ancestor of ‘Pinot Blanc’ and ‘Pinot Gris’ (Yakushiji et al. 2006). Initially, somatic mutations take place in a single meristematic cell associated with the DNA replication and cell division processes. Somatic mutations are additionally defined by the tissue structure of the grapevine meristem i.e. the composition of two cell layers L1 (tunica) and L2 (corpus). While L1 layers give rise to the epidermal cells, all internal cells including the gamete development in the flowers are composed by cells of the L2 layer. The L1 cell layer divides mostly in anticlinal orientation and the L2 layer divides predominantly in periclinal orientation. Therefore, the two layers evolve

## General Introduction

into distinct sections with only rare events of cell exchange between the layers (Thompson and Olmo 1963). Given that mutations spontaneously emerge in either the L1 or L2 layer, grapevine plants are genetic chimeras with, to some extent, different genetic composition in L1- and L2-derived cell layers. If the mutation is propagated in the L1 or the L2 of a shoot apical meristem, it could be transmitted by bud propagation representing the starting point of a new clone of a cultivar (Carbonell-Bejerano et al. 2019).

Exploiting the intravarietal diversity in genetic and phenotypic studies, the causal DNA sequence variants of various economically important traits have been revealed by comparing phenotypically contrasting clone variants from the same cultivar. Recently Carbonell-Bejerano et al. (2019) reviewed some viticultural and oenological relevant mutations captured in somatic clones of widely used varieties. Somatic clones were used to reveal the genetic basis of Muscat flavor (Crespan and Milani 2001; Emanuelli et al. 2010), berry color variations in grapevine (Yakushiji et al. 2006) and berry seedlessness (Royo et al. 2018). Plants derived from the L1 cell layer of 'Pinot Meunier' (showing hairy leaves) revealed the causal mutations for a reduced juvenile phase and a dwarf phenotype (Boss and Thomas 2002). Direct comparison of intra-cultivar sequence variation is even able to identify genetic determinants at gene-level for as complex traits as grapevine cluster architecture. Rossmann et al. (2020) used a next generation sequencing (NGS) approach and 'Pinot Noir' clones with different levels of cluster compactness and revealed a causal mutation in the gene encoding transcription factor *VvGRF4* leading to a loosely clustered phenotype. **In Chapter 3 of this thesis (Richter et al. 2020), the assertion that *VvGRF4* expression determines loose cluster architecture as revealed by (Rossmann et al. 2020) could be broadened to a range of 20 'Pinot Noir' clones showing either loose or compact cluster architecture.** Moreover, 14 additional candidate genes emerged as significant differentially expressed over diverse environments, regardless the application of organic and integrated vineyard managements. Identified mutations causing the observed phenotypic variation of economically important traits as discussed above have the potential for precision breeding using genome editing with CRISPR/cas as new technology for the introduction of SNPs at the desired locations (Rossmann et al. 2020).

### 1.3 Grapevine breeding

#### Breeding history

The data, accessible via the 'Vitis International Variety Catalogue' ([www.vivc.de](http://www.vivc.de)), emphasize that the genetic variation of the *V. vinifera* gene pool was shaped through crosses between early cultivated varieties. Supporting this notion, the kinship analysis reported in Laucou et al. (2018) identified 118 full parentages and 490 parent-offspring duos in a set of 783 different prominent cultivars. So, these results confirm a close pedigree relationship within the cultivated (*V. vinifera*) grapevine varieties. However, it remains an open question if these cultivars are the result of organized breeding activities or of random selections for higher yield and quality (Töpfer et al. 2011). Reasonable evidence for controlled grapevine breeding is found in America during the late 18th century. *Vitis vinifera* varieties brought from Europe to North America (with Eurasian genetic background), showed high levels of susceptibility to endemic North American fungal pathogens e.g. (*Plasmopara viticola*, Berk. & Curt ex. De Bary) causing downy mildew (Spring et al. 2018) and (*Erysiphe* (syn. *Uncinula*) *necator*, Schwein) causing powdery mildew (Gadoury et al. 2012). Driven by this susceptibility, targeted breeding activities with American wild species resulted in resistant interspecific plants and varieties known as 'American hybrids'. The introduction of the 'New World' pathogens to Europe provoked breeding activities in the 'Old World', particularly in France, resulting in 'French hybrids' with considerable resistance but poor wine quality (Töpfer et al. 2011). Mendelian genetics were applied in grapevine breeding since the beginning of the 20th century (Hedrick and Anthony 1915). The results of this attempt were limited to major genes (inherited in a Mendelian manner, with allelic forms that give qualitatively distinct phenotypes) and the progress was slow. Husfeld (1962) concluded that the restricted success in breeding of resistant as well as tasty varieties was due to the poor understanding of the genetic complexity of the plant material that has been used for crosses.

#### Molecular breeding

The turning point from heuristic to information-based grapevine breeding was the advent of molecular marker techniques in the 1990s (Töpfer et al. 2011; Williams et al. 1990). Since that time, it is possible to resolve the contributions of single loci of a multi-genic inherited trait and associate it with quantitative phenotypic features (for an introduction in the principles of segregation, recombination and linkage in a molecular marker map for a

## General Introduction

population see Jones et al. (1997)). Over the last decades molecular marker types have continuously been developed. The first genetic mapping studies used the RAPD (random amplified polymorphic DNA) marker technique (Weeden et al. 1994). A further major improvement was reached with the publication of the reference genome for *Vitis vinifera*, available since the year 2007 (Jaillon et al. 2007). With this reference genome, simple sequence repeat (SSR) markers could be developed individually and improved mapping and marker-assisted selection in terms of reproducibility. The co-dominant SSR markers showed a high transferability among *Vitis* varieties and in inter specific crosses, even allowing the generation of integrated maps of several different mapping populations based on their marker synteny. This combines data over all populations integrating a higher genetic diversity (Di Gaspero et al. 2007; Doligez et al. 2006; Vezzulli et al. 2008). To some content, SSRs are amenable to automation. Hence, they were used for detailed analysis of genetically determined grapevine traits such as pathogen resistance (Rex et al. 2014; Schwander et al. 2012; Zhang et al. 2009a), variable phenology (Fechter et al. 2014) or morphology (Battilana et al. 2013; Fechter et al. 2012). Over the last decades, SSR markers have evolved to the reliable and cost-effective standard application in marker-assisted grapevine breeding (Zini et al. 2019). Single nucleotide polymorphisms (SNP) represent the next marker generation used for genetic analysis in grapevine breeding. They allowed to exploit next generation sequencing data based on the detection of SNP present at genome scale (Di Gaspero and Foria 2015). Currently chip based approaches using an 18k SNP assay allowed to use thousands of SNPs per genotyping. This embodies an average marker resolution of 315 to 650 markers per chromosome i.e. on genome wide average, one SNP every 47 kilo base pair (Laucou et al. 2018). Nevertheless, SNP chips showed clear limitations because the transferability of SNPs is rather low, the implementation costs are high, and the SNP chip is not flexible once produced (Delrot et al. 2020). Direct genotyping of entire mapping populations with genotyping by sequencing (GBS) as in Tello et al. (2019) following the Restriction site Associated DNA Sequencing (RAD Seq) approach (Elshire et al. 2011) seems to be the current method of choice for the construction of SNP-based genetic maps.

Heterozygous and homozygous species demand for different population types. In plant breeding the generation of linkage maps derived from segregating populations based on two phenotypically differing parents was commonly utilized e.g. for model plants and annual crops (Tanksley et al. 1989) as well as for perennial species (Lodhi et al. 1995). The majority of

## General Introduction

the biparental populations used for linkage mapping in plants are progenitors of homozygous parental lines where the parental individuals differ from each other regarding their phenotype and genotype (Mendelian testcrosses). This is different in grapevine genetic analyses. The wild dioeciously and therefore outcrossing ancestors of domesticated grape varieties have consequently heterozygous genomes and strong inbreeding depression prevents the selection of homozygous genotypes. Thus, the routinely practice of vegetative propagation conserves high heterozygosity even in centuries old cultivars. Indeed, retracing the pedigree of the parental genotypes of the cross described in Chapter 2 of this thesis (GF.GA-47-42 (syn. 'Calardis Musqué') x 'Villard Blanc') suggested the contribution of six wild (out-crossing) *Vitis* species within a distance of only eight meiotic events (based on the information at VIVC [www.vivc.de](http://www.vivc.de) (Maul et al. 2019)). This high level of heterozygosity greatly facilitated genetic studies in grapevine and thus each variety is already a first filial generation (F1). The progeny of a controlled cross between two varieties segregates for all the loci that are heterozygous in that cross with an expected ratio of 3 : 1, 1 : 2 : 1, or 1 : 1 : 1 : 1. Alternatively, with 1:1 ratio if both parents are homozygous at this locus (Weeden et al. 1994). A drawback of the high heterozygosity in clonally propagated plants is the inbreeding depression due to a high number of accumulated deleterious recessive mutations (McKey et al. 2010). Consequently, the establishment of populations based on selfing or backcrossing (RIL, NIL, F2, BC1, etc.) is not realistic in grapevine breeding (Delrot et al. 2020). Taken together, unlike other crop or model species, quantitative genetics in grapevine utilizes F1 plants based upon a cross of highly heterozygous parental individuals. To circumvent the deleterious effects of accumulated mutations, a "double pseudo test-cross" approach is applied (Cipriani et al. 2011; Grattapaglia and Sederoff 1994). In the usual test cross of two homozygous parents, only two alleles of a genetic locus segregate in the F1 progeny, for grapevine in a double pseudo testcross up to four alleles may segregate. Because of this approach, two separated genetic maps, one from each parent, are obtained (Lodhi et al. 1995). Codominant markers like SSRs, with segregating alleles from both parents, often allow the combination of both parental maps into an integrated genetic map. This provides a higher marker density and a combined coherent marker order of the parental maps, providing additional segregating alleles (Delrot et al. 2020). **Chapter 2 of this thesis (Richter et al. 2019) reports the stable detection of QTL (quantitative trait locus) for important cluster architecture traits calculated with a genetic map based on SSR and SNP markers segregating in a double pseudo testcross population.**

## General Introduction

Plant breeding focusses on the identification of genotype-to-phenotype associations. Various successful QTL mapping studies, using bi-parental mapping populations, have proved the useful application of this approach. However, there are some limitations regarding the genetic diversity of the crossing parents i.e. their segregating alleles and the degree of recombination. The latter determines the resolution of the QTL localization (Korte and Farlow 2013). In addition, grapevine as a large space consuming perennial species with a long seed to seed cycle of about three years makes the establishment of a cross population a costly attempt. This interferes with the fact that the size of the population decides the minimal detectable phenotypic effect i.e. minor genetic effects are below the statistical threshold required for the detection of a genotype-to-phenotype association if the population comprises an inadequate number of individuals (Töpfer et al. 2016).

Several thousand grapevine accessions, representing almost the entire genetic variation, are maintained in germplasm repositories in different environments (Maul et al. 2019). Together with NGS techniques, this is a source for genetic investigations without the need of creating cross populations. The exploitation of standing germplasm collections with NGS and bioinformatics are a promising combination to accelerate the identification of transferable DNA markers that are essential for breeding and genetics. Recently, bioinformatics analysis in form of genome-wide efficient mixed-model association was used to associate GBS derived SNPs with berry traits, in a population consisting of 179 grape genotypes in a genome wide association study (Guo et al. 2019). The RNase H2 enzyme-dependent amplicon sequencing (rhAmpSeq) approach, introduced by Zou et al. (2020), provides a strategy to identify SNP markers that are transferable even between distantly related *Vitis* species.

### **1.4 Cluster architecture determines the physical resilience to pathogens**

Due to climate change, extreme weather conditions are expected more frequently, extending the phases with dry or moist weather (Stocker et al. 2013), late spring frost, hail etc. A prolonged time span with wet or moist conditions favors fungal infections. Loose cluster architecture (CA) acts as physical feature restricting the favorable moist conditions for fungal infections (Igounet et al. 1995). Grapevine varieties with genetically determined loose cluster architecture provide enhanced airflow within clusters without the need for extra viticultural

measures. This sustainable effect usually avoids additional fungicide applications for *Botrytis*, energy and effort.

### **Grape cluster organization and function**

Grapevine berries are organized in a panicle. The term inflorescence is used until flowering, after fruit set the terms bunch or cluster are used, respectively. The peduncle is the part of the stalk connected with the shoot ongoing to the first branching point where a shoulder may be inserted. From there the main axis is termed rachis, bearing the lateral branches. Each single flower and later the berry is attached to the lateral structures or to the rachis with a pedicel (Keller 2015) (Figure 2). Besides its framework function, the stalk contains various vascular bundles, forming the pathway for water and nutrient supply from the vine to single flowers and berries, respectively (Gourieroux et al. 2016).

### **Cluster architecture affecting factors**

CA sub-traits are sensitive to environmental conditions and respond, depending on the phenological stage of a grapevine, in a complex manner (for a review see Tello and Ibáñez (2017)). Primed by these environmental conditions the sink-source relationship between vegetative and generative growth and the accumulation of starch reserves is changed (Li-Mallet et al. 2016). Management systems i.e. integrated, organic and biodynamic viticulture show impact on cluster architecture sub-traits (Döring et al. 2015). There is also an impact of vineyard management practices to CA. For example, the berry number can be reduced due to application of anti-transpirant agents or if leaf removal is performed around flowering-time leading to a diminished capacity for photosynthesis. Artificial shading and leaf removal applied as pre-flowering treatment is causing smaller berries. The application of gibberellins at flowering time has a reducing effect on berry number, too. An application of gibberellins prior to flowering leads to elongated inflorescence axes (Tello and Ibáñez 2017). Recently, the naturally occurring phytohormone concentration was correlated to cluster architecture traits. Grimplet et al. (2019) reported significantly different abundance of auxin and gibberellic acid between loosely and compactly clustered clones of 'Tempranillo'. The arrangement of rachis related and berry related CA sub-traits determines the compactness of a cluster i.e. the available space for a single berry within the panicle (Figure 2).

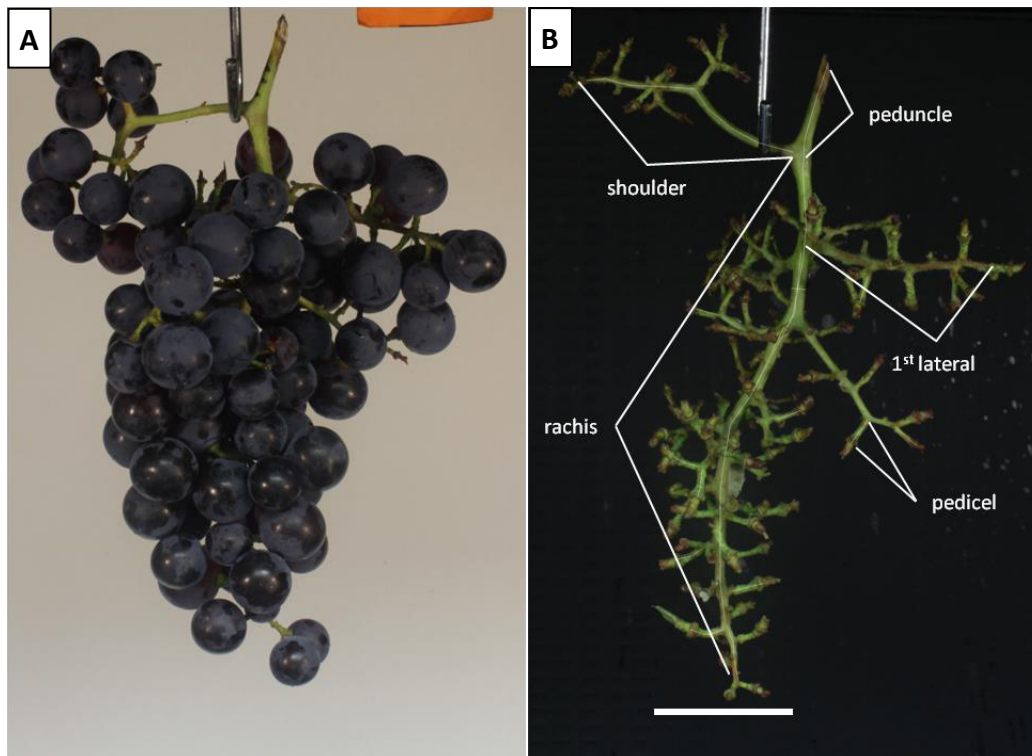


**Figure 2.** A) 'Uva Rara' Cluster with 98 berries and 182g berry weight at BBCH89 (ripe for harvest). B) The same cluster after destemming the berries. Cluster architecture sub-traits characterize the supportive structure and define the distribution of the berries in the accessible space. The size standards in orange and white represents 3cm.

### Impact of cluster architecture on the phytosanitary condition of a grape cluster

Cluster compactness is of utmost importance for the maintenance of physical properties, which universally prevent pest infections. Compact cluster architecture is involved in the loss of physical resilience against pathogens caused by micro cracks (Becker and Knoche 2012) and macro cracks in the epidermis of the berry (Smart and Robinson 1991). Also, higher infestation rates of the grape berry moth *Lobesia botrana*, the ochratoxine producing fungus *Aspergillus* spp. and the bacterial pathogen *Cladosporium* spp. are related to compact clusters (Fermaud 1998; Latorre et al. 2011; Leong et al. 2006). In a compact cluster, berries are in close contact. Consequently, berries at these contact zones have less cuticle content and show an amorphous structure in the waxy layers with restricted protective capacity against *Botrytis cinerea* (Gabler et al. 2003; Marois et al. 1986). However, the spatially wide arrangement of the berries supports the formation of thicker and waxier skin. The wax layers of the cuticle function as physical barriers against rot-inducing pathogens (Herzog et al. 2015). Additionally, within a loose cluster, ultra-violet radiation can trigger the biosynthesis of secondary metabolites such as resveratrol. Resveratrol acts as a phytoalexin, improving the resistance to

## General Introduction

molds (Jeandet et al. 1991) and even causes damage on *B. cinerea* conidia when treated with it (Adrian and Jeandet 2012). Fungal infections are dependent on suitable temperature and humidity conditions. *B. cinerea* infects green tissues of grapevine including berries over a wide temperature range (5~35°C). However, the requirement for wetness is amplified with growing distance to the optimum infection temperature of 20.8°C (Nair and Allen 1993). Ciliberti et al. (2015) investigated the impact of temperature and wetness duration on the infection rate of several *B. cinerea* strains, their results are in line with those reported in Nair and Allen (1993). The optimal temperature for infections with *B. cinerea* is analogous to temperatures regularly encountered at harvest in wine growing regions. However, in loosely structured grape clusters accelerated air exchange and lower temperatures reduce the internal vapor content. Thus, the driving factors for *Botrytis* resilience conveyed by loose cluster architecture are the shorter wet periods and, but to a lesser extent, the reduced internal temperature (Igounet et al. 1995).

### Scaling options for cluster compactness

The level of cluster compactness can be estimated based on visual or tactile impressions of judging persons. These subjective methods classify grapevine bunches in predefined categories according to their overall appearance. This is simple and non-destructive but entails the need for trained evaluators to produce replicable results. The OIV descriptor 204 for bunch compactness is a widely used framework to grade bunches according to five ordinal ranks from very loose to very compact. A further advantage of this descriptor is that the OIV describes certain varieties as reference for each class of compactness e.g. 'Uva Rara' (depicted in Figure 2) or 'Prosecco' for very loose and for loose cluster architecture respectively (OIV 2015). This is useful for training of evaluating panel members or in machine learning for the generation of reference data. Even so, a range of other ranking schemes has been published (for a review see Tello and Ibáñez (2017)).

In contrast, cluster compactness indices, where the level of compactness is captured with measured values of multiple cluster architecture sub-traits result, in objective and continuous data sets. Studies applying these indices proved their usefulness for the estimation of bunch compactness at inter and at intra cultivar level (Tello and Ibáñez 2017). However, cluster shape differs considerably between varieties e.g. the OIV descriptor 208 for bunch shape includes three classes. It might be reasonable to conclude that, depending on the cluster

## General Introduction

shape, architecture sub-traits contribute with different impact to the total compactness of a given bunch. In Chapter 2 of this work, thorough measurements of 16 CA sub-traits describe cluster compactness. Only Six sub-traits confirmed their importance for compactness in the highly diverse cluster architecture context represented in the F1 progeny used for the study. Future studies may benefit from recently reported automated solutions for the assessment of single sub-traits contribution to the overall phenotype. These have the potential to minimize time and effort inherent to the measurement of the multi-factorial trait cluster compactness (Rist et al. 2018).

### 1.5 Aims and Scope

The work described in this thesis intends to elucidate phenotypic and genetic determinants of loose cluster architecture of grapevine, as a prerequisite for the incorporation of this complex trait in marker assisted selection processes. To this end, this work was set out with the following overall aims:

- Identification of phenotypic sub-traits with a seasonally independent and a high contribution to overall cluster architecture. (Chapter 2).
- Determination of QTLs linked to main drivers of cluster architecture (Chapter 2).
- Inference of first molecular markers for key sub-traits with high impact on cluster compactness (Chapter 2 and Chapter 4).
- Validation of candidate gene expression with association to cluster architecture by exploiting the contrast between gene expression measured in loosely and compactly clustered varieties and in somatic variants of 'Pinot Noir' over multiple environments (Chapter 3).
- The general discussion (Chapter 4) aims at integrating the results elaborated in the frame of the joint project Molecular Analysis of Grapevine Cluster architecture (MATA). Further aspects of experiments that are not covered in detail in the published articles are discussed. The discussion intensifies the reflection about candidate genes that are supported by multiple lines of evidence.
- A marker assisted negative selection scenario for compact clustered individuals in a bi-parental cross is discussed as a proof of principle for the applicability of the trait linked genomic regions of this thesis in marker-assisted selection.
- The work ends with a résumé of the main findings and gives an outlook on possible exercises aiming at a broader understanding of the genetic cues determining cluster architecture traits.

## **2 - Identification of co-located QTLs and genomic regions affecting grapevine cluster architecture**

Robert Richter, Doreen Gabriel, Florian Rist, Reinhard Töpfer, Eva Zyprian

Theoretical and Applied Genetics (2019) 132:1159–1177

<https://doi.org/10.1007/s00122-018-3269-1>

Reprinted by permission from Springer Nature Customer Service Centre GmbH:  
Springer Nature, Theoretical and Applied Genetics, Identification of co-located QTLs  
and genomic regions affecting grapevine cluster architecture, Richter et al. , © (2018)



# Identification of co-located QTLs and genomic regions affecting grapevine cluster architecture

Robert Richter<sup>1</sup> · Doreen Gabriel<sup>2</sup> · Florian Rist<sup>1</sup> · Reinhard Töpfer<sup>1</sup> · Eva Zyprian<sup>1</sup> 

Received: 23 July 2018 / Accepted: 12 December 2018 / Published online: 19 December 2018  
© Springer-Verlag GmbH Germany, part of Springer Nature 2018

## Abstract

Loose cluster architecture is an important aim in grapevine breeding since it has high impact on the phytosanitary status of grapes. This investigation analyzed the contributions of individual cluster sub-traits to the overall trait of cluster architecture. Six sub-traits showed large impact on cluster architecture as major determinants. They explained 57% of the OIV204 descriptor for cluster compactness rating in a highly diverse cross-population of 149 genotypes. Genetic analysis revealed several genomic regions involved in the expression of this trait. Based on the linkage of phenotypic features to molecular markers, QTL calculations shed new light on the genetic determinants of cluster architecture. Eight QTL clusters harbor overlapping confidence intervals of up to four co-located QTLs. A physical projection of the QTL clusters by confidence interval-flanking markers onto the PN40024 reference genome sequence revealed genes enriched in these regions.

## Introduction

Grapevine (*Vitis vinifera* L. subsp. *vinifera*) is one of the most important and valuable fruit crops. Globally, 7.5 million hectares are under viticulture. The annual grape yield reached 75.8 million tons in 2016. The largest part of the harvested grapes (47.3%) sustains wine production (267 million hl). The remaining shares are sold as fresh grapes (35.8% of the annual yield), followed by raisins and the production of juice (13.5%; OIV 2017).

High-quality fruits are crucial for winemakers and the fruit processing industry. However, *V. vinifera* grapevine cultivars are susceptible to several diseases and pests, so viticulture depends on intense protective sprayings. The obligate

biotrophic pathogens *Erysiphe necator* (the causal agent of powdery mildew) and *Plasmopara viticola* (the causal agent of downy mildew), both specific pathogens of grapevine, as well as the ubiquitous fungus *Botrytis cinerea* (teleomorph *Botryotinia fuckeliana*, the causal agent of gray mold) represent the major threats (Pertot et al. 2017). Recent grapevine breeding efforts succeeded in the introgression of resistance loci for *Erysiphe necator* and for *Plasmopara viticola* from *Vitis* wild species into new high-quality cultivars (Töpfer et al. 2011). Grapevine varieties with enhanced genetically determined resistance against those pathogens became available. However, this strategy is not a solution to obtain resistance to *Botrytis cinerea*. There is no efficient cellular defense response known against this fungus. Due to the lack of resistance donors, grapevine breeding and clonal selection for resilience to *Botrytis* have to rely on the utilization of physical factors, e.g., the selection of genotypes with loose cluster architecture, thick berry skin and hydrophobic berry surface (Gabler et al. 2003; Herzog et al. 2015; Shavrukov et al. 2004). Loosely structured grape clusters have enhanced resilience to *B. cinerea* due to improved ventilation within the grape cluster. The accelerated drying process of residual humidity after rainfall or the precipitation of dew functions as a physical barrier against infections with fungal pathogens (Hed et al. 2010; Molitor et al. 2012). Several studies underline the importance of wetness duration for the successful infection by *B. cinerea* (Broome et al. 1995; Nair and Allen 1993; Nelson 1956). In addition, fungicide applications can

---

Communicated by Matthias Frisch.

---

**Electronic supplementary material** The online version of this article (<https://doi.org/10.1007/s00122-018-3269-1>) contains supplementary material, which is available to authorized users.

---

✉ Eva Zyprian  
eva.zyprian@julius-kuehn.de

<sup>1</sup> Institute for Grapevine Breeding Geilweilerhof, Julius Kuehn Institute, Federal Research Centre of Cultivated Plants, Geilweilerhof, 76833 Siebeldingen, Germany

<sup>2</sup> Institute for Crop and Soil Science, Julius Kuehn Institute, Federal Research Centre of Cultivated Plants, Bundesallee 58, 38116 Brunswick, Germany

better reach the berries surface within the cluster in the case of a more open, loose cluster (Hed et al. 2010). Furthermore, spatial temperature gradients between the inner and outer berries of a cluster are less pronounced. Solar radiation can much better reach the internally situated berries. Fruit maturity thus reaches a higher rate of uniformity in a loosely structured grapevine cluster (Pieri et al. 2016; Vail and Marois 1991). The formation of micro-cracks and the subsequent loss-of-barrier effect of the berry's epidermis against pathogens (Becker and Knoche 2012) appear reduced. According to Smart and Robinson (1991) berries may even burst due to high pressure inside of compact clusters and thereby lose any kind of barrier against pathogens. Loose cluster architecture thus contributes to healthier grapes and harmonized ripening periods for the production of supreme yield and quality.

The grade of density or openness of a grapevine cluster relates to the ratio between the volume occupied by berries and the total cluster volume. This ratio describes the free space between the berries. Cluster architecture (CA) determines the arrangement of berries in a cluster and the distribution of free space. The components of CA comprise berry traits and stalk traits. The interplay of berry traits, e.g., berry number and berry volume, and stalk traits, e.g., rachis length or pedicel length, determines the final grade of compactness (discussed in Tello and Ibáñez 2017). The International Organization of Vine and Wine (OIV) developed descriptors to score and measure morphologic grape cluster traits (OIV 2015). Based on the assessment of the available space between single berries, the descriptor “OIV204 (cluster density)” is applicable to score the cluster compactness (OIV 2015). Furthermore, cluster architecture can be assessed by measuring cluster architecture sub-traits, e.g., the length of single rachis internodes (Shavrukov et al. 2004) or berry size and number (Rist et al. 2018; Kicherer et al. 2013). These measurements of single sub-traits can be assembled into CA factors, e.g., the ratio of cluster weight by length (Tello and Ibáñez 2014).

Although environmental and management conditions affect CA traits (Li-Mallet et al. 2016; Tello and Ibáñez 2017), their expression is also under genetic control. Houel et al. (2013) studied the genetic variability of berry size in a wide range of grapevine genotypes and found an immense variation of berry volume. For berry weight, Ban et al. (2016) detected the genetic influence in the offspring of a hybrid cross. Genetic characterization of 140  $F_1$  individuals from a table grape cross-population indicated significant genotypic effects for all of the 23 CA traits under investigation (Correa et al. 2014). Shavrukov et al. (2004) compared four grapevine genotypes and found that rachis size variation is due to rachis cells size variation. Tello et al. (2015) compared 125 genotypes in an association genetic study and described major variations concerning the lengths of the rachis and secondary branches.

Fanizza et al. (2005) detected genetic variation in the offspring of a table grape cross associated with berry number per cluster. Wine grapes and table grapes belong to different gene pools and show, among other characteristics, considerable variations in berry and cluster architecture sub-traits (Migicovsky et al. 2017). The authors revealed genetic differences associated with bigger berries and less dense clusters in table grapes as compared to wine grapes. Di Genova et al. (2014) compared a genetic draft sequence of the table grape cultivar “Sultanina” with the reference genome for grapevine derived from an inbred line of “Pinot Noir,” a wine grape cultivar. In total, 2000 genes were found affected by structural variants. Among these genes, more than 50 genes are associated with the GO (gene ontology) term “anatomical structure development” (GO:0048854) providing a source of genetic diversity potentially involved in cluster architecture differences. Grimplet et al. (2017) compared clones with loose or compact CA of the same cultivar (near-isogenic lines). These authors found 470 genes differentially expressed (two loose clones vs. two compact clones). More specifically, compact clones showed a higher gene activity in genes involved in the production of cellular material and in genes of the cell cycle network. Shiri et al. (2018) performed a co-expression experiment with a compactly clustered table grape variety along the development from pre-flowering to pre-harvest. The authors identified gene expression networks with influence on cluster architecture via regulation of gibberellin abundance.

In this study, detailed phenotyping and statistics of CA sub-traits classified the investigated sub-traits according to their impact on the overall grade of compactness/openness. The linkage of phenotypic characteristics of CA with molecular markers identified quantitative trait loci (QTLs). These QTLs should be involved in the manifestation of multiple sub-traits that contribute to CA. A transfer of the genetic positions of the QTLs to the physical map by projection of the confidence interval-flanking markers onto the reference genome of PN40024 (12x) revealed clusters of overlapping confidence intervals from QTLs of strong impact on CA traits. The elucidated genomic regions, i.e., the novel knowledge about linked molecular markers, restrict the size of genomic regions for investigation in further studies. The here presented  $LOD_{max}$ -associated markers for cluster architecture sub-traits are first steps to marker-assisted selection and could be further evaluated for their transferability in molecular breeding for cultivars with loose clusters.

## Materials and methods

### Plant material

The parents and 151  $F_1$  genotypes from a controlled cross of GF.GA-47-42 × “Villard Blanc” (G × V) were used in

this work. The vines were located in two neighboring vineyards at the Institute for Grapevine Breeding Geilweilerhof (N49°21.675, E8°04.433). In the first vineyard (vineyard 1), for each of the individual 151 F<sub>1</sub> genotypes two vegetatively propagated clones were planted on their own roots with 1.8 m row spacing and 0.9 m plant spacing in the year 2000. The second vineyard (vineyard 2) with eight additional clonal replicates (made from wooden cuttings grafted on rootstock SO4) was planted in 2010. Here, the vines were grown with 2 m (row) × 1 m (plant) spacing. The vines underwent “Guyot pruning” with 10 to 12 buds remaining and were grown in a vertical shoot position trellis system. An integrated pesticide spray program according to best practice policies for viticulture (BMELV 2010) protects the plantation.

The maternal parent, the fungus-resistant breeding line GF.GA-47-42, and the paternal parent, the fungus-resistant white wine cultivar “Villard Blanc”, exhibit reduced cluster densities according to OIV204 as evaluated over 3 years at six plants each (Online Resource 1). The resulting segregating population includes transgressive phenotypes with extreme differences in CA. Two genotypes were excluded from the evaluation process since they showed no or unusually poor fruit set during consecutive growing seasons. Moreover, the population provides 45 plants with female flowers and 106 plants with hermaphrodite flowers.

## Sampling

Phenotypic investigations used 3 to 12 clusters per genotype harvested from different vines per season. In the year 2013, 12 samples came from two vines, while in the years 2014 to 2017, three to six independent samples originated from different vines (Table 1). When the first vines of the population reached véraison the clusters were inspected two times per week. To avoid the loss of berries during harvest and transport of the clusters the samples were harvested when the clusters showed characteristics of maturity, but were not overripe. At this time, the berries had a sugar content of ~10° to 20° Brix. The clusters were strictly sampled from the basal insertions of three central shoots on the fruit cane. The analyzed clusters were cut directly at the connection with the shoot and stored at 5 °C until use.

## Investigated sub-traits

In total, data for 19 sub-traits of cluster architecture (Table 1) collected for at least two growing seasons entered this study. During the seasons of 2013 and 2014 pilot studies generated data for 12 and 8 CA traits, respectively. In the seasons of 2015 and 2016, data collection covered 16 sub-traits. Measurements assessed 3 to 12 biological replications per genotype and season. Pedicel measurements encompassed

at least 60 pedicels per genotype. Cluster compactness was evaluated according to OIV204 descriptor in five classes (i.e., 1, 3, 5, 7 and 9) from grade 1 = very loose to grade 9 = very dense. A panel of four trained experts did an independent OIV204 rating to reduce the impact of subjectivity. Subsequently, the mode value of the four ratings was used. Image-based Berry Analysis Tool (BAT) generated data on berry volume and berry number according to the description in Kicherer et al. (2013). The BAT segmentation algorithm, trained with destemmed berries in BBCH79 condition as ground truth data, is able to recognize berries when presented on a standardized picture. Once the berries are individually identified, the number and the size of berries are estimated. In addition, all pictures were personally inspected and manually interpreted if the automatic assessment was not plausible. The length measurements of rachis-related sub-traits were determined using ImageJ (Schneider et al. 2012). Pictures of the rachis were taken together with a size standard to transform the pixel-based image data into SI-unit-based length values. The size standard was measured using the “straight line tool”, and the cluster architecture was measured using the “segmented line tool”. The peduncle length was measured from the cutting edge to the insertion of a wing or tendril, respectively. The wing length was measured from its insertion to the point where the pedicels separate. The rachis length was measured from the first lateral insertion to the end of the spike without the terminal pedicel. Laterals were measured from their insertion at the main rachis without the terminal pedicel. Rachis internodes were measured from the middle of the flanking nodes. Rachis diameter was measured in the middle of the second internode. Pedicels were measured from dyad or triad junctions to the contact surface where the berries have been removed. Gravimetric measurements were taken using an electronic balance, with deviance = 0.1 g (EMB 3000-1 KERN & SOHN GmbH, Balingen, Germany). °Brix measurements used an electronic refractometer (DWN2 Risun, Beijing, China).

## Statistics

Statistical analyses applied R software, version 3.4.1 (R Core Team 2017), and various packages as described below. The significance level of measurement results was set at  $p < 0.05$  as obtained by one-way ANOVA, if not stated otherwise. Data quality and model assumptions were checked by inspecting normal Q–Q plots, density distributions and scatter plots.

Measures of 16 cluster architecture sub-traits recorded in 2015 ( $n = 851$ ) and 2016 ( $n = 896$ ) at vineyard 2 (Table 1) were analyzed by: (i) correlation analysis between cluster architecture traits, (ii) principle component analysis (PCA) to reflect the influence of flower sex (FS) and growing

**Table 1** Overview of the measurements and sampling used in this work

No	Sub-trait (unit)	Notation	2013	2014	2015	2016	2017	Overall (n = 1747) mean <sup>a</sup> (SD)	2015 (n = 851)	2016 (n = 896)	Female 2015 (n = 262)	Hermaphrodite 2015 (n = 589)	Female 2016 (n = 278)	Hermaphrodite 2016 (n = 618)
1	Berry number per bunch	BN	x	x	x	x	x	185.2 (87.0)	174.0 (83.1)	195.8 (89.4)	138.6 (78.3)	189.7 (80.3)	180.1 (90.0)	202.9 (88.3)
2	Sugar content of juice (°Brix)	BRX	x	x	x	x	x	68.5 (11.5)	71.0 (11.0)	66.1 (11.4)	75.4 (10.3)	69.0 (10.8)	67.5 (11.3)	65.4 (11.4)
3	Berry weight (g)	BW	x	x	x	x	x	261.7 (131.1)	228.4 (109.6)	293.3 (141.6)	191.8 (104.6)	244.7 (108.0)	271.6 (139.3)	303.0 (141.6)
4	Berry weight/rachis weight	BW/RW	x	x	x	x	x	22.8 (8.9)	20.9 (7.0)	24.7 (10.1)	17.5 (6.5)	22.4 (6.8)	20.7 (8.5)	26.4 (10.3)
5	Cluster weight (g)	CW	x	x	x	x	x	273.6 (134.7)	239.6 (113.0)	305.8 (145.3)	203.1 (108.7)	255.8 (111.2)	285.3 (143.6)	315.1 (145.2)
6	Mean single berry volume (cm <sup>3</sup> )	MBV	x	x	x	x	x	0.93 (0.57)	0.49 (0.39)	1.34 (0.37)	0.45 (0.37)	0.51 (0.39)	<b>1.33 (0.43)</b>	<b>1.35 (0.35)</b>
7	Compactness	OIV204	x	x	x	x	x	3.84 (1.79)	3.36 (1.68)	4.30 (1.76)	2.18 (1.27)	3.88 (1.58)	3.44 (1.45)	4.69 (1.75)
8	Pedical length (cm)	PED	x	x	x	x	x	0.53 (0.08)	0.51 (0.08)	0.54 (0.08)	0.50 (0.08)	0.52 (0.08)	0.52 (0.08)	0.55 (0.08)
9	Peduncle length (cm)	PL	x	x	x	x	x	2.24 (1.01)	2.15 (1.00)	2.31 (1.00)	2.39 (1.08)	2.05 (0.95)	2.49 (1.08)	2.23 (0.96)
10	Length of first internode of rachis (cm)	L1I	x	x	x	x	x	13.7 (6.4)	14.0 (6.4)	13.3 (6.5)	14.9 (6.7)	13.6 (6.2)	14.4 (6.5)	12.8 (6.4)
11	Length of second internode of rachis (cm)	L2I	x	x	x	x	x	11.9 (5.4)	11.5 (5.4)	12.3 (5.3)	<b>12.0 (6.1)</b>	<b>11.3 (5.1)</b>	13.1 (5.6)	11.9 (5.1)
12	Length of third internode of rachis (cm)	L3I	x	x	x	x	x	-	-	10.61 (2.50)	-	-	11.12 (2.40)	10.39 (2.52)
13	Diameter of second internode of rachis (cm)	RD	x	x	x	x	x	0.45 (0.09)	<b>0.45 (0.08)</b>	<b>0.45 (0.10)</b>	0.48 (0.09)	0.44 (0.08)	0.49 (0.10)	0.43 (0.09)
14	Rachis length (cm)	RL	x	x	x	x	x	15.9 (3.8)	15.3 (3.5)	16.5 (3.9)	16.7 (4.0)	14.7 (3.1)	17.9 (4.3)	15.8 (3.5)
15	Rachis weight	RW	x	x	x	x	x	11.9 (5.3)	11.2 (4.8)	12.6 (5.8)	<b>11.3 (5.6)</b>	<b>11.1 (4.3)</b>	13.7 (6.5)	12.0 (5.3)
16	Shoulder length	SL	x	x	x	x	x	10.6 (3.8)	9.4 (3.5)	11.7 (3.7)	10.5 (4.2)	9.0 (3.1)	12.6 (3.8)	11.3 (3.6)
17	Total berry volume	TBV	x	x	x	x	x	176.6 (140.5)	91.1 (96.3)	257.8 (127.1)	63.8 (70.2)	103.2 (103.6)	234.0 (124.8)	268.5 (126.7)
18	Total length of laterals	TLL	x	x	x	x	x	-	-	23.34 (7.07)	-	-	24.94 (6.96)	22.18 (6.99)
19	Presence/absence of a “shoulder”	Wing	x	x	x	x	x	-	-	-	-	-	-	-

Analyzed sub-traits of cluster architecture and number of assessed growing seasons in a segregating population of 149 F<sub>1</sub> individuals from a GF.GA-47-42 × “Villard Blanc” cross during the growing seasons 2013 to 2017. Mean and in brackets standard deviation of sub-traits are given for the measurements records of 2015 and 2016, and for each combination between flower sex of the genotypes and growing season. In bold, sub-traits which do not differ ( $p < 0.05$ ) in mean values between groups (2015 vs. 2016, female vs. hermaphrodite in 2015 and 2016, respectively) <sup>a</sup>Pearson’s Chi-square test was used to test whether the ordinal OIV204 differed across groups. A Welch test was used for continuous data to compare means of sub-traits between groups

season on the cluster architecture traits and (iii) random forest models and cumulative link models to assess the effect and relative importance of cluster architecture traits on visual compactness. Some genotypes did exhibit some missing data for different reasons: In 2015 for example, berry rot caused 37% missing data for “total berry volume” and “mean berry volume” and in 2016, “shoulder length” could not be recorded in 13% of the data since not all of the progeny plants produced a shoulder in each cluster. However, overall, the amount of missing values was less than 5%. Since the presence of missing data does not allow the comparison of statistical models with the “Akaike information criterion” (AIC), multiple imputations using chained equations were calculated with the R-package “mice” (van Buuren and Groothuis-Oudshoorn 2011). The averaged results of five imputations were used after visual comparison of the density distributions and the range of original and implemented data. Since metric data and ordinal data, i.e., measurements of rachis architecture sub-traits and the ordinal OIV204 descriptor scores for cluster compactness, were considered in this work, Kendall’s  $\tau_b$  correlation coefficient was used to perform a correlation analysis using the R-package “cormat” (Kassambara 2017) (Online Resource 2). A principle component analysis based on covariance was applied to the scaled cluster architecture traits of 2015 and 2016 using the R-packages “factoMineR” (Lê et al. 2008) and “factoextra” (Kassambara 2017). Only variables with a Kendall’s  $\tau_b$  correlation coefficient  $< 0.8$  were used (Online Resource 2). To assess whether the data contain any inherent grouping structure with respect to flower sex (FS) and growing season (2015 and 2016) the clustering tendencies in the PCA scores were statistically evaluated by computing the Hopkins statistics ( $H_o$ ) with the R-package “clustertend” (Han et al. 2012).  $H_o > 0.5$  would indicate a significant cluster within a dataset (Han et al. 2012).

Random forest (RF) models and cumulative link models (CLMs) with scaled data assessed the effect and the relative importance of 15 cluster architecture traits measured in 2015 and 2016 (Table 1). Additionally, the effect of flower sex and year on OIV204 ranking was assessed. The random forests were established for an ordinal response (OIV204 descriptor) using the function “cforest” of the R-package “party” (Hothorn et al. 2006; Strobl et al. 2007, 2008). It utilizes the commonly applied random forest method introduced by Breiman (2001) (for a recent overview of the methodology, see Boulesteix et al. 2012). Prediction accuracy measurement for response levels with uniform distances was performed with ranked probability scores (RPS), appropriate for ordinal response variables, as described in Janitzka et al. (2016). Variable importance measurements (VIMs) for RF were performed with RPS-based VIMs. Hence, the incorporated ordering information, contained in the ordinal responsive variable, was respected in the VIM calculation,

i.e., the accelerating compactness in five classes from 1 to 9. To further study the model performance, RF calculations were repeated four times, using error rate (ER), mean standard error (MSE), mean absolute error (MAE) and RPS to compare the prediction accuracy contained in the VIM results. Cumulative link models for ordinal response were fitted with the same explanatory variables as in random forest using the R-package “ordinal” (Christensen 2018). The model selection was performed in a two-step procedure (due to processing time) and based on an information-theoretic approach (Burnham and Anderson 2002) using the R-package “glmulti” (Calcagno and de Mazancourt 2010). In a first step, various candidate models with up to eight different main terms were fitted and compared using the “Akaike information criterion” (AIC) (Burnham and Anderson 2002), where a lower AIC indicates a better fit. All variables with a model-averaged importance of  $> 0.75$  were used in a second step to fit candidate models with main terms and two-way interactions, which were compared via AIC as above. The models within a range of  $\Delta AIC < 2$  were used for interpretation of effects. The relative importance of explanatory variables was then assessed by fitting models where each explanatory variable was removed at a time and calculating the  $\Delta AIC$  relative to the best model. The more the  $\Delta AIC$  rises, the more important is the variable that was removed from the model. The overall error rate and rank-wise error rate indicated the prediction quality of a CLM. In order to assess the collinearity between the predictor variables of the best models we calculated the variance inflation factors (VIFs) with the R-package “car” using the function “vif” (Fox and Monette 1992).

## Genetic evaluation

As described in Zyprian et al. (2016) a genetic map has been established based on 546 molecular markers. This map and the corresponding parental maps provided the basis in this work for the identification of QTLs related to the sub-traits of cluster architecture.

## Quantitative trait locus analysis

Quantitative trait locus (QTL) analysis applied the software tool MapQTL6.0 (van Ooijen 2009). The determination of segregation of trait-linked markers and QTL detection used the interval mapping (IM) procedure with a mapping step size of 1 cM. Based on a permutation test with 1000 iterations a linkage group-specific “logarithm of the odds” (LOD) threshold was calculated (with  $p < 0.05$ ). Additionally, an IM with flower sex as co-variable was computed. Regions that exceeded the LG-wide LOD threshold were recorded as QTL. This work considered QTLs that have been: (i) reproduced at least three times; or (ii) reproduced two times, but were

physically co-located to other QTLs for two seasons and were found accumulated with overlapping confidence intervals on the reference genome; or (iii) identified in other crosses than in  $G \times V$  according to literature references (Correa et al. 2014; Marguerit et al. 2009). For each QTL, the maximum LOD score, the percentage of explained phenotypic variation and the extension of the confidence intervals (in cM) are recorded.

The molecular markers in direct neighborhood to the  $LOD_{max} - 1$  positions delimited the confidence intervals. These flanking markers were used to project the QTL regions on the grapevine reference genome of (PN40024)12x V2 (Canaguier et al. 2017) as retrieved from <https://urgi.versailles.inra.fr/Species/Vitis/Data-Sequences/Genome-sequences>. The physical position of proximate confidence intervals assessed the accumulation of cluster architecture-linked QTLs.

### Gene set enrichment analyses

The projection of confidence intervals for cluster architecture QTLs on the physical regions of the reference genome (PN40024) 12x V2 delimits gene sets that were statistically associated with cluster architecture-related traits. Genes contained in these confidence intervals were transferred to the protein classification system (PANTHER) via the gene ontology consortium online platform (Ashburner et al. 2000; The Gene Ontology Consortium 2017) available at <http://geneontology.org/>. The redundancy of annotated biological functions assigned to the genes within these confidence intervals was then compared to the redundancy of biological functions in the total set of genes of the reference genome. Significantly overrepresented or underrepresented ( $p < 0.05$  Fisher's exact with FDR multiple test correction) gene ontology (GO) terms were assessed using PANTHER, version 13.1, as described in Mi et al. (2017). The enriched GO term was used to prioritize the search for candidate genes from multiple QTLs.

### Weather records

Climate data were acquired in approx. 500 m distance to the trial fields with the records of the meteorological station 88 Siebeldingen type AME 16, 192 m sea level, longitude 8.047925770315487, and latitude 49.216499765308136. Data were downloaded from <http://www.am.rlp.de>.

## Results

### Evaluation of cluster compactness according to descriptor OIV204

The parental varieties of the  $G \times V$  population were rated for their cluster density according to OIV descriptor 204

during the three seasons from 2015 to 2017. The maternal genotype GF.GA-47-42 showed a loose cluster architecture (mode for OIV204 = 3). The paternal type of the population, "Villard Blanc", showed a very loose (mode for OIV204 = 1) cluster structure. The OIV204 scorings of the  $F_1$  individuals of the  $G \times V$  population covered all classes from 1 = very loose (Fig. 1a) to 9 = very compact (Fig. 1b). The  $F_1$  progeny showed a mode value for OIV204 between 3 and 5 in the years 2013, 2015, 2016 and 2017. In 2015 the probability for a lower OIV204 score was significantly higher ( $p > 0.001$  Pearson's Chi-square test) as compared to 2016 (Fig. 1c). In addition, genotypes with female flowers showed significantly smaller OIV204 scores ( $p < 0.001$ ; Pearson's Chi-square test) during consecutive seasons (Fig. 1c).

### Cluster architecture sub-traits and their correlation

All CA sub-traits and corresponding notations are presented in Table 1. Correlation analysis (Online Resource 2) indicated the highest correlation for the CA sub-traits cluster weight and berry weight ( $\tau_{-b} = 1$ ). OIV204 and berry traits were in general slightly positively correlated ( $\tau_{-b} = 0.1 - 0.4$ ), while rachis traits were slightly negatively correlated to OIV204 ( $\tau_{-b} = -0.1 - 0.2$ ) in 2015 and 2016. The correlation of berry weight/rachis weight with OIV204 was positive ( $\tau_{-b} = 0.3$  and  $0.4$ ) during the two consecutive years. The correlation among the various rachis sub-traits was found less pronounced ( $-0.1$  to  $0.5$ ), but stable over the 2 years. Quite in contrast, the correlation among berry traits varied between years. In 2015, the correlation between total berry volume and berry number or mean berry volume was  $\tau_{-b} = 0.4$  and  $0.7$ , while in 2016, it was  $\tau_{-b} = 0.7$  and  $0.3$ . Hence, total berry volume appeared to be determined by the components berry number and single berry volume in a contrasting way in the 2 years. The correlation between the cluster architecture sub-traits that determine OIV204 (i.e., rachis length, shoulder length, cluster weight, berry number, mean berry volume and pedicel length, see below) was generally weak and ranged between  $\tau_{-b}$  0.0 and 0.3, with the exception of cluster weight and berry number ( $\tau_{-b} = 0.6$ ) in 2015 and 2016 and RL and SL ( $\tau_{-b} = 0.5$ ) in 2016 (Online Resource 2).

### Identification of major components of cluster architecture and influence of flower sex

The OIV204 scores showed some influence of flower sex, indicating a shift toward higher OIV204 scores in the hermaphrodite vs. female genotypes (Fig. 1c). Therefore, a PCA was applied to the measurements of the 15 sub-traits recorded in 2015 and 2016. The PCA identified five main components that explained 69% of the variation in the data. Principal component 1 (PC1) and principal component 2

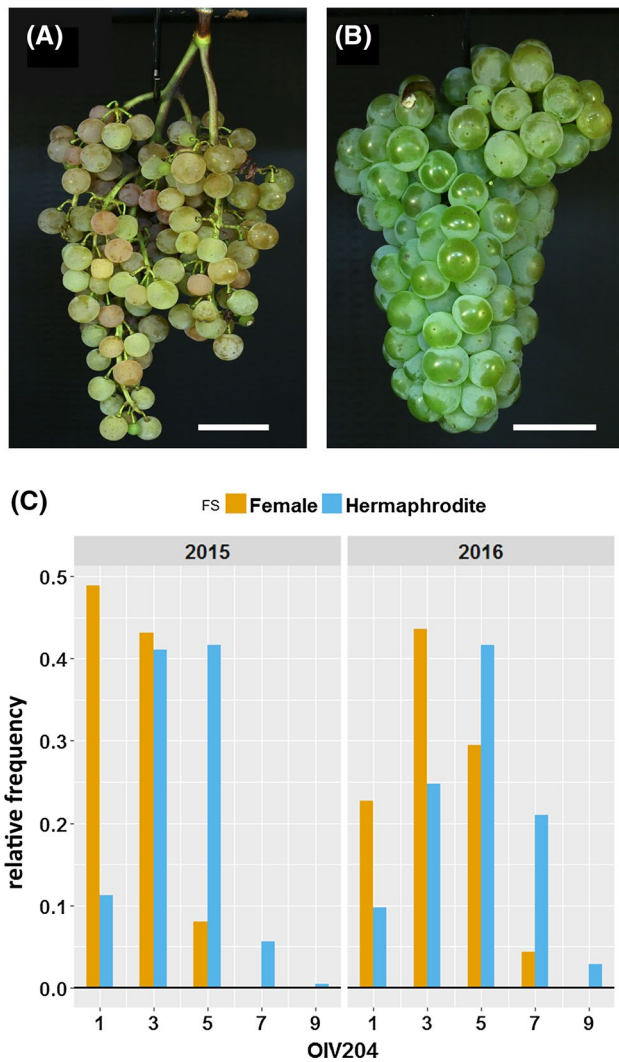


**Fig. 1** Variation of cluster architecture in the cross-population GF.GA-47-42 × “Villard Blanc” during two seasons and between the flowering types female and hermaphrodite. The OIV descriptor 204 for compactness scores from **a** 1 = very loose, where rachis and pedicels are visible, to **b** 9 = very compact, where berries are non-circularly deformed (scale bar = 35 mm). **c** Histogram showing the relative frequency (density) of OIV204 scorings in 46 female and 103 hermaphroditic  $F_1$  genotypes from the GF.GA-47-42 × “Villard Blanc” cross measured at BBCH85 in 2015 and 2016

(PC2) explained 47% of the variation. PC1 was associated with berry features cluster weight, total berry volume, berry number and the rachis features rachis weight and shoulder length (Fig. 2). The contribution to PC1 was as follows: cluster weight (18.5%), total berry volume (17.3%), berry number (15.2%), rachis weight (13.7%) and shoulder length (7.0%). PC2 was positively associated with rachis traits with a contribution of rachis length (17.7%), rachis diameter (14.2%), shoulder length (10.6%) and rachis weight (7.9%). PC2 was negatively related to the ratio of berry weight to rachis weight (20.1%) and the OIV204 score

(10.9%) (Fig. 2). PCA scores displayed a pattern depending on flower sex and year. PC1 displayed higher scores for the year 2016 vs. 2015, indicating higher berry weight and volume in 2016. PC2 displayed higher scores for female genotypes, indicating elongated rachis sub-traits. However, the separation of the concentration ellipses of the PCA scores was moderate as indicated by  $H_o$  of 0.13.

### Identification of cluster architecture sub-traits that predict cluster compactness

The sub-traits (aligned according to their relevance for cluster architecture) pedicel length < rachis weight < mean berry volume < berry weight/rachis weight < shoulder length < berry number < flower sex < total berry volume < rachis length < cluster weight are important variables that predict OIV204 according to random forest (Table 2). The application of the four different prediction accuracy estimates ER, MSE, MAE and PRS for the VIM calculation showed no influence on the importance rank order (Online Resource 3).

CLMs for the prediction of OIV204 showed that the sub-traits pedicel length < shoulder length < berry number < rachis length < cluster weight had the largest impacts (in ascending order) on compactness levels (OIV204 values) of the 149  $F_1$  genotypes of the cross-population when the season was included as predictor variable (Table 2). MBV was an important predictor variable, when the variable season was not included. The collinearity of the predictor variables in the selected models was quite low. The variance inflation factor values ranged between 1.09 for pedicel length and 3.38 for cluster weight. All sub-traits that reflect berry features were positively related to compactness, while all sub-traits measuring rachis features showed negative relationship to OIV204 scores (Online Resource 4). Genotypes with female flower organs and samples from 2015 showed a higher probability to be loosely clustered as compared to samples from 2016 and hermaphroditic flowered genotypes, respectively (Online Resource 4). The interaction between berry number and cluster weight was a predictor in CLMs regardless of whether season was in the model (Table 2). The overall error rate was 0.42 and 0.44 for the CLMs without and with season as additional predictor variable. A comparison of the error rates across OIV204 categories showed that the prediction accuracy for class three and five (loose to medium cluster architecture) was considerably higher than for the compact levels (Online Resource 5). The majority of the genotypes (over 70%) were member of these two classes (3 and 5), where the ER was 0.39 and 0.32, respectively.

According to the random forest VIM results berry weight/rachis weight and total berry volume were important sub-traits for cluster compactness, but were not included in the CLMs as predictor variable. Due to these inconsistencies,

**Fig. 2** Principal component analysis of cluster architecture sub-traits recorded in 2015 and 2016. The biplot shows the first principal component (PC1) where berry sub-traits are dominant contributors and the second principal component (PC2) representing mainly rachis sub-traits. The scaled cluster architecture trait values of the principal components 1 and 2 display 47% of the total variance. Concentration ellipses indicate the location of 95% of the data. **a** Separated by the year (growing season). **b** Separated by flower sex. For notation of sub-traits see Table 1

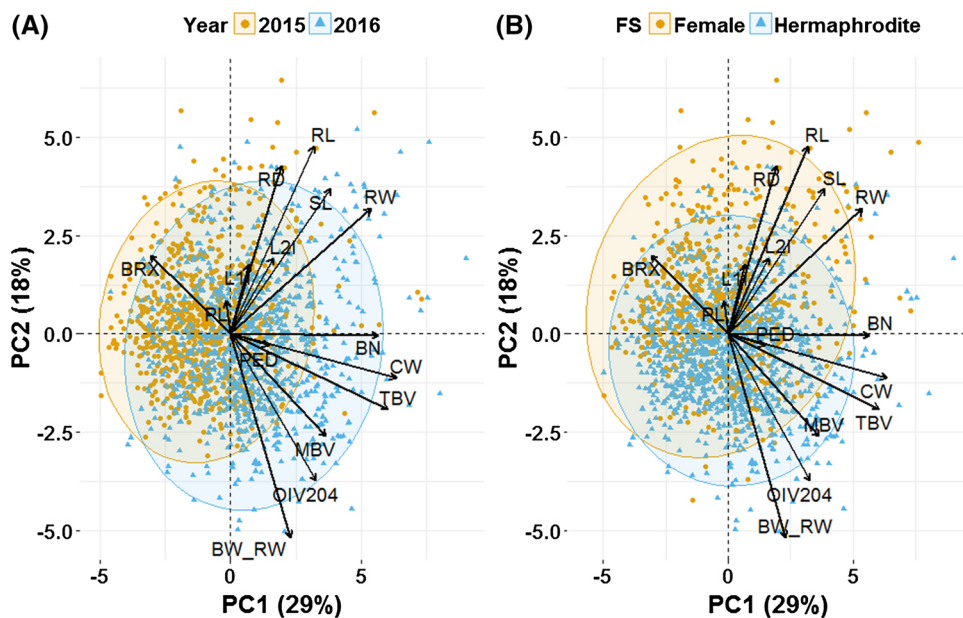


**Table 2** Importance of cluster architecture sub-traits for the OIV204 compactness descriptor using random forest and cumulative link models. For sub-trait abbreviations see Table 1

Dataset	15/16 –season	15/16 +season	15/16 –season	15/16 +season	15/16 –season	15/16 +season
Model type	RF <sup>a</sup>	RF	CLM-full <sup>b</sup>	CLM-full	CLM-red <sup>c</sup>	CLM-red
Measure	RPS-VIM <sup>d</sup>	RPS-VIM	$\Delta$ -AIC <sup>e</sup>	$\Delta$ -AIC	$\Delta$ -AIC	$\Delta$ -AIC
Season	–	<b>0.014</b>	–	<b>157.6</b>	–	<b>156.6</b>
FS	<b>0.037</b>	<b>0.036</b>	<b>99.6</b>	<b>98.9</b>	<b>84.6</b>	<b>82.9</b>
BN	<b>0.021</b>	<b>0.025</b>	<b>50.8</b>	<b>27.1</b>	<b>61.7</b>	<b>46.5</b>
BW_RW	0.014	0.016	–	–	–	–
CW	<b>0.073</b>	<b>0.074</b>	<b>114.5</b>	<b>137.1</b>	<b>135.6</b>	<b>236.9</b>
LII	0.001	0.001	–	–	–	–
L2I	0.001	0.001	–	–	–	–
MBV	<b>0.011</b>	0.009	<b>98</b>	–	<b>93.6</b>	–
PED	<b>0.006</b>	<b>0.006</b>	<b>8.4</b>	<b>13.2</b>	<b>10.7</b>	<b>13.8</b>
PL	0.002	0.002	–	–	–	–
RD	0.004	0.003	9.6	–	–	–
RL	<b>0.058</b>	<b>0.057</b>	<b>135</b>	<b>143.3</b>	<b>125.5</b>	<b>132.3</b>
RW	0.008	0.009	–	11.5	–	–
SL	<b>0.013</b>	<b>0.017</b>	<b>20</b>	<b>51.9</b>	<b>22.3</b>	<b>46.1</b>
TBV	0.056	0.05	–	–	–	–
BN:CW	–	–	–	–	33	42.5

Predictor variables in bold confirm the high importance in random forest and cumulative link models. The modeling was performed without (–season) or with season as explanatory variable (+season)

<sup>a</sup>Random forest for ordinal response produced with the “cforest” function of the R-package “party”; <sup>b</sup>cumulative link models for ordinal response using all predictor variables with the R-package ordinal; <sup>c</sup>cumulative link models with trait–trait interaction for ordinal response using predictor variables with a model-averaged importance value > 0.75 as determined in b; <sup>d</sup>ranked probability score prediction accuracy used for variable importance measurements; <sup>e</sup>delta AIC, when the predictor was removed from the model. For further details see text

the sub-traits total berry volume and berry weight/rachis weight were not considered for further analysis. The sub-traits rachis diameter and rachis weight contributed weakly and inconsistently to CLMs when main effects only were

fitted, but were not important when interactions were fitted. Interestingly, the sub-traits length of the first lateral, length of the second lateral and peduncle length were of minor importance.

## QTL detection

Mean values of the cluster architecture sub-traits measurements recorded in the years 2013 to 2017 were applied for QTL analysis using interval mapping (IM) on the genetic constitutions of 149  $F_1$  individuals and the consensus map of  $G \times V$  (Zyprian et al. 2016).

IM detected 24 QTLs for CA sub-traits reproducibly (Online Resource 6). These QTLs were found on the following 10 linkage groups (LGs):  $LG_1$  (pedicel length a, pedicel length b, rachis weight, peduncle length, total berry volume),  $LG_2$  (cluster weight, rachis length, shoulder length, OIV204),  $LG_3$  (mean berry volume, shoulder length, rachis length),  $LG_{10}$  (cluster weight, berry number),  $LG_{11}$  (pedicel length),  $LG_{12}$  (cluster weight, mean berry volume),  $LG_{14}$  (peduncle length),  $LG_{15}$  (OIV204),  $LG_{17}$  (mean berry volume, cluster weight, OIV204) and  $LG_{18}$  (cluster weight, pedicel length).

With respect to the presence of 45 female and 106 hermaphroditic individuals in the population, flower sex was used as a co-variable in an explorative additional calculation of “IM + FS.” This approach yielded six additional QTLs on  $LG_3$  (pedicel length),  $LG_{10}$  (berry number, berry weight),  $LG_{14}$  (wing),  $LG_{17}$  (berry number) and  $LG_{18}$  (berry number) cluster architecture traits (Online Resource 6). Remarkably, three QTLs for berry number and one for berry weight were identified newly by application of flower sex as a co-factor for IM. Furthermore, a QTL for cluster complexity, i.e., the presence/absence of a shoulder at the cluster, was reproduced using flower sex as co-factor in an IM. In total, 30 QTLs for traits related to CA were reproducibly detected over two to four seasons (Online Resource 6).

The QTLs identified by IM and IM + co-variable (flower sex) showed no significant differences for the average  $LOD_{max}$  values, the size of the average confidence interval (CI) and the explained phenotypic variance (Online Resource 7). The sub-traits rachis length, mean berry volume, berry number, cluster weight and pedicel length show high contribution to cluster density (Table 2). QTLs for these important traits were reproducible over three seasons (Table 3). For the sub-trait shoulder length, also statistically important, QTLs were reproducible over two seasons. Notably, the QTL found on  $LG_2$  for shoulder length was linked for two seasons with the same  $LOD_{max}$  marker (VVIB23\_312) than the one found for rachis length (Table 3). The major QTL for OIV204 cluster compactness was identified on  $LG_2$  in the vicinity of marker GF02-12 with an average impact explaining 20% of the variance of the OIV204 scores and  $LOD_{max}$  of 11.07. For berry-related sub-traits the average maximum explained variance (15%) was found with a QTL on  $LG_{10}$  for berry weight associated with marker VRZAG7. The major QTL for rachis-related sub-traits was found on  $LG_1$  for peduncle length correlated

to the SNP marker 55553gene\_1\_GF\_WRKY. This QTL explains on average 24% of the phenotypic variance and had a  $LOD_{max}$  value of 10.79 (Online Resource 6).

## Relevant QTLs accumulate in eight clusters

Based upon the multivariate statistical analysis of the CA data described above, the rachis features (rachis length, shoulder length and pedicel length) and specific berry sub-traits (cluster weight, berry number, mean berry volume) showed high impact on OIV204. For these traits of prominent importance, 19 QTLs were detected reproducibly. In addition, four QTLs for compactness according to OIV204 scores were identified. The major QTLs were found on  $LG_2$  (rachis length, cluster weight),  $LG_3$  (rachis length),  $LG_{11}$  (pedicel length),  $LG_{17}$  (mean berry number) and  $LG_{18}$  (berry number). On average, the QTLs for these traits explained approximately 14% of the total variance (ranging from 11 to 18%) (Table 3 and Online Resource 6). Beside the QTL for pedicel length on  $LG_{11}$ , correlated to marker VMC6C3, all other high-impact QTLs were co-located in groups with two to four different QTLs for CA sub-traits. To facilitate the application of these new findings in marker-assisted grapevine breeding, these QTLs were analyzed to check whether they are spatially concentrated in a specific region of a chromosome. To this purpose the confidence intervals (positions of  $LOD_{max} - 1$ ) of the 23 QTLs were projected on the reference genome from PN40024 12x v2 (Canaguier et al. 2017) and screened for overlaps. This approach identified eight genomic regions where QTLs of cluster architecture shared the same stretch of genomic sequence as confidence interval. Twenty QTLs were co-located in reference to the PN40024 sequence (Table 4). These eight clusters cover all major QTLs for architecture sub-traits with high impact on compactness and explain 87% of the variance.

## Gene set enrichment analyses

The genomic regions of the eight QTL clusters for sub-traits of cluster architecture enclose 3691 annotated genes. Using gene ontology categories related to biological processes for a GO term enrichment analysis, 3462 of the genes (93.8%) could be successfully assigned to a category. 229 genes could not be mapped to the protein database. Significant GO term enrichments were found in all confidence interval-associated gene subsets except in the cluster on  $LG_2$ . Reducing the gene subset on  $LG_2$  to genes enclosed in the central 2 Mb range of the confidence interval showed that the GO term “regulation of microtubule-based process” was 50 times overrepresented in this region. *VIT\_202s0025g04960* was one of the GO-term-associated genes. It encodes a cell-cycle-regulated microtubule-associated protein. Moreover, this approach revealed 45 overrepresented GO terms in

**Table 3** Important results of QTL analysis

Calculation method <sup>a</sup>	LG <sup>b</sup>	Trait/season <sup>c</sup>	LOD <sub>max</sub> position <sup>d</sup> (cM)	LOD value <sup>e</sup>	% Explained phenotypic variance <sup>f</sup>	Marker name
IM	2	OIV204_15	13.003	11.07	29	GF02_12_170
IM	2	OIV204_16	13.003	5.32	15.2	GF02_12_170
IM	2	OIV204_17	13.003	6.65	18.6	GF02_12_170
IM	2	RL_14	12.027	3.07	9.3	VVIB23_312
IM	2	RL_15	12.027	4.09	12.4	VVIB23_312
IM	2	RL_16	12.027	3.98	11.6	VVIB23_312
IM	2	SL_15	12.027	2.64	8.1	VVIB23_312
IM	2	SL_16	12.027	2.93	8.6	VVIB23_312
IM+FS	10	BN_14	69.861	3.47	10.1	VRZAG7_106
IM+FS	10	BN_15	69.861	3.09	8.9	VRZAG7_106
IM+FS	10	BN_16	69.861	6.27	17.4	VRZAG7_106
IM	10	CW_14	69.861	2.96	8.9	VRZAG7_106
IM	10	CW_15	69.861	5.03	14.4	VRZAG7_106
IM	10	CW_16	69.861	4.02	11.8	VRZAG7_106
IM	11	PED_13	3	7.64	23.6	VMC6C3
IM	11	PED_14	0	5.06	14.8	VMC6C3
IM	11	PED_15	3	6.57	19.1	VMC6C3
IM	11	PED_16	0	5.49	15.6	VMC6C3
IM	17	MBV_14	27.514	5.03	14.9	VRZAG15
IM	17	MBV_15	27.514	5.92	17	VRZAG15
IM	17	MBV_16	27.514	4.68	13.6	VRZAG15

Main QTLs for compactness and for major cluster architecture sub-traits in 149 F1 individuals of the segregating population of the cross GF.GA-47-42 × “Villard Blanc” calculated with interval mapping (IM) and interval mapping with flower sex as co-factor (FS)

<sup>a</sup>QTL calculation method: interval mapping (IM) or interval mapping using flower sex as co-variable (IM+FS); <sup>b</sup>position on linkage group (LG); <sup>c</sup>trait and season for calculated QTL; <sup>d</sup>genetic position of the LOD<sub>max</sub> marker in centimorgan (cM) on the consensus map (Zyprian et al. 2016); <sup>e</sup>logarithm of the odds value (LOD); <sup>f</sup>percentage of explained phenotypic variance

the gene subsets when compared to the GO annotations of all genes in the reference genome, including the category “response to auxin.” The terms “ion transport,” “anion transport” and “response to endogenous stimulus” were overrepresented in two clusters. In total, 219 genes (Online Resource 8) were assigned to at least one of the significantly overrepresented GO classes ( $p < 0.05$  Fisher’s exact test).

## Discussion

### The segregating population

A population segregating for the trait of interest and a linkage map for this population are prerequisite for QTL analysis. The genetic map of the G × V population used here has been elaborated earlier and was already successfully applied to detect QTLs affecting resistance to pathogens and ripening traits of grapevines (Zyprian et al. 2016).

The loose cluster architecture (CA) inherent to the parent GF.GA-47-42 (G; OIV204 = 3) and the very loose CA of the parent “Villard Blanc” (V; OIV204 = 1) suggested that the G × V population could segregate for CA. Indeed, the F<sub>1</sub> genotypes exhibited variable and even transgressive phenotypes, showing OIV 204 density scores from very loose (1) to very dense (9). The paternal grandparent variety Seibel 6468 showed significantly lower rachis length and a higher mean berry volume in comparison with the parental varieties (data not shown). This could be used for a genetic determination of the transgressive phenotypes. The field plantation of the population was established in 2000 and in a multiplied form in 2010. The phyllotaxic phase shift inherent to grapevine development from juvenile to adult plants was completed at the time of investigation. Therefore, any phenotypic bias due to juvenile anomalism was avoided. The CA segregation pattern could be verified for consecutive seasons and thus was exploited for the detection of reproducible QTLs associated with CA.

**Table 4** Physical position of markers related to the maximum LOD value of QTLs for cluster architecture traits and their physical confidence interval region on the reference genome PN40024 (12x) V2

QTL cluster		QTLs in V × B			Physical position on PN40024 12X V2 (bp)		
LG	QTL cluster/traits in cluster	Calculation method	Trait/season	Marker name	LOD <sub>max</sub> marker	Confidence interval upper limit	Confidence interval lower limit
1	CL_1 OIV204 + PEDa	IM	OIV204_16	SNP1241_207FEM	12.608.167	10.569.689	19.375.466
		IM	OIV204_17	SNP1241_207FEM	12.608.167	10.569.689	19.375.466
		IM	PED_14	SNP1241_207FEM	12.608.167	5.948.674	19.375.466
		IM	PED_15	SNP1241_207FEM	12.608.167	5.948.674	19.375.466
2	CL_2 RL + SL + CW + OIV204	IM	RL_14	VVIB23_312	4.807.391	2.068.206	5.632.401
		IM	RL_15	VVIB23_312	4.807.391	2.068.206	5.632.401
		IM	RL_16	VVIB23_312	4.807.391	2.068.206	5.000.200
		IM	SL_15	VVIB23_312	4.807.391	2.068.206	8.335.117
		IM	SL_16	VVIB23_312	4.807.391	2.068.206	5.632.401
		IM	CW_13	GF02_12_170	5.012.979	2.068.206	4.993.382
		IM	CW_14	GF02_12_170	5.012.979	2.068.206	5.632.401
		IM	OIV204_15	GF02_12_170	5.012.979	4.807.391	5.084.681
		IM	OIV204_16	GF02_12_170	5.012.979	2.068.206	5.000.200
		IM	OIV204_17	GF02_12_170	5.012.979	2.068.206	5.084.681
3	CL_3.1 PED + MBV	IM	MBV_13	1044J09FFEM	1.900.405	1.900.405	609.887
		IM	MBV_14	1044J09FFEM	1.900.405	1.900.405	609.887
		IM + FS	PED_13	1044J09FFEM	1.900.405	1.900.405	609.887
		IM + FS	PED_15	1044J09FFEM	1.900.405	1.900.405	609.887
		IM + FS	PED_16	1044J09FFEM	1.900.405	1.900.405	609.887
	CL_3.2 SL + RL	IM	SL_15	GF03_07_273	16.500.873	9.542.014	20.541.773
		IM	RL_15	GF03_07_236	16.500.873	9.542.014	20.541.773
		IM	RL_16	GF03_07_236	16.500.873	9.542.014	20.541.773
		IM	SL_16	GF03_07_236	16.500.873	9.542.014	20.541.773
		IM	SL_16	GF03_07_236	16.500.873	9.542.014	20.541.773
10	CL_10 CW + BN	IM	CW_14	VRZAG7_106	23.172.655	21.301.493	23.172.655
		IM	CW_15	VRZAG7_106	23.172.655	21.301.493	23.172.655
		IM	CW_16	VRZAG7_106	23.172.655	16.604.597	23.172.655
		IM + FS	BN_14	VRZAG7_106	23.172.655	21.301.493	23.172.655
		IM + FS	BN_15	VRZAG7_106	23.172.655	9.424.409	23.172.655
		IM + FS	BN_16	VRZAG7_106	23.172.655	21.301.493	23.172.655
12	CL_12 MBV + CW	IM	CW_15	GF12_07	22.414.306	18.369.473	23.795.082
		IM	MBV_13	GF12_09_87	23.246.484	22.414.306	23.795.082
		IM	CW_13	GF12_09_83	23.246.484	23.246.484	23.795.082
		IM	MBV_14	GF12_09_83	23.246.484	18.369.473	23.795.082
		IM	MBV_16	GF12_09_83	23.246.484	20.203.052	23.795.082
		IM	MBV_15	SNP1119_176CMZ	23.795.082	20.203.052	23.795.082
17	CL_17 OIV204 + CW + MBV + BN	IM	MBV_15	SCU_06	3.290.363	38.382	6.588.726
		IM	CW_16	VvEDS1gene_1GF	3.930.996	6.588.726	17.980.880
		IM + FS	BN_16	VvEDS1gene_1GF	3.930.996	8.686.027	9.613.080
		IM	MBV_16	VRZAG15	6.588.726	38.382	8.686.027
		IM	MBV_14	VRZAG15	6.588.726	38.382	8.686.027
		IM	CW_15	VRZAG15	6.588.726	3.290.363	8.686.364
		IM	OIV204_15	EDS1_CF_SNP1837GF	8.686.027	6.588.726	9.613.080
		IM	OIV204_16	EDS1_CF_SNP1837GF	8.686.027	6.588.726	9.613.080
		IM	OIV204_17	EDS1_CF_SNP1837GF	8.686.027	6.588.726	3.930.996
		IM + FS	BN_15	EDS1_CF_SNP1837GF	8.686.027	6.588.726	9.613.080

**Table 4** (continued)

QTL cluster		QTLs in V × B			Physical position on PN40024 12X V2 (bp)		
LG	QTL cluster/traits in cluster	Calculation method	Trait/season	Marker name	LOD <sub>max</sub> marker	Confidence interval upper limit	Confidence interval lower limit
18	CL_18 BN + CW + PED	IM	CW_15	VMC2A3	948.244	948.244	6.487.637
		IM	CW_16	SCU_10	4.520.661	321.045	6.487.637
		IM + FS	BN_16	SCU_10	4.520.661	3.362.208	5.605.673
		IM + FS	BN_15	VV_18_6624520FEM	6.720.583	5.539.873	9.582.805
		IM	PED_14	VMCNG1B09	5.645.610	3.362.208	9.582.805
		IM	PED_15	VMCNG1B09	5.645.610	3.362.208	9.582.805
		IM	PED_16	VMCNG1B09	5.645.610	3.362.208	9.582.805

Note that the confidence intervals of several cluster architecture traits traverse the same physical region on a chromosome

### Stability and interrelationship of cluster architecture sub-traits

The compactness of the cluster is the result of an interaction of multiple cluster architecture sub-traits (Rist et al. 2018; Tello et al. 2015; Correa et al. 2014; Shavrukov et al. 2004). This study used 16 different sub-traits for the statistical evaluation of the individual contribution to cluster compactness in two consecutive growing seasons. The correlation analysis among them showed high variation concerning the intensity and the direction of correlations between individual cluster architecture sub-traits and to the official OIV204 descriptor.

Seasonal conditions had an impact regarding the berry traits, i.e., total berry volume correlated with berry number and mean berry volume but in a divergent manner for the two seasons of 2015 and 2016 (Online Resource 2). To further assess the seasonal impact on the berry sub-traits even the traits with stronger correlation were considered in principal component analysis. Here again the berry-related sub-traits were more affected by the season compared to the rachis-related sub-traits. Climate conditions from budburst to flowering on to harvest affected berry number. However, the weather conditions recorded for this period did not provide evident differences (recorded as monthly average for air and ground temperature or for photoactive radiation) during the first weeks of growth and inflorescence development. Nevertheless, 2016 had 50% more days with rainfall compared to 2015 and therefore provided less favorable conditions for berry set during this time period. However, the berry number in 2016 was higher than in 2015. The Hopkins statistics value for clustering tendency was far below the threshold that would indicate a cluster within the dataset of measured cluster architecture sub-traits. This supports our assumption of a quantitative multiple trait genetic determinism.

### The complexity of cluster architecture

Cluster density (as characterized by OIV descriptor 204) is a highly complex trait since it depends on the interaction of multiple berry and rachis sub-traits. Several previous studies concern the variability of CA sub-traits. Fanizza et al. (2005) reported berry number variation. The average berry size is highly variable from 0.5 to 11.5 cm<sup>3</sup> according to Houel et al. (2013). Shavrukov et al. (2004) highlighted rachis internodes' length as major contributor to CA variation. Gabler et al. (2003) and Sarooshi (1977) reported variation in CA due to elongated pedicels. Complexity of CA, i.e., the presence or absence of a “shoulder” segregated in a cross from table and wine grapes (Marguerit et al. 2009). In addition, the contribution of sub-traits to overall CA appeared to be variable among *Vitis* cultivars (Tello et al. 2015). In agreement with the findings of Migicovsky et al. (2017) this study here showed that there is a negative correlation of sugar content with mean berry volume evident in 2015 and in 2016 data (Online Resource 2 and Fig. 2). Hence, an important step of this work was to determine the sub-traits that substantially contribute to the CA phenotype in the given G × V cross.

### Determination of the most relevant sub-traits to predict cluster architecture

Forests of regression trees and automated multi-model inference using CLMs with the CA dataset predicted the compactness level (OIV204) with CA sub-traits. Explorative, random forest VIM calculations gave an overview of the importance of single sub-traits for OIV204 prediction. The assessment of the prediction accuracy as described in Janitza et al. (2016) using four different prediction performance measures showed no impact on the VIM order (Online Resource 3). Hence, in subsequent CLMs the prediction

accuracy was measured straightforward with the calculation of the error rate. This revealed that the models had a lower error rate if the compactness was lower, i.e., in season 2015, in the group of female phenotypes and the group with loose cluster OIV204 rankings (Online Resource 5). One possibility may be that the subjective visual classification of compactness might be less accurate with increasing levels of compactness which leads to a reduced predictive power of the models.

Nevertheless, within the available CA sub-traits, the best CLMs to predict the OIV204 descriptor consisted of the predictors rachis length, shoulder length, cluster weight, berry number, mean berry volume and pedicel length. Therefore, these traits were of major importance for genetic analysis. Notably, the derived measures berry weight/rachis weight and total berry volume were not included as predictor variables in the best CLMs. Instead, the models used for the ranking of the sub-traits considered original measurements as predictor variables only. The variance inflation factors for the unassembled variables in the obtained best models were quite low (between 1.09 and 3.38). The obtained values were considered to be low enough to assume no bias due to collinearity (Hair et al. 2010). However, expressed as variable importance value based on regression trees or as delta AIC value elaborated with a leave-one-out model comparison, the importance of these sub-traits in the models for compactness was diverse. In this study, rachis length and cluster weight showed the highest impact followed by the total berry volume. Tello et al. (2015) reported rachis length and berry number as highly correlated to OIV204 scorings in a wide range of cultivars over three growing seasons. Tello and Ibáñez (2014) combined up to six sub-traits to form compactness indices. In their work, the indices showing the highest correlations with the visual OIV204 classification contained the sub-traits cluster weight, rachis length, berry number and pedicel lengths (among others). Their findings are supporting our modeling results where the same traits show large effects on ordinal OIV204 values. Among cluster architecture sub-traits with elevated importance for compactness, pedicel length was least important in this study. Nevertheless, it is important enough to be recognized as determining factor for cluster compactness (Table 2). In Tello et al. (2015) the sub-trait pedicel length produced the highest correlation with cluster compactness in one of three seasons. However, the authors found a low relevance of pedicel length to the overall compactness in their study. Although our work in general corresponds to the findings of Tello et al. (2015) the study presented here revealed a higher likelihood for open cluster with longer pedicels (Online Resource 4). Supporting our notion, Gabler et al. (2003) reported that pedicel length showed impact on cluster architecture. The same was found by Sarooshi (1977) after growth regulator treatment. Additionally, on LG1, the

co-localization of QTLs for compactness (OIV204) with QTLs for pedicel length supports the importance of pedicel length for compactness on genetic level (Fig. 3).

In the work of Shavrukov et al. (2004) rachis internode length was the main determinant of cluster openness of compact wine grape varieties (“Riesling” and “Chardonnay”) compared to openly structured table grape cultivars (“Exotic” and “Sultanina”). This is not in line with our findings where the length of the first and second internodes (estimated with 149  $F_1$  genotypes of the  $G \times V$  population) was not important for the prediction of compactness (OIV204 classes) with random forest and cumulative link models. Moreover, in their work they could not find significantly different pedicel lengths, discriminating compact and open cultivars, whereas in this study, elongated pedicel lengths raise the likelihood of showing loose cluster architecture (Online Resource 4). Together, this suggests that table grapes achieve their cluster openness with divergent sub-trait contributions or the highly diverse set of  $F_1$  genotypes was highlighting other genetic determinants of cluster architecture sub-traits than the wine grape versus table grape comparison.

### QTLs for cluster architecture

The overall aim of this study was to reveal QTLs for cluster architecture to deduce cluster architecture-associated markers for marker-assisted selection (MAS) in grapevine breeding. Due to the complexity of the trait “cluster architecture”, several QTLs with various levels of contribution to the phenotypic variance were expected. Indeed, this investigation revealed an elevated number of 30 QTLs for cluster architecture sub-traits (Table 3 and Online Resource 6). The statistical evaluation of 16 cluster architecture sub-traits recorded in 2015 and 2016 (~1700 data points per trait) showed that six of the cluster architecture sub-traits had high impact on the compactness level of the cluster (OIV204).

Focusing on these statistically most relevant sub-traits for cluster architecture berry number, cluster weight, mean berry volume, pedicel length, rachis length and shoulder length reduced the number to 24 QTLs for close investigation (Table 3 and Online Resource 6). Many QTL regions accumulate in specific genomic regions. The confidence intervals of 21 QTLs were co-located on the reference genome in eight genomic regions (Table 4). This fact of clustered QTLs alleviates the task to deduce trait-linked markers for assays of applicability in grapevine breeding for loose cluster architecture. An overview of cluster architecture-related QTLs is shown in Online Resource 6.

On LG1, limited by the markers VVIN61 and VMC2B3, a cluster of the QTLs for OIV204 and pedicel length (PEDa) was detected. Pedicel length is a predictor variable in the majority of the linear models. The  $LOD_{max}$ -associated marker for OIV204 and for pedicel

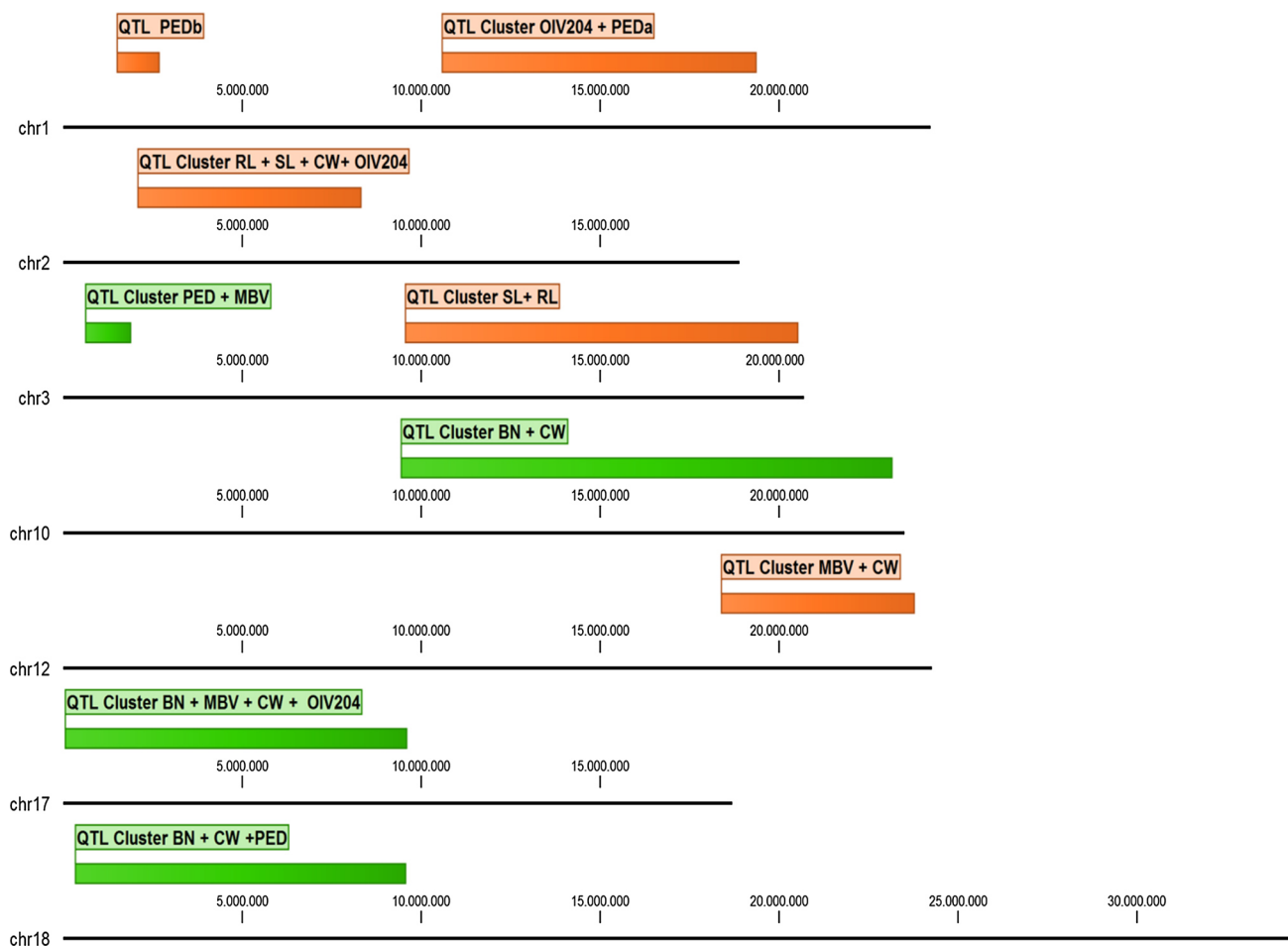


**Fig. 3** Graphical overview of co-located QTLs linked to cluster architecture sub-traits. Physical position for confidence interval regions of QTLs related to sub-traits of cluster architecture projected onto the reference genome of grapevine PN40024 12x V2. In orange the location of confidence interval clusters for QTLs calculated with interval

mapping. In green the location of confidence interval clusters determined with contribution of interval mapping and interval mapping + flower sex as co-variable during QTL calculation. For trait abbreviations see Table 1. For positions and details see Table 4 and Online Resource 6

length was SNP1241\_207FEM. This SNP is located in the mRNA sequence of the gene *VIT\_201s0026g02580*. The gene product, a “zinc finger DOF5.2-like” protein, is a plant-specific transcription factor of the DOF (DNA-binding One Zinc Finger) family. In the model plant *A. thaliana*, Fornara et al. (2015) reported that an alteration in the expression level of cycling DOF factors affected flowering and growth. However, besides *VIT\_201s0026g02580*, there are 718 more genes encompassed in the confidence interval of the QTL; 39 of them are also found in the GO enrichment (Online Resource 8). In addition, LG1 harbors a second QTL for pedicel length (PEDb) associated with the  $LOD_{max}$  marker GF01-24. Approximately 700 kb downstream of GF01-24 Marguerit et al. (2009) also reported a QTL for pedicel length, which was associated with the marker IRT1f in their study. Costantini et al. (2008) described a QTL for berry weight on LG1

in a table grape cross, associated with AFLP marker “mCACeATC4.” The AFLP technique of this marker prevents a precise determination of the position on the reference genome, but the closest SSR marker on their consensus map was VVIF52 at 23 Mb. In this region a QTL for peduncle length was found in the  $G \times V$  cross during three seasons, but with different  $LOD_{max}$  positions (Online Resource 6).

Incorporated on LG2, the confidence intervals of the QTLs found for rachis length, shoulder length, cluster weight and OIV204 were co-located between the markers GF02-07 and VMC5G7. The associated  $LOD_{max}$  marker for rachis length and shoulder length was VVIB23. The QTLs for cluster weight and OIV204 share GF02-12 as common  $LOD_{max}$  marker. In a former study Marguerit et al. (2009) found the region close to marker VVIB23 on LG2 associated with rachis sub-traits in their interspecific cross of “Cabernet

Sauvignon"  $\times$  *V. riparia* "Gloire de Montpellier," e.g., rachis length, rachis length combined with peduncle length and the presence/absence of a wing.

The markers GF02-07 and VVIB23 are linked to cluster architecture sub-traits and also closely linked to flower sex. Using the offspring of a cross, performed with a root-stock cultivar and a wine grape breeding line, Fechter et al. (2012) pinpointed genetic determinants of flower sex within a 143 kb region between the markers VVIB23 and GF02-12. Marguerit et al. (2009) found a high association of flower sex to the marker VVIB23 in their cross. Analyzing exclusively the 103 hermaphroditic individuals of the  $G \times V$  population (omitting the 46 female  $F_1$ -individuals) no QTL was detectable in this region. A QTL calculation based on the paternal map (data not shown) did not show any QTL for cluster architecture in this genomic region, either. However, the QTL calculation using the maternal map showed QTLs for OIV204, rachis length and shoulder length in this region spanning the confidence interval between the markers VVIB23 and GF02-12 (data not shown). This indicates maternal heredity of these QTLs for cluster architecture sub-traits on LG2. This finding is consistent with a genetic determination for elongated rachis sub-traits and more open cluster architecture in female genotypes as visible in the PCA calculation at PC2 (Table 1 and Fig. 2).

An interval mapping using flower sex as co-variable detected a QTL for pedicel length on LG3. The marker GF03-09 was the upper limit of the  $LOD_{max} - 1$  confidence interval, and the marker 1044j09FEM was the lower limit and the  $LOD_{max}$  marker at the same time (1.9 Mb). As far as we know, this is the first report for cluster architecture QTLs in this genomic region. Nevertheless, the confidence interval for this QTL harbors 170 genes; 34 of them were reported as differentially expressed between loosely and compactly clustered "Tempranillo" clones in a study of Grimplet et al. (2017). Moreover, it displays the additional power of IM using a co-variable (flower sex) for QTL calculation since the pedicel length QTL was not detectable without the application of this co-variable.

The QTL for pedicel length shares its  $LOD_{max}$  marker with the one for mean berry volume on LG3. In grapevine, the berry size and seed number are directly related. This correlation results likely from the fact that gibberellins produced by seeds are required to promote berry growth during late berry development (Coombe 1960, 1973; Perez et al. 2000). This study here did not record seed number, but an elevated phytohormone concentration could also be the reason for longer pedicels. Gourieroux et al. (2016) discussed that phytohormones released by grape ovaries may promote the elongation of the rachis so that adequate space becomes available for the growing berries.

LG3 carries a second QTL cluster delimited by the markers VCHR03a and 2018J24 at around 16.5 Mb. This cluster

covers the QTLs for rachis length and shoulder length. Both QTLs shared GF03-07 as  $LOD_{max}$  marker. In the cross-population used by Marguerit et al. (2009), it was possible to detect QTLs for rachis length and length of the first rachis internode also on LG3, but in a different region at  $\sim 7.8$  Mb. It remains to be explored whether these two loci correspond.

On LG10, the application of interval mapping calculation with flower sex as co-factor identified co-localized QTLs for berry number and cluster weight. Depending on the season the upper limit of the confidence interval varied considerably between 9.42 and 21.30 Mb. The lower limit and the  $LOD_{max}$  were stable at marker VRZAG7 positioned at 23.17 Mb. The varying range of the confidence intervals over the seasons is probably a result of the influence of climate conditions on the development of berry traits, which requires two consecutive years for the full cycle [as discussed in Li-Mallet et al. (2016) or in Tello and Ibáñez (2017)]. This QTL cluster also encloses further QTLs for berry weight in 2015 and 2016, rachis weight in 2015 and 2016 and total berry volume in 2014 and 2016. In this region, with QTLs for berry-related sub-traits of cluster architecture, Tello et al. (2016) found two SNPs at around 19.17 Mb associated with the length of the first lateral. LG10 also contains QTLs for shoulder length between  $\sim 5$  and  $\sim 15$  Mb in the  $G \times V$  cross. Associated with the marker VMC2A10 (5.98 Mb) Marguerit et al. (2009) detected QTLs for peduncle, rachis and rachis internode length on LG10 in the interspecific cross in their work. Their QTL was co-localized with AGAMOUS, a floral organ development gene. As a key finding of their work Shiri et al. (2018) have recently reported that AGAMOUS is involved in the compactness of table grape clusters.

On LG12, the QTLs for mean berry volume and cluster weight co-localized between 17.92 and 23.76 Mb. Within this 5.84-Mb-wide region, an additional QTL for OIV204 was detected, but only in the season of 2017. During 2 years (2015 and 2016) the  $LOD_{max}$  for the QTL for OIV204 was located also on LG12, but at different positions of VV\_12\_3836836FEM (3.88 Mb) and VV\_12\_6764538FEM (6.05 Mb), respectively. Trying to explain the positional shift of the OIV204 QTL in the year 2017, the climatic conditions around the time of flowering were compared between the three seasons (14 days pre-bloom until 14 days post-bloom counted from the median of the flowering time range of a given season). The most prominent climatic event between the seasons was a heavy rain storm on June 3, 2017 (31 l/m<sup>2</sup> in 6 h), at the beginning of the flowering time of the cross-population with the potential to affect the pollination rate. Such an event could have influenced the expression of the trait. Interestingly, Costantini et al. (2008) reported a QTL for berry weight in the region of the confidence interval for OIV204 at 5.44 Mb. Berry weight is significantly correlated with OIV204 in the population investigated here over 2 years. Assuming that the QTL for OIV204 reported

here is influenced by berry weight Costantini et al. (2008) may thus have indirectly confirmed the position of the QTL for OIV204 in the range of 3.88–6.05 Mb by their finding. In the work of Tello et al. (2016) a SNP associated with cluster compactness was located in this region also, directly supporting the QTL position for OIV204 in the upper third of the chromosome.

On LG17, QTLs for berry number, cluster weight, mean berry volume and OIV204 were found between the LOD<sub>max</sub> markers SCU06 (3.29 Mb) and UDV092 (9.61 Mb) in this work. Several studies using populations with diverse genetic background reported QTLs for cluster architecture traits in this chromosomal region. Fanizza et al. (2005) found a QTL for berry number associated with an AFLP marker (17mCTG eATC8) at the very top of LG17. Correa et al. (2014) reported a QTL for rachis traits linked to the marker VMC2H3 at 3.68 Mb. Linked to the marker VVIN73 (5.63 Mb), Doligez et al. (2013) reported a QTL for berry weight. Marguerit et al. (2009) reported VVIN73 as LOD<sub>max</sub> marker for rachis internode length. Hence, the region on LG17 seems to be strongly engaged in the genetic determination of cluster architecture. The fact that the same marker was linked to rachis as well as to berry traits, in two different studies, could probably be explained by the dependency of rachis traits on the manifestation of flower and berry traits as explained in Gourieroux et al. (2016). With the resolution of QTL analysis it is not feasible to dissect underlying candidate genes for single sub-traits. It remains elusive to suggest a pleiotropic effect of a locus on several phenotypic features. Indeed, the proximity of QTLs for berry- and rachis-related sub-traits in this region provides the opportunity for marker-assisted selection. It may be possible to take advantage of this situation by applying a small range of molecular markers from this QTL region to select less berry volume with large rachis features tagging several traits that might be co-inherited.

On LG18, the confidence interval of the QTL for cluster weight flanks the confidence interval for the QTL for pedicel length. Both confidence intervals were co-located additionally with the confidence interval for berry number, when flower sex was used as a co-factor in IM calculation. This QTL-saturated region is flanked by markers VMC2A3 (0.95 Mb) and VV18\_8582805FEM (9.58 Mb). In addition, the sub-trait QTLs for berry weight and rachis weight were co-located in this cluster.

Several recent reports for cluster architecture sub-traits identified QTLs on LG18. In the studies of Correa et al. (2014), Doligez et al. (2013), Costantini et al. (2008) and Cabezas et al. (2006) the marker VMC7F2 at 30.31 Mb was linked to berry volume, berry weight and seed traits. In the close vicinity of this marker Tello et al. (2016) reported a SNP in the 5'UTR of a MADS-box SEEDSTICK encoding gene correlated with ramification length. Correa et al. (2014)

could show the linkage of rachis node number to the markers VMC2A7 and VMCNG2F12 at 13.39 and 22.85 Mb. Downstream of this region, in proximity of the marker UDV108, they reported the QTL position for berry number and berry number after gibberellic acid treatment.

On LG18, all so far reported QTLs for berry-related cluster architecture sub-traits from table grape crosses were located at the lower arm of the group. Quite in contrast, the QTLs detected in this work were exclusively located on the upper arm of LG18. Doligez et al. (2013) used three cross-populations to investigate the coupling of berry size and seed content. Two of these were table grape crosses and one was a wine grape cross. Only in the cross of wine grape cultivars they found a QTL for berry sub-traits, also on the upper arm linked to marker VVIN83 at 10.67 Mb.

### Survey of GO classes enriched in the QTL cluster regions

Looking at the highly enriched GO classes and the corresponding annotated genes reveals six groups of GO-term-related genes enriched between 30- and 90-fold in the QTL clusters for cluster architecture-associated traits (Online Resource 8). The first group comprises a set of genes encoding a component of menaquinone biosynthesis, a 2-oxoglutarate decarboxylase hydro-lyase magnesium ion binding protein and a gene encoding naphthoate synthase, enriched 45-fold in the QTL cluster on chromosome 1. These genes are involved in the formation of co-factors for the electron transfer machinery of photosystem I (PSI) (Gross et al. 2006). At a similar level of enrichment (36-fold) there are copper transporter systems encoded in cluster 3.2. Copper is a crucial element in electron transport, but may also be implicated in other processes like free radical elimination, signaling and hormone perception (Sancenón et al. 2003). It remains to be elucidated whether electron transfer systems of PSI are particularly involved in cluster architecture determination. The role of copper transporters may be ambiguous with the possibility to contribute to PSI or to participate in signaling during cellular development. In cluster 2 there is a strong enrichment (50-fold) for genes encoding a cell-cycle-regulated microtubule-associated protein and armadillo repeat-containing kinesin-like protein 2. The products of these genes are involved in cell division and intracellular transport along microtubuli using motor proteins like kinesins. This function is in line with the strong enrichment (90-fold) of as yet uncharacterized proteins assigned to the GO classes for bidirectional movement of large protein complexes along microtubules (GO:0035721 and 42073) found in cluster 10. These functions are intrinsic to cell development and may be an important part of the formation of the cluster architecture sub-traits. The genes strongly enriched (37-fold) in cluster 18 encode flavonol synthase (FLS1), an

iron-binding light-responsive oxidoreductase that contributes to flavonoid biosynthesis. It acts on dihydroflavonols to yield quercetin, kaempferol and myricetin in grapevine. These substances serve as UV protectants. Five FLS genes have been shown to be expressed in flower buds and flowers of grapevine. Two FLS genes keep on being expressed from véraison (the transition point of berry growth from hard, green berries to berry softening and sugar accumulation) to harvest stage (Fujita et al. 2006). Heijde and Ulm (2012) reported enhanced FLS expression after UV-B photon perception by the UV-B photoreceptor (UVR8) pathway in *A. thaliana*. Also Hayes et al. (2014) reported for *A. thaliana* that the perception of UV-B radiation was maintained with the UVR8-mediated UV-B responses. They could link the UVR8 pathway to growth patterns, i.e., shade avoidance responses in *Arabidopsis thaliana* by antagonizing the phytohormones auxin and gibberellin. Nevertheless, how a higher level of UV protectants may be beneficial for a more loosely structured inflorescence remains to be revealed. The cluster 3.1 contains a prominent group of SAUR family proteins and auxin-induced genes in 33.5-fold enrichment. SAURs (“Small Auxin Up” RNAs) are early auxin-responsive genes that play a role in the regulation of plant cell growth (cell expansion and cell division). The plant-specific SAUR genes are generally present in tandem arrays with high redundancy and arranged in large genomic blocks due to segmental duplications of very closely related genes. These genes are induced by auxins, but may also be regulated by brassinosteroids, gibberellins, abscisic acid and jasmonate. They are involved in cell differentiation and patterning. The SAURs also respond to environmental conditions (light, drought) and may modulate auxin transport (Ren and Gray 2015). From all the genes enriched in the QTL clusters, this block in cluster 3.1, together with the finding of highly enriched intracellular microtubule-guided transporter functions involved in cell development in the cluster on chromosome 2, provides the best candidates to explain different growth patterns that result in the phenotypes of loose or compact cluster architecture traits. However, their functional relevance awaits further investigation.

## Conclusions

The combination of statistical methods, i.e., correlation analysis, PCA, RF and CLM modeling, enabled the determination of the most relevant sub-traits that determine cluster architecture in the evaluated  $G \times V$  cross. For those highly effective sub-traits of cluster architecture, it was possible to identify 19 reproducible QTLs. As compared to literature references, some QTLs already reported could be verified and new QTLs in yet unreported regions became accessible. Co-localized QTLs determined 87% of the total phenotypic

variation of traits with high impact on cluster architecture detected in this study. Projection of confidence intervals of co-localized QTLs onto the reference genome for grapevine (PN40024) revealed eight QTL clusters, and the QTL clustering facilitates marker deduction for MAS. GO term enrichment analysis suggested accumulation of genes related to biological functions as first ideas on the molecular basis underlying the phenotype of cluster architecture.

**Author contribution statement** EZ designed the study, acquired funding and supervised the work. RR performed the experiments, measurements and calculations. FR contributed phenotypic data. DG provided statistical expertise and tools. RT provided all plant materials, infrastructure and special advice. RR and EZ wrote the paper. All authors read the manuscript.

**Acknowledgements** We wish to thank Sarina Elser for expert technical assistance. This work was funded by the “Federal Program for Ecologic Landuse and other forms of Sustainable Agriculture” (Bundesprogramm Ökologischer Landbau und andere Formen nachhaltiger Landwirtschaft, BÖLN) of BLE (Bundesanstalt für Landwirtschaft und Ernährung) Federal Office for Agriculture and Food under the title “MATA- Molekulare Analyse der Traubenarchitektur” (Molecular analysis of cluster architecture) FKZ 2811NA056 ([www.ble.de](http://www.ble.de)).

## Compliance with ethical standards

**Conflict of interest** The authors declare that they have no conflict of interest.

## References

- Ashburner M, Ball CA, Blake JA, Botstein D, Butler H, Cherry JM, Davis AP, Dolinski K, Dwight SS, Eppig JT et al (2000) Gene ontology: tool for the unification of biology. *Nature Genet* 25:25
- Ban Y, Mitani N, Sato A, Kono A, Hayashi T (2016) Genetic dissection of quantitative trait loci for berry traits in interspecific hybrid grape (*Vitis labruscana* × *Vitis vinifera*). *Euphytica* 211(3):295–310
- Becker T, Knoche M (2012) Water induces microcracks in the grape berry cuticle. *Vitis* 51(3):141–142
- BMELV (2010) Gute fachliche Praxis im Pflanzenschutz: Bundesministerium für Ernährung Landwirtschaft und Verbraucherschutz (BMELV)
- Boulesteix AL, Janitza S, Kruppa J, König I (2012) Overview of random forest methodology and practical guidance with emphasis on computational biology and bioinformatics. *Wiley Interdiscip Rev Data Min Knowl Discov* 2(6):493–507
- Breiman L (2001) Random forests. *Mach Learn* 45(1):5–32
- Broome JC, English JT, Marois JJ, Latorre BA, Aviles JC (1995) Development of an infection model for Botrytis bunch rot of grapes based on wetness duration and temperature. *Phytopath* 85(1):97–102. <https://doi.org/10.1094/Phyto-85-97>
- Burnham KP, Anderson DR (2002) Model selection and multimodel inference: a practical information-theoretic approach, 2nd edn. Springer, New York

- Cabezas JA, Cervera MT, Ruiz-Garcia L, Carreno J, Martinez-Zapater JM (2006) A genetic analysis of seed and berry weight in grapevine. *Genome* 49(12):1572–1585. <https://doi.org/10.1139/G06-122>
- Calcagno V, de Mazancourt C (2010) glmulti: an R package for easy automated model selection with (generalized) linear models. *J Stat Softw* 34(12):1–29
- Canaguier A, Grimplet J, Di Gaspero G, Scalabrin S, Duchêne E, Choïse N, Mohellibi N, Guichard C, Rombauts S, Le Clainche I, Bérard A, Chauveau A, Bounon R, Rustenholz C, Morgante M, Le Paslier MC, Brunel D, Adam-Blondon AF (2017) A new version of the grapevine reference genome assembly (12X.v2) and of its annotation (VCost.v3). *Genom Data* 14:56–62. <https://doi.org/10.1016/j.gdata.2017.09.002>
- Christensen RHB (2018) Ordinal-regression models for ordinal data. R package version 2018, pp 4–19
- Coombe BG (1960) Relationship of growth and development to changes in sugars, auxins and gibberellins in fruit of seeded and seedless varieties of *Vitis vinifera*. *Plant Physiol* 35(2):241–250
- Coombe BG (1973) The regulation of set and development of the grape berry. International Society for Horticultural Science (ISHS), Leuven, Belgium, p 261
- Correa J, Mamani M, Munoz-Espinoza C, Laborie D, Munoz C, Pinto M, Hinrichsen P (2014) Heritability and identification of QTLs and underlying candidate genes associated with the architecture of the grapevine cluster (*Vitis vinifera* L.). *Theor Appl Genet* 127:1143–1162
- Costantini L, Battilana J, Lamaj F, Fanizza G, Grando MS (2008) Berry and phenology-related traits in grapevine (*Vitis vinifera* L.): from quantitative trait loci to underlying genes. *BMC Plant Biol* 8(1):38. <https://doi.org/10.1186/1471-2229-8-38>
- Di Genova A, Almeida AM, Munoz-Espinoza C, Vizoso P, Travisany D, Moraga C, Pinto M, Hinrichsen P, Orellana A, Maass A (2014) Whole genome comparison between table and wine grapes reveals a comprehensive catalog of structural variants. *BMC Plant Biol* 14:7. <https://doi.org/10.1186/1471-2229-14-7>
- Doligez A, Bertrand Y, Farnos M, Grolier M, Romieu C, Esnault F, Dias S, Berger G, Francois P, Pons T, Ortigosa P, Roux C, Houel C, Laucou V, Bacilieri R, Peros JP, This P (2013) New stable QTLs for berry weight do not colocalize with QTLs for seed traits in cultivated grapevine (*Vitis vinifera* L.). *BMC Plant Biol* 13:217. <https://doi.org/10.1186/1471-2229-13-217>
- Fanizza G, Lamaj F, Costantini L, Chaabane R, Grando (2005) QTL analysis for fruit yield components in table grapes (*Vitis vinifera*). *Theor Appl Genet* 111(4):658–664. <https://doi.org/10.1007/s00122-005-2016-6>
- Fechter I, Hausmann L, Daum M, Sorensen TR, Viehöver P, Weisshaar B, Töpfer R (2012) Candidate genes within a 143 kb region of the flower sex locus in *Vitis*. *Mol Genet Genomics* 287(3):247–259. <https://doi.org/10.1007/s00438-012-0674-z>
- Fornara F, de Montaigu A, Sánchez-Villarreal A, Takahashi Y, Loren Ver, van Themaat E, Huettel B, Davis SJ, Coupland G (2015) The GI-CDF module of *Arabidopsis* affects freezing tolerance and growth as well as flowering. *Plant J* 81(5):695–706
- Fox J, Monette G (1992) Generalized collinearity diagnostics. *J Am Stat Assoc* 87(417):178–183. <https://doi.org/10.1080/01621459.1992.10475190>
- Fujita A, Goto-Yamamoto N, Aramaki I, Hashizume K (2006) Organ-specific transcription of putative flavonol synthase genes of grapevine and effects of plant hormones and shading on flavonol biosynthesis in grape berry skins. *Biosci Biotechnol Biochem* 70(3):632–638
- Gabler FM, Smilanick JL, Mansour M, Ramming DW, Mackey BE (2003) Correlations of morphological, anatomical, and chemical features of grape berries with resistance to *Botrytis cinerea*. *Phytopathology* 93(10):1263–1273. <https://doi.org/10.1094/Phyto.2003.93.10.1263>
- Gourieroux AM, McCully ME, Holzapfel BP, Scollary GR, Rogiers SY (2016) Flowers regulate the growth and vascular development of the inflorescence rachis in *Vitis vinifera* L. *Plant Physiol Biochem* 108:519–529
- Grimplet J, Tello J, Laguna N, Ibanez J (2017) Differences in flower transcriptome between grapevine clones are related to their cluster compactness, fruitfulness, and berry size. *Front Plant Sci* 8:17
- Gross J, Cho WK, Lezhneva L, Falk J, Krupinska K, Shinozaki K, Seki M, Herrmann RG, Meurer J (2006) A plant locus essential for phyloquinone (Vitamin K1) biosynthesis originated from a fusion of four eubacterial genes. *J Biol Chem* 281:17189–17196. <https://doi.org/10.1074/jbc.M601754200>
- Hair J, Anderson R, Tatham R, Black W (2010) Multivariate data analysis, 7th edn. Pearson, New York
- Han J, Kamber M, Pei J (2012) Data Mining: concepts and techniques. In: Data mining, 3rd edn. Morgan Kaufmann, Boston, pp 443–541. <https://doi.org/10.1016/B978-0-12-381479-1.00016-2>
- Hayes S, Velanis CN, Jenkins GI, Franklin KA (2014) UV-B detected by the UVR8 photoreceptor antagonizes auxin signaling and plant shade avoidance. *Proc Natl Acad Sci* 111:11894
- Hed B, Ngugi HK, Travis JW (2010) Use of gibberellic acid for management of bunch rot on Chardonnay and Vignoles grape. *Plant Dis* 95(3):269–278. <https://doi.org/10.1094/PDIS-05-10-0382>
- Heijde M, Ulm R (2012) UV-B photoreceptor-mediated signalling in plants. *Trends Plant Sci* 17:230–237
- Herzog K, Wind R, Töpfer R (2015) Impedance of the grape berry cuticle as a novel phenotypic trait to estimate resistance to *Botrytis cinerea*. *Sensors* 15(6):12498–12512. <https://doi.org/10.3390/s150612498>
- Hothorn T, Buehlmann P, Dudoit S, Molinaro A, Van Der Laan M (2006) Survival ensembles. *Biostat* 7(3):355–373
- Houel C, Martin-Magniette ML, Nicolas SD, Lacombe T, Le Cunff L, Franck D, Torregrosa L, Conejero G, Lalet S, This P, Adam-Blondon AF (2013) Genetic variability of berry size in the grapevine (*Vitis vinifera* L.). *Aust J Grape Wine Res* 19(2):208–220. <https://doi.org/10.1111/ajgw.12021>
- Janitza S, Tutz G, Boulesteix A-L (2016) Random forest for ordinal responses: prediction and variable selection. *Comput Stat Data Anal* 96:57–73
- Kassambara A (2017) Practical guide to cluster analysis in R: unsupervised machine learning, vol 1. STHDA
- Kicherer A, Roscher R, Herzog K, Šimon S, Förstner W, Töpfer R (2013) BAT (Berry Analysis Tool): a high-throughput image interpretation tool to acquire the number, diameter, and volume of grapevine berries. *Vitis* 52(3):129–135
- Lê S, Josse J, Hussen F (2008) FactoMineR: an R package for multivariate analysis. *J Stat Softw* 25(1):18. <https://doi.org/10.18637/jss.v025.i01>
- Li-Mallet A, Rabot A, Geny L (2016) Factors controlling inflorescence primordia formation of grapevine: their role in latent bud fruitfulness? A review. *Botany* 94(3):147–163. <https://doi.org/10.1139/cjb-2015-0108>
- Marguerit E, Boury C, Manicki A, Donnart M, Butterlin G, Nemorin A, Wiedemann-Merdinoglu S, Merdinoglu D, Ollat N, Decroocq S (2009) Genetic dissection of sex determinism, inflorescence morphology and downy mildew resistance in grapevine. *Theor Appl Genet* 118(7):1261–1278. <https://doi.org/10.1007/s00122-009-0979-4>
- Mi H, Huang X, Muruganujan A, Tang H, Mills C, Kang D, Thomas PD (2017) PANTHER version 11: expanded annotation data from gene ontology and reactome pathways, and data analysis tool enhancements. *Nucleic Acids Res* 45(Database issue):D183–D189. <https://doi.org/10.1093/nar/gkw1138>

- Migicovsky Z, Sawler J, Gardner KM, Aradhya MK, Prins BH, Schwaninger HR, Bustamante CD, Buckler ES, Zhong G-Y, Brown PJ, Myles S (2017) Patterns of genomic and phenomic diversity in wine and table grapes. *Hortic Res* 4:17035
- Molitor D, Behr M, Hoffmann L, Evers D (2012) Impact of grape cluster division on cluster morphology and bunch rot epidemic. *Am J Enol Vitic* 63(4):508
- Nair NG, Allen RN (1993) Infection of grape flowers and berries by *Botrytis cinerea* as a function of time and temperature. *Mycol Res* 97(8):1012–1014. [https://doi.org/10.1016/S0953-7562\(09\)80871-X](https://doi.org/10.1016/S0953-7562(09)80871-X)
- Nelson KE (1956) The effect of *Botrytis* infection on the tissue of Tokay grapes. *Phytopath* 46(4):223–229
- OIV (2017) 2017 World Vitiviniculture Situation. OIV Statistical Report on World Vitiviniculture. International Organisation of Vine and Wine, Paris. <http://www.oiv.int/>. Accessed Dec 2018
- OIV (2015) 2nd edition of the OIV descriptor list for grape varieties and *Vitis* species. <http://www.oiv.int/>. Accessed Dec 2018
- Perez FJ, Viani C, Retamales J (2000) Bioactive gibberellins in seeded and seedless grapes: identification and changes in content during berry development. *American J Enol Vitic* 51(4):315–318
- Pertot I, Caffi T, Rossi V, Mugnai L, Hoffmann C, Grando MS, Gary C, Lafond D, Duso C, Thiery D, Mazzoni V, Anfara G (2017) A critical review of plant protection tools for reducing pesticide use on grapevine and new perspectives for the implementation of IPM in viticulture. *Crop Prot* 97:70–84. <https://doi.org/10.1016/j.cropro.2016.11.025>
- Pieri P, Zott K, Gomes E, Hibert G (2016) Nested effects of berry half, berry and bunch microclimate on biochemical composition in grape. *Oeno One* 50(3):145–159
- R Core Team (2017) R: a language and environment for statistical computing. R Foundation for Statistical Computing, Vienna, Austria. <http://www.r-project.org>. Accessed Sept 2018
- Ren H, Gray WM (2015) SAUR proteins as effectors of hormonal and environmental signals in plant growth. *Mol Plant* 8(8):1153–1164. <https://doi.org/10.1016/j.molp.2015.05.003>
- Rist F, Herzog K, Mack J, Richter R, Steinhage V, Töpfer R (2018) High-precision phenotyping of grape bunch architecture using fast 3D sensor and automation. *Sensors* 18(3):763
- Sancenón V, Puig S, Mira H, Thiele DJ, Peñarrubia L (2003) Identification of a copper transporter family in *Arabidopsis thaliana*. *Plant Mol Biol* 51:577–587
- Sarooshi R (1977) Some effects of girdling, gibberellic acid sprays, bunch thinning and trimming on the sultana. *Austr J Exp Agric* 17(87):700–704. <https://doi.org/10.1071/EA9770700>
- Schneider CA, Rasband WS, Eliceiri KW (2012) NIH Image to ImageJ: 25 years of image analysis. *Nat Methods* 9(7):671–675. <https://doi.org/10.1038/nmeth.2089>
- Shavrukov YN, Dry IB, Thomas MR (2004) Inflorescence and bunch architecture development in *Vitis vinifera* L. *Aust J Grape Wine Res* 10(2):116–124. <https://doi.org/10.1111/j.1755-0238.2004.tb00014.x>
- Shiri Y, Solouki M, Ebrahimie E, Emamjomeh A, Zahiri J (2018) Unraveling the transcriptional complexity of compactness in sistan grape cluster. *Plant Sci* 270:198–208
- Smart R, Robinson M (1991) Sunlight into wine. A handbook for wine-grape canopy management. Winetitles, Adelaide
- Strobl C, Boulesteix A-L, Zeileis A, Hothorn T (2007). Bias in random forest variable importance measures: illustrations, sources and a solution. *BMC Bioinfo* 8(25). <http://www.biomedcentral.com/1471-2105/8/25>
- Strobl C, Boulesteix A-L, Kneib T, Augustin T, Zeileis A (2008) Conditional variable importance for random forests. *BMC Bioinforma* 9(307). <http://www.biomedcentral.com/1471-2105/9/307>
- Tello J, Ibáñez J (2014) Evaluation of indexes for the quantitative and objective estimation of grapevine bunch compactness. *Vitis* 53(1):9–16
- Tello J, Ibáñez J (2017) What do we know about grapevine bunch compactness? A state-of-the-art review. *Austr J Grape Wine Res*. <https://doi.org/10.1111/ajgw.12310>
- Tello J, Aguirrezabal R, Hernaiz S, Larreina B, Montemayor MI, Vaquero E, Ibáñez J (2015) Multicultivar and multivariate study of the natural variation for grapevine bunch compactness. *Austr J Grape Wine Res* 21(2):277–289. <https://doi.org/10.1111/ajgw>
- Tello J, Torres-Perez R, Grimplet J, Ibanez J (2016) Association analysis of grapevine bunch traits using a comprehensive approach. *Theor Appl Genet* 129:227–242
- The Gene Ontology Consortium (2017) Expansion of the gene ontology knowledgebase and resources. *Nucleic Acids Res* 45(Database issue):D331–D338. <https://doi.org/10.1093/nar/gkw1108>
- Töpfer R, Hausmann L, Harst M, Maul E, Zyprian E, Eibach R (2011) New horizons for grapevine breeding. In: Flachowsky H, Hanke M-V (eds) *Methods in temperate fruit breeding*. Global Science Books Ltd, Ikenobe, pp 79–100
- Vail ME, Marois JJ (1991) Grape cluster architecture and the susceptibility of berries to *Botrytis cinerea*. *Phytopath* 81(2):188–191. <https://doi.org/10.1094/phyto-81-188>
- van Buuren S, Groothuis-Oudshoorn K (2011) mice: Multivariate imputation by chained equations in R. *J Stat Softw* 45(3):1–67
- van Ooijen J (2009) MapQTL 6, software for the mapping of quantitative trait loci in experimental populations of diploid species. Kyazma b. V, The Netherlands
- Zyprian E, Ochssner I, Schwander F, Simon S, Hausmann L, Bonow-Rex M, Moreno-Sanz P, Grando MS, Wiedemann-Merdinoglu S, Merdinoglu D, Eibach R, Töpfer R (2016) Quantitative trait loci affecting pathogen resistance and ripening of grapevines. *Mol Gen Genom* 291(4):1573–1594. <https://doi.org/10.1007/s00438-016-1200-5>

**Publisher's Note** Springer Nature remains neutral with regard to jurisdictional claims in published maps and institutional affiliations.

**3 - Differential expression of transcription factor- and further growth related genes correlates with contrasting cluster architecture in *Vitis vinifera* 'Pinot Noir' and *Vitis* spp. genotypes**

Robert Richter, Susanne Rossmann, Doreen Gabriel, Reinhard Töpfer, Klaus Theres  
and Eva Zyprian

Theoretical and Applied Genetics (2020) 133:3249–3272

<https://doi.org/10.1007/s00122-020-03667-0>



# Differential expression of transcription factor- and further growth-related genes correlates with contrasting cluster architecture in *Vitis vinifera* ‘Pinot Noir’ and *Vitis* spp. genotypes

Robert Richter<sup>1</sup> · Susanne Rossmann<sup>2</sup> · Doreen Gabriel<sup>3</sup> · Reinhard Töpfer<sup>1</sup> · Klaus Theres<sup>2</sup> · Eva Zyprian<sup>1</sup>

Received: 18 March 2020 / Accepted: 3 August 2020 / Published online: 18 August 2020  
© The Author(s) 2020

## Abstract

Grapevine (*Vitis vinifera* L.) is an economically important crop that needs to comply with high quality standards for fruit, juice and wine production. Intense plant protection is required to avoid fungal damage. Grapevine cultivars with loose cluster architecture enable reducing protective treatments due to their enhanced resilience against fungal infections, such as *Botrytis cinerea*-induced gray mold. A recent study identified transcription factor gene *VvGRF4* as determinant of pedicel length, an important component of cluster architecture, in samples of two loose and two compact quasi-isogenic ‘Pinot Noir’ clones. Here, we extended the analysis to 12 differently clustered ‘Pinot Noir’ clones from five diverse clonal selection programs. Differential gene expression of these clones was studied in three different locations over three seasons. Two phenotypically opposite clones were grown at all three locations and served for standardization. Data were correlated with the phenotypic variation of cluster architecture sub-traits. A set of 14 genes with consistent expression differences between loosely and compactly clustered clones—independent from season and location—was newly identified. These genes have annotations related to cellular growth, cell division and auxin metabolism and include two more transcription factor genes, *PRE6* and *SEPI*-like. The differential expression of *VvGRF4* in relation to loose clusters was exclusively found in ‘Pinot Noir’ clones. Gene expression studies were further broadened to phenotypically contrasting F1 individuals of an interspecific cross and OIV reference varieties of loose cluster architecture. This investigation confirmed *PRE6* and six growth-related genes to show differential expression related to cluster architecture over genetically divergent backgrounds.

---

Communicated by Mingliang Xu.

**Electronic supplementary material** The online version of this article (<https://doi.org/10.1007/s00122-020-03667-0>) contains supplementary material, which is available to authorized users.

---

✉ Eva Zyprian  
eva.zyprian@julius-kuehn.de

<sup>1</sup> Federal Research Centre for Cultivated Plants, Institute for Grapevine Breeding Geilweilerhof, Julius Kühn Institute, 76833 Siebeldingen, Germany

<sup>2</sup> Department of Plant Breeding and Genetics, Max Planck Institute for Plant Breeding, Carl-von-Linné-Weg 10, 50829 Cologne, Germany

<sup>3</sup> Federal Research Centre for Cultivated Plants, Institute for Crop and Soil Science, Julius Kühn Institute, Bundesallee 58, 38116 Brunswick, Germany

## Introduction

Grapevine (*Vitis vinifera* L.) is one of the most important fruit crops at global scale. The worldwide grape production reached 74 million tons in 2018 (OIV 2019). The world gross production value for grapes in 2016 was above 67.5 billion USD (FAOSTAT 2016). Regardless of the use as wine grapes, table grapes or dried fruits (raisins), only high-quality fruits are acceptable for marketing. Unfortunately, *V. vinifera* grapevine varieties are susceptible to several pathogens. Viticulture requires intense application of plant protection products (PPP) to meet the market’s demands. Fungicides are unavoidable to control the pathogens (Perrot et al. 2017) causing powdery mildew, *Erysiphe necator* (syn. *Uncinula necator*, (Schw.) Burr), downy mildew, *Plasmopara viticola* (Berk. & Curt) Berl. & de Toni and *Botrytis cinerea* (teleomorph *Botryotinia fuckeliana* (de Bary) Whetzel), provoking gray mold. The use of PPP, irrespective of their inorganic (copper and sulfur) or synthetic origin, contributes to a decrease in biodiversity and raises

consumers' concerns (Keulemans et al. 2019). One strategy to reduce their use is the breeding of pathogen-resistant grapevine varieties, e.g., by introgression of genetically traceable resistance loci against *E. necator* and *P. viticola* from wild American or Asian *Vitis species* into *V. vinifera* quality cultivars. In the last years, several improved varieties with resistance traits against the mildews became available (Töpfer et al. 2011). However, for *B. cinerea*, there is only preliminary knowledge on a putative resistance locus (Sapkota et al. 2019). Current cultivar development focuses on the enforcement of physical barriers, e.g., a thick berry skin, a hydrophobic berry surface and loose cluster architecture, to increase resilience toward *B. cinerea* (Gabler et al. 2003; Herzog et al. 2015; Shavrukov et al. 2004). Within a loose grape cluster, improved ventilation accelerates the drying-off after rainfall or morning dew. Reduced humidity diminishes infections with fungal pathogens (Hed et al. 2009; Molitor et al. 2012). In addition, fungicide sprays can better spread into a loosely clustered bunch as compared to a compact one (Hed et al. 2010). The high physical stress arising in between the berries of compact clusters upon ripening provokes micro-cracks or even bursting of the berry skin (Becker and Knoche 2012; Smart and Robinson 1991). This problem is avoided in loosely clustered bunches. Moreover, there are less pronounced temperature gradients within loosely structured clusters as solar radiation can better reach the interior berries. This conveys more uniform fruit maturity (Pieri et al. 2016; Vail and Marois 1991). Overall, loose cluster architecture results in grapes with less *B. cinerea* infections and a better harmonized ripening process. It is a highly desired trait in grapevine breeding. Understanding its genetic basis would help to develop novel tools for efficient grapevine breeding and clonal selection.

Worldwide, several thousands of grapevine cultivars exist and are registered in data repositories, e.g., the 'Vitis International Variety Catalogue' (<http://www.vivc.de>; Maul 2019). A plethora of genetic diversity subsists and includes the gene pools of wine grapes and table grapes that show remarkable differences in berry and cluster architecture (Di Genova et al. 2014; Migicovsky et al. 2017). The variability of cluster density is characterized by OIV (Office International de la Vigne et du Vin, International Organisation of Vine and Wine, Paris, France) descriptors like OIV#204, and reference varieties for the scores of this descriptor are available (OIV 2015). However, despite the impressive genetic diversity, only 33 (*V. vinifera* L. subsp. *vinifera*) cultivars account for 50% of the totally used acreage for commercial production (OIV 2017). Promoted by the long cultivation time and large acreage covered with the predominant cultivars, somatic mutations causing intra-cultivar genetic variation are detectable and exploitable to select clonal variants

(De Lorenzis et al. 2017). For example, about 500 different clones are available for 'Pinot Noir' (PN) (Forneck et al. 2009), a variety of high economic importance. Clonal selection programs in this cultivar identified phenotypic variants for relevant agronomic traits including cluster architecture. Apart from the mutation, these clones provide the opportunity to perform genomic diversity studies in a 'pseudo' near isogenic background (Blaich et al. 2007; Konradi et al. 2007). Phenotypic and genotypic diversity can further be uncovered in segregating cross populations intended for genetic mapping and development of trait-linked markers for breeding purposes. Several such populations for genetic tagging of cluster architecture traits were reported (Correa et al. 2014; Marguerit et al. 2009; Richter et al. 2019).

Bunch architecture is controlled by environmental and genetic factors (Döring et al. 2015; Tello and Ibáñez 2017). It is a complex trait composed of berry and stalk characteristics (Li et al. 2019; Richter et al. 2019; Rist et al. 2018). Some of these sub-traits are under genetic control as reported for berry size, berry volume and berry weight (Ban et al. 2016; Houel et al. 2015; Mejia et al. 2007; Tello et al. 2015), berry number (Dry et al. 2010; Fanizza et al. 2005) and other rachis sub-traits (Correa et al. 2014; Marguerit et al. 2009; Tello et al. 2016).

Intravarietal diversity in cluster architecture sub-traits of grapevine has been reported for only few cases, comprising clones of cultivars 'Garnacha Tinta', 'Tempranillo', 'Aglanico' and 'Muscat of Alexandria' (Grimplet et al. 2019, 2017; De Lorenzis et al. 2017). For 'Albariño' clones and for PN clones, the studies of Alonso-Villaverde et al. (2008) and Konrad et al. (2003) provided evidence that loosely clustered clones show reduced susceptibility to *B. cinerea*. PN is a member of the very old 'Pinot' family (Regner et al. 2000) and is used in viticulture for centuries. Presently, with an acreage of 115.000 ha, PN is among the top thirteen international varieties (OIV 2017). The 'Pinot' family accumulated a high number of somatic mutations and gave rise to a wide range of clones displaying divergent phenotypic features (different berry color, varying levels of acidity, different aroma compounds, different vigor and cluster architecture) (Forneck et al. 2009). Concerning cluster architecture (CA), the PN clones were classified into three categories, i.e., compactly clustered clones (CCC) with a dense arrangement of berries, loosely clustered clones (LCC) with berries not touching each other and loose clones with mixed berry size (MBC) producing bunches containing small and large berries at the same time (Bleyer 2001; Ruehl et al. 2004).

In PN, the gene *VvGRF4* was recently detected as a major component affecting inflorescence architecture (Rossmann et al. 2019). Two loosely clustered PN clones from the 'Mariafeld' selection line (M171) and

the Geisenheim clonal selection program (Gm1-86) were compared to two compactly clustered clones ('Frank Charisma' and 'Frank Classic'). This investigation included RNA-Seq analysis and revealed a mutation in the microRNA mi396 binding site of *VvGRF4*, a gene encoding a growth-promoting transcription factor. The mutation prevents down-regulation of the *VvGRF4* transcript, specifically in the LCC clones. Two mutated alleles were identified, one specific for M171 and the other one found in Gm1-86. Both operate in heterozygous state, lead to an enhancement of cell numbers in pedicels in the loose clusters and thus contribute to loose cluster architecture (Rossmann et al. 2019).

In this work, we explored the variation of cluster architecture in an extended set of twelve PN clones from five different selection lines and linked it to the differential transcriptional activity of genes selected from the previous RNA-Seq study. Two OIV reference varieties for loose cluster architecture and 16 selected F1 genotypes from a controlled cross ('Calardis Musqué' (formerly GF.GA-47-42) × 'Villard Blanc') segregating for cluster architecture traits (Richter et al. 2019) were included to broaden the analysis and validate the results. Besides *VvGRF4*, 14 more genes including two genes encoding additional transcription factors were found to be stably regulated in the quasi-isogenic 'Pinot Noir' plants, independent from their growth in different places and through several seasons. Out of these, a set of seven genes were

found to be involved in the genetic regulation of cluster architecture sub-traits in different genetic backgrounds.

## Materials and methods

### Plant material

The *V. vinifera* variety 'Pinot Noir' (abbreviated PN, VIVC No. 9279) was investigated in 12 clones showing different cluster architecture. These comprised compactly clustered clones (CCCs), loosely clustered clones (LCCs) and clones bearing berries with mixed size (MBCs), the latter also resulting in loose clusters. The plants were distributed over three plantations in three German viticulture areas (Palatinate, Baden and Hesse) with partial overlap (Table 1). The vineyard in Palatinate is a trial field of Julius Kuehn Institute for Grapevine Breeding Geilweilerhof (JKI). The vineyards in Baden and Hesse originated from certified material and were managed by grapevine nurseries. All vineyards were submitted to regular visual monitoring for their phytosanitary state.

Trueness to type of the PN plants over all locations was confirmed with six SSR markers (VMC3a9, VMC5g7, VMC8g6, VrZAG79, VVMD32 and VVS2) described to monitor clonal variation in PN (Pelsy et al. 2010) in two snap samples per clone and location (44 samples in total,

**Table 1** Sampling schedules for 12 'Pinot Noir' clones spread over three locations during two seasons for phenotyping

Cluster type	Sample	Abbreviation	Palatinate BBCH 89	Hesse BBCH 89	Baden BBCH 89
CCC	Frank Charisma	FkCH	10 <sup>a</sup>	10 <sup>a</sup>	10 <sup>a</sup>
CCC	Frank Classic	FkCL	10 <sup>a</sup>	10 <sup>a</sup>	–
CCC	Entav 777	En777	–	10 <sup>a</sup>	10 <sup>a</sup>
Variable	Geisenheim 18	Gm18	–	10 <sup>b</sup>	–
MBC	Geisenheim 20-13	Gm20-13	10 <sup>a</sup>	10 <sup>a</sup>	10 <sup>a</sup>
MBC	Freiburg 1801	Fr1801	–	10 <sup>a</sup>	10 <sup>b</sup>
LCC	Geisenheim 1-86	Gm1-86	10 <sup>a</sup>	10 <sup>a</sup>	–
LCC	Freiburg 12-L	Fr12L	–	10 <sup>a</sup>	10 <sup>a</sup>
LCC	Freiburg 13-L	Fr13L	–	10 <sup>a</sup>	10 <sup>a</sup>
LCC	Weinsberg M1	WeM1	–	10 <sup>a</sup>	–
LCC	Weinsberg M171	WeM171	10 <sup>a</sup>	–	–
LCC	Weinsberg M242	WeM242	–	10 <sup>b</sup>	–

For phenotyping of cluster traits, samples of ripe bunches at BBCH89 were taken with 10 replicates from randomly selected independent vines. The measurements of the PN clones 'Frank Charisma' (FkCH) and 'Gm20-13,' present at all three locations, enabled to model the environmental impact on cluster architecture sub-traits (Online resource 6 a, b and c)

– not available

<sup>a</sup>Biological samples taken in 2015 and 2016

<sup>b</sup>Biological samples taken in 2016

Online resource 1). SSR analysis was done as described (Zyprian et al. 2016).

The PN clones were well established (~20-year-old vines), and all grafted on the same rootstock (Kober 125AA, VIVC No. 12344). ‘Guyot pruning’ was applied throughout, and a vertical shoot position trellis system with 1.8–2.2 m<sup>2</sup> space per vine was used. Vineyards in Baden and Hesse were maintained with integrated management. The PN field of JKI was managed according to organic farming rules (Online resource 2). All the plantations contained ample material of PN plants to permit random sampling from the individual clones. Samples were taken exclusively from plants without any symptom of infection or aberration from the typical clonal type of appearance. The OIV reference varieties for loose cluster architecture, ‘Uva Rara’ (VIVC No. 12830) and ‘Prosecco’ (Prime name ‘Glera,’ VIVC No. 9741), were maintained in triplicates as part of the germplasm collection at JKI. The vines are grafted on rootstock ‘Selektion Oppenheim 4’ (SO4, VIVC 11473) and were planted in 2011. A set of 16 phenotypically extreme F1 genotypes (concerning the lengths of pedicels and rachises) from a controlled cross of ‘Calardis Musqué’ (synonym GF.GA-47-42, VIVC No. 4549) × ‘Villard Blanc’ (VIVC No. 13081) (Zyprian et al. 2016) used in this work (Table 2) were planted in eight replicates on rootstock SO4 at JKI in 2010. The OIV reference varieties and the F1 individuals underwent ‘Guyot pruning’ with approximately 10 buds remaining. They were grown in a vertical shoot position trellis system with 2 m (row) × 1 m (plant) spacing. An integrated pesticide spray program according to the best practice policies for viticulture (BMELV 2010) protects this plantation.

## Sampling

Sampling for phenotypic evaluation: For phenotyping of PN clones at BBCH89 (ripe for harvest), ten vines per

**Table 2** Sampling schedules for phenotypically extreme F1 individuals of the cross ‘Calardis Musqué’ (formerly GF.GA-47-42) × ‘Villard Blanc’ grown in the Palatinate vineyard

Cluster type	Sample	Abbreviation	BBCH 89
Long pedicel	F1# 212, 294, 354, 380 <sup>a</sup>	PEDmax	3–12 <sup>b</sup>
Short pedicel	F1# 194, 558, 594, 598 <sup>a</sup>	PEDmin	3–12 <sup>b</sup>
Long rachis	F1# 059, 405, 484, 503 <sup>a</sup>	RLmax	3–12 <sup>b</sup>
Short rachis	F1# 052, 241, 647, 680 <sup>a</sup>	RLmin	3–12 <sup>b</sup>

For phenotyping of cluster traits, samples of ripe bunches at BBCH89 were taken randomly with 3–12 replicates from replicated ( $n=8$ ) vines of individuals with extreme phenotype

<sup>a</sup>F1 individuals reported in (Richter et al. 2019) with extreme rachis or pedicel length

<sup>b</sup>Biological samples taken in 2013–2017 as stated in Online resource 4

clone were chosen randomly. From each vine, a basally inserted cluster from the central shoot of the fruit cane was collected in the years 2015 and 2016 in every vineyard. A total of 16 F1 genotypes of the cross population ‘Calardis Musqué’ (GF.Ga-47-42) × ‘Villard Blanc’ with extreme rachis length and pedicel length as monitored over four years (Richter et al. 2019) were sampled with 3 to 12 biological replicates over four seasons. Bunches were cut directly at the connection with the shoot and stored at 5 °C until use.

Sampling for gene expression experiments: In the years from 2015 to 2017, the sampling time of the different ‘Pinot Noir’ clones in the three vineyard locations was fitted to hit the same developmental stage by a nonlinear cumulative degree-day (CDD)-based model (Molitor et al. 2014). The target temperature sum was 400° CDD for BBCH57 and 700° CDD for BBCH71. The CDD calculation was based on air temperatures recorded at 2 m height by the nearest weather station. Samples for gene expression analyses were collected from three randomly selected individual plants from the plantation (of about 100–200 individual plants per clone) from the lowest cluster insertion point during the developmental stages BBCH57 (just before flowering) and BBCH71 (at early fruit set) in the three years 2015, 2016 and 2017. OIV reference cultivars ‘Uva Rara’ (OIV#204 grade 1), ‘Prosecco’ (OIV#204 grade 3) and 16 F1 genotypes of the cross population ‘Calardis Musqué’ × ‘Villard Blanc’ with extreme rachis length and pedicel length were sampled with three biological replicates. Complete inflorescences were cut at the connection of peduncle and shoot and shock-frozen immediately in liquid nitrogen. A detailed schedule of the sampling and the temperature records is presented in Tables 3, 4 and Online resource 3.

## Evaluation of vegetative growth

The vigor of the PN clones was determined by measuring the mass of the annual outgrowth, i.e., the weight of the ten most basally located branches on ten vines per season and location (Online resource 2, Table 5).

## Phenotypic evaluation of cluster architecture sub-traits

Measurements of 12 cluster architecture sub-traits (Table 5) were used for the phenotypic assessment of the 12 PN clones. Three indices for cluster compactness were calculated. The calculation of the ratio ‘berry number/rachis length’ [BN/RL (cm), Hed et al. (2009)] and indices CI-12 [berry weight (g)/[rachis length (cm)]<sup>2</sup> and CI-18 [berry weight (g) × berry number/[peduncle length (cm) + rachis

**Table 3** Sampling schedules for 12 ‘Pinot Noir’ clones spread over three locations during three seasons

Cluster type	‘Pinot Noir’ clone	Abbreviation	Palatinate		Hesse		Baden	
			BBCH		BBCH		BBCH	
			57	71	57	71	57	71
CCC	Frank Charisma	FkCH	3 <sup>a</sup>					
CCC	Frank Classic	FkCL	3 <sup>a</sup>	3 <sup>a</sup>	3 <sup>a</sup>	3 <sup>a</sup>	–	–
CCC	Entav 777	En777	–	–	3 <sup>a</sup>	3 <sup>a</sup>	3 <sup>a</sup>	3 <sup>a</sup>
Unsteady	Geisenheim 18	Gm18	–	–	3 <sup>b</sup>	3 <sup>b</sup>	–	–
MBC	Geisenheim 20-13	Gm20-13	3 <sup>a</sup>					
MBC	Freiburg 1801	Fr1801	–	–	3 <sup>b</sup>	3 <sup>b</sup>	3 <sup>a</sup>	3 <sup>a</sup>
LCC	Geisenheim 1-86	Gm1-86	3 <sup>a</sup>	3 <sup>a</sup>	3 <sup>a</sup>	3 <sup>a</sup>	–	–
LCC	Freiburg 12-L	Fr12L	–	–	3 <sup>b</sup>	3 <sup>b</sup>	3 <sup>b</sup>	3 <sup>b</sup>
LCC	Freiburg 13-L	Fr13L	–	–	3 <sup>b</sup>	3 <sup>b</sup>	3 <sup>b</sup>	3 <sup>b</sup>
LCC	Weinsberg M1	WeM1	–	–	3 <sup>b</sup>	3 <sup>b</sup>	–	–
LCC	Weinsberg M171	WeM171	3 <sup>a</sup>	3 <sup>a</sup>	–	–	–	–
LCC	Weinsberg M242	WeM242	–	–	3 <sup>b</sup>	3 <sup>b</sup>	–	–

For gene expression studies, samples of whole inflorescences at BBCH57 and BBCH71 were taken with three replicates from randomly selected independent vines. The expression measurements of the PN clone ‘Gm20-13’ were used for normalization of the relative PN gene expression at all three locations

– not available

<sup>a</sup>Three biological samples taken in 2015, 2016 and 2017

<sup>b</sup>Three biological samples taken in 2016 and 2017

**Table 4** Sampling schedules for phenotypically extreme F1 individuals of the cross ‘Calardis musqué’ (formerly GF.GA-47-42) × ‘Villard Blanc’ and OIV reference varieties for loose cluster architecture

Cluster type	Variety name # F1 individual	Abbreviation	Palatinate BBCH71
OIV 204 reference for very loose cluster <sup>a</sup>	‘Uva Rara’	OIV LCC	3 <sup>b</sup>
OIV 204 reference for loose cluster <sup>a</sup>	‘Prosecco’	OIV LCC	3 <sup>b</sup>
Long pedicel <sup>c</sup>	F1# 212, 294, 354, 380	PEDmax	3 <sup>b</sup>
Short pedicel <sup>c</sup>	F1# 194, 558, 594, 598	PEDmin	3 <sup>b</sup>
Long rachis <sup>c</sup>	F1# 059, 405, 484, 503	RLmax	3 <sup>b</sup>
Short rachis <sup>c</sup>	F1# 052, 241, 647, 680	RLmin	3 <sup>b</sup>

For gene expression studies, samples of whole inflorescences at BBCH57 and BBCH71 were taken randomly with three replicates from eight cloned phenotypically extreme vines of the segregating population and three replicates of the OIV reference varieties

<sup>a</sup>Reference varieties for loose cluster architecture according to the OIV descriptor 204 for cluster density (OIV 2015)

<sup>b</sup>Three biological samples taken in 2015, 2016 and 2017

<sup>c</sup>F1 individuals reported in (Richter et al. 2019) with extreme measurements for rachis length and pedicel length

length (cm)]<sup>2</sup> × rachis length (cm) × pedicel length (mm)] followed the proceedings stated in Tello and Ibáñez (2014). The 16 F1 individuals of the cross population ‘Calardis Musqué’ × ‘Villard Blanc’ were phenotypically studied for cluster architecture sub-traits during four seasons as described (Richter et al. 2019) (Online resource 4).

### RNA extraction and cDNA synthesis

For RNA extraction and cDNA synthesis, pre-bloom flowers (BBCH57) and fruit setting berries (BBCH71) were carefully removed from the inflorescence. The complete remaining stalk structure including peduncle, rachis and pedicels was ground into fine powder. All steps were performed in liquid nitrogen. Aliquots of sample tissue were mixed with 50 mg polyvinylpyrrolidone Polyclar® AT (Serva Electrophoresis GmbH, Heidelberg, Germany). Total RNA extraction used the Spectrum™ Plant Total RNA Kit (Sigma Aldrich, Darmstadt, Germany), following protocol ‘A’. An on-column DNaseI digestion with RNase-Free DNase (QIAGEN, Hilden, Germany) was performed according to the manufacturer’s protocol. RNA integrity and quantity were analyzed by spectrophotometry (Clario Star 0430, BMG Labtech, Ortenberg, Germany) and checking 500 ng of total RNA by non-denaturing agarose gel (1%) electrophoresis. 250 ng of total RNA was used for first-strand cDNA

**Table 5** Morphometric measurements on cluster architecture for 12 ‘Pinot Noir’ clones at BBCH89 recorded over three locations and two seasons

Trait	Abbrevia- tion	En777	FKCH	FKCL	Fr12L	Fr13L	Fr1801	Gm20-13	Gm1-86	WeM1	WeM171	WeM242	Gm18
		Compact	Compact	Compact	Loose	Loose	Loose	Loose	Loose	Loose	Loose	Loose	Unsteady
<b>Berry number</b>	BN (#)	157.41 (±5.85)abc	167.1 (±4.82)bc	161.4 (±5.93)abc	164.97 (±6.17)bc	165.69 (±6.05)bc	141.01 (±6.13)ab	139.72 (±4.53)ab	171.7 (±6.29)c	146.68 (±7.73)abc	149.49 (±8.32)abc	174.58 (±12.78)abc	159.23 (±11.71)abc
<b>Cluster weight</b>	CW (g)	181.04 (±6.94)bc	211.87 (±6.32)bc	193.43 (±7.34)cd	248.11 (±9.62)de	254.19 (±9.63)e	166.76 (±7.46)ab	129.5 (±4.29)a	246.51 (±9.35)de	214.26 (±11.71)cd	222.05 (±12.57)cd	267.91 (±20.62)de	168.84 (±12.99)abc
<b>Mean berry volume</b>	MBV (cm <sup>3</sup> )	0.84 (±0.03)ab	0.87 (±0.02)ab	0.86 (±0.03)ab	1.15 (±0.03)d	1.06 (±0.03)d	0.82 (±0.03)d	0.66 (±0.02)a	1.05 (±0.03)cd	1.15 (±0.04)d	1.12 (±0.04)d	1.17 (±0.05)d	0.85 (±0.05)abc
<b>Total berry Volume</b>	TBV (cm <sup>3</sup> )	129.11 (±5.35)bc	143.24 (±4.62)cd	134.08 (±5.5)bcd	190.15 (±7.98)f	173.19 (±7.09)ef	112.12 (±5.42)ab	91.1 (±3.26)a	170.65 (±7)ef	164.86 (±9.74)def	158.3 (±9.69)cd	195.35 (±16.25)f	133.53 (±11.11)bcde
<b>Rachis length</b>	RL (cm)	10.91 (±0.25)a	13.18 (±0.2)b	12.62 (±0.25)ab	15.77 (±0.26)ef	15.6 (±0.25)e	16.26 (±0.3)ef	12.83 (±0.22)ab	12.61 (±0.51)abc	15.26 (±0.36)de	15.74 (±0.38)def	17.55 (±0.51)f	14.39 (±0.25)cd
<b>Shoulder length</b>	SL (cm)	6.93 (±0.45)a	9.16 (±0.35)bcd	8.01 (±0.45)ab	10.34 (±0.46)cd	10.17 (±0.45)cd	11.04 (±0.53)d	9.44 (±0.39)bcd	9.11 (±0.45)bcd	9.36 (±0.65)abcd	9.76 (±0.67)bcd	11.7 (±0.91)d	7.3 (±0.91)abc
<b>Pedicle length</b>	PL (cm)	0.47 (±0.01)a	0.48 (±0.01)a	0.47 (±0.01)a	0.56 (±0.01)d	0.56 (±0.01)d	0.5 (±0.01)ab	0.48 (±0.01)ab	0.56 (±0.01)d	0.56 (±0.01)d	0.52 (±0.01)bc	0.59 (±0.01)d	0.5 (±0.01)ab
<b>Peduncle length</b>	PL (cm)	1.24 (±0.1)abcd	1.16 (±0.07)abc	1.13 (±0.09)ab	1.38 (±0.11)abcd	1.58 (±0.11)bcd	1.14 (±0.11)abc	1.02 (±0.08)a	1.72 (±0.12)d	1.65 (±0.17)bcd	1.42 (±0.16)abcd	1.93 (±0.27)cd	1.05 (±0.19)abcd
<b>Rachis weight</b>	RW (g)	7.4 (±0.36)abc	8.76 (±0.28)cd	8.25 (±0.36)abcd	8.94 (±0.37)cd	8.21 (±0.36)abcd	8.12 (±0.42)abcd	6.69 (±0.31)a	9.62 (±0.36)de	6.78 (±0.52)ab	8.72 (±0.53)bcde	10.97 (±0.73)e	7.81 (±0.73)abcde
<b>Rachis diameter</b>	RD (cm)	0.4 (±0.01)bc	0.35 (±0.01)a	0.39 (±0.01)bc	0.4 (±0.01)bc	0.4 (±0.01)bc	0.38 (±0.01)bc	0.39 (±0.01)ab	0.42 (±0.01)c	0.38 (±0.01)ab	0.38 (±0.01)abc	0.43 (±0.02)bc	0.37 (±0.02)abc
<b>first internode length</b>	L1I (cm)	1.27 (±0.11)a	1.31 (±0.09)a	1.26 (±0.11)a	1.53 (±0.12)a	1.26 (±0.11)a	1.6 (±0.13)a	1.3 (±0.1)a	1.45 (±0.11)a	1.53 (±0.16)a	1.46 (±0.17)a	2.08 (±0.23)a	1.45 (±0.23)a
<b>second internode length</b>	L2I (cm)	1.28 (±0.09)a	1.27 (±0.07)a	1.29 (±0.09)a	1.49 (±0.09)a	1.54 (±0.09)a	1.13 (±0.11)a	1.21 (±0.08)a	1.37 (±0.09)a	1.46 (±0.13)a	1.47 (±0.14)a	1.49 (±0.19)a	1.35 (±0.19)a
<b>seasonal wood gain</b>	WG (g)	790 (±30)bc	716 (±21)abc	613 (±23)a	702 (±27)abc	672 (±25)ab	807 (±36)bc	790 (±26)bc	807 (±31)c	677 (±37)abc	676 (±38)abc	693 (±53)abc	755 (±58)abc
<b><sup>a</sup>Index</b>	BN/ RL (cm)	14.39 (±0.51)f	12.73 (±0.35)ef	12.81 (±0.45)ef	10.57 (±0.38)bcd	10.77 (±0.37)bcd	8.84 (±0.36)a	10.94 (±0.33)bcd	12.01 (±0.42)de	9.8 (±0.49)abc	9.48 (±0.49)ab	10.16 (±0.72)abcde	12.71 (±0.7)cd
<b><sup>b</sup>Index</b>	CL <sub>12</sub>	1.49 (±0.07)f	1.19 (±0.04)ef	1.17 (±0.05)de	0.99 (±0.05)cd	1.04 (±0.05)cd	0.63 (±0.03)a	0.78 (±0.03)b	1.17 (±0.05)de	0.93 (±0.06)bcd	0.87 (±0.06)bc	0.87 (±0.08)abcd	1.06 (±0.09)bcde
<b><sup>c</sup>Index</b>	CL <sub>18</sub>	4.91 (±0.43)f	3.24 (±0.22)ef	3.24 (±0.28)de	1.77 (±0.16)abc	1.96 (±0.17)abc	1.31 (±0.13)a	2.26 (±0.17)bcd	2.31 (±0.2)ab	1.58 (±0.2)ab	1.89 (±0.24)abc	1.33 (±0.23)ab	3.26 (±0.57)cd

Estimated (marginal) means of sub-traits and compactness indices for each clone adjusted for the effects of ‘location’ and ‘season’ as predicted from the generalized linear model ‘sub-trait’ ~ loc\*year+clone (details in Online resource 6). (±) represents the standard error. Different letters indicate significantly divergent values for sub-traits and compactness indices as identified with a Tukey HSD test at significance level  $\alpha = 0.05$

<sup>a</sup>According to Hed et al. (2009)

<sup>b</sup>According to Tello and Ibáñez (2014)

<sup>c</sup>Based on CL-18 stated in Tello and Ibáñez (2014) but omitting seed number. Cluster architecture sub-traits indicated in bold are major contributors to cluster density levels (Richter et al. 2019)

synthesis with the high-capacity cDNA Transcription Kit (Applied Biosystems, Thermo Fisher Scientific, Waltham, MA, USA).

### Primer design for RT-qPCR

Primer pairs (Online resource 5) for quantitative RT-PCR (RT-qPCR) were designed as recommended in (Citri et al. 2012) using the CLC main workbench primer design software tool (CLC Main Workbench Version 8.0.1, QIAGEN [www.qiagenbioinformatics.com](http://www.qiagenbioinformatics.com)). PCR amplification efficiencies of the primer pairs for the 91 targets and 2 endogenous control genes were validated as suggested by Schmittgen and Livak (2008). Standard RT-qPCRs were performed using the Power SYBR-Green PCR Master Mix (Applied Biosystems). The specificity of the amplification was affirmed by visual inspection of the amplification products followed by melting curve analysis and gel electrophoresis of the PCR products (after 40 thermal cycles, size inspection on 3% agarose gels).

### Expression analysis using high-throughput quantitative real-time PCR

Expression analysis applied the high-throughput BioMark™ HD (Fluidigm Corporation, Munich, Germany) system with dynamic array chips (96.96 GE IFC; Fluidigm) according to the manufacturer's instruction. Fluorescence data recording and processing were done with the BioMark Real-Time PCR Analysis Software 3.0.2 (Fluidigm).

The overall quality score of the experiment was 0.945. Variation between the chips was low (0.92–0.97).  $C_t$  values of several 96.96 IFC chips were combined with their metadata in an expression set using the R-package 'HT-q-PCR' (Dvinge and Bertone 2009). All  $C_t$  values below 5 and  $C_t$  values of genes showing little variation between the samples (with an inter-quartile range below 0.6) were discarded.

The relative amount of mRNA was calculated based on the  $C_t$  value (cycle number at threshold). The cycle threshold was determined with the automatic linear baseline setting. For normalization of the relative gene expression values, the genes *VIT\_17s0000g10430* encoding glyceraldehyde-3-phosphate dehydrogenase (*GAPDH*) and *VIT\_08s0040g00040* encoding ubiquitin-conjugating enzyme E2 (*UBIc*) served as references. These genes have already been successfully applied in other grapevine RT-qPCR studies, e.g., (Monteiro et al. 2013; Reid et al. 2006; Selim et al. 2012; Upadhyay et al. 2015). Their expression proved to be stable (rank invariant) in rachis tissue over clones, locations and growing seasons (as revealed with

the function 'normalizectdata' of the package 'HT-qPCR'). To obtain the  $\Delta C_t$  value, the  $C_t$  value of each target gene was normalized by subtraction of the mean  $C_t$  values of the two endogenous reference genes (*GAPDH* and *UBIc*). For gene expression comparisons between F1 siblings, varieties, clones, seasons and vineyard locations, the  $2^{-\Delta\Delta C_t}$  value was calculated (Livak and Schmittgen 2001).

### Statistics

All statistics employed R-software version 3.5.3 (R Core Team 2013). All statistic tests were set to a significance threshold of  $p = 0.05$ .

Cluster architecture: The environmental impact on each cluster architecture sub-trait was assessed using generalized linear models (GLM) with clone, location, season and the two-way interaction between location and season as explanatory variables. For count data, a GLM with Poisson distribution or (when overdispersed) negative binomial distribution was fitted. For strictly positive continuous responses, a Gamma-GLM with log link or a linear model was applied. Model residuals were visually assessed, and dispersion was checked when applicable. Effects were tested using type three analysis of variance and the function 'Anova' of the package 'car' (Fox and Weisberg 2011) and visualized using the function 'alleffects' of the package 'effects' (Online resource 6). Estimated marginal means, post hoc tests and pairwise comparisons with compact letter display were calculated for the effect of 'clone' on the response while accounting for the effects of 'season' and 'location' using the functions 'emmeans' and 'CLD' of the package 'emmeans' (Lenth 2019). The significance level was set to 0.05 (Table 5).

Differential gene expression, denoted as fold change (FC), was calculated using the package 'limma' (Matthew et al. 2015). A design matrix containing the experimental data for all investigated PN clones, varieties and F1 siblings, at up to three trial locations and three seasons, was generated with the function 'model.matrix'. The correlation between technical replicates was estimated with the function 'duplicatecorrelation.' Differential gene expression was analyzed by fitting gene-wise linear models using the design matrix, the estimated correlation and the function 'lmFit.' To interpret different gene expression values, the empirical Bayes method was used to modify the standard errors toward a common value using the 'eBayes' function.

Contrast: The  $\log_{(2)} FC (-\Delta\Delta C_t)$  for each gene was calculated by the expression difference to the selected standard PN clone Gm20-13 using the function 'contrasts.fit'. The relative expression ( $2^{-\Delta C_t}$ ) of each Gm20-13 gene at any

individual location and season of was subtracted from the ( $2^{-\Delta C_t}$ ) of the test genes in all the other investigated PN clones for standardization. Following the same principle, a contrast was calculated by subtracting the ( $2^{-\Delta C_t}$ ) of the genes active in compactly clustered PN clones from those in the loosely clustered varieties ‘Uva Rara’ and ‘Prosecco.’ The contrast for the F1 siblings was calculated by subtracting the ( $2^{-\Delta C_t}$ ) of the test genes in F1 siblings with short pedicels and rachis lengths from the ( $2^{-\Delta C_t}$ ) of the test genes in F1 individuals with extreme long rachises and pedicels, respectively. The identification of ‘regulated genes’ applied the limma package that determined differential gene expression with a threshold level of  $p \leq 0.05$ .

The results of relative gene expression were displayed in heatmaps as  $\log_2$  FC ( $-\Delta\Delta C_t$ ) using the package ‘pheatmap’ (Kolde 2015). Row-scaled data (gene-wise) and Euclidian distance were used for hierarchical clustering. Expression data of tested genes ( $\log_2$  FC), displayed in box–whisker plots, were obtained in the same way as stated above, but with the contrast matrix containing additionally the biological replication (Fig. 7b, c).

Variance partition: To estimate the variation in this multilevel gene expression experiment, the package ‘variancePartition’ was used with the  $\log_2$  of  $\Delta C_t$ . A linear mixed model with the random effects season, location, batch, biological replicate, cluster type, clone and gene pool identified the typical drivers of variance. These factors can be classified as environmental (‘season’ and ‘location’), technical (two repeated ‘batches’), biological (three independent ‘replicates’), phenotypic (‘cluster type’) and genetic (‘clone’ and ‘gene pool,’ i.e., selection background of ENTAV, Frank, Fr (Freiburg), Gm (Geisenheim) and We (Weinsberg) clones) (Hoffman and Schadt 2016).

Correlation between relative test gene expression, expressed as  $\log_2$  FC ( $-\Delta C_t$ ), and cluster architecture sub-trait records of PN clones for 2015 and 2016 were calculated with Spearman rank correlation test using the function ‘rcorr’ from the package ‘Hmisc’ (Harrell Jr 2015).

## Gene annotation

The gene identifiers of the Gramene database version IGGP\_12x.54 ([http://ensembl.gramene.org/Vitis\\_vinifera/Info/Index](http://ensembl.gramene.org/Vitis_vinifera/Info/Index)) were used to retrieve the nucleotide sequences of the candidate genes. These sequences were submitted to Blast searches (Altschul et al. 1990) in the NCBI GenBank (<https://www.ncbi.nlm.nih.gov/Blast.cgi>). The best match (Blastx) of the translated sequences of candidate genes with homologous genes from non *Vitis* species is used as functional annotation.

## Analysis of co-expression

An analysis of co-expression was performed with the gene expression compendium ‘Vespucci’ (Moretto et al. 2016a). The expression profiles of 14 candidate genes and *VvGRF4* were determined in 21 selected samples containing inflorescence, rachis and tendril tissue of the *V. vinifera* cultivars ‘Corvina’ and ‘Tempranillo,’ reported by Fasoli et al. (2012) and Diaz-Riquelme et al. (2014). The following ‘Vespucci’ Sample IDs have been used for co-expression analysis: ID 2210, 2211, 2225, 227, 229, 334, 335, 336, 347, 346, 348, 228, 230, 231, 232, 233, 234, 235, 307, 308 and 309. The ‘Vespucci’ inference was based on the publicly available transcriptomics data and integrated by the COLOMBOS v3.0 database (Moretto et al. 2016b).

## Results

### Trueness to type of the investigated PN clones

Microsatellite-derived markers known for their ability to reveal polymorphisms in PN clones (Pelsy et al. 2010) were applied to check the integrity of the plant material over the three plantations in Palatinate, Hesse and Baden. The data (Online resource 1) confirmed the trueness of type of the plants over all locations. The PN clones ENTAV777 and Geisenheim 1-86 showed the same genetic variation at the different locations, in agreement with the data reported by Pelsy et al. (2010).

### Cluster architecture characteristics and vitality of PN clones

The typical differences in cluster architecture (CA) exhibited by PN clones at stage BBCH89 (berries ripe for harvest) are depicted in Fig. 1. The morphological characteristics of ripe bunches were evaluated in 12 PN clones spread over the three geographic locations in 2015 and 2016 at BBCH89 (Table 1, Online resource 2).

The ratio ‘berry number/rachis length’ (Hed et al. 2009) and indices CI-12 and CI-18 (Tello and Ibáñez 2014) were used to categorize the PN clones according to their cluster density. In this way, the general visual classification in loose and compact clones (Ruehl et al. 2004) was confirmed, and the clones were characterized as three CCC, two MBC and six LCC (Tables 1, 5). The clone Gm18 remained unclassified due to high variability in the measurement results recorded for the sub-traits represented in the indices.

In total, 12 sub-traits of cluster architecture (CA) were evaluated. Between the clones, 10 out of the 12 sub-traits differed significantly (The lengths of the first rachis

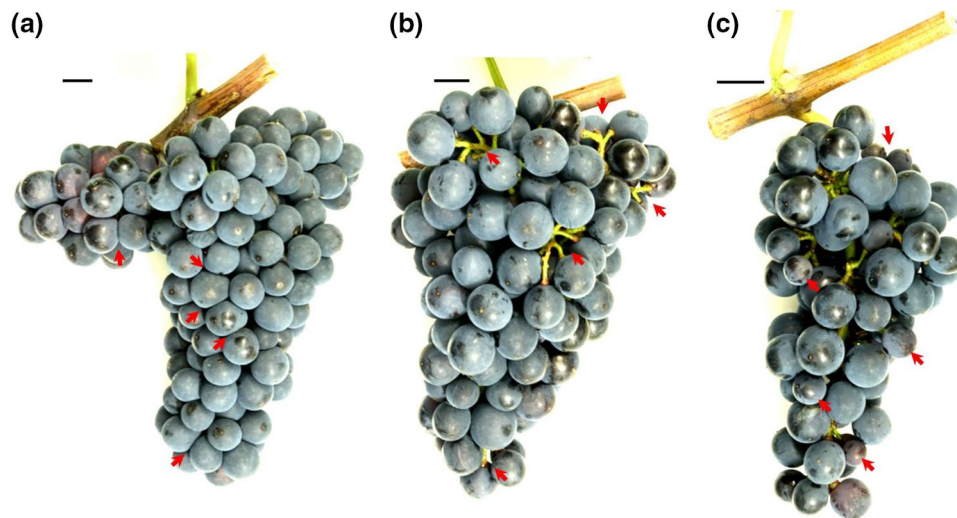


**Fig. 1** Clones of *V. vinifera* cv. ‘Pinot Noir’ with different cluster architecture. Phenological stage BBCH89 (berries ripe for harvest) was used for cluster architecture assessment. **a** The PN clone ‘Frank Charisma’ as an example for compactly clustered clones with non-circular-shaped berries due to high pressure between the berries. **b** The PN clone ‘Geisenheim 1-86’ as an example for loosely clustered

clones with visibly extended pedicel length. **c** The PN clone ‘Freiburg 1801’ as an example for clones partially bearing smaller berries leading to reduced compactness (mixed berried clones). Red arrows highlight the emphasized cluster architecture feature. The size standard depicts 1 cm. Developmental stages according to Lorenz et al. (1995) (color figure online)

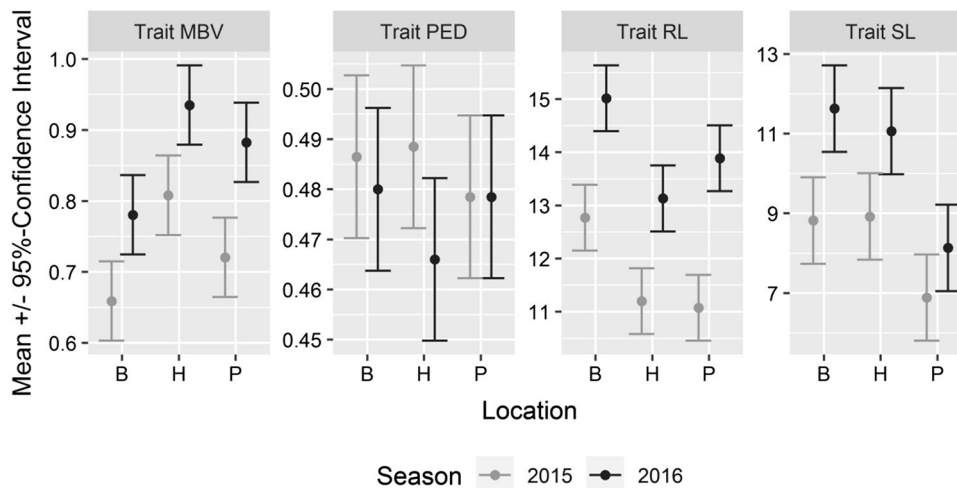


**Fig. 2** Effects of sampling locations and growing seasons on cluster architecture sub-traits for the ‘Pinot Noir’ clones Gm20-13 and FkCH. These two clones could be sampled across all seasons and locations ( $n=120$ ). Estimated marginal means and 95% confidence intervals were obtained from generalized linear models. The CA sub-

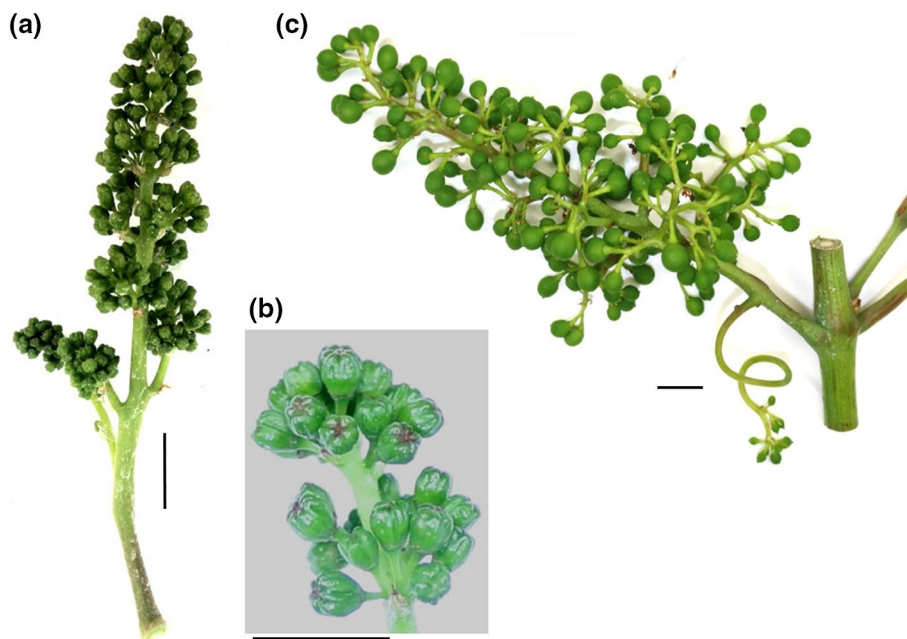
traits rachis length (RL), shoulder length (SL) and mean berry volume (MBV) were clearly influenced by ‘season.’ In contrast, pedicel length (PED) was affected neither by ‘season’ nor by ‘location’ (Online resource 6)

internode (I1L) and second rachis internode (I2L) did not vary). Table 5 summarizes the morphometric data of the bunches. The loosely clustered clones from Freiburg (Fr12L, Fr13L) and from Weinsberg (WeM1, WeM171, WeM242) shared long rachis lengths and larger berry volume. The clones Fr12L, Fr13L and WeM242 showed extended pedicel lengths, as did the loosely clustered clone Gm1-86 from Geisenheim. However, the latter clone (Gm1-86) formed

shorter rachises. Compact PN clones in general produced small berries with short pedicels at reduced rachis lengths. This analysis also revealed mixed berried clones that differed concerning berry volume and berry number in comparison with their co-members from the same clonal selection lines. They also exhibited a loose CA.

The effects of the environmental factors ‘season’ and ‘location’ on CA were evaluated using the clones Gm20-13

**Fig. 3** For differential gene expression studies, BBCH57 (a) (just before flowering with still closed flower caps (b)) and BBCH71 (c) (berry set) samples were used. For each time point, three biological replicates were collected from different vines. The sampled vines were chosen randomly within a plantation of several hundred individuals of each clonal variant. Only vines without any indication of pathogen infection or physiological disorder were sampled



and FkCH since these clones were common to all three locations (Hesse, Baden and Palatinat). The evaluation of generalized linear models revealed that ‘season’ affected berry number (BN), mean berry volume (MBV), total berry volume (TBV), rachis length (RL), shoulder length (SL) and rachis weight (RW). The factor ‘location’ influenced cluster weight (CW), mean berry volume (MBV), total berry volume (TBV), rachis length (RL), shoulder length (SL) and rachis weight (RW). The values for peduncle lengths (PL) and pedicel lengths (PED) in Gm20-13 and FkCH were stable and did not differ between locations and seasons (Fig. 2, Online resource 6a and 6b).

In addition to CA sub-traits, the annual wood gain was recorded as indicator of plant vigor (Table 5). The values of clones Gm20-13 and FkCH attained during the seasons 2015 and 2016 differed significantly between the three locations (Online resource 2). The highest wood gain per vine was achieved in Baden (average 1136 g, integrated management), followed by Hesse (average 758 g, integrated management) and Palatinat (average 456 g, vineyard under organic management). Wood gain (WG) was not significantly affected by season (Online resource 6). The morphometric measurements served to study differential gene expression in association with cluster architecture features.

### Identification of genes regulated in association with cluster architecture sub-traits

In total, 80 candidate genes were selected based on a previous RNA-Seq study reported by analysis of each two loosely and compactly clustered PN clones (Rossmann et al. 2019).

These genes had shown a significant fold change of at least 1.5 between loose and compact clones. In addition, 11 candidate genes were selected for analysis based on their implication in inflorescence development as reported in the literature. A list of all genes is presented in Online resource 5. The gene *VvGRF4* was included to check its implication in cluster compactness in an extended set of ‘quasi isogenic’ PN clones from various selection backgrounds and over multiple environments.

Accelerated inflorescence growth of loosely as compared to compactly clustered PN clones just before flowering (BBCH57) and at early fruit set (BBCH71) has been reported (Richter et al. 2017). Hence, these time points were chosen for the expression analysis in the 11 PN clones of LCC, MBC and CCC phenotype (Fig. 3). The clone Gm20-13 had a special distinct phenotype (small berries, short rachises) and served as reference to standardize the gene expression data.

Quantitative real-time PCR was performed on developed inflorescences (BBCH57) and on young clusters at fruit set (BBCH71). Data were normalized to the internal controls (*GAPDH* and *UBIc*), standardized with Gm20-13 values and reported as logarithm of the fold change ( $-\Delta\Delta C_t$ ). In total, 40 genes at BBCH57 and 81 genes at BBCH71 appeared differentially expressed between the PN clones of LCC, MBC or CCC phenotype (Online resource 7). Out of these, 15 genes were differentially expressed over all conditions, independently from environmental factors ‘season’ and ‘location’ (as inferred with moderated T-statistics using empirical Bayesian modeling, Smyth 2004). Three genes were consistently differentially active at the early stage of BBCH57 (Fig. 4). They included the gene encoding

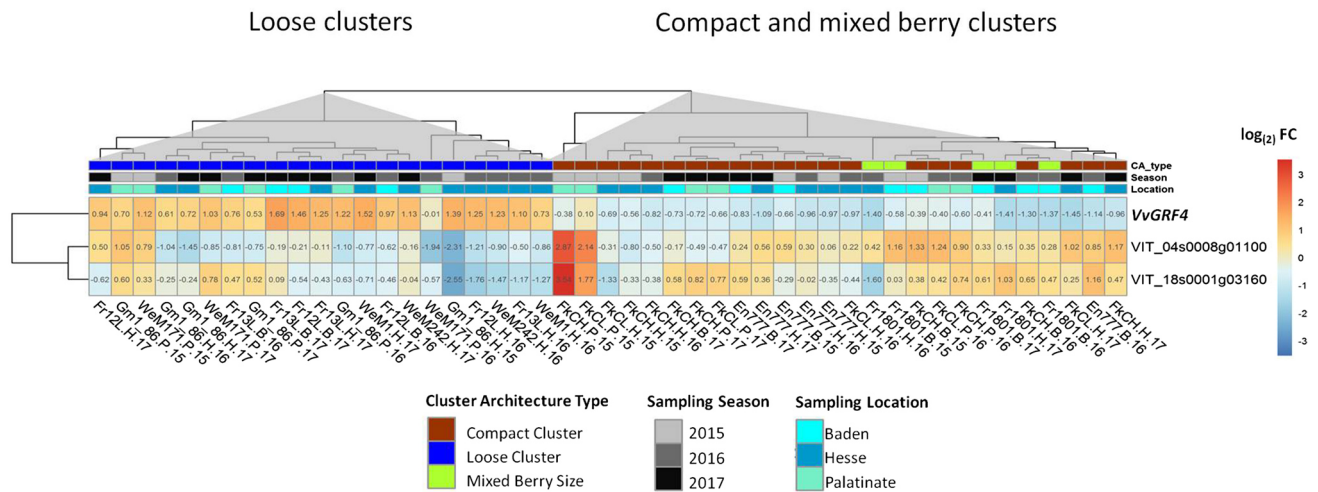


**Fig. 4** Heatmap of the averaged (three biological and two technical replicates) relative gene expression values as  $\log_2 FC$  ( $-\Delta\Delta C_t$ ) of selected genes at BBCH57. The gene expression relative to the mean of *GAPDH* and *UBIc* was analyzed just before flowering (BBCH57) and standardized relative to the PN clone Gm20-13. The rows show the relative expression of the genes. The columns represent the ‘Pinot

Noir’ samples. The clones are indicated at the bottom with their abbreviated name, their location (*B*=Baden, *H*=Hesse, *P*=Palatinate) and the year of sampling (15=2015, 16=2016, 17=2017). Hierarchical clustering (based on Euclidian distances) revealed similarities in gene regulation in the PN clones depending on their cluster architecture (CA) type. LCCs are separated from CCCs and MBCs

transcription factor *VvGRF4*, as expected from the former study (Rossmann et al. 2019), assessed here in a larger clone set. In addition, the two genes *VIT\_04s0008g01100* (encoding a cytochrome P450 CYP711A1-like gene, named *MAX1* in Arabidopsis) and *VIT\_18s0001g03160* (annotated as a WAT1-related protein) were differentially expressed at this early stage under all conditions.

*VvGRF4* was differentially expressed both at BBCH57 and at BBCH71. In agreement with former results, its activity was high in LCC clones and down-regulated in CCC (Figs. 4, 5). The expression of *VvGRF4* in MBCs resembled the pattern seen in CCCs.

After fruit set and begin of fruit development (BBCH71), 11 more genes were found to be differentially expressed between loose and compact PN clones independently from all seasons and locations.

Hierarchical clustering based on their expression values grouped them into five clusters of similar expression patterns (Table 6, Fig. 5). Clustering of PN clones showed a clear separation of LCCs from CCCs and MBCs (Fig. 5).

In expression cluster I, the transport- and phytohormone-related genes *VIT\_04s0008g01100* (*CYP711A1*-like), *VIT\_08s0007g01370* (*DIR1*-like), *VIT\_18s0001g03160* (*WAT1*-like) and *VIT\_18s0001g0489* (*SULTRA3*-like) were down-regulated in the majority of LCCs, while they showed only little expression changes in most MBCs and CCCs. The gene *VvGRF4* formed a separate cluster II and followed a homogenous differential expression pattern specific to loose and compact/mixed berried clones,

respectively. It was more active in LCC clones. Cluster III combined the genes *VIT\_17s0000g05000* (*SEP1*-like), *VIT\_18s0001g03540* (*AUX1*-like) and *VIT\_18s0001g11160* (*MIZU-KUSSELI*-like). The products of these genes relate to transcription regulation (transcription factor *SEPAL-LATA1*-like), auxin transport and auxin homeostasis. They were up-regulated in most LCCs to a much larger extent than in CCCs. Cluster IV contains gene *VIT\_01s0026g02030*. It probably encodes a non-DNA binding basic helix-loop-helix (bHLH) transcription factor *PRE6*. For this transcription factor gene, the LCCs showed higher expression than the CCCs. The MBCs showed a heterogeneous range of differential expression extending from  $-4.35$  to  $0.39$ . In cluster V, expression patterns showed the highest heterogeneity. The genes *VIT\_01s0010g02430* (*MAD2*-like), *VIT\_01s0127g00870* (*PG1*-like), *VIT\_17s0000g03750* (*LYM1*) and *VIT\_17s0053g00990* (*EXPA1*-like) encode proteins related to cell wall synthesis or cellular growth. The products of the genes *VIT\_02s0025g04720* (*LDOX*) and *VIT\_18s0001g05060* (*PGM*) are associated with proanthocyanidin synthesis resp. glycolysis/gluconeogenesis. Few CCC samples showed divergent (up-regulated) gene expression affected by ‘season’ and ‘location’ (e.g., Hesse 2015). Interestingly, the LCC samples from Palatinate (under organic farming) showed repression for four genes in cluster V in contrast to the clones from the other locations managed by integrated viticulture practices (Fig. 5). The expression changes are summarized in Table 6.

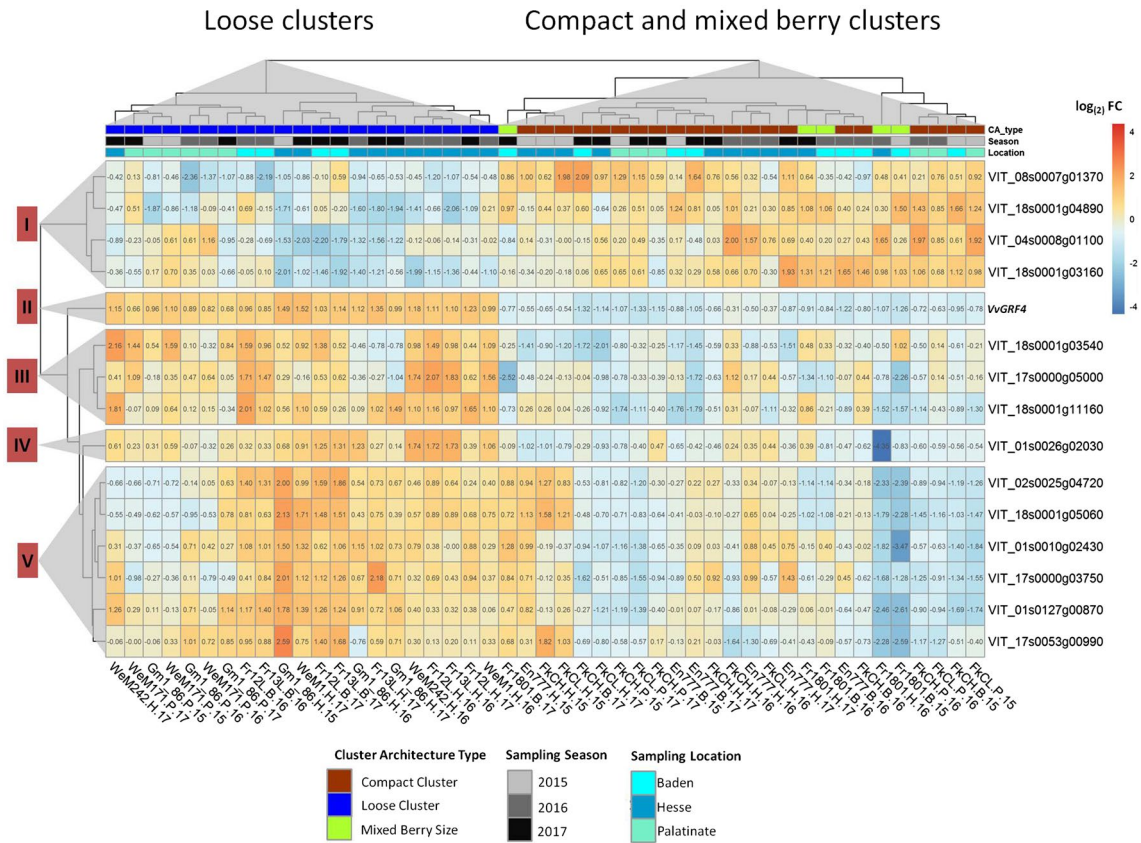


**Fig. 5** Heatmap of the averaged (three biological and two technical replicates) relative gene expression values as  $\log_2 FC$  ( $-\Delta\Delta C_t$ ) of selected genes at BBCH71. The gene expression relative to the mean of *GAPDH* and *UBIc* was analyzed just after flowering (BBCH71) and standardized relative to the PN clone Gm20-13. The rows show the relative expression of the genes. The columns represent the ‘Pinot Noir’ samples. The clones are indicated at the bottom with their

abbreviated name, their location (*B*=Baden, *H*=Hesse, *P*=Palatinate) and the year of sampling (15=2015, 16=2016, 17=2017). Hierarchical clustering (based on Euclidian distances) revealed similarities in gene regulation in the PN clones depending on their cluster architecture (CA) type. LCCs are separated from CCCs and MBCs. The genes expression data form five clusters of similar patterns (as indicated by numbers at the left-hand side)

### Variance of gene expression in PN explained by experimental factors

In order to determine to which extent the modulations of gene expression were affected by the experimental factors, a variance partition analysis was carried out. For all the identified genes, the factor ‘cluster type’ explained a substantial percentage of the variance in gene expression. The factors ‘location’ and ‘season’ also showed clear effects (Fig. 6, Online resource 8).

At the early time point, (BBCH57) the main cause of variance for *VvGRF4* was ‘cluster type’ (58% explained variance). For *VIT\_18s0001g03160* (a vacuolar auxin transporter, *WAT1*-like), it was ‘season’ (26%). The variance of *VIT\_04s0008g01100* (*CYP711A1*-like) was mainly explained by the factor ‘location’ (22%) at this early developmental stage.

At the later developmental stage, BBCH71, the factor ‘cluster type’ was the major determinant of gene

expression variation of almost all 15 investigated genes. The sole exception was *VIT\_18s0001g03540* (*AUX1*-like, with only 14% of variance explained by ‘cluster type’ but over 20% by the factor ‘location’). The variance of *VvGRF4* gene expression was explained to more than 80% by ‘cluster type,’ and the environment caused little variation (‘location’ 0%, ‘season’ 2.6%). The factor ‘season’ was an important determinant of gene expression variation explaining more than 20% of variance for the genes *VIT\_08s0007g01370* (*DIR1*-like), *VIT\_17s0000g05000* (*SEP1*-like), *VIT\_17s0053g00990* (*EXPA1*-like) and *VIT\_18s0001g03540* (*AUX1*-like) (Fig. 6, Online resource 8).

The gene *VIT\_18s0001g04890* (*SULTR2*-like) was affected by factor ‘batch’ (technical replicates), and the genes *VIT\_01s0010g02430* (*MAD2*), *VIT\_01s0026g02030* (*PRE6*), *VIT\_01s0127g00870* (*PG1*-like) and *VIT\_18s0001g11160* (*Mizu-Kussell*-like) varied to some extent also over the biological replicates (Online resource 8).

**Table 6** Average gene expression fold change  $\log_2$  FC ( $-\Delta\Delta C_i$ ) at early fruit development stage (BBCH71) in loosely clustered clones (LCCs), mixed berried clones (MBCs) and compactly clustered clones (CCCs) as compared to the standard ‘Pinot Noir’ clone Gm20-13

Cluster <sup>a</sup>	Mean <sup>b</sup> (median) LCCs	Mean <sup>b</sup> (median) MBCs	Mean <sup>b</sup> (median) CCCs	Gene ID <sup>c</sup> (gramene)	Gene symbol	Annotated function (GenBank NCBI)	Gene ID <sup>d</sup> (NCBI)	Description NCBI blastp for protein sequence <sup>e</sup>	E- valu e <sup>f</sup>	Accession no. of homologu e <sup>g</sup>
c1	-0.79 (-0.59)	-0.17 (-0.22)	-0.03 (-0.11)	VIT_04s0008g01100	CYP711A1-like	PREDICTED: cytochrome P450 711A1 [Vitis vinifera]	LOC100243924	Cytochrome P450 711A1-like isoform X1 [Juglans regia]	0.0	XP_018844671.1
c1	-0.91 (-0.92)	-0.15 (-0.11)	0.03 (0.07)	VIT_08s0007g01370	DIR1-like	Uncharacterized protein [Vitis vinifera]	LOC100240776	Putative lipid-transfer protein DIR1 [Camellia sinensis]	3e-53	XP_028090966.1
c1	-1.29 (-1.22)	-0.10 (0.01)	-0.34 (-0.27)	VIT_18s0001g03160	WAT1-like	WAT1-related protein [Vitis vinifera]	LOC100242142	PREDICTED: WAT1-related protein At4g08300-like [Populus euphratica]	0.0	XP_011027560.1
c1	-0.93 (-0.87)	-0.15 (-0.12)	-0.34 (-0.39)	VIT_18s0001g04890	SULTR2-like	PREDICTED: low affinity sulfate transporter 3 [Vitis vinifera]	LOC100252269	PREDICTED: low affinity sulfate transporter 3-like [Quercus suber]	0.0	XP_023904544
c2	2.88 (2.93)	0.05 (0.13)	0.24 (0.28)	VIT_16s0003g01450	VvGRF4	PREDICTED: growth-regulating factor 4 isoform X2 [Vitis vinifera]	LOC100259737	Growth-regulating factor 4 (Citrus clementina)	0.0	XP_006437422.1
c3	0.69 (0.65)	-0.07 (0.02)	0.39 (0.39)	VIT_17s0000g05000	SEPI-like	PREDICTED: MADS-box protein CMB1 isoform X2 [Vitis vinifera]	LOC100251943	Developmental protein SEPALLATA1 [Nelumbo nucifera]	2e-136	XP_010257958.1
c3	0.48 (0.57)	0.23 (0.29)	-0.24 (-0.16)	VIT_18s0001g03540	AUX1-like	PREDICTED: auxin transporter-like protein 3 [Vitis vinifera]	LOC100243769	Auxin transporter-like protein 3 [Durio zibethinus]	0.0	XP_022753165.1
c3	0.56 (0.62)	0.04 (0.01)	0.04 (0.09)	VIT_18s0001g11160	MIZU-KUSSELI	PREDICTED: protein MIZU-KUSSELI [Vitis vinifera]	LOC100245545	Protein MIZU-KUSSELI 1-like [Durio zibethinus]	3e-141	XP_022752310.1
c4	1.61 (1.49)	-0.41 (-0.05)	0.37 (0.25)	VIT_01s0026g02030	PRE6	PREDICTED: Vitis vinifera transcription factor PRE6	LOC100256731	Transcription factor IL16 [Hibiscus syriacus]	1e-46	KAE8792984.1
c5	0.87 (0.95)	0.15 (0.48)	0.35 (0.34)	VIT_01s0010g02430	MAD2	PREDICTED: Vitis vinifera mitotic spindle checkpoint protein MAD2	LOC100254488	Mitotic spindle checkpoint protein MAD2-like [Olea europaea var. sylvestris]	4e-145	XP_022885664.1
c5	1.54 (1.51)	0.31 (0.98)	0.59 (0.69)	VIT_01s0127g00870	PGI-like	PREDICTED: Vitis vinifera polygalacturonase 1 beta-like protein 1	LOC100258559	Polygalacturonase-1 non-catalytic subunit beta like [Actinidia chinensis var. chinensis]	0.0	PSS26864.1
c5	1.20 (1.27)	-0.02 (0.04)	0.65 (0.61)	VIT_02s0025g04720	LDOX	Leucoanthocyanidin dioxygenase [Vitis vinifera]	LDOX	Anthocyanidin synthase [Nekemias (=Ampelopsis grossedentata)]	0.0	AGO02175.1
c5	0.91 (0.98)	0.30 (0.30)	0.41 (0.29)	VIT_17s0000g03750	LYM1	PREDICTED: Vitis vinifera lysM domain-containing GPI-anchored protein 1	LOC100247526	lysM domain-containing GPI-anchored protein 1-like [Pistacia vera]	1e-151	XP_031279065.1
c5	1.10 (1.09)	0.04 (0.39)	0.42 (0.29)	VIT_17s0053g00990	EXPA1-like	PREDICTED: Vitis vinifera expansin-like	LOC100261426	Expansin-A1 [Herrania umbraica]	1e-164	XP_021299559.1
c5	1.05 (1.18)	-0.09 (0.08)	0.51 (0.50)	VIT_18s0001g05060	PGM	PREDICTED: Vitis vinifera 2,3-bisphosphoglycerate-dependent phosphoglycerate mutase	LOC100245371	2,3-Bisphosphoglycerate-dependent phosphoglycerate mutase [Actinidia chinensis var. chinensis]	0.0	PSS31654.1

(a) Hierarchical clusters (Euclidian distances) of the relative gene expression (Figs. 4, 5) (b) Clone group specific mean and median values of relative expression. The color code corresponds to the colors used in the heatmap in Figs. 4 and 5 and indicates changes based on the mean expression value. (c) Identifier from the Gramene data base ([http://ensembl.gramene.org/Vitis\\_vinifera/](http://ensembl.gramene.org/Vitis_vinifera/)) and functional annotation of the genes at NCBI Genbank (<https://www.ncbi.nlm.nih.gov/nucleotide>) (d) Gene identifier from NCBI (e) Best match (Blastp) of the translated amplified sequences of candidate genes with homologous genes from non Vitis species (<https://blast.ncbi.nlm.nih.gov/Blast.cgi>) (f) Quality estimator value for similarity between sequences (g) Accession number of homologous genes in the NCBI database

### Correlation of gene expression with sub-traits of cluster architecture and wood gain

At the early stage of BBCH57, the relative expression of *VvGRF4* ( $\log_2$  FC) was strongly correlated with

the sub-traits mean berry volume (MBV;  $r=0.87/0.90$ ) and pedicel length (PED;  $r=0.92/0.89$ ) in both years. In contrast, the activity of genes *VIT\_04s0008g01100* and *VIT\_18s0001g03160* correlated inversely with MBV and

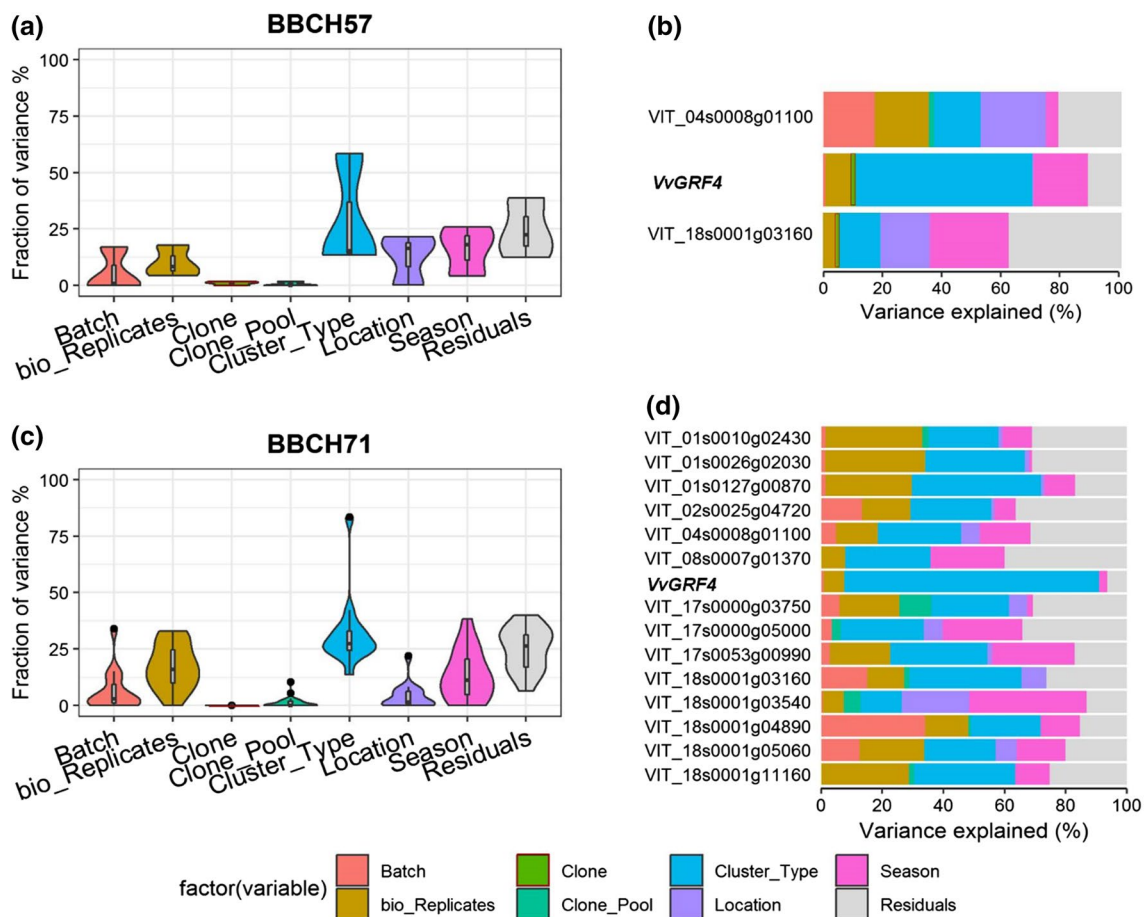


**Fig. 6** Variance partition analysis using experimental factors to assess the percentage of the explained variance of gene expression. The violin plots (**a**, **c**) indicate the explained variances in overall gene expression values  $\log_{(2)}(\Delta C_T)$  on the *y*-axis, while the *x*-axis depicts the factors of variance: cluster type (loose, mixed berried, compact), bio-

replicates, (biological replicates,  $n=3$ ), season, batch (technical replicates,  $n=2$ ), location, gene pool (selection background), clone (11 ‘Pinot Noir’ clones) and the residuals. The bar plots (**b**, **d**) depict the amount of variance explained by each factor on the individual gene’s expression

PED (Table 7). At this time, there was no significant correlation to shoulder length (SL).

During 2015 and 2016, at developmental stage BBCH71, all selected genes changed expression correlated with at least one of the sub-traits mean berry volume (MBV), pedicel length (PED) or shoulder length (SL) (Table 7). Three main trends appeared in both seasons. I) 11 genes with significant correlation with MBV also correlated with PED in the same sense (positive or negative correlation). Genes with correlation with SL often co-correlated with plant vigor (measured as wood gain, WG). II) The correlations with MBV/PED in general appeared inverse to the correlations observed to SL/WG (Table 7, Online resource 9). III). None of the 15 genes showed any significant correlation with the sub-traits berry number (BN), cluster weight (CW) or rachis length (RL) (Online resource 9).

Interestingly, at BBCH71 the correlation of the genes expression with MBV was generally stronger than to PED. All genes showed regulation correlated with the sub-trait shoulder length (SL) in at least one season.

### Correlation in between the modulated genes

In general, the correlation among the differentially expressed genes was strong, with the sole exception of *VIT\_18s0001g03540* (Online resource 9).

Consistent with the gene expression clusters (Fig. 5), the genes that were positively correlated with MBV and PED also correlated positively with the genes of the expression clusters II to V, but negatively with the genes of cluster I. On the contrary, the genes that correlated negatively with MBV and PED also correlated negatively with all genes in

**Table 7** Coefficient of correlation (*r*) between the relative expression changes of selected genes and key sub-traits of cluster architecture and wood gain (for abbreviations see Table 5)

BBCH57	Year	MBV	PED	SL	WG
<i>VIT_04s0008g01100</i>	2015	-0.94*** *	-0.82**	-0.10	0.50
	2016	-0.78**	-0.93***	0.31	0.77**
<i>VvGRF4</i>	2015	0.87**	0.92***	-0.07	-0.78**
	2016	0.90***	0.89***	-0.56	-0.93***
<i>VIT_18s0001g03160</i>	2015	-0.83**	-0.83**	0.16	0.83**
	2016	-0.88***	-0.84**	0.42	0.88***
BBCH71	Year	MBV	PED	SL	WG
<i>VIT_01s0010g02430</i>	2015	0.90***	0.63**	-0.81*** *	-0.97***
	2016	0.82***	0.63**	-0.62**	-0.54*
<i>VIT_01s0026g02030</i>	2015	0.85***	0.72***	-0.71***	-0.89***
	2016	0.77***	0.48*	-0.52*	-0.61**
<i>VIT_01s0127g00870</i>	2015	0.88***	0.65**	-0.81*** *	-0.96***
	2016	0.92***	0.74***	-0.69***	-0.70***
<i>VIT_02s0025g04720</i>	2015	0.81***	0.61**	-0.80*** *	-0.94***
	2016	0.76***	0.51*	-0.57**	-0.59**
<i>VIT_04s0008g01100</i>	2015	-0.87*** *	-0.66***	0.73***	0.94***
	2016	-0.88*** *	-0.79*** *	0.75***	0.87***
<i>VIT_08s0007g01370</i>	2015	-0.86*** *	-0.69***	0.67***	0.91***
	2016	-0.88*** *	-0.70***	0.55**	0.53*
<i>VvGRF4</i>	2015	0.83***	0.72***	-0.76*** *	-0.90***
	2016	0.84***	0.66***	-0.58**	-0.55**
<i>VIT_17s0000g03750</i>	2015	0.78***	0.70***	-0.76*** *	-0.90***
	2016	0.56**	0.24	-0.44*	-0.30
<i>VIT_17s0000g05000</i>	2015	0.59**	0.48*	-0.69***	-0.71***
	2016	0.63**	0.23	-0.38	-0.48*
<i>VIT_17s0053g00990</i>	2015	0.81***	0.65***	-0.77*** *	-0.93***
	2016	0.88***	0.70***	-0.66***	-0.65***
<i>VIT_18s0001g03160</i>	2015	-0.82*** *	-0.61**	0.81***	0.96***
	2016	-0.89*** *	-0.61**	0.70***	0.80***
<i>VIT_18s0001g03540</i>	2015	-0.28	0.26	0.78***	0.51*
	2016	-0.79*** *	-0.65***	0.75***	0.96***
<i>VIT_18s0001g04890</i>	2015	-0.90*** *	-0.61**	0.80***	0.98***
	2016	-0.88*** *	-0.82*** *	0.72***	0.86***
<i>VIT_18s0001g05060</i>	2015	0.88***	0.61**	-0.81*** *	-0.98***
	2016	0.76***	0.51*	-0.61**	-0.63**
<i>VIT_18s0001g11160</i>	2015	0.92***	0.63**	-0.79*** *	-0.98***
	2016	0.66***	0.33	-0.39	-0.35

**Table 7** (continued)

The gene expression relative to *GAPDH* and *UBIc* ( $\log_2FC$ ) was measured just before flowering (BBCH57) and just after flowering (BBCH71). The results for cluster architecture sub-traits of ‘Pinot Noir’ clones were recorded at ripe grape clusters stage BBCH89. Wood gain was recorded after leaves had fallen (BBCH97)

Spearman correlation ( $r$ ) is significant with \* $p < 0.05$ , \*\* $p < 0.01$ , \*\*\* $p < 0.001$  and \*\*\*\* $p < 0.0001$

Positive correlation is highlighted in light red, negative correlation in light blue

**Table 8** Coefficient of correlation for relative gene expression ( $\log_2FC$ ) between the three putative transcription factors and differentially regulated genes

BBCH	Gene Id	Season	<i>VIT_01s0026g02030</i>	<i>VvGRF4</i>	<i>VIT_17s0000g05000</i>	Annotation according to NCBI blastX results
57	<i>VIT_04s0008g01100</i>	2015		− 0.83**		Cytochrome P450 711A1-like
57		2016		− 0.90***		
57	<i>VIT_18s0001g03160</i>	2015		− 0.98****		WAT1-related protein
57		2016		− 0.95****		
71	<i>VIT_01s0026g02030</i>	2015		0.97****	0.79****	Transcription factor PRE6
71		2016		0.87****		
71	<i>VvGRF4</i>	2015	0.97****		0.85****	Growth-regulating factor 4
71		2016	0.87****		0.74****	
71	<i>VIT_17s0000g05000</i>	2015	0.79****	0.85****		SEPALLATA1-like protein
71		2016	0.89****	0.74****		
71	<i>VIT_01s0010g02430</i>	2015	0.95****	0.93****	0.70***	Mitotic spindle checkpoint protein MAD2-like
71		2016	0.92****	0.97****	0.72***	
71	<i>VIT_01s0127g00870</i>	2015	0.92****	0.95****	0.73***	Polygalacturonase 1 beta-like protein
71		2016	0.82****	0.96****	0.66***	
71	<i>VIT_02s0025g04720</i>	2015	0.88****	0.92****	0.79****	Anthocyanidin synthase
71		2016	0.98****	0.92****	0.83****	
71	<i>VIT_17s0000g03750</i>	2015	0.89****	0.94****	0.81****	lysM domain-containing GPI-anchored protein 1-like
71		2016	0.89****	0.83****	0.84****	
71	<i>VIT_17s0053g00990</i>	2015	0.90****	0.92****	0.75****	Alpha-expansin
71		2016	0.86****	0.97****	0.68***	
71	<i>VIT_18s0001g05060</i>	2015	0.90****	0.92****	0.71***	Bisphosphoglycerate-dependent phosphoglycerate mutase-like
71		2016	0.97****	0.89****	0.81****	
71	<i>VIT_18s0001g11160</i>	2015	0.92****	0.92****	0.69***	Protein MIZU-KUSSEL 1-like
71		2016	0.89****	0.86****	0.89****	
71	<i>VIT_04s0008g01100</i>	2015	− 0.90****	− 0.87****	− 0.60**	Cytochrome P450 711A1-like
71		2016	− 0.67***	− 0.74****	− 0.42*	
71	<i>VIT_08s0007g01370</i>	2015	− 0.90****	− 0.86****	− 0.56**	Putative lipid-transfer protein DIR1
71		2016	− 0.72***	− 0.88****	− 0.64**	
71	<i>VIT_18s0001g03160</i>	2015	− 0.89****	− 0.92****	− 0.74****	WAT1-related protein
71		2016	− 0.91****	− 0.89****	− 0.74****	
71	<i>VIT_18s0001g03540</i>	2015	− 0.25	− 0.35	− 0.39	Auxin influx carrier (AUX1 LAX family)
71		2016	− 0.56**	− 0.57**	− 0.38	
71	<i>VIT_18s0001g04890</i>	2015	− 0.91****	− 0.91****	− 0.68***	Low affinity sulfate transporter 3-like
71		2016	− 0.62**	− 0.72****	− 0.42	

Spearman correlation ( $r$ ) is significant with \* $p < 0.05$ , \*\* $p < 0.01$ , \*\*\* $p < 0.001$  and \*\*\*\* $p < 0.0001$

Positive correlation is highlighted in magenta, negative correlation in light blue

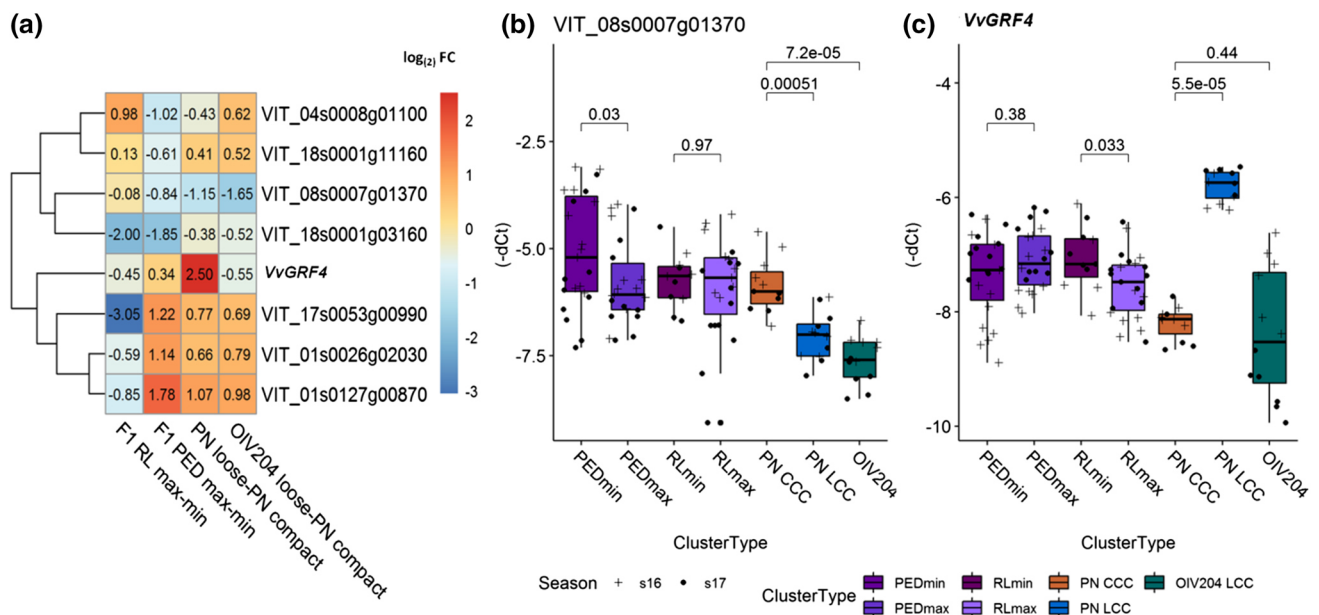


**Fig. 7** Differential expression of CA-related genes identified in PN in genetically distant backgrounds. Values from PN clones are included for comparison. **a** Heatmap of the averaged relative gene expression values as  $\log_2 FC$  ( $-\Delta\Delta C_i$ ) at BBCH71 (just after flowering). The gene expression relative to the mean of *GAPDH* and *UBIc* was analyzed in three biological replicates. For gene activity in F1 individuals, a contrast to the mean of four individuals with short pedicels and short rachis was used, respectively. For standardization of loosely clustered individuals of OIV reference varieties, a contrast to the two compactly clustered PN clones, Frank Classic and Frank Charisma, was calculated. **b, c** Fold change ( $-\Delta C_i$ ) of *VIT\_08s0007g01370* (**b**) and *VvGRF4* (**c**) relative to the internal control genes during two sea-

sons at BBCH71 as measured in phenotypic and genotypic diverse individuals grouped according to their cluster architecture type. Cluster architecture types consist of the following individuals: PEDmin and PEDmax, four F1 hybrids each were grouped according to pedicel length. RLmin and RLmax, four F1 hybrids each were grouped according to rachis length. PN CCC, compactly clustered ‘Pinot Noir’ clones Gm1-86 and WeM171. PN LCC, loosely clustered ‘Pinot Noir’ clones Frank Classic and Frank Charisma. OIV 204, ‘Uva Rara’ and ‘Prosecco,’ two OIV reference varieties of cluster density OIV descriptor#204 for loose cluster architecture. Indicated *p* values were generated with Wilcoxon’s test between group means of cluster architecture types

expression clusters II to V, but positively with the genes in cluster I (Online resource 9).

The three genes *VIT\_01s0026g02030* (*PRE6*), *VvGRF4* and *VIT\_17s0000g05000* (*SEP1*-like) encode putative transcription factors. At BBCH57, the expression of *VvGRF4* correlated negatively with the genes differentially expressed at this developmental stage. This negative correlation continued to the later stage. At BBCH71, the expression of the ten other regulated genes was always correlated with the transcriptional activity of the three transcription factor genes in the same sense (with the sole exception of the gene *VIT\_18s0001g04890* that correlated with *VIT\_17s0000g05000* only during the season of 2015) (Table 8). The three transcription factor genes correlated positively with each other.

### Expression of cluster architecture-associated genes in alternative genetic backgrounds

The differential gene expression of the 15 genes identified in the PN clones was tested for maintenance of their association with the sub-traits of CA in completely different genetic backgrounds. To this purpose, the OIV reference varieties

for loose cluster architecture ‘Uva Rara’ and ‘Prosecco’ were analyzed. In addition, 16 interspecific F1 hybrids from a cross population of ‘Calardis Musqué’ (formerly GF.GA-47-42)  $\times$  ‘Villard Blanc’ (Zyprian et al. 2016) were chosen for this broadened analysis. These samples comprised four genotypes each showing maximal or minimal pedicel lengths and each four individuals of maximal or minimal rachis lengths as characterized in Richter et al. (2019) and detailed (including *T* Test) in Online resource 4. They were included in the high-throughput RT-qPCR chips at stage BBCH71. Out of the 15 genes with differential expression between loose and compact quasi-isogenic PN clones, seven genes maintained their differential expression in individuals of contrasting cluster architecture sub-traits in this diverse genetic background (Fig. 7a, Online resources 10 and 11).

The gene encoding *VvGRF4* lost its association with CA within these genetically different grapevine samples (Fig. 7a, c). Its differential expression was restricted to the PN clones. It was neither regulated in the OIV reference varieties ‘Uva Rara’ and ‘Prosecco’ nor the F1 hybrids of the cross population. Although the investigated F1 siblings exhibited extreme pedicel lengths difference, and pedicel

length is a discriminant between loose and compact PN clones, no significant correlation of *VvGRF4* gene expression modulation in relation to pedicel lengths was identified (Fig. 7c).

Particularly, the three genes *VIT\_01s0026g02030* (*PRE6*), *VIT\_01s0127g00870* (*PG1*-like) and *VIT\_17s0053g00990* (*EXPA1*-like) genes were significantly up-regulated (FC ~ 1.6–2.1) in the OIV reference varieties for loose cluster architecture ‘Uva Rara’ and ‘Prosecco’ (related to compact PN clones, Fig. 7a).

The gene *VIT\_08s0007g01370* (*DIR1*-like), which showed down-regulation in loose PN clones, was also expressed at considerably reduced level in the loose OIV reference varieties (Fig. 7a, b).

Regarding the F1 siblings with long rachises, the three genes *VIT\_01s0026g02030* (*PRE6*), *VIT\_01s0127g00870* (*PG1*-like, *jp650*-like) and *VIT\_17s0053g00990* (*EXPA1*-like) showed reduced expression as compared to siblings with short rachis length. In contrast, F1 siblings with long pedicels showed higher expressions of these genes in comparison with their siblings with short pedicels (Fig. 7a, Online resource 10).

The expression of *VIT\_18s0001g03160* (*WAT1*-like) appeared 3.6–4-fold down-regulated in F1 hybrids with long pedicels and large rachis length. The F1 genotypes #484 and #503 appeared particularly diminished for expression of *VIT\_18s0001g03160* and likewise for the gene *VIT\_17s0053g00990*.

The genes *VIT\_04s0008g01100* (*CYP711A1*-like) and *VIT\_18s0001g11160* (*MIZU-KUSSELI*-like) showed a contrasting regulation pattern regarding the four experimental sets (Fig. 7a). The loosely clustered OIV#204 reference varieties and F1 hybrids with long rachis were more actively expressing these genes, while F1 hybrids with long pedicels were found reduced in the activity of these two genes.

### Co-expression network analysis

To learn more about the regulatory networks involved in cluster morphogenesis, the gene expression data obtained in this study were checked for co-expression within other publicly available grapevine transcriptomic datasets. The co-expression network, calculated with the grapevine gene expression compendium ‘Vespucci’ (Moretto et al. 2016a), revealed that 11 of the 15 genes are part of a co-expression network when examined within the expression data of ‘Corvina’ (Fasoli et al. 2012) and ‘Tempranillo’ (Diaz-Riquelme et al. 2014) samples. The genes within the network had manually annotated functions comprising auxin signaling, auxin transport, cell cycle and flower development. The genes *VIT\_04s0008g01100* (*CYP711A1*-like), *VIT\_08s0007g01370* (*DIR1*-like), *VIT17s0000g05000*

(*SEP1*-like) and *VIT\_18s0001g05060* (*PGM*) do not belong to any co-expression network (Diaz-Riquelme et al. 2014, Fasoli et al. 2012) represented in the available data sets.

### Discussion

This study analyzed 92 genes involved in the determination of loose cluster architecture in different PN clones. The implication of *VvGRF4*, recently identified as an important regulator of cluster architecture in four PN clones (Rossmann et al. 2019), was confirmed here in a wider genetic range of PN. Seven of these genes could be validated for their association with cluster architecture in completely different genetic background, in OIV reference varieties for loose cluster architecture and in phenotypically extreme F1 siblings from a controlled cross. These included the gene annotated as encoding transcription factor *PRE6*. The regulation of *VvGRF4*, in contrast, was limited to the PN clones of selection lines with different pedicel length. Such restriction of intravarietal variance was also reported in Fernandez et al. (2010, 2014). The authors detected a mutation causing alterations of inflorescence morphology in the promoter of *VvTFLIA* in somatic variants of the cultivar ‘Carignan.’ However, the authors could not find that specific mutation in a population of 140 varieties with diverse cluster architecture.

The phenotype of an organism is determined by a combination of its genotype (*G*), the environment (*E*) and their interaction (*G* × *E*) (Grishkevich and Yanai 2013). Considering this fact, it is desirable to dispose high numbers of clonal individuals spread over several locations for investigation. However, for perennial crops like grapevine, this requirement is difficult to fulfill. Establishment of controlled vineyards raised from certified plant material with ample material to allow random sampling is time-consuming and expensive. The PN clones in this study needed to be grown in homogeneous plots and grafted on the same rootstock cultivar to avoid transcriptomic shifts in the scion and influences on yield and vigor by the rootstock (Chitarra et al. 2017). The experimentation here was therefore restricted to clonal material available at the collaborating nurseries and the cultivar repository at the JKI. The three plantations were under different viticulture systems with organic viticulture at Geilweilerhof and integrated management at the nurseries. This fact should delimit the identification of genetic components affecting the phenotype of cluster architecture to those that operate autonomously from environmental conditions.

Organic or integrated vineyard management may influence CA development. Döring et al. (2015) used ‘Riesling’ vines (on rootstocks ‘Börner’ and ‘SO4’) to compare growth and yield parameters in relation to viticulture systems of

integrated and organic production. The authors reported significant lower cluster and berry weight under organic management. The latter parameter (berry weight) could be regarded as equivalent to mean berry volume (MBV) analyzed in this study. Interestingly, in the study here, the vineyard in Baden (integrated) had lower MBV as compared to the organically maintained field in Palatinate. It might be possible that there is a difference in grapevine cultivars regarding their requirements for nutrients and a cultivar-specific shift to promote generative development under nutrient shortage. This may be indicated by the lower wood gain observed in the organically managed vineyard.

In total, 12 different PN clones of various cluster architecture types were characterized for cluster sub-traits. Ripe bunches were measured for two seasons in three different environments. Enlarging the range of CA types investigated previously (conducted on two loose and two compact PN clones), the additional cluster type of ‘mixed berried-clones’ was included newly in this investigation. These MBC clones result in rather loose bunches at ripeness, due to the presence of interspersed small berries within the clusters. Among the cluster architecture characteristics studied over all clones, the sub-traits MBV (mean berry volume), RL (rachis length) and PED (pedicel lengths) emerged as the most relevant determinants of overall cluster architecture. This finding is in agreement with the results from the former genetic study on QTLs related to cluster architecture mapped on a segregating population independent from the PN gene pool (Richter et al. 2019). Particularly, the sub-trait PED (pedicel length) was clearly discriminant between compact and loosely clustered PN clones (Table 5). Formation of the pedicel is largely influenced by cell number, and the long pedicels possess a higher number of cells in comparison with short pedicels of compact bunches in PN (Rossmann et al. 2019). This phenomenon is linked to the differential gene regulation of *VvGRF4* due to its mutation in the microRNA binding site. In this case, there appears to be an obvious direct influence of the genetic constitution, specific for ‘Pinots.’ Quite in contrast, the phenotypically extreme F1 siblings concerning pedicel length were differentially regulated in the activity of transcription factor gene *PRE6*, but not in *VvGRF4* expression (Fig. 7a, c). The gene encoding *PRE6* is enclosed in the confidence interval of a QTL for pedicel length and cluster architecture scored according to OIV descriptor #204 identified in the former genetic study (Richter et al. 2019). These findings may allow us to conclude that specifically the sub-trait pedicel length is primarily controlled by the genetic constitution and less affected by environmental effects. This finding is of high relevance for promising application in grapevine breeding and the development of genetic markers.

Genetic components affecting mean berry volume (MBV) are also operating, since many genes differentially expressed

in association with this sub-trait were identified. In the PN samples, essentially all of the 15 generally CA-associated genes correlated with MBV (Table 7). The sub-trait rachis length (RL) turned out as relevant characteristic of overall cluster architecture, but did not show any significant correlation with the genes investigated.

The developmental period from pre-anthesis to beginning berry formation was chosen to study gene regulation as the stage relevant for the constitution of final cluster compactness (Tello and Forneck 2018). This period was reported to be important for the modulation of cluster architecture sub-traits berry number (Bessis and Fournioux 1992), rachis length (Shavrukov et al. 2004) and berry volume (Houel et al. 2013). Particularly, the latter traits constitute loose or compact CA in a cultivar-dependent manner (Tello and Forneck 2018). This developmental phase encompasses a period of differential growth rate of rachis structures, which is accelerated during the development of loose clusters (Richter et al. 2017) compared to compact bunches. Gene regulation was studied during three seasons in the samples from three different environments. This approach should allow identifying CA-associated genes that work comprehensively, independently from season and vineyard location.

This study revealed 15 genes that were differentially expressed between loosely and compactly clustered ‘Pinot Noir’ clones under all different environmental conditions. The regulation of these genes was primarily related to cluster architecture (Fig. 5). As expected, it was partially affected also by environmental and experimental fluctuations to various extents (Fig. 6).

At the early stage of BBCH57, the expression of *VvGRF4* was already higher in the loosely clustered clones than in compact and mixed berried clones. A subtle modulation was observed in the genes *VIT\_04s0008g01100* (*CYPP711A1-like*) and *VIT\_18s0001g03160* (*WAT1-like*) at this early point. These two genes are members of cluster I of the regulatory groups at the later stage BBCH71. They maintained expression changes at fruit set, with an explicit down-regulation in loosely clustered clones. *VIT\_18s0001g03160* is annotated as a *WAT1*-like (‘walls are thin’) encoding gene, a vacuolar transporter of auxin characterized in *Arabidopsis* (Ranocha et al. 2013). The gene *VIT\_04s0008g01100* encodes a homolog to cytochrome P450 711A1, a monooxygenase involved in the metabolism of strigolactones (conversion of carlactone to carlactonic acid). Its function has been identified in the *MAX1* mutation in *Arabidopsis*, which shows increased axillary growth. *MAX1* suppresses shoot branching in *Arabidopsis* (Abe et al. 2014). The findings here indicate additional or diversified functions of this gene in grapevine. The cluster I genes with down-regulation in loose clusters further encompass *VIT\_08s0007g01370* (*DIR1-like*) and *VIT\_18s0001g04890* (*SULTR2-like*), annotated as a putative lipid transfer protein resp. a sulfate transporter.

The genes *VIT\_18s0001g04890* and *VIT\_18s0001g03160* have also been described to be repressed in ‘Garnacha Tinta’ clones with larger berries (Grimplet et al. 2017). Homologs of *DIR1* have been implicated in long-distance signal transduction during systemic acquired resistance in plant–pathogen interactions (Shah and Zeier 2013). Its transcript reduction in the context of emerging loose cluster architecture is a new aspect. Hypothetically, it may have a role in the transmission of growth-related cellular signals.

Besides the gene encoding *VvGRF4* that was definitely higher expressed in the LCC-type PN clones at BBCH71, expression of the transcription factor-like gene encoding *PRE6* (*VIT\_01s0026g02030*) was significantly enhanced in LCCs. *PRE6* belongs to the atypical bHLH transcription factor class with no direct DNA binding ability that mediates auxin, brassinosteroid and light signaling and affects photomorphogenesis. A homolog from rice called *IL11* (increased lamina inclination 1) increased cell elongation (Zhang et al. 2009). Cell elongation may well contribute to important cluster features such as rachis length and shoulder length.

Genes with autonomous up-regulation in LCCs included *VIT\_17s0000g05000*. This gene encodes a *SEPALLATA1*-like developmental regulator. It has probable transcription factor function and is part of the network that regulates flower development in *Arabidopsis* where it prevents indeterminate growth of the flower meristem (Pelaz et al. 2000). Recently, Palumbo et al. (2019) reported *VIT\_17s0000g05000* as homeotic gene associated with whorl differentiation in grapevine during the period of pre-anthesis on to post-fertilization. A functional role of *SEP1-like* is supported by data available in a transcriptomic atlas derived from spatial–temporal gene expression studies on the grapevine cultivar ‘Corvina’ (Fasoli et al. 2012). In this study, growing rachis tissue showed up-regulation of *VIT\_17s0000g05000*, whereas its expression was close to the reference tissue (mesocarp at BBCH77) in tendrils, seed, roots and mature rachis tissue.

In addition to auxin transport functions (*VIT\_18s0001g03540*, *LAX3-like*) and auxin homeostasis [*VIT\_18s0001g11160*, *MIZU-KUSSELL1* (Moriwaki et al. 2011)], further genes with up-regulation, particularly in loosely clustered PN clones, encompass functions involved in cell wall extension (*VIT\_17s0053g00990*, *EXPA1-like*), cell size (*VIT\_01s0127g00870*, *PG1-like*) and cell division (*VIT\_01s0010g02430*, *MAD2*). The gene *VIT\_17s0053g00990* encodes  $\alpha$ -expansin that was found up-regulated in rapidly growing grape berries and permits to enlarge cell size by loosening the fibrillar net in plant cell walls (Suzuki et al. 2015).

In a previous genetic study, QTL clusters associated with loose bunch architecture were localized in a CA segregating population from a cross of ‘Calardis Musqué (formerly named GF.GA-47-42) × ‘Villard Blanc’ (Richter et al.

2019). Arrays of overlapping QTL regions were found on seven chromosomes, including chromosome 1 and 17. Interestingly, the three genes *VIT\_01s0026g02030* (*PRE6*), *VIT\_17s0000g05000* (*SEP1-like*), and *VIT\_17s0053g00990* (*EXPA1-like*), associated with cluster architecture characteristics found here for PN clones, are located in QTL areas. Two of them code for transcription factors that may have a comprehensive function, which needs to be further investigated.

Furthermore, 16 selected individuals from this cross population exhibiting extreme phenotypes for pedicel and rachis lengths were included in the gene expression study. The aim was to check the differential gene regulation of the 15 CA-related genes found in PN in this genetically completely different sample set. Indeed, the expression level of the gene encoding transcription factor *VvPRE6* and six more genes (homologs of *CYP711A1-like*, *Mizu-Kussell1*, *DIR1*, *WAT1*, *EXPA1* and *PG1-like*, Fig. 7a) was significantly linked to extreme CA phenotypes in this divergent germplasm. A corresponding result was obtained in the loosely clustered reference varieties ‘Uva Rara’ and ‘Prosecco’ (Fig. 7a, b). Particularly, the three genes encoding transcription factor *PRE6* and the cell wall-related functions *EXPA1-like* and *PG1-like* exhibit increased expression levels in loosely clustered plants of diverse genetic background, especially in relation to pedicel length (Fig. 7a). Quite in contrast, the role of *VvGRF4* is specific for the ‘Pinot’ clones, as also inferred from sequencing studies that show the absence of the mutated microRNA binding site in the OIV reference varieties (Rossmann et al. 2019).

This study thus revealed a set of genes with wide relevance for loosely clustered grapevines. These genes enclose components of auxin transport and homeostasis (*WAT1*, *AUX1*, *Mizu-Kussell1*), cell wall structure and loosening (*PG1*, *EXPA1*), in addition to strigolactone metabolism (*CYP711A1*, *MAX1*) and the regulatory transcription factor *PRE6*. These genes deserve further investigation. This novel knowledge facilitates development of gene-targeted markers of loose cluster types for grapevine breeding.

## Conclusions

This study revealed 15 genes with differential gene expression between loosely and compactly clustered PN clones, independently from year and location (or any other environmental variation encountered). It confirmed the role of *VvGRF4* in the control of cluster architecture in ‘Pinot Noir.’ It newly identified two more transcription factor genes, encoding a *SEPALLATA1* homolog and a homolog of *PRE6*, that are more active in the loosely clustered than in the compact bunch type clones. Compared to the recent literature, these regulator genes may have new or additional

functions in affecting the structure of the ‘Pinot Noir’ grapevine bunch. Furthermore, genes involved in auxin metabolism, cellular growth and transport were found to be regulated. A gene homolog of CYP711A1, encoding an enzyme of strigolactone metabolism, was also involved. Strigolactones function as shoot branching inhibitors (Gomez-Roldan et al. 2008). This gene is repressed in loose clusters, possibly releasing some inhibition, and thus seems to contribute to the loose-clustered phenotype in grapes.

These results were confirmed for seven genes in completely different genetic backgrounds: the transcription factor gene *PRE6* and six genes related to auxin metabolism, cell wall loosening and strigolactones. They improve the basic knowledge on grapevine cluster phenotype.

This study revealed several major regulators of cluster architecture in ‘Pinot Noir’ and other grapevines, which deserve further attention and functional studies. Future investigation will show if they are applicable as molecular tools for breeding of advantageous loosely clustered grapevine cultivars with improved resilience to *Botrytis cinerea*.

**Acknowledgements** Open Access funding provided by Projekt DEAL. This work was funded by the ‘Federal Program for Ecologic Landuse and other forms of Sustainable Agriculture’ (Bundesprogramm Ökologischer Landbau und andere Formen nachhaltiger Landwirtschaft, BÖLN) of BLE (Bundesanstalt für Landwirtschaft und Ernährung) Federal Office for Agriculture and Food under the title ‘MATA-Molekulare Analyse der Traubenarchitektur’ (Molecular analysis of cluster architecture) FKZ 2811NA056 ([www.ble.de](http://www.ble.de)). We thank Daniel Zender for fruitful discussion and Margareta Schneider for technical help. We wish to thank the grapevine nurseries Reben Sibbus GmbH, Sasbach-Jechtingen, Germany, and Antes Viticulture and Grafting GbR, Heppenheim, Germany, for providing access to their clonal material and maintaining the trial fields in Baden and Hesse.

**Author contribution statement** EZ acquired funding and supervised the work. EZ and RR designed the study. RR performed the experiments, measurements and calculations. SR and KT contributed RNA sequencing data. DG provided statistical expertise. RT provided plant material, infrastructure and special advice. RR and EZ wrote the paper. All authors read the manuscript.

**Funding** Open Access funding provided by Projekt DEAL.

## Compliance with ethical standards

**Conflict of interest** The authors declare that they have no conflict of interest.

**Open Access** This article is licensed under a Creative Commons Attribution 4.0 International License, which permits use, sharing, adaptation, distribution and reproduction in any medium or format, as long as you give appropriate credit to the original author(s) and the source, provide a link to the Creative Commons licence, and indicate if changes were made. The images or other third party material in this article are included in the article’s Creative Commons licence, unless indicated otherwise in a credit line to the material. If material is not included in the article’s Creative Commons licence and your intended use is not permitted by statutory regulation or exceeds the permitted use, you will

need to obtain permission directly from the copyright holder. To view a copy of this licence, visit <http://creativecommons.org/licenses/by/4.0/>.

## References

- Abe S, Sado A, Tanaka K, Kisugi T, Asami K, Ota S, Kim HI, Yoneyama K, Xie X, Ohnishi T, Seto Y, Yamaguchi S, Akiyama K, Yoneyama K, Nomura T (2014) Carlactone is converted to carlactonoic acid by MAX1 in *Arabidopsis* and its methyl ester can directly interact with AtD14 in vitro. *Proc Natl Acad Sci USA* 111:18084–18089
- Alonso-Villaverde V, Boso S, Luis Santiago J, Gago P, Martínez M-C (2008) Relationship between susceptibility to *Botrytis* bunch rot and grape cluster morphology in the *Vitis vinifera* L. cultivar Albariño. *Int J Fruit Sci* 8:251–265
- Altschul SF, Gish W, Miller W, Myers EW, Lipman DJ (1990) Basic local alignment search tool. *J Mol Biol* 215(3):403–410
- Ban Y, Mitani N, Sato A, Kono A, Hayashi T (2016) Genetic dissection of quantitative trait loci for berry traits in interspecific hybrid grape (*Vitis labruscana* × *Vitis vinifera*). *Euphytica* 211:295–310
- Becker T, Knoche M (2012) Water induces microcracks in the grape berry cuticle. *Vitis* 51:141–142
- Bessis R, Fournioux J (1992) Zone d’abscission et coulure de la vigne. *Vitis* 31:9–21
- Blaich R, Konradi J, Ruehl E, Forneck A (2007) Assessing genetic variation among Pinot noir (*Vitis vinifera* L.) clones with AFLP markers. *Am J Enol Vitic* 58:526–529
- Bleyer K (2001) Klonzüchtung beim Blauen Spätburgunder. *Rebe Wein* 11:22–26
- BMELV (2010) Gute fachliche Praxis im Pflanzenschutz: Bundesministerium für Ernährung Landwirtschaft und Verbraucherschutz (BMELV)
- Canaguier A, Grimplet J, Di Gaspero G, Scalabrin S, Duchêne E, Choisine N, Mohellibi N, Guichard C, Rombauts S, Le Clainche I, Bérard A, Chauveau A, Bounon R, Rustenholz C, Morgante M, Le Paslier MC, Brunel D, Adam-Blondon AF (2017) A new version of the grapevine reference genome assembly (12X.v2) and of its annotation (VCost.v3). *Genom Data* 14:56–62
- Chitarra W, Perrone I, Avanzato CG, Minio A, Boccacci P, Santini D, Gilardi G, Siciliano I, Gullino ML, Delledonne M, Mannini F, Gambino G (2017) Grapevine grafting: scion transcript profiling and defense-related metabolites induced by rootstocks. *Front Plant Sci* 8:654
- Citri A, Pang ZPP, Sudhof TC, Wernig M, Malenka RC (2012) Comprehensive qPCR profiling of gene expression in single neuronal cells. *Nat Protoc* 7:118–127
- Correa J, Mamani M, Munoz-Espinoza C, Laborie D, Munoz C, Pinto M, Hinrichsen P (2014) Heritability and identification of QTLs and underlying candidate genes associated with the architecture of the grapevine cluster (*Vitis vinifera* L.). *Theor Appl Genet* 127:1143–1162
- Dal Santo S, Vannozzi A, Tornielli GB, Fasoli M, Venturini L, Pezzotti M, Zenoni S (2013) Genome-wide analysis of the expansin gene superfamily reveals grapevine-specific structural and functional characteristics. *PLoS ONE* 8:e62206
- De Lorenzis G, Squadrito M, Rossoni M, Di Lorenzo GS, Brancadoro L, Scienza A (2017) Study of intra-varietal diversity in biotypes of Aglianico and Muscat of Alexandria (*Vitis vinifera* L.) cultivars. *Aust J Grape Wine Res* 23:132–142
- Di Genova A, Almeida AM, Munoz-Espinoza C, Vizoso P, Travisany D, Moraga C, Pinto M, Hinrichsen P, Orellana A, Maass A (2014) Whole genome comparison between table and wine grapes reveals a comprehensive catalog of structural variants. *BMC Plant Biol* 14:7. <https://doi.org/10.1186/1471-2229-14-7>

- Diaz-Riquelme J, Martinez-Zapater JM, Carmona MJ (2014) Transcriptional analysis of tendrils and inflorescence development in grapevine (*Vitis vinifera* L.). PLoS ONE 9:e92339
- Döring J, Frisch M, Tittmann S, Stoll M, Kauer R (2015) Growth, yield and fruit quality of grapevines under organic and biodynamic management. PLoS ONE 10:e0138445
- Dry PR, Longbottom ML, McLoughlin S, Johnson TE, Collins C (2010) Classification of reproductive performance of ten wine-grape varieties. Aust J Grape Wine Res 16:47–55
- Dvinge H, Bertone P (2009) HTqPCR: high-throughput analysis and visualization of quantitative real-time PCR data in R. Bioinformatics 25:3325–3326
- Fanizza G, Lamaj F, Costantini L, Chaabane R, Grando MS (2005) QTL analysis for fruit yield components in table grapes (*Vitis vinifera*). Theor Appl Genet 111:658–664
- FAOSTAT (2016) <http://www.fao.org/faostat/en/#data/>. Value of agricultural production. Food and Agriculture Organization of the United Nations, last accessed Feb 2, 2020
- Fasoli M, Dal Santo S, Zenoni S, Tornielli GB, Farina L, Zamboni A, Porceddu A, Venturini L, Bicego M, Murino V, Ferrarini A, Delledonne M, Pezzotti M (2012) The grapevine expression atlas reveals a deep transcriptome shift driving the entire plant into a maturation program. Plant Cell 24:3489–3505
- Fernandez L, Torregrosa L, Segura V, Bouquet A, Martinez-Zapater JM (2010) Transposon-induced gene activation as a mechanism generating cluster shape somatic variation in grapevine. Plant J 61(4):545–557
- Fernandez L, Le Cunff L, Tello J et al (2014) Haplotype diversity of *VvTFLIA* gene and association with cluster traits in grapevine (*V. vinifera*). BMC Plant Biol 14:209
- Forneck A, Benjak A, Rühl E (2009) Grapevine (*Vitis* spp.): example of clonal reproduction in agricultural important plants. In: Schön I, Martens K, Van Dijk P (eds) Lost sex: the evolutionary biology of parthenogenesis. Springer, Dordrecht
- Fox J, Weisberg S (2011) An companion to applied regression, 2nd edn. Sage, Thousand Oaks
- Gabler FM, Smilanick JL, Mansour M, Ramming DW, Mackey BE (2003) Correlations of morphological, anatomical, and chemical features of grape berries with resistance to *Botrytis cinerea*. Phytopathology 93:1263–1273
- Gomez-Roldan V, Femas S, Brewer PB, Puech-Pages V, Dun EA, Pilot JP, Letisse F, Matusova R, Danoun S, Portais JC, Bouwmeester H, Becard G, Beveridge CA, Rameau C, Rochange SF (2008) Strigolactone inhibition of shoot branching. Nature 455:U189–U194
- Grimplet J, Tello J, Laguna N, Ibáñez J (2017) Differences in flower transcriptome between grapevine clones are related to their cluster compactness, fruitfulness, and berry size. Front Plant Sci 8:17
- Grimplet J, Ibáñez S, Baroja E, Tello J, Ibáñez J (2019) Phenotypic, hormonal, and genomic variation among *Vitis vinifera* clones with different cluster compactness and reproductive performance. Front Plant Sci 9:1917
- Grishkevich V, Yanai I (2013) The genomic determinants of genotype × environment interactions in gene expression. Trends Genet 29:479–487
- Harrell FE Jr (2015) Package ‘Hmisc’. CRAN2018: <https://cran.r-project.org/web/packages/Hmisc/Hmisc.pdf>
- Hed B, Ngugi HK, Travis JW (2009) Relationship between cluster compactness and bunch rot in vigneles grapes. Plant Dis 93:1195–1201
- Hed B, Ngugi HK, Travis JW (2010) Use of gibberellic acid for management of bunch rot on Chardonnay and Vigneles grape. Plant Dis 95:269–278
- Herzog K, Wind R, Töpfer R (2015) Impedance of the grape berry cuticle as a novel phenotypic trait to estimate resistance to *Botrytis cinerea*. Sensors 15:12498–12512
- Hoffman GE, Schadt EE (2016) Variance partition: Interpreting drivers of variation in complex gene expression studies. BMC Bioinform 17:483
- Hoffmann P (2015) Lockerbeerigkeit bei Klonen von Spätburgunder (Pinot noir): analyse von molekularen Markern und der Einfluss von Gibberellin auf die Traubenmorphologie. Dissertation, University of Hohenheim <http://opus.uni-hohenheim.de/volltexte/2015/1022/>
- Houel C, Martin-Magniette ML, Nicolas SD, Lacombe T, Le Cunff L, Franck D, Torregrosa L, Conejero G, Lalet S, This P, Adam-Blondon AF (2013) Genetic variability of berry size in the grapevine (*Vitis vinifera* L.). Aust J Grape Wine Res 19:208–220
- Houel C, Chatbanyong R, Doligez A, Rienth M, Foria S, Luchaire N, Roux C, Adiveze A, Lopez G, Farnos M, Pellegrino A, This P, Romieu C, Torregrosa L (2015) Identification of stable QTLs for vegetative and reproductive traits in the microvine (*Vitis vinifera* L.) using the 18 K Infinium chip. BMC Plant Biol 15:23
- Jiang Y, Bao L, Jeong SY, Kim SK, Xu C, Li X, Zhang Q (2012) XIAO is involved in the control of organ size by contributing to the regulation of signaling and homeostasis of brassinosteroids and cell cycling in rice. Plant J 70:398–408
- Keulemans W, Bylemans D, De Coninck B (2019) Farming without plant protection products. <https://doi.org/10.2861/05433PE634.416>. ISBN: 978-92-846-3993-9
- Kolde R (2015) Pheatmap: Pretty Heatmaps. R package version 1.0.8
- Konrad H, Lindner B, Bleser E, Rühl EH (2003) Strategies in the genetic selection of clones and the preservation of genetic diversity within varieties, 603rd edn. International Society for Horticultural Science (ISHS), Leuven, pp 105–110
- Konradi J, Blaich R, Forneck A (2007) Genetic variation among clones and sports of ‘Pinot noir’ (*Vitis vinifera* L.). Eur J Horticult Sci 72:275–279
- Kriventseva EV, Kuznetsov D, Tegenfeldt F (2019) OrthoDB v10: sampling the diversity of animal, plant, fungal, protist, bacterial and viral genomes for evolutionary and functional annotations of orthologs. Nucl Acids Res. <https://doi.org/10.1093/nar/gky1053>
- Lenth R (2019) Emmeans: estimated marginal means, aka least-squares means (version 1.3.4)
- Li M, Klein LL, Duncan KE, Jiang N, Chitwood DH, Londo JP, Miller AJ, Topp CN (2019) Characterizing 3D inflorescence architecture in grapevine using X-ray imaging and advanced morphometrics: implications for understanding cluster density. J Exp Bot 70(21):6261–6276. <https://doi.org/10.1093/jxb/erz394>
- Livak KJ, Schmittgen TD (2001) Analysis of relative gene expression data using real-time quantitative PCR and the 2(T)(ΔΔC) method. Methods 25:402–408
- Lorenz DH, Eichhorn KW, Bleiholder H, Klose R, Meier U, Weber E (1995) Growth Stages of the Grapevine: Phenological growth stages of the grapevine (*Vitis vinifera* L. ssp. *vinifera*)—codes and descriptions according to the extended BBCH scale. Aust J Grape Wine Res 1:100–103
- Marguerit E, Boury C, Manicki A, Donnart M, Butterlin G, Nemorin A, Wiedemann-Merdinoglu S, Merdinoglu D, Ollat N, Decroocq S (2009) Genetic dissection of sex determinism, inflorescence morphology and downy mildew resistance in grapevine. Theor Appl Genet 118:1261–1278
- Matthew ER, Belinda P, Di W, Yifang H, Charity WL, Wei S, Gordon KS (2015) limma, powers differential expression analyses for RNA-sequencing and microarray studies. Nucl Acids Res 43:47
- Maul E (2019) *Vitis* international variety catalogue. [www.vivc.de](http://www.vivc.de)

- Mejia N, Gebauer M, Munoz L, Hewstone N, Munoz C, Hinrichsen P (2007) Identification of QTLs for seedlessness, berry size, and ripening date in a seedless  $\times$  seedless table grape progeny. *Am J Enol Vitic* 58:499–507
- Migicovsky Z, Sawler J, Gardner KM, Aradhyia MK, Prins BH, Schwaninger HR, Bustamante CD, Buckler ES, Zhong G-Y, Brown PJ, Myles S (2017) Patterns of genomic and phenomic diversity in wine and table grapes. *Horticult Res* 4:17035
- Molitor D, Behr M, Hoffmann L, Evers D (2012) Impact of grape cluster division on cluster morphology and bunch rot epidemic. *Am J Enol Vitic* 63:508
- Molitor D, Junk J, Evers D, Hoffmann L, Beyer M (2014) A high-resolution cumulative degree day-based model to simulate phenological development of grapevine. *Am J Enol Vitic* 65:72–80
- Monteiro F, Sebastiana M, Pais MS, Figueiredo A (2013) Reference gene selection and validation for the early responses to downy mildew infection in susceptible and resistant *Vitis vinifera* cultivars. *PLoS ONE* 8:e72998
- Moretto M, Sonogo P, Pilati S, Malacarne G, Costantini L, Grzeskowiak L, Bagagli G, Grando MS, Moser C, Engelen K (2016a) VESPUCCI: exploring patterns of gene expression in grapevine. *Front Plant Sci* 7:633
- Moretto M, Sonogo P, Dierckxsens N, Brilli M, Bianco L, Ledezma-Tejeida D, Gama-Castro S, Galardini M, Romualdi C, Laukens K, Collado-Vides J, Meysman P, Engelen K (2016b) COLOMBOS v3.0
- Moriwaki T, Miyazawa Y, Kobayashi A, Uchida M, Watanabe C, Fujii N, Takahashi H (2011) Hormonal regulation of lateral root development in *Arabidopsis* modulated by *MIZ1* and requirement of GNOM activity for *MIZ1* function. *Plant Physiol* 157:1209–1220
- OIV (2015) 2nd edition of the OIV descriptor list for grape varieties and *Vitis* species. <http://www.oiv.int/>
- OIV (2017) Focus OIV 2017 distribution of the world's grapevine varieties. In: OIV (ed) OIV—international organization of vine and wine 18 rue d'Aguesseau F-75008 Paris, France [www.oiv.in](http://www.oiv.in). Last Accessed Feb 2, 2020
- OIV (2019) 2018 world vitiviniculture situation. OIV statistical report on world vitiviniculture. International Organisation of Vine and Wine. <http://www.oiv.int/public/medias/6782/oiv-2019-statistica-1-report-on-world-vitiviniculture.pdf>. Last Accessed May 7, 2020
- Palumbo F, Vannozzi A, Magon G, Lucchin M, Barcaccia G (2019) Genomics of flower identity in grapevine (*Vitis vinifera* L.). *Front Plant Sci* 10:316. <https://doi.org/10.3389/fpls.2019.00316>
- Pelaz S, Ditta GS, Baumann E, Wisman E, Yanofsky MF (2000) B and C floral organ identity functions require SEPALLATA MADS-box genes. *Nature* 405:200–203
- Pelsy F, Hocquigny S, Moncada X, Barbeau G, Forget D, Hinrichsen P, Merdinoglu D (2010) An extensive study of the genetic diversity within seven French wine grape variety collections. *Theor Appl Genet* 120:1219–1231
- Pertot I, Caffi T, Rossi V, Mugnai L, Hoffmann C, Grando MS, Gary C, Lafond D, Duso C, Thiery D, Mazzoni V, Anfora G (2017) A critical review of plant protection tools for reducing pesticide use on grapevine and new perspectives for the implementation of IPM in viticulture. *Crop Protect* 97:70–84
- Pieri P, Zott K, Gomès E, Hilbert G (2016) Nested effects of berry half, berry and bunch microclimate on biochemical composition in grape. *Oeno One* 50:145–159
- R Core Team (2013) R: a language and environment for statistical computing, Vienna. <http://www.r-project.org/index.html>
- Ranocha P, Dima O, Nagy R, Felten J, Corratge-Faillie C, Novak O, Morreel K, Lacombe B, Martinez Y, Pfrunder S, Jin X, Renou JP, Thibaud JB, Ljung K, Fischer U, Martinoia E, Boerjan W, Goffner D (2013) *Arabidopsis* WAT1 is a vacuolar auxin transport facilitator required for auxin homeostasis. *Nat Commun* 4:2625
- Regner F, Stadlbauer A, Eisenheld C, Kaserer H (2000) Genetic relationships among Pinots and related cultivars. *Am J Enol Vitic* 51:7–14
- Reid KE, Olsson N, Schlosser J, Peng F, Lund ST (2006) An optimized grapevine RNA isolation procedure and statistical determination of reference genes for real-time RT-PCR during berry development. *BMC Plant Biol* 6:27
- Richter R, Rossmann S, Töpfer R, Theres K, Zyprian E (2017) Genetic analysis of loose cluster architecture in grapevine. In: Aurand JM (ed) 40th world congress of vine and wine
- Richter R, Gabriel D, Rist F, Töpfer R, Zyprian E (2019) Identification of co-located QTLs and genomic regions affecting grapevine cluster architecture. *Theor Appl Genet* 132(4):1159–1177
- Rist F, Herzog K, Mack J, Richter R, Steinhage V, Töpfer R (2018) High-Precision phenotyping of grape bunch architecture using fast 3D sensor and automation. *Sensors* 18:763
- Rossmann S, Richter R, Sun H, Schneeberger K, Töpfer R, Zyprian E, Theres K (2019) Mutations in the miR396 binding site of the growth-regulating factor gene *VvGFR4* modulate inflorescence architecture in grapevine. *Plant J*. <https://doi.org/10.1111/tbj.14588>
- Ruehl E, Konrad H, Lindner B, Bleser E (2004) Quality criteria and targets for lonal selection in grapevine. *Acta Hort* 625:29–33
- Sapkota SD, Chen LL, Yang S, Hyma KE, Cadle-Davidson LE, Hwang CF (2019) Quantitative trait locus mapping of downy mildew and Botrytis bunch rot resistance in a *Vitis aestivalis*-derived 'Norton'-based population, 1248th edn. International Society for Horticultural Science (ISHS), Leuven, pp 305–312
- Schmittgen TD, Livak KJ (2008) Analyzing real-time PCR data by the comparative C–T method. *Nat Protoc* 3:1101–1108
- Selim M, Legay S, Berkelmann-Löhnertz B, Langen G, Kogel K-H, Evers D (2012) Identification of suitable reference genes for real-time RT-PCR normalization in the grapevine-downy mildew pathosystem. *Plant Cell Rep* 31:205–216
- Shah J, Zeier J (2013) Long-distance communication and signal amplification in systemic acquired resistance. *Front Plant Sci* 4:30. <https://doi.org/10.3389/fpls.2013.00030>
- Shavrukov YN, Dry IB, Thomas MR (2004) Inflorescence and bunch architecture development in *Vitis vinifera* L. *Aust J Grape Wine Res* 10:116–124
- Smart R, Robinson M (1991) Sunlight into wine: a handbook for wine-grape canopy management. Winetitles, Adelaide, South Australia
- Smyth GK (2004) Linear models and empirical Bayes methods for assessing differential expression in microarray experiments. *Stat Appl Genet Mol Biol* 3:1–25
- Suzuki H, Oshita E, Fujimori N, Nakajima Y, Kawagoe Y, Suzuki S (2015) Grape expansins, *VvEXPA14* and *VvEXPA18* promote cell expansion in transgenic *Arabidopsis* plant. *Plant Cell Tissue Organ Cult (PCTOC)* 120:1077–1085
- Tello J, Forneck A (2018) A double-sigmoid model for grapevine bunch compactness development. *OENO One* 52:4. <https://doi.org/10.20870/oeno-one.2018.52.4.2132>
- Tello J, Ibáñez J (2014) Evaluation of indexes for the quantitative and objective estimation of grapevine bunch compactness. *Vitis* 53:9–16
- Tello J, Ibáñez J (2017) What do we know about grapevine bunch compactness? A state-of-the-art review. *Aust J Grape Wine Res* 24:6–23
- Tello J, Aguirrezabal R, Hernaiz S, Larreina B, Montemayor MI, Vaquero E, Ibáñez J (2015) Multicultivar and multivariate study

- of the natural variation for grapevine bunch compactness. *Aust J Grape Wine Res* 21:277–289
- Tello J, Torres-Perez R, Grimplet J, Ibáñez J (2016) Association analysis of grapevine bunch traits using a comprehensive approach. *Theor Appl Genet* 129:227–242
- Töpfer R, Hausmann L, Eibach R (2011) Molecular breeding. In: Adam-Blondon AF, Martínez-Zapater JM (eds) *Genetics, genomics, and breeding of grapes*. CRC Press, Boca Raton, pp 160–185
- Upadhyay A, Jogaiah S, Maske SR, Kadoo NY, Gupta VS (2015) Expression of stable reference genes and SPINDLY gene in response to gibberellic acid application at different stages of grapevine development. *Biol Plant* 59:436–444
- Vail ME, Marois JJ (1991) Grape cluster architecture and the susceptibility of berries to *Botrytis cinerea*. *Phytopathology* 81:188–191
- Vargas AM, Fajardo C, Borrego J, De Andres MT, Ibanez J (2013) Polymorphisms in *VvPel* associate with variation in berry texture and bunch size in the grapevine. *Aust J Grape Wine Res* 19:193–207
- Zhang L-Y, Bai M-Y, Wu J, Zhu J-Y, Wang H, Zhang Z, Wang W, Sun Y, Zhao J, Sun X, Yang H, Xu Y, Kim S-H, Fujioka S, Lin W-H, Chong K, Lu T, Wang Z-Y (2009) Antagonistic HLH/bHLH transcription factors mediate brassinosteroid regulation of cell elongation and plant development in rice and *Arabidopsis*. *Plant Cell* 21:3767–3780
- Zyprian E, Ochssner I, Schwander F, Šimon S, Hausmann L, Bonow-Rex M, Moreno-Sanz P, Grando MS, Wiedemann-Merdinoglu S, Merdinoglu D, Eibach R, Töpfer R (2016) Quantitative trait loci affecting pathogen resistance and ripening of grapevines. *Mol Genet Genomics* 291:1573–1594

**Publisher's Note** Springer Nature remains neutral with regard to jurisdictional claims in published maps and institutional affiliations.

## **4 - General Discussion**

## General Discussion

The overall aim of this thesis was to infer the phenotypic main factors of grapevine cluster compactness, to reveal molecular indications for cluster determining traits. Furthermore, first markers should be developed that have the capacity to differentiate between loosely and compactly clustered grapevines for MAS. The following chapter aims at linking the successful outcome of the different approaches of this thesis with the results of our collaborators, discussing aspects of experiments that are not covered in detail in the published articles, and adds results of yet unpublished experiments to the discussion.

### **4.1 Considerations on grapevine cluster architecture as breeding target**

An essential task of the conducted experiments was to reveal the key drivers of cluster architecture in defined genetic backgrounds of grapevine. As described above, cluster compactness is a complex composition of cluster architecture sub-traits (Chapter 1.4 Figure 2). However, six phenotypic key factors for cluster compactness could be identified in a diverse set of F1 individuals from a mapping population segregating for the trait cluster compactness. These factors are also important in the intra-varietal context of 'Pinot Noir' clones, however, to a different extent. For grapevine breeding, these results are of high value for two reasons: **I)** Individuals with loose grape clusters are significantly more resilient to *B. cinerea* reported in inter- and intra-varietal context (Alonso-Villaverde et al. 2008; Hed et al. 2009; Konrad et al. 2003; Vail and Marois 1991). **II)** The detailed knowledge of a diverse set of sub-traits, potentially contributing to loose cluster architecture, raises the degree of freedom in a breeding scheme aiming at achieving a loosely structured grape cluster. Some of the discovered loci and candidate genes for cluster architecture sub-traits are physically linked to additional traits like resistances e.g. the resistance loci for *E. necator* and *P. viticola* does co-localize with the loci for berry volume and cluster weight on Chr.12 (Appendix III Figure 1). Hence, it might be feasible that several beneficial traits are jointly selected and introgressed in a new cultivar. On the other hand, if the additional beneficial locus is tightly linked with a disadvantageous compact CA allele, uncoupling of the two loci by recombination becomes difficult. In such a case, it is possible in principal to select one of the 29 other loci for CA sub-traits for the introgression of loose CA in new cultivars.

The correlation analysis performed with the CA measurement results of F1 individuals in Chapter 2 revealed, that berry related cluster architecture sub-traits had a considerably stronger correlation with the compactness ranking in the F1 individuals as compared to the

## General Discussion

sub-traits based on rachis measurements (online resource 2 in Richter et al. 2019). This indicates that berry-related sub-traits could serve as a more effective target in a breeding program. However, *V. vinifera* varieties have been selected over centuries (Kui et al. 2020) for their yield (tons per hectare) or quality (berry pulp to skin ratio) features (Barbagallo et al. 2011; Gil et al. 2015; Matthews and Nuzzo 2007). Thus, targeting berry aspects in a breeding scheme aiming at the introduction of advantageous CA bears the chance for a conflict of interest: the already achieved breeding value in terms of yield and quality may compete with the selection of berry traits associated to loose CA. In Chapter 2, a modeling approach confirms already reported phenotypic key features associated with grapevine cluster compactness (for a review on already determined cluster architecture sub-traits see Tello and Ibáñez (2017)) e.g. cluster weight, berry size, berry number in the genetic background of the cross ‘Calardis Musqué’ x ‘Villard Blanc’. In addition, with the utilization of random forest and cumulative linked models, also the rachis-related sub-trait rachis length turned out to be a major factor for cluster compactness. Interestingly, to some degree, the rachis measurements “pedicel length” and “shoulder length” could be confirmed as predictors for cluster compactness in the phenotypically diverse set of F1 individuals as well. This allows the berry-trait independent selection of loose cluster phenotypes based on features of the rachis avoiding negative aspects of altered berry-volume ratios (Chapter 2).

In the multi seasonal data set from the F1 individuals of the cross population two tendencies were revealed with a principal component analysis of the phenotypic data (Richter et al. 2019 Figure 2). Firstly, the model factor ‘season’ had a higher impact on berry volume/mass related traits as compared to non-berry architecture features. This is comparable with results reported for rapeseed (*Brassica napus*) where the plant yield components varied greatly from year to year but the plant architecture factors were much more consistent during several seasons (Cai et al. 2016). In experiments with a table grape cross population, all fruit and yield components showed only moderate repeatability during three consecutive seasons (Fanizza et al. 2005) pointing out that also for table grapes the environmental influence on berry traits is high. On the other hand, in accordance with findings in Chapter 2 an intra-varietal survey with ‘Granacha’ clones revealed that rachis features were influenced by environment to a lesser extent (Lorenzo et al. 2019). Taken together, berry related sub-traits can have significant impact on CA but might not be preferable traits in a smart breeding

## General Discussion

program aiming at loose cluster architecture if more constant rachis-based sub-traits segregate and contribute to loose cluster architecture as well.

The cross population scrutinized in Chapter 2 consists of 46 F1 individuals with female flowers and 103 hermaphrodites. This leads to the second tendency observed in the phenotypic data set. For the individuals of the cross population, flower sex (FS) had influenced cluster density during both seasons. Individuals with female flower organs showed elongated rachis sub-traits and were consequently less compact. The impact of FS on grapevine cluster architecture was also reported in Marguerit et al. (2009). In their study, the individuals with male and female flowers showed significantly longer rachis length compared to individuals having hermaphrodite flowers. Congruently, the study of Marguerit et al. (2009) and Chapter 2 of this thesis report that the rachis length differences are genetically co-located with the sex-determining locus on linkage group 2, supporting the link of cluster architecture and flower sex. Plant hormone levels showed their capacity to alter cluster architecture e.g. gibberellin causes elongated rachis and laterals of the bunch (Correa et al. 2014; Molitor et al. 2012). Isci and Gökbayrak (2015) reported elongated bunch length after brassinosteroid (BR) application. An analysis, of the dioecious wild *Vitis* flower transcriptome, revealed a differential gene expression of genes that control hormone behavior among the three possible *Vitis* flower types during flower development (Ramos et al. 2017). Arguably, this might support the notion of a FS dependent manifestation of rachis length based on different hormone levels encountered in different flower types during the sex determining process.

Although, the phenotypic variability observed in the 149 F1 individuals in terms of compactness was extreme, including very loose and very compact phenotypes, a significant positive correlation of cluster weight with cluster compactness was observed (Chapter 2 online resource 2). This met the expectations, since several studies report that cluster weight is a compactness-determining factor (Tello et al. 2015; Vail and Marois 1991; Valdes-Gomez et al. 2008). Cluster weight is an amalgamated feature that is based on two factors i.e. berry number and single berry mass. These traits are influenced by sink source modulating viticultural practices and by the environment as reviewed in Li-Mallet et al. (2016), Tello et al. (2015) and references therein. Further, it was reported that different viticultural management systems influence grapevine mean berry weight/volume (Döring et al. 2015). Experiments in Chapter 3 of this thesis include three trial locations and show that cluster weight was significantly influenced by location. The generalized linear models that were used to equate the clones over

## General Discussion

environments accounted for the effects of season and location that allowed the comparison between clones in different environments. However, 'Pinot Noir' clones –counter intuitively– show a negative correlation between cluster weight and compactness. The 'Pinot Noir' clones with the highest cluster weight were among the loosely clustered clones e.g. the Weinsberg (We) clones and some Freiburg (Fr) clones (Chapter 3 Table 2). A further peculiarity of the 'Pinot Noir' clone group is the sub-trait pedicel length. It showed the capacity to contribute significantly to cluster compactness and was capable to discriminate compactly clustered clones in all environments. These findings were supported by a ten-year trial assessing 42 'Pinot' clones, in which elongated pedicel length was identified as a key feature for reduced cluster compactness in 'Pinot' clones with subsequently less *B. cinerea* infections (Konrad et al. 2003). This underlines the cultivar specific sub-trait contribution to the overall compactness at inter- and intra-cultivar level. Notably, among the ten sub-traits with differences between the assessed 'Pinot Noir' clones (Online resource 6c in Richter et al. (2020)), only the traits pedicel length and peduncle length were not significantly affected by environment. The results reported here suggest that reliable phenotypic assessments of cluster architecture need to be based on repeated observations at different field trial locations to account for the environmental impact on the results of this important trait.

Results in Tello et al. (2015) support the cultivar dependent manifestation of cluster architecture. The comparison of cluster density at intra- and inter-cultivar level revealed a low but significant correlation with almost all measured cluster architecture sub-traits. Indeed, studies that compare only a few cultivars or a restricted phenotypic range, report various traits as key determining factors for cluster compactness e.g. berry number (Dry et al. 2010; Tello et al. 2016), single berry volume (Alonso-Villaverde et al. 2008; Schildberger et al. 2011), rachis internode length (Shavrukov et al. 2004) and pedicel length (Rossmann et al. 2020). In Tello et al. (2015), the authors explicitly suggest that any in general minor contributor may play important roles in certain cultivars. This is reflected by the finding that long pedicel length is a main driver of loose clusters in 'Pinot Noir' clones (Chapter 3) but showed less impact on compactness in the phenotypically diverse background of the cross population in Chapter 2. In contrast, Alonso-Villaverde et al. (2008) reported in an intra-varietal study based on 'Albariño' clones that the clone having the shortest pedicels, had the lowest cluster compactness. This is giving an additional hint on the individuality of the importance of cluster architecture sub-traits for a given cultivar.

## General Discussion

Nevertheless, the multi factorial analysis of cluster architecture of 149 F1 genotypes of the cross population in Richter et al. (2019) revealed berry volume, berry number, rachis and shoulder length as pivotal contributors for cluster density. After assessing over 100 wine and table grape varieties for the impact of specific cluster architecture characteristics on cluster compactness, also Tello et al. (2015) reported similarly the number of berries, berry dimensions and length of the first lateral branch as important sub-traits. This suggests that key features for cluster architecture with the capacity to contribute in a more general manner to loose cluster architecture exist. Providing the possibility that transferable marker for pivotal cluster architecture sub-traits could be uniformly used in MAS for loose cluster architecture.

The complexity of cluster architecture sub-traits urges the desire to simplify the observations. Numerous compactness indices that combine several measurements into an index are reported and reviewed (Tello and Ibanez 2014). However, the use of combined measurements in an index for cluster compactness leads to less discriminating power in follow up experiments. For example, cluster weight is composed of berry number and berry mass/volume as described above. In Chapter 2, four QTLs for cluster weight could be identified during consecutive seasons at four linkage groups. Two QTLs for cluster weight co-localize with QTLs for berry number, a third QTL is co-localized with QTL for mean berry volume and the fourth is co-localized with QTLs for berry number and mean berry volume. Therefore, it seems suitable not to combine single measurements to aggregated indices but use the original records for single sub-traits in order to obtain precise results in follow up experiments.

Recently, phenotyping approaches have been reported which utilize new visualization procedures next to the standard RGB images to describe cluster compactness. Rist et al. (2018) used dense 3D point clouds of grapevine bunches and was capable to identify berry number, mean berry volume and bunch length, among other cluster sub-traits. Interestingly, using the automated imaging process to evaluate the cluster architecture phenotype of the same cross population that was analyzed in Chapter 2 of this thesis, Rist et al. (2019) identified similar QTLs compared to the QTLs revealed with conventional measurement methods in the course of this work (Chapter 2; Richter et al. (2019)). These promising results for automated phenotyping may allow indirect investigations of cluster architecture with the assessment of correlated morphological traits e.g. leaf area as reviewed by Paulus (2019). This would enable

sensor-based phenotyping of CA under field conditions at early developmental and phenological stages.

### **4.2 QTLs related to cluster architecture**

#### **QTLs for cluster architecture in corresponding genomic regions**

An important aim of this thesis was to determine genetic regions that are linked to phenotypic traits involved in loose cluster architecture. This was achieved in the studies presented in Chapter 2 of this thesis. In total 30, stable QTLs for compactness-levels and cluster architecture sub-traits with high impact on the formation of a loose grape cluster were identified. The transfer of markers that flank the confidence intervals of these QTLs revealed that eight regions can be found where two to four cluster architecture related QTLs do co-localize in the grapevine reference genome PN 40024 12X.v2, (Canaguier et al. 2017). These regions harbor 60% of all detected cluster architecture related QTLs but represent 87% of the cluster architecture variance that could be explained with the complete range of all QTLs detected in Chapter 2. When projected on the reference genome, several thousand genes reside within the flanking markers of the confidence intervals for these QTLs. Using the parental individuals of the segregating population for comparative NGS based analysis of the QTL regions, could represent the starting point for candidate gene identification.

#### **QTLs for cluster architecture compared to QTLs for alternative breeding goals**

Studies exploiting more than 50 cross populations revealing loci for over 100 traits are reported in Delrot et al. (2020). Notably, the population used for the genetic analysis of cluster architecture in Chapter 2 of this thesis, ('Calardis Musqué' x 'Villard Blanc'), was already part of these reports. It was successfully utilized for the detection of resistance loci and phenology related loci (Zyprian et al. 2016). Markedly, the previously reported QTLs for phenology and resistances calculated in Zyprian et al. (2016) with this population do not physically correspond with the cluster architecture loci identified in this thesis (Figure 1 Appendix III). Very recently, Kamal et al. (2019) used this population for a study to reveal the genetics of flowering time point and reported stable QTLs for flowering time (FTi) in grapevine. Comparing the inflorescence specific candidate genes for flowering time in Kamal et al. (2019) with the positional candidate genes for cluster architecture in Chapter 2 of this thesis revealed an overlap. Eight genes were correlated to cluster architecture and coincidentally to the time

## General Discussion

point for flowering. Amid these genes are interesting candidates for both traits e.g. VIT\_17s0000g00430, reported to be a switch gene for the first developmental transition in ripening berries (Fasoli et al. 2018) and VIT\_02s0025g03560 differentially modulated in wine grapes infected with the fungus *Botrytis* (Fortes and Gallusci 2017). In the studies of Kamal et al. (2019) and Richter et al. (2019), the phenotypical evaluations leading to identical positional candidate genes for flowering time and CA were made in the same cross at the same plant organ. The manifestation of cluster architecture and date of flowering is determined in an overlapping time range between BBCH57 to BBCH65. Using inflorescence samples of this time range for differential gene expression assays between contrasting individuals in terms of FTi and CA might help to reveal the association of the genes to each of the traits. This highlights the necessity of additional studies aiming at the assessment of the gene expression of a gene in a specific tissue at several time points as further indicator for a probable function of the gene.

The reported physical positions for cluster architecture QTLs in Chapter 2 and the physical positions for QTLs for other traits in other crosses as stated in the VIVC database ([www.vivc.de/loci](http://www.vivc.de/loci)) are co-localized in three physically overlapping regions (Figure 1 Appendix III). The QTL (fleshless berries *Flb*) at the upper telomeric part of chromosome 18 is based on a mutation in the *PISTILLATA-like* MADS-box gene (*VvPI*) causal for the impaired mesocarp formation leading to reduced mean berry volume and cluster weight (Fernandez et al. 2013). Correspondingly, a QTL for cluster weight was reported at that position in this thesis. However, in Richter et al (2019) the QTL for cluster weight was co-located with a QTL for berry number. Hence, cluster weight is influenced by different sub-traits, i.e. mean berry volume in Fernandez et al. (2013) and berry number in the study presented here, not suggesting further commonality. Again, this demonstrates the value of precise CA phenotyping at sub-trait resolution.

### **QTLs for cluster architecture on chromosome 2 and the effect of flower sex**

The genetic region that determines flower sex in domesticated *V. vinifera* was linked to the marker VVIB23 and is located at the upper chromosomal arm of chromosome two. Although the flower sex-determining locus was pinpointed to a small genomic region the causal genes are yet not fully understood (reviewed in Delrot et al. (2020)). Two crossing populations, both segregating for flower sex and cluster architecture traits, showed influence of FS on sub-traits of CA (Marguerit et al. 2009; Richter et al. 2019). The genetic investigations

## General Discussion

presented in Chapter 2 revealed that four QTLs for CA overlap at the position of the FS-locus in the reference genome around the markers VVIB23 and GF02-12. The capacity of FS to cause cluster density variation was further implied by the finding that the phenotypic data of 103 hermaphrodite individuals of the cross ('Calardis Musqué' × 'Villard Blanc') showed no QTL linked with those markers. However, the phenotype data of the entire population of the cross including the female individuals (n=46) lead to the detection of a QTL at that position for cluster density explaining 15 to 29% of the variation in cluster density during three consecutive seasons (Figure 2 Appendix III). Therefore, the markers of this genetic region could be potentially linked to both traits. Indeed, the allele assessment of the marker GF02-12 revealed effects on both traits. Regarding cluster architecture, the LOD<sub>max</sub> marker for cluster density on LG 2 was the SSR marker GF02-12 (Richter et al. 2019). Scrutinizing the allele effect of this marker reveals that the 174 bp allele was linked to dense cluster architecture. Moreover, the absence of the allele in was highly linked to loose cluster architecture (Figure 3 Appendix III). Regarding FS determination, in Chapter 2, all 46 F1 individuals with a female flower type also lack the 174 bp SSR allele at this locus. Whereas, 102 hermaphrodite F1 individuals had a heterozygous or homozygous 174 bp amplification product at this locus. This suggests the linkage of the marker GF02-12 to a flower sex-determining locus as reported in Fechter et al. (2012). However, the F1 genotype Gf.1989-30-0361 in the cross population recombines a hermaphrodite flower type with the absence of the 174 bp allele at this locus. This recombination seems to uncouple the in general unwanted female flower type from the desired loose cluster architecture (Figure 3 Appendix III). A sequence-based analysis including this recombinant genotype could help to identify the causal link between FS and loose cluster architecture. Using the confidence interval sequence at this locus for QTL-sequencing, including female genotypes, hermaphrodite genotypes and the recombinant genotype (Gf.1989-30-0361), would provide the resolution to detect the causal sequence variants for loose cluster architecture.

Preliminary results for this physical region on chromosome 2 report genetic cues directly involved in resistance to *B. cinerea* (Sapkota et al. 2019). The link between those studies remains to be shown since the study of Sapkota et al. (2019) did not focus on experiments based on cluster architecture but on scoring the disease severity of *B. cinerea* infections at detached berries. The experiments in Chapter 2 of this thesis associated two LOD<sub>max</sub> markers for important rachis traits i.e. the marker VVIB23 correlating to rachis length and GF02-12 to

cluster density. These are localized in the region of the reference genome were Sapkota and colleagues reported the QTL for *B. cinerea* resistance. The marker GF02-12 explains ~ 20% of the total variation in cluster density (OIV204) observed in this crossing population. This might be an additional indicator for the importance of a loosely clustered bunch to enhanced *B. cinerea* resilience although the mechanism remains to be elucidated.

### **4.3 Proof-of-concept for marker assisted selection of dense cluster architecture**

QTL mapping allows breeders to use marker-assisted selection (MAS) for the precise introgression of beneficial QTL alleles into elite cultivars for crop improvement (Maloof (2003). However, due to the complex contribution of cluster architecture sub-traits to cluster compactness, as reported in Chapter 2, it is not to be expected to find a single genetic marker that is capable to efficiently discriminate individuals with loose / compact clusters in a given cross. Indeed, the work presented in Chapter 2 (Richter et al. 2019) identified a total of 30 stable QTLs for cluster compactness (OIV204) and related traits, respectively. Moreover, a set of molecular markers linked to the key traits of cluster architecture could be described (Table 3 in Richter et al. 2019). In addition, a non-parametric mapping reported in Appendix III showed that 36 further markers carry alleles with the capacity to identify significant variation of compactness. For applied grapevine breeding, a combination of trait-associated markers, instead utilizing a single marker, may be an intermediate step for marker-assisted selection of cluster architecture aspects. For example, a set of three carefully chosen genetic markers could reduce the number of undesirable compact clustered genotypes by 29% without selecting a single false positive in the investigated population (Figure 3). This negative selection would help to cut down the costs for follow up maintenance and phenotyping, improving the throughput with the given resources. In addition, the selective markers for compactness are linked to both categories of variation i.e. berry related traits and rachis related traits (Table 1 Appendix III). This fact enables the selection of loose cluster architecture by markers for rachis traits without automatically involving berry features. With the application of markers that are linked primarily to rachis features, the trade-off between loose cluster architecture at the one side and quality plus quantity aspects inherent to the berry related sub-traits at the other side could be avoided.

## General Discussion

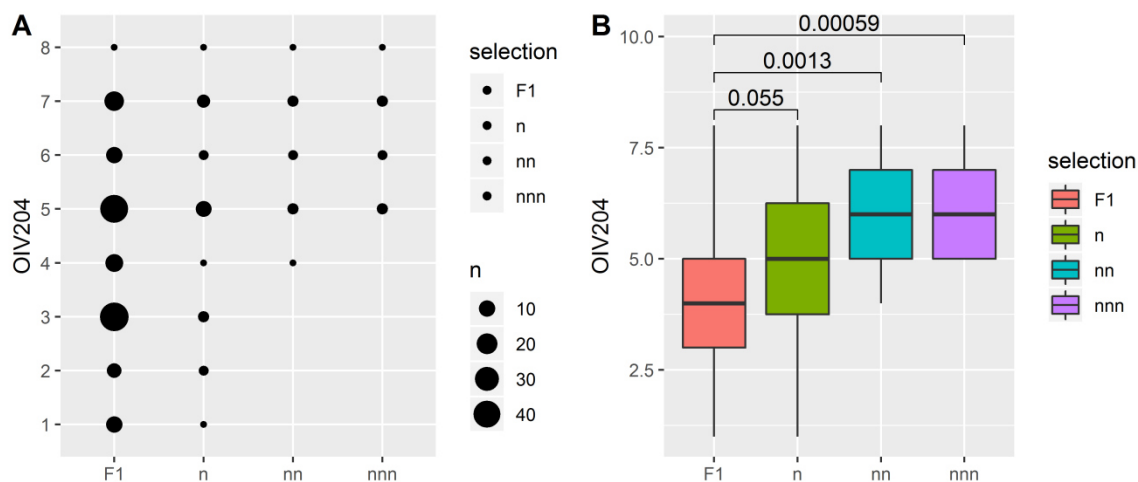


**Figure 3** Negative selection of compactly clustered individuals in 149 F1 genotypes of the cross population ('Calardis Musqué' x 'Villard Blanc'). 29% of the genotypes with compact cluster architecture ( $OIV204 > 5$ ) could be identified using three markers. n) = selection with the allele 116 bp of the marker GF01\_07. nn) selection of genotypes having n + the 337 bp allele of the marker GF09\_48. nnn) having nn+ selection of genotypes with the marker EDS1\_CF\_SNP1520GF nt polymorphism (A) at 17:8554736. For detailed marker information, see Zyprian et al. (2016) and table 2 Appendix III.

A) Count distribution for the scoring with the descriptor OIV204 (cluster compactness) in all 149 genotypes of the population (F1) and for marker based selections combining up to three alleles (n, nn, nnn). B) Average compactness for 149 F1 genotypes, 24 n selected genotypes, 10 nn genotypes and 9 nnn genotypes. The  $p$ -values report the Kruskal Wallis test results for different group means of marker selected sub-groups with the entire population.

### 4.4 Candidate genes derived in the framework of the 'MATA' project

The molecular and genetic analysis presented in this thesis, was part of a joint effort ('MATA-Molekulare Analyse der Traubenarchitektur' funded by BÖLN funding code: 2811NA056 and 2811NA093) in cooperation with partners of the Max Planck Institute for Plant Breeding Research in Cologne (MIPZ). Mainly in parallel, four different approaches were undertaken to understand the genetic basis involved in phenotypic differences of grapevine cluster architecture. **I)** Positional candidate genes for cluster architecture were inferred by QTL calculations based on the linkage of marker alleles to the phenotype of the F1 offspring in a biparental cross (Richter et al. 2019). **II)** Transcriptome analysis in two loosely and in two compactly clustered 'Pinot Noir' clones revealed over 1500 genes differentially expressed between two loosely and two compactly clustered phenotypes at one trial location (Rossmann et al. 2020). **III)** When compared to the compact clones, over 1600 DNA structure variants were detected in the loosely clustered clones with DNA sequencing. The combination of whole

## General Discussion

genome sequencing and transcriptomic analysis revealed the growth regulating factor gene *VvGRF4* as causal contributor for the long pedicel phenotype in 'Pinot Noir' clones (Rossmann et al. 2020). IV) High throughput RT-q-PCR was applied to assess the relative expression of 92 candidate genes. In preliminary RNA sequencing experiments, performed by our colleges of the MPIPZ, these genes were differentially expressed between 'Pinot Noir' clones with loose and compact clusters. Interestingly, these genes were to some extent physically located in the confidence intervals of QTLs for cluster architecture sub-traits reported in Richter et al. (2019) or their function in cell growth and proliferation was already reported for other crops (for an overview see online resource 3 Richter et al. 2020). The differential gene expression of these selected candidate genes was subsequently assessed in an expanded set of 12 'Pinot Noir' clones of five selection lines in different environments. In addition, the candidate gene expression was assessed in loosely clustered reference varieties for cluster density (OIV204) and in selected F1 individuals of the cross population with extreme rachis and pedicel length as reported in Richter et al. (2020). This approach identified seven candidates with differential gene expression between loose and compact individuals in a broader genetic range. These genes as well were positional candidate genes located in the confidence intervals of QTLs for cluster architecture. Hence, the candidate genes reported in this thesis emphasize on several lines of evidence i.e. up to three different technical approaches and multiple independent genetic backgrounds confirm their possible involvement in CA. These genes may have the capacity to be successfully involved in marker development for MAS and could guide breeders to identify optimized breeding material. An overview of the results derived with the four different approaches and their overlaps are presented in figure 4. Aside the candidate genes that have been implicitly reported in Chapter 3 of this thesis, further five genes showed cluster architecture association in the divergent genetic backgrounds i.e. 'Pinot Noir' clones and in the offspring of the cross 'Calardis Musqué' x 'Villard Blanc' (Figure 4). Likewise, these genes are of special interest since they provide the possibility to be causal for cluster architecture differences across diverse genetic backgrounds.

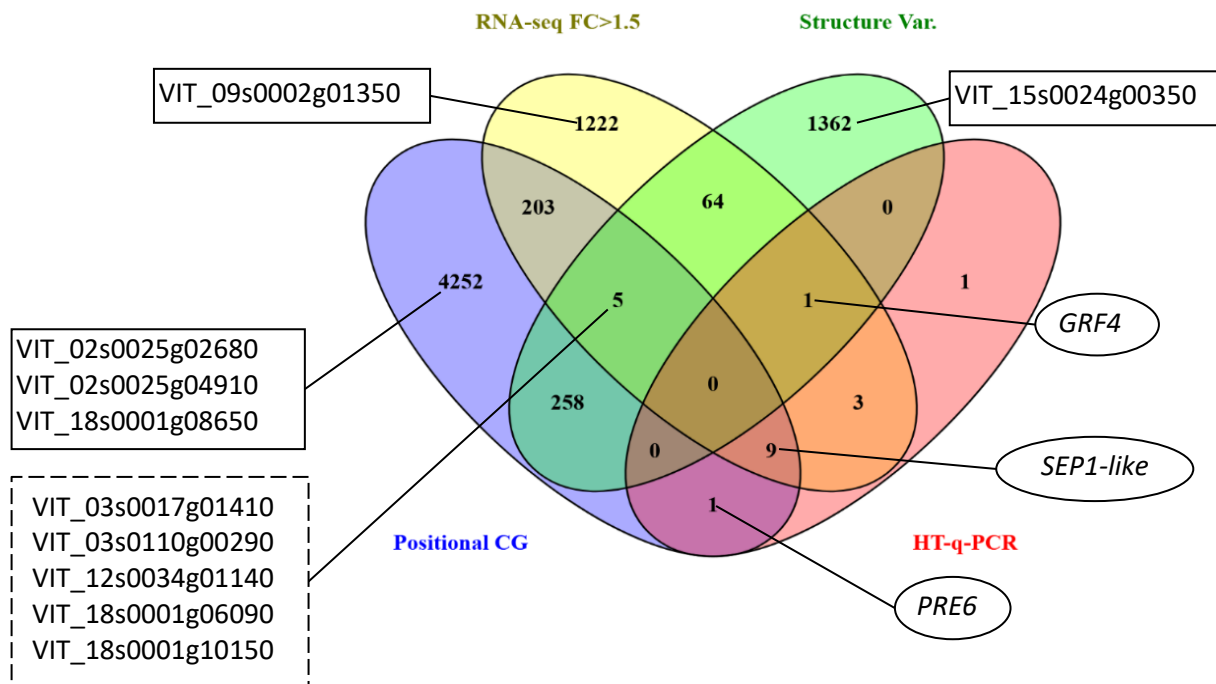


**Figure 4.** Number of candidate genes related to cluster architecture inferred by means of four different approaches. RNA sequencing and HT-q-PCR revealed differential gene expression between loosely and compactly clustered individuals. DNA sequencing of loosely and compactly clustered individuals revealed structure variances. QTL calculations defined positional candidate genes located in the physical regions of confidence intervals for cluster architecture sub-traits at the reference genome (PN40024 version 12X.v2). Differentially expressed transcription factor genes (in ellipses) and additional target genes of miRNA396d (in rectangles) are assigned according to their subgroup membership. Notably, further five genes are co supported candidate genes for cluster architecture (rectangle with dashed line).

#### 4.5 Differentially expressed transcription factors and related candidate genes

An important objective of this thesis was the identification of candidate genes associated to cluster architecture and to develop first markers for the early detection of the desired trait, loose cluster architecture. Transcription factors are of special interest for marker development based on their high impact on downstream genes involved in the trait of interest. Three genes among the 15 differentially expressed genes in Chapter 3 are annotated with transcription factor function i.e. VIT\_01s0026g02030 encoding PACLOBUTRAZOLE-RESISTANCE 6 (PRE6), VIT\_16s0039g01450 encoding GROWTH REGULATION FACTOR 4 (GRF4) and VIT\_17s0000g05000 coding for SEPALLATA1-like (SEP1-like). In addition, multiple experiments supported their association with cluster architecture (Figure 4). The transcript abundance of these three genes was coherent positively correlated with the sub-trait

## General Discussion

measurements for mean berry volume (MBV) and pedicel length (PED) and negatively correlated with the sub-trait shoulder length (SL). Except for one gene, the coefficient of correlation for relative gene expression between the three putative transcription factors and the other differentially regulated genes was also highly significant (Table 7 and 8 Richter et al. 2020). This provides the option that the genes exert their function as part of an expression network. Though, an evidence-based network analysis using the 'Search Tool for the Retrieval of Interacting Genes' (STRING) (Szklarczyk et al. 2019) revealed no direct significant interactions among the three transcriptions factors. This might point to the possibility that they contribute independently to different growth mechanisms e.g. cell division and enlargement. The tissue samples for the differential gene expression experiments have been collected during a period of intense growth driven by process of cell division and elongation at BBCH57 and BBCH71. During that time, loosely cluster PN clones show more increment of growth compared to compactly clustered PN clones (Richter et al. 2017). The same phenomena were measured in loosely and compactly clustered F1 individuals of the cross population (Figure 4 Appendix III). Especially pedicels and considerably rachis and laterals develop at this time (Figure 3 Richter et al. 2020). Characteristically, irreversible extension (cell elongation) is facilitated with pH dependent relaxing of the cell wall (Cosgrove 2005). The beginning of this cell wall loosening process was clearly visible at the later time point (BBCH71) when the inflorescences began to change from erected to hanging position at the branch. The knowledge of this particular growth pattern might contribute to the identification of candidate genes in this tissue, integrating different growth regimes driven by cell division and/or cell elongation.

### ***PRE6 and brassinosteroid related candidate genes***

Investigating the interactions of PRE6 with other proteins, by means of evidence-based networks implemented with STRING, showed that the highest evidence for interaction was reached with the two genes VIT\_15s0021g02140 and VIT\_17s0000g01560 (Table 2 Appendix III). The first contains a RING domain and codes for a protein involved in translational initiation. The latter is a tethering factor involved in vesicle mediated protein transport (Wong et al. 2013). In addition, VIT\_15s0021g02140 belongs to a wider network with significant overrepresentation of proteins belonging to the pathway for ubiquitin-mediated proteolysis. In the cell, proteolysis has a vital role in altering protein load through degradation by means of ubiquitin-mediated response to diverse stimuli (Stone and Callis 2007). The degradation of

## General Discussion

proteins affects many cellular activities particularly plant growth and cell division (Sharma et al. 2016). If the gene VIT\_15s0021g02140 connects grapevine *PRE6* with proteolysis, this could be a hint that variations in cluster architecture phenotype might be based on postponed time points of *PRE6* degradation rather than by different levels of *PRE6* expression in varieties with loose or compact CA.

Hormones integrate endogenous and exogenous signals in order to employ the proteolytic process as the plant's response to environmental conditions (Stone and Callis 2007). Also for CA, hormone dependent alterations have been reported recently (Grimplet et al. 2019; Isci and Gökbayrak 2015). Several literature reports link *PRE6* expression with brassinosteroid levels in different tissues and plant species. VIT\_01s0026g02030 (*PRE6*) is an orthologue of *Oryza sativa* *INCREASED LEAF INCLINATION (IL1)*. In Jiang et al. (2012), *IL1* was mentioned as a brassinosteroid responsive gene measured in a study on a rice dwarf mutant. Regarding growth, plants respond to brassinosteroids (BR) with elongation and expansion of cells promoting shoot and root growth. Brassinosteroids are perceived by BRASSINOSTEROID INSENSITIVE 1 (BRI1) receptor kinase at the cell surface. After a kinase cascade the BR signal also activates PP2A, a phosphatase that phosphorylates and activates the transcription factor BRASSINAZOLE-RESISTANT1 (BZR1) (Anwar et al. 2018). In *Arabidopsis thaliana* and rice the transcription factor gene *IL1* acts downstream of (*BZR1*), regulating plant development. Overexpression of *IL1* increases cell elongation and suppresses dwarf phenotypes in *A. thaliana* (Zhang et al. 2009b). Chapter 3 of this thesis shows that *PRE6* was higher expressed in loosely clustered individuals of diverse genetic backgrounds when compared to compactly clustered individuals (Figure 7 Richter et al. 2020). However, this observation was made at BBCH71 but not at BBCH57. Tissue growth in early developmental stages is based on cytoplasmic growth, turgor-driven wall extension, and mitotic cycles. At later stages of organ development, it is based on turgor-driven extension (Sablowski & Carnier 2014). Thus, genes involved in growth, may target different cellular processes at different developmental stages and different cellular growth regimes (Breuninger and Lenhard 2010). Arguably, prolonged transcription or increased *PRE6* transcript levels in grapevine may contribute to increased cell elongation conveying elongated cluster architecture sub-traits in a brassinosteroid responsive manner in a growth regime depending mainly on cell elongation.

Within the 15 differentially expressed candidate genes, two interacting pairs have been identified by means of evidence-based linkage obtained with STRING (Table 2 Appendix III).

## General Discussion

Interestingly, among these genes are further brassinosteroid related genes i.e. the orthologue of VIT\_04s0008g01100, *Dwarf4* (*DWF4*) and the orthologue of VIT\_17s0053g00990 *EXPANSIN 8* (*EXP8*). *DWF4* is an *A. thaliana* cytochrome P450 putative steroid 22-hydroxylase of the brassinosteroid biosynthetic pathway that correlates with brassinosteroid deficiency in planta (Shimada et al. 2003). *EXP8* and *DWF4* are mentioned together as candidate genes for plant architecture in *B. napus* (Shen et al. 2018) or are involved in phytohormone-regulated developmental plant stages (Glazinska et al. 2017; Liu et al. 2018; Tian et al. 2018). In *A. thaliana*, the transcripts of *EXP8* are induced, but the transcripts of *DWF4* are down regulated by transcription factor BRASSINAZOLE-RESISTANT 1 (BRZ1), resulting in increased cell size in *Arabidopsis* (Tian et al. 2018). During this thesis, individuals with long PED had a similar expression profile for those genes at BBCH71. Actually, the orthologue for *EXP8* was also found to be induced (VIT\_17s0053g00990) whereas *DWF4* (VIT\_04s0008g01100) was down regulated, respectively. Disputably, the expression pattern of VIT\_17s0053g00990 and VIT\_04s0008g01100 in *Vitis* spp. with contrasting pedicel length could depend to some extent on a regulation with the brassinosteroid signaling pathway as reported for *A. thaliana* in Tian et al. (2018). Supporting this notion, Hoffmann et al. (2006) and Anhalt et al. (2013) reported allelic variants for the gene VIT\_17s0053g00990 related to loose and compact cluster architecture of 'Pinot Noir'.

The genes VIT\_04s0008g01100 (*DWF4*), VIT\_17s0053g00990 (*EXP8*) and VIT\_01s0026g02030 (*PRE6*) showed differential expression between PN clones and F1 siblings with divergent loosely and compactly cluster architecture (Richter et al. 2020). In addition, all three genes were connected to brassinosteroid regulation. For the first time, brassins were isolated from pollen extracts of *B. napus*. Comparing the internode length of beans after application of brassins and gibberellic acid showed that brassins had a significantly higher growth promoting effect (Mitchell et al. 1970). Artificial homobrassinolide application at anthesis caused elongated bunches in the table grape variety 'Alphonse Lavallée' (Isci and Gökbayrak 2015). In *A. thaliana*, the BR concentration was highest in flowers whereas rachis tissue had much lower concentrations (Shimada et al. 2003). Interestingly, Gourieroux et al. (2017) could show that the artificial removal of flowers prior to anthesis reduces the rachis length distinctively. It would be interesting to infer if the reduction of flowers corresponds with the BR concentration in rachis tissue. For the analysis of brassinosteroids in plants, different analytical methods have been used for isolation, detection, and characterization of

BR from composite plant materials (Kanwar et al. 2017). Investigating the BR content in individuals with divergent cluster architecture would provide further evidence for the role of this plant hormone in loose grapevine cluster architecture.

### **The miR396–*VvGRF4* interaction**

The most abundant class of small non-coding RNAs are miRNAs. They are involved in post-transcriptional regulations and fine-tuning of genetic programming during plant development (Belli Kullan et al. 2015). Compared to all other tissues, the grapevine miRNA expression atlas shows that samples derived from tendril, inflorescence and rachis tissue had the highest numbers of detected miRNA interaction. Over 150 different miRNAs were expressed in these tissues (Belli Kullan et al. 2015). In rice, miRNA396d is a direct target of the brassinosteroid responsive transcription factor BZR1, and therefore connects the transcription factor PRE6 and the miR396–*VvGRF4* interaction by way of the brassinosteroid regulation. The rice miRNA396d controls various yield traits through different downstream targets. In particular, the growth regulating factor *GRF4* expression with influence on plant architecture (Tang et al. 2018). This is comparable with the role of miRNA396 in grapevine where high transcript abundance of miRNA396 corresponds to low levels of *VvGRF4* (Rossmann et al. 2020).

In the recent work presented by Rossmann et al. (2020), *VvGRF4* was up regulated in loosely clustered ‘Pinot Noir’ clones. This was due to heterozygous *VvGRF4* structure variants hindering the binding of miRNA396a at the *VvGRF4* binding site. Thus, it impairs the miRNA-cleavage of *VvGRF4* resulting in longer PED and higher MBV in all loose clustered ‘Pinot Noir’ clones of the Gm-1 and ‘Mariafeld’ derived selection lines. The two independent SNPs detected in this work could be used e.g. in a KASP™ marker genotyping assay for the detection of the desirable loose cluster architecture in a MAS. The value of *VvGRF4* allelic variants as marker for cluster architecture is underlined with the finding that all ‘Gm-1’ and ‘Mariafeld’ PN clones show an uniformly divergent regulation of *VvGRF4* between loosely and compactly clustered clones over different environments independent of season and location (Richter et al. 2020). Together, these are the first reports for an applicable PED related marker with the relevance for an utilization in applied grapevine breeding aiming at MAS of loosely clustered genotypes in a commercially important variety (worldwide PN is among the top ten cultivated wine varieties (OIV 2017)). Using these loosely clustered PN clones as quality donors in a cross

## General Discussion

with resistance donors allows the introgression of active molecular resistance mechanisms into the genetic background of an organoleptic desired and physically resilient variety. In the offspring of this cross, the causal SNPs in *GRF4* could serve as marker for loose CA. This is especially interesting when aiming at the resilience to *B. cinerea* infections. Currently loose CA is one of a few options in grapevine breeding to introduce physical resilience against this pathogen. In addition, the half parentage of the iconic PN might support the marketing of the new variety.

According to Belli Kullan et al. (2015), the miRNA396d targets further five genes that were associated with CA in the experiments related to this thesis (Figure 4). Using the information provided by the grapevine specific co-expression database (Wong et al. 2013), the gene VIT\_15s0024g00350 is functionally annotated as a TATA-binding protein-associated factor therefore involved in transcription. The genes *VIT\_02s0025g02680*, *VIT\_02s0025g04910*, *VIT\_09s0002g01350* and *VIT\_18s0001g08650* encode the growth regulation factors GRF5-1, GRF5-3, GRF7 and GRF1, respectively. The information accessible by STRING database search, suggests nine homolog proteins of VvGRF4 in *V. vinifera* as further candidate genes with probable cluster architecture related function (Table2 Appendix III). Nevertheless, varieties with divergent genetic background e.g. table grapes of the ‘Cardinal’ family or even the closely related loosely clustered ‘Pinot Gris’ clones did not have the PN-specific *GRF4* SNP but did also show loosely clustered bunches (Supporting table 3, Rossmann et al. 2020). The accumulation of *TEOSINTE-BRANCHED/CYCLOIDEA/PROLIFERATING CELL FACTORS 4* (*TCP4*) transcripts cause an increase in miR396 abundance and a reduction in the transcript levels of all GRFs in *A. thaliana* (Omidbakhshfard et al. 2015). Therefore, TCPs provide structure variant independent regulation options of GRFs suggesting TCPs for further studies as superordinate targets for the search of markers related to CA.

### *VvSEP1-like*

VIT\_17s0000g05000 (*SEP1-like*) was the third differentially regulated transcription factor. VIT\_17s0000g05000 is an E-class gene of the grapevine “ABCDE” model for flowering. According to this model, class A+E genes specify sepals, A+B+E specify petals, B+C+E specify stamens, C+E specify carpels, and C+D+E specify ovules (Palumbo et al. 2019). During this interaction, *SEP1-like* was induced in the flower caps just before flowering. Evidently, *SEP1-like* expression was different between PN clones with divergent cluster architecture during the

## General Discussion

experiments of this thesis suggesting additional roles related to cluster architecture for this gene. However, flowering takes place in a variably expanded time window influenced by genetic and environmental factors (Kamal et al. 2019). This could raise the question whether the detected differential gene expression is due to cluster architecture and represents an additional function for this gene, or was it confounded by the sampling time point just ahead and after flowering.

To avoid such bias, a phenology dependent sampling schedule was implemented in the experimental design in Chapter 3. Firstly, the sampling dates were harmonized over three locations and seasons with the application of cumulated target temperatures for phenological stages as suggested in Molitor et al. (2014). Secondly, based on the availability of several hundred plants per clone at all trial locations, exclusively inconspicuous (unchallenged) looking vines could be used for sampling. Thirdly, the inflorescences were picked from basal insertions at shoots from the center of the fruit cane. So, the phenological stage was not biased by spatial variation present on a plant as described in Shavrukov et al. (2004). Hence, it seems reasonable to assume that based on the multiple lines of evidence (Figure 4), *SEP1-like* has a function in the formation of divergent cluster architecture. Nevertheless, for the reason that 26.2% of the observed gene expression variance were explained by season, considerable environmental influence on the gene expression of *SEP1-like* has to be recognized (Figure 6 Richter et al. 2020).

For most 'Pinot Noir' clones, differing in cluster architecture, the expression correlation among the 15 candidate genes followed a pattern of significantly positive and negative correlation (Online resource 9 Richter et al. 2020). This raises the question whether these genes exert their function in a network. Indeed, the evidence-based linkage (STRING (Szklarczyk et al. 2019)) revealed interactions between the homologues for VIT\_17s0053g00990 with homologues of VIT\_04s0008g01100 and for VIT\_18s0001g03160 with VIT\_18s0001g03540. The genes VIT\_17s0053g00990 and VIT\_04s0008g01100 have been discussed above already due to their linkage to the transcription factor *PRE6*. The additional identified interaction between the homologues for VIT\_18s0001g03160 and VIT\_18s0001g03540 supported a function as auxin transporters with transmembrane domain. Text mining results for this network revealed various situations for interaction of these genes. This ranges from nodule-like structure formation, necessary for mutualistic interaction with nitrogen fixing bacteria in rice (Hiltbrand et al. 2016), to the association with yield and phenology related traits revealed in

## General Discussion

chickpea (Li et al. 2018). Due to the diverse potential roles for VIT\_18s0001g03540, it could be possible that this gene is differentially expressed between 'Pinot Noir' clones but due to biotic or abiotic interactions and not because of cluster architecture traits. This might be reflected by the mostly insignificant and exceptional low correlation to the other genes of the gene expression study (Online resource 9 Richter et al. 2020) and by the high percentage of gene expression that was explained by the factors season and location (Figure 6d Richter et al. 2020).

### 4.6 Conclusion and outlook

This thesis provides an in-depth analysis of plant material, genetic data, candidate genes and molecular markers which in turn are valuable resources to breed physically resilient grape varieties, thus promoting a viticulture which is more resilient to climate change and requires the application of fewer pesticides. In particular, they provide a basis for marker-assisted selection (MAS) of key traits, which have a profound impact on cluster compactness across a broad genetic range. The partitioning of cluster compactness by contributing sub-traits makes it possible to combine markers linked to berry and rachis features. This allows a more effective selection of cluster architecture and provides the chance for a combined introgression with other traits of interest. However, cluster architecture is a complex trait influenced by environmental conditions and controlled by multiple regulatory mechanisms during cell division and enlargement. The integration of phytohormone metabolomics with the expression data of growth-related transcription factors discussed in this thesis, may possibly contribute to a better understanding of the candidate gene expression interacting with variable environmental cues. This could provide further insights into the molecular basis of loose cluster architecture – a key feature in further breeding for resilient grape varieties in particular against pathogens with no known resistance mechanism such as *B. cinerea*.

## 5 - Summary

Cultivated grapevine (*Vitis vinifera*) is one of the most widely grown fruit crops in the world and held in high regard for its nourishing fruits, sweet juices and iconic wines. Global viticulture predominantly utilizes *Vitis vinifera* varieties, because they convey sensory attributes corresponding to the current consumer ideal of product quality. However, they are also highly susceptible to fungal pathogens, and therefore require intense applications of plant protection products with adverse side effects. Consumers criticize the use of pesticides for food production but simultaneously request perfect product quality.

Viticulture could prove it is possible to reduce the demand for pesticides while keeping high quality standards by introducing newly bred varieties with resistances against downy and powdery mildew, two main fungal threats. Nevertheless, plant–pathogen interactions are cycles of resistance and susceptibility, and some strains of these pathogens have developed mechanisms to overcome the resistance within a few decades. Recently, grapevine breeding has started drawing on trait-linked molecular markers to combine several resistance loci within new cultivars for more enduring resistance. For grey mold, a third severe threat in viticulture, an active resistance mechanism is still not feasible. Therefore, grapevine-breeding aims at introducing fungi-static physical properties, e.g. wax layers, more or rigid cells in the berry skin and loose cluster architecture as additional defense mechanisms. This is a way to reduce the susceptibility to pathogens in general and in particular if physical resilience is the only effective option. The central hub of these physical barriers is a loosely clustered variety. The enhanced available space between the berries provides the framework for the effective formation of a firm berry surface and waxy cover and is restricting the time-span with favorable moisture conditions for fungal infections even inside of the cluster.

The overall aim of this thesis was to shed light on genetic cues involved in cluster architecture and to derive first molecular markers that have the capacity to differentiate between loosely and compactly clustered genotypes. This provides the prerequisite for MAS of the desired loosely clustered individuals. To this end, the experimental design of this thesis draws on different sources of natural variance: Firstly, the F1 generation of the cross (‘Calardis Musqué’ × ‘Villard Blanc’) and secondly, somatic variants of the variety ‘Pinot Noir’ showing significantly different cluster compactness. Both sources of natural variation were successfully

## Summary

used to elucidate cluster architecture sub-traits that trigger phenotypic differences between loose and compact clusters.

The genetic approach, applied in Chapter 2, exposed overlapping regions with up to four QTLs for cluster architecture sub-traits that are physically co-located on the grapevine reference genome. Based on co-location on the chromosome, this finding provides the option for a joint introgression of multiple genetic variations in a breeding scheme with an overall considerable effect on CA. In addition, several molecular markers with strong linkage to these cluster architecture sub-traits could be proposed (Richter et al. 2019). A ‘proof of concept’ study (Chapter 4) showed that it was possible to exploit three of these markers for MAS against unwanted compactly clustered individuals. This demonstrates their capacity as selective markers for a complex morphological trait among the individuals of the cross (‘Calardis Musqué’ × ‘Villard Blanc’).

The survey in Chapter 3 reveals that the gene expression of 15 candidate genes consistently correlates to cluster architecture variations of ‘Pinot Noir’ clones in a multi environmental experiment. The genetic approach applied in Richter et al. (2019), the gene expression experiments in Richter et al. (2020) and the results of the RNA-sequencing previously described in Rossmann et al. (2020) provide multiple lines of evidence for the reported candidate genes. In further phenotypically divergent individuals from a genetically diverse background, the transcription factor gene *PRE6* and six genes related to auxin metabolism, cell wall loosening and strigolactones showed differential expression (Richter et al. 2020). Implementing an evidence-based network, allowing a wider view on the interaction of the candidate genes, shows multiple associations of the candidate genes with brassinosteroids, a class of growth-promoting phytohormones. Thus, the candidate genes presented here may have the capacity to be successfully involved in marker development with the aim of selecting cluster architecture traits in MAS enabling breeders to identify optimized breeding material with physical resilience to fungal pathogens such as *B. cinerea*

## 6 – Zusammenfassung

Weltweit rangieren domestizierte Reben (*Vitis vinifera*) unter den meistangebauten Obstkulturen. Die geernteten Trauben werden geschätzt als nahrhaftes Obst, für die Herstellung von Traubensaft und für die Vinifikation begehrter Weine. Im Wesentlichen dominieren *Vitis vinifera* Sorten den globalen Weinbau, da sie die von Verbrauchern gewünschten Merkmale für Produktqualität aufweisen. Jedoch sind diese Sorten hoch anfällig gegenüber pilzlichen Schaderregern und müssen intensiv mit Pestiziden behandelt werden, was abträglichen Nebeneffekten Vortrieb leistet. Der Einsatz von Pestiziden in der Lebensmittelherstellung wird von Verbrauchern zunehmend weniger gebilligt, wobei gleichzeitig makellose Produktqualität erwartet wird.

Für den Weinbau zeigte sich, dass diesem Interessenkonflikt mit der Verwendung von neugezüchteten Sorten begegnet werden kann, welche Resistenzen gegenüber dem Falschen- und Echten Mehltau aufweisen. Sorten mit Resistenzen gegen diese Hauptschaderreger erlauben einen deutlich reduzierten Aufwand an Pflanzenschutz bei hoher Produktqualität. Jedoch verlaufen Interaktionen zwischen Pflanzen und ihren Pathogenen als Zyklen gegenseitiger Anpassung. In deren Abfolge einzelne Pathogen Stämme die Resistenzmechanismen der Pflanzen binnen weniger Jahrzehnte überwinden. Merkmalsgekoppelte molekulare Marker ermöglichen es, mehrere aktive Resistenzmechanismen in einer Sorte zu vereinen. Dies trägt zu einer anhaltenderen Resistenz gegen Schaderreger bei. Grauschimmel verursacht durch *B. cinerea* ist die dritte schwerwiegende Bedrohung für den Weinbau. Dafür sind derzeit keine Marker für zelluläre Resistenzmechanismen bekannt. Deshalb zielt die Züchtung auf das Einkreuzen physikalischer Eigenschaften ab, die das Wachstum oder den Infektionsmechanismus dieses Pathogens behindern. Dazu zählen passive Abwehrmechanismen wie beispielsweise dickere Wachsschichten auf der Epidermis, robustere Zellschichten in der Beerenhaut und lockere Traubenarchitektur. Dies erhöht die Resistenz gegen Schaderreger im Allgemeinen ist jedoch von herausragender Bedeutung, wenn die physikalische Resistenz die einzige verfügbare Resistenz ist. Lockere Traubenarchitektur hat hierbei eine zentrale Rolle, da sie das Ausbilden von effektiven physikalischen Barrieren erst ermöglicht. Zusätzlich fördert die lockere Beschaffenheit der Traube ein zügiges abtrocknen auch der innenliegenden Teile des

## Zusammenfassung

Fruchtstandes. Die reduzierte Zeitspanne mit feuchten Bedingungen verkürzt das Zeitfenster, das für eine erfolgreiche Infektion durch pilzliche Schaderreger zur Verfügung steht.

Das Ziel der Studien dieser Thesis war es genetische Faktoren für lockere Traubenarchitektur zu definieren. Weiterhin sollten erste molekulare Marker ermittelt werden, die für die Differenzierung von Genotypen mit lockeren und kompakten Trauben geeignet sind. Dies schafft die Voraussetzung für die Marker gestützte Selektion der gewünschten lockerbeerigen Individuen. Um dies zu erreichen wurden unterschiedliche Quellen natürlicher Varianz in den Experimenten berücksichtigt: Erstens, F1 Individuen aus der Kreuzung ('Calardis Musqué' × 'Villard Blanc'). Zweitens, somatische Varianten der Sorte 'Pinot Noir' mit signifikanter Varianz der Traubenkompaktheit. Die natürliche Varianz beider Herkünfte konnte dabei erfolgreich zur Identifizierung von Faktoren für lockere Traubenarchitektur herangezogen werden.

Mit den genetischen Untersuchungen in Kapitel 2 konnten deckungsgleiche Regionen des Referenzgenoms für Reben ermittelt werden auf denen quantitative Loci für bis zu vier Faktoren für lockere Traubenarchitektur gemeinsam lokalisiert sind. Bedingt durch die Kolokalisierung auf dem Chromosom, kann so die Introgression mehrerer Faktoren mit substantiellem Effekt auf lockere Traubenarchitektur in einem Zuchtgang gelingen. Darüber hinaus können molekulare Marker mit starker Kopplung zu Faktoren der Traubenarchitektur benannt werden (Richter et al. 2019). Mit einer Konzeptstudie (Kapitel 4) kann der Nachweis erbracht werden, dass drei der ermittelten molekularen Marker gemeinsam geeignet sind um eine Selektion der unerwünschten kompakten Genotypen in der Kreuzungspopulation ('Calardis Musqué' × 'Villard Blanc') durchzuführen.

Die Untersuchungen in Kapitel 3 berücksichtigen Experimente an mehreren Standorten. So zeigt sich, dass die Genexpression von 15 Kandidatengen stabil mit Traubenarchitekturparametern von 'Pinot Noir' Klonen korreliert. Der genetische Untersuchungsansatz in Richter et al. (2019), die Ergebnisse der RNA-Sequenzierungsstudie von Rossmann et al. (2020) und die Genexpressionsstudien in Richter et al. (2020) untermauern gemeinsam die Bedeutung der Kandidatengene für Traubenarchitektur. In weiteren Studien mit, in Bezug auf Traubenarchitektur, stark unterschiedlichen Individuen aus diversem genetischem Hintergrund ergibt sich, dass das Transkriptionsfaktor kodierende Gen *PRE6* und weitere sechs Gene differentiell exprimiert sind. Diese Gene haben Beziehung zu Auxinmetabolismus, Zellwandlockerung und Strigolaktone (Richter et al. 2020). Die

## Zusammenfassung

Ergebnisse einer evidenzbasierten Netzwerkanalyse verweisen auf weitere Interaktionen der Kandidatengene mit Brassinosteroiden, einer Klasse von Phytohormonen mit wachstumsförderndem Effekt. Basierend auf den Ergebnissen der unterschiedlichen Experimente, können die hier vorgestellten Kandidatengene für Traubenarchitektur dazu geeignet sein um molekulare Marker für diese Eigenschaft zu entwickeln. Diese Marker können dann zur MAS von optimiertem Zuchtmaterial mit physikalischer Resilienz gegen *B. cinerea* eingesetzt werden.

## 7 - References

- Adam-Blondon, A. F., Martinez-Zapater, J. M., & Kole, C. (Eds.). (2016). *Genetics, Genomics, and Breeding of Grapes*. CRC Press.
- Adrian, M., & Jeandet, P. (2012). Effects of resveratrol on the ultrastructure of *Botrytis cinerea* conidia and biological significance in plant/pathogen interactions. *Fitoterapia*, *83*(8), 1345-1350.
- Alonso-Villaverde, V., Boso, S., Luis Santiago, J., Gago, P., & Martínez, M. C. (2008). Relationship between susceptibility to *Botrytis* bunch rot and grape cluster morphology in the *Vitis vinifera* L. cultivar Albariño. *International Journal of Fruit Science*, *8*(4), 251-265
- Anhalt, U. C., Martini, K., Ruehl, E. H., & Forneck, A. (2013). Tracing Heterozygosity in the *Vvlexp1* Locus in Grapevine by Sequencing and High-resolution Melt Analysis. *Journal of the American Society for Horticultural Science*, *138*(2), 120-124.
- Anwar, A., Liu, Y., Dong, R., Bai, L., Yu, X., & Li, Y. (2018). The physiological and molecular mechanism of brassinosteroid in response to stress: a review. *Biological research*, *51*(1), 46.
- Bacilieri, R., Lacombe, T., Le Cunff, L., Di Vecchi-Staraz, M., Laucou, V., Genna, B., Péros, J.-P., This, P. & Boursiquot, J. M. (2013). Genetic structure in cultivated grapevines is linked to geography and human selection. *BMC plant biology*, *13*(1), 25.
- Barbagallo, M. G., Guidoni, S., & Hunter, J. J. (2011). Berry size and qualitative characteristics of *Vitis vinifera* L. cv. Syrah. *South African Journal of Enology and Viticulture*, *32*(1), 129-136.
- Battilana, J., Lorenzi, S., Moreira, F. M., Moreno-Sanz, P., Failla, O., Emanuelli, F., & Grando, M. S. (2013). Linkage mapping and molecular diversity at the flower sex locus in wild and cultivated grapevine reveal a prominent SSR haplotype in hermaphrodite plants. *Molecular biotechnology*, *54*(3), 1031-1037.
- Becker, T., & Knoche, M. (2012). Water induces microcracks in the grape berry cuticle. *VITIS*, *51*(3), 141-142.
- Belli Kullán J., Lopes Paim Pinto D., Bertolini E., Fasoli M., Zenoni S., Tornielli G. B., Pezzotti M., Meyers B. C., Farina L., Pè M. E., Mica E. (2015). miRVine: a microRNA expression atlas of grapevine based on small RNA sequencing. *BMC genomics* *16*(1):393
- Bessis R., Fournioux J. C. (1992) Zone d'abscission et coulure de la vigne. *VITIS* *31*(1):9-21
- Boss, P. K., & Thomas, M. R. (2002). Association of dwarfism and floral induction with a grape 'green revolution' mutation. *Nature*, *416*(6883), 847-850.
- Breuninger, H., & Lenhard, M. (2010). Control of tissue and organ growth in plants. In *Current topics in developmental biology* (Vol. 91, pp. 185-220). Academic Press.
- Cai, G., Yang, Q., Chen, H., Yang, Q., Zhang, C., Fan, C., & Zhou, Y. (2016). Genetic dissection of plant architecture and yield-related traits in *Brassica napus*. *Scientific reports*, *6*, 21625.
- Canaguier A., Grimplet J., Di Gaspero G., Scalabrin S., Duchêne E., Choisne N., Mohellibi N., Guichard C., Rombauts S., Le Clainche I., Bérard A., Chauveau A., Bounon R., Rustenholz C., Morgante M., Le Paslier M. C., Brunel D., Adam-Blondon A. F. (2017). A new version of the grapevine reference genome assembly (12X. v2) and of its annotation (VCost. v3). *Genomics data*, *14*, 56.

## References

- Carbonell-Bejerano, P., Royo, C., Mauri, N., Ibáñez, J., & Zapater, J. M. M. (2019). Somatic variation and cultivar innovation in grapevine. In *Advances in Grape and Wine Biotechnology*. IntechOpen.
- Carmona, M. J., Chaïb, J., Martínez-Zapater, J. M., & Thomas, M. R. (2008). A molecular genetic perspective of reproductive development in grapevine. *Journal of experimental botany*, 59(10), 2579-2596.
- Ciliberti, N., Fermaud, M., Languasco, L., & Rossi, V. (2015). Influence of fungal strain, temperature, and wetness duration on infection of grapevine inflorescences and young berry clusters by *Botrytis cinerea*. *Phytopathology*, 105(3), 325-333.
- Cipriani G., Di Gaspero G., Canaguier A., Jusseaume J., Tassin J., Lemainque A., Thareau V., Adam-Blondon A-F., Testolin R. (2011). Molecular linkage maps: strategies, resources and achievements. *Genetics, Genomics and Breeding of Grapes*, 111-136.
- Cochetel N., Minio A., Vondras A. M., Figueroa-Balderas R., Cantu D. (2020). Diploid chromosome-scale assembly of the *Muscadinia rotundifolia* genome supports chromosome fusion and disease resistance gene expansion during *Vitis* and *Muscadinia* divergence. bioRxiv:2020.2006.2002.119792
- Coombe, B. G. (1995). Growth stages of the grapevine: adoption of a system for identifying grapevine growth stages. *Australian journal of grape and wine research*, 1(2), 104-110.
- Correa, J., Mamani, M., Muñoz-Espinoza, C., Laborie, D., Muñoz, C., Pinto, M., & Hinrichsen, P. (2014). Heritability and identification of QTLs and underlying candidate genes associated with the architecture of the grapevine cluster (*Vitis vinifera* L.). *Theoretical and applied genetics*, 127(5), 1143-1162.
- Cosgrove, D. J. (2005). Growth of the plant cell wall. *Nature reviews molecular cell biology*, 6(11), 850.
- Crespan, M., & Milani, N. (2001). The Muscats: A molecular analysis of synonyms, homonyms and genetic relationships within a large family of grapevine cultivars. *VITIS*, 40(1), 23-30
- Delrot S., Grimplet J., Carbonell-Bejerano P., Schwandner A., Bert P-F., Bavaresco L., Costa L. D., Di Gaspero G., Duchêne E., Hausmann L., Malnoy M., Morgante M., Ollat N., Pecile M., Vezzulli S. (2020). Genetic and Genomic Approaches for Adaptation of Grapevine to Climate Change. In *Genomic Designing of Climate-Smart Fruit Crops* (pp. 157-270). Springer, Cham.
- Di Gaspero, G., Cipriani, G., Adam-Blondon, A. F., & Testolin, R. (2007). Linkage maps of grapevine displaying the chromosomal locations of 420 microsatellite markers and 82 markers for R-gene candidates. *Theoretical and Applied Genetics*, 114(7), 1249-1263.
- Di Gaspero, G., & Foria, S. (2015). Molecular grapevine breeding techniques. In *Grapevine breeding programs for the wine industry* (pp. 23-37). Woodhead Publishing.
- Doligez A., Adam-Blondon AF., Cipriani G., Di Gaspero G., Laucou V., Merdinoglu D., Meredith C. P., Riaz S., Roux C., This P. (2006). An integrated SSR map of grapevine based on five mapping populations. *Theoretical and applied genetics*, 113(3), 369-382.
- Döring, J., Frisch, M., Tittmann, S., Stoll, M., & Kauer, R. (2015). Growth, yield and fruit quality of grapevines under organic and biodynamic management. *PLoS One*, 10(10), e0138445.
- Dry, P. R., Longbottom, M. L., McLoughlin, S., Johnson, T. E., & Collins, C. (2010). Classification of reproductive performance of ten winegrape varieties. *Australian Journal of Grape and Wine Research*, 16, 47-55.

## References

- Duchêne E. (2016). How can grapevine genetics contribute to the adaptation to climate change? *OENO ONE*, 50(3) DOI: <https://doi.org/10.20870/oeno-one.2016.50.3.98>
- Eibach, R., & Töpfer, R. (2015). Traditional grapevine breeding techniques. In *Grapevine breeding programs for the wine industry* (pp. 3-22). Woodhead Publishing.
- Elshire, R. J., Glaubitz, J. C., Sun, Q., Poland, J. A., Kawamoto, K., Buckler, E. S., & Mitchell, S. E. (2011). A robust, simple genotyping-by-sequencing (GBS) approach for high diversity species. *PloS one*, 6(5), e19379.
- Emanuelli, F., Battilana, J., Costantini, L., Le Cunff, L., Boursiquot, J. M., This, P., & Grando, M. S. (2010). A candidate gene association study on muscat flavor in grapevine (*Vitis vinifera* L.). *BMC plant biology*, 10(1), 241.
- Fanizza, G., Lamaj, F., Costantini, L., Chaabane, R., & Grando, M. S. (2005). QTL analysis for fruit yield components in table grapes (*Vitis vinifera*). *Theoretical and Applied Genetics*, 111(4), 658-664.
- FAOSTAT (2016). Value of agricultural production. Food and Agriculture Organization of the United Nations. <http://www.fao.org/faostat/en/#data/QC> Accessed: 22nd June 2020
- Fasoli, M., Richter, C. L., Zenoni, S., Bertini, E., Vitulo, N., Dal Santo, S., Dokoozlian N., Pezzotti M. Tornielli, G. B. (2018). Timing and order of the molecular events marking the onset of berry ripening in grapevine. *Plant Physiology*, 178(3), 1187-1206.
- Fechter, I., Hausmann, L., Daum, M., Sörensen, T. R., Viehöver, P., Weisshaar, B., & Töpfer, R. (2012). Candidate genes within a 143 kb region of the flower sex locus in *Vitis*. *Molecular Genetics and Genomics*, 287(3), 247-259.
- Fechter, I., Hausmann, L., Zyprian, E., Daum, M., Holtgräwe, D., Weisshaar, B., & Töpfer, R. (2014). QTL analysis of flowering time and ripening traits suggests an impact of a genomic region on linkage group 1 in *Vitis*. *Theoretical and Applied Genetics*, 127(9), 1857-1872.
- Fermaud, M. (1998). Cultivar susceptibility of grape berry clusters to larvae of *Lobesia botrana* (Lepidoptera: Tortricidae). *Journal of Economic Entomology*, 91(4), 974-980.
- Fernandez, L., Chaïb, J., Martinez-Zapater, J. M., Thomas, M. R., & Torregrosa, L. (2013). Mis-expression of a *PISTILLATA*-like MADS box gene prevents fruit development in grapevine. *The Plant Journal*, 73(6), 918-928.
- Fortes, A. M., & Gallusci, P. (2017). Plant stress responses and phenotypic plasticity in the epigenomics era: perspectives on the grapevine scenario, a model for perennial crop plants. *Frontiers in plant science*, 8, 82.
- Fraga, H., Malheiro, A. C., Moutinho-Pereira, J., & Santos, J. A. (2012). An overview of climate change impacts on European viticulture. *Food and Energy Security*, 1(2), 94-110.
- Gabler, F. M., Smilanick, J. L., Mansour, M., Ramming, D. W., & Mackey, B. E. (2003). Correlations of morphological, anatomical, and chemical features of grape berries with resistance to *Botrytis cinerea*. *Phytopathology*, 93(10), 1263-1273.
- Gadoury, D. M., CADLE-DAVIDSON, L. A. N. C. E., Wilcox, W. F., Dry, I. B., Seem, R. C., & Milgroom, M. G. (2012). Grapevine powdery mildew (*Erysiphe necator*): a fascinating system for the study of the biology, ecology and epidemiology of an obligate biotroph. *Molecular plant pathology*, 13(1), 1-16.
- Galet, P. (1979). *A practical ampelography*. Cornell University Press.
- Gascuel, Q., Diretto, G., Monforte, A. J., Fortes, A. M., & Granell, A. (2017). Use of natural diversity and biotechnology to increase the quality and nutritional content of tomato and grape. *Frontiers in plant science*, 8, 652.

## References

- Gerrath, J. M., Posluszny, U., Ickert-Bond, S. M., & Wen, J. (2017). Inflorescence morphology and development in the basal rosoid lineage Vitales. *Journal of Systematics and Evolution*, 55(6), 542-558.
- Gil, M., Pascual, O., Gómez-Alonso, S., García-Romero, E., Herмосín-Gutiérrez, I., Zamora, F., & Canals, J. M. (2015). Influence of berry size on red wine colour and composition. *Australian Journal of Grape and Wine Research*, 21(2), 200-212.
- Glazinska, P., Wojciechowski, W., Kulasek, M., Glinkowski, W., Marciniak, K., Klajn, N., Kesy, J. & Kopcewicz, J. (2017). De novo transcriptome profiling of flowers, flower pedicels and pods of *Lupinus luteus* (yellow lupine) reveals complex expression changes during organ abscission. *Frontiers in plant science*, 8, 641.
- Gourieroux, A. M., Holzapfel, B. P., McCully, M. E., Scollary, G. R., & Rogiers, S. Y. (2017). Vascular development of the grapevine (*Vitis vinifera* L.) inflorescence rachis in response to flower number, plant growth regulators and defoliation. *Journal of plant research*, 130(5), 873-883.
- Gourieroux, A. M., McCully, M. E., Holzapfel, B. P., Scollary, G. R., & Rogiers, S. Y. (2016). Flowers regulate the growth and vascular development of the inflorescence rachis in *Vitis vinifera* L. *Plant Physiology and Biochemistry*, 108, 519-529.
- Grattapaglia, D., & Sederoff, R. (1994). Genetic linkage maps of *Eucalyptus grandis* and *Eucalyptus urophylla* using a pseudo-testcross: mapping strategy and RAPD markers. *Genetics*, 137(4), 1121-1137.
- Grimplet, J., Ibáñez, S., Baroja, E., Tello, J., & Ibáñez, J. (2019). Phenotypic, hormonal, and genomic variation among *Vitis vinifera* clones with different cluster compactness and reproductive performance. *Frontiers in plant science*, 9, 1917.
- Guo, D. L., Zhao, H. L., Li, Q., Zhang, G. H., Jiang, J. F., Liu, C. H., & Yu, Y. H. (2019). Genome-wide association study of berry-related traits in grape [*Vitis vinifera* L.] based on genotyping-by-sequencing markers. *Horticulture research*, 6(1), 1-13.
- Hed, B., Ngugi, H. K., & Travis, J. W. (2009). Relationship between cluster compactness and bunch rot in Vignoles grapes. *Plant disease*, 93(11), 1195-1201.
- Hedrick, U. P., & Anthony, R. D. (1915). *Inheritance of certain characters of grapes*. *J Agr Res* 4:315-330.
- Herzog, K., Wind, R., & Töpfer, R. (2015). Impedance of the grape berry cuticle as a novel phenotypic trait to estimate resistance to *Botrytis cinerea*. *Sensors*, 15(6), 12498-12512.
- Hickey, C. C., Smith, E. D., Cao, S., & Conner, P. (2019). Muscadine (*Vitis rotundifolia* Michx., syn. *Muscandinia rotundifolia* (Michx.) Small): The Resilient, Native Grape of the Southeastern US. *Agriculture*, 9(6), 131.
- Hiltenbrand, R., Thomas, J., McCarthy, H., Dykema, K. J., Spurr, A., Newhart, H., Winn, M. E., & Mukherjee, A. (2016). A developmental and molecular view of formation of auxin-induced nodule-like structures in land plants. *Frontiers in Plant Science*, 7, 1692.
- Hoffmann, P., Vaclavicek, A., Blach, R., & Forneck, A. (2006, July). A SNP Marker Can Differentiate Loose Clustered Clones of 'Pinot Noir'. In *IX International Conference on Grape Genetics and Breeding* 827 (pp. 471-474).
- Houel, C., Martin-Magniette, M. L., Nicolas, S. D., Lacombe, T., Le Cunff, L., Franck, D., Torregrosa, L., Conejero, G., Lalet, S., This, P., & Adam-Blondon, A. F. (2013). Genetic variability of berry size in the grapevine (*Vitis vinifera* L.). *Australian Journal of Grape and Wine Research*, 19(2), 208-220.
- Husfeld B. (1962). Reben. In: Kappert H., Rudolf W. (Eds). *Handbuch der Pflanzenzüchtung VI Paul Parey, Berlin und Hamburg*, pp 723-773.

## References

- Igounet, O., Baldy, C., Suard, B., Sauvage, F. X., López, F., Boulet, J. C., & Robin, J. P. (1995). Thermal regime of the grape (*Vitis vinifera* L. Syrah grapes) during maturation. Influence of the berry coloration, the compactness degree of the grape and the local wind regime. *OENO One*, 29(4), 193-204.
- Isci, B., & Gökbayrak, Z. (2015). Influence of brassinosteroids on fruit yield and quality of table grape 'Alphonse Lavallée'. *VITIS*, 54(1), 17-19.
- Jaillon O., Aury J-M., Noel B., Policriti A., Clepet C., Casagrande A., Choisne N., Aubourg S., Vitulo N., Jubin C., Vezzi A., Legeai F., Huguene y .P, Dasilva C., Horner D., Mica E., Jublot D., Poulain J., Bruyere C., Billault A., Segurens B., Gouyvenoux M., Ugarte E., Cattonaro F., Anthouard V., Vico V., Del Fabbro C., Alaux M., Di Gaspero G., Dumas V., Felice N., Paillard S., Juman I., Moroldo M., Scalabrin S., Canaguier A., Le Clainche I., Malacrida G., Durand E., Pesole G., Laucou V., Chatelet P., Merdinoglu D., Delledonne M., Pezzotti M., Lecharny A., Scarpelli C., Artiguenave F., Pe M. E., Valle G., Morgante M., Caboche M., Adam-Blondon A-F., Weissenbach J., Quetier F., Wincker P., (2007), The grapevine genome sequence suggests ancestral hexaploidization in major angiosperm phyla. *Nature* 449:463–467.
- Jeandet, P., Bessis, R., & Gautheron, B. (1991). The production of resveratrol (3, 5, 4'-trihydroxystilbene) by grape berries in different developmental stages. *American Journal of Enology and Viticulture*, 42(1), 41-46.
- Jiang, Y., Bao, L., Jeong, S. Y., Kim, S. K., Xu, C., Li, X., & Zhang, Q. (2012). XIAO is involved in the control of organ size by contributing to the regulation of signaling and homeostasis of brassinosteroids and cell cycling in rice. *The Plant Journal*, 70(3), 398-408.
- Jones, N., Ougham, H., & Thomas, H. (1997). Markers and mapping: we are all geneticists now. *New Phytologist*, 137(1), 165-177.
- Kamal, N., Ochßner, I., Schwandner, A., Viehöver, P., Hausmann, L., Töpfer, R. & Holtgräwe, D. (2019). Characterization of genes and alleles involved in the control of flowering time in grapevine. *PloS one*, 14(7), e0214703.
- Kanwar, M. K., Bajguz, A., Zhou, J., & Bhardwaj, R. (2017). Analysis of brassinosteroids in plants. *Journal of Plant Growth Regulation*, 36(4), 1002-1030.
- Kassambara A. (2018). ggpubr: 'ggplot2' based publication ready plots. R package version 0.1, 7.
- Keller M. (2015). *The science of grapevines: anatomy and physiology*. (pp. 194-264). Academic Press (Second Edi).
- Konrad, H., Lindner, B., Bleser, E., & Rühl, E. (2002, August). Strategies in the genetic selection of clones and the preservation of genetic diversity within varieties. In *VIII International Conference on Grape Genetics and Breeding 603* (pp. 105-110).
- Korte, A., & Farlow, A. (2013). The advantages and limitations of trait analysis with GWAS: a review. *Plant methods*, 9(1), 1-9.
- Kui, L., Tang, M., Duan, S., Wang, S., & Dong, X. (2020). Identification of Selective Sweeps in the Domesticated Table and Wine Grape (*Vitis vinifera* L.). *Frontiers in Plant Science*, 11, 572.
- Latorre, B. A., Briceño, E. X., & Torres, R. (2011). Increase in *Cladosporium* spp. populations and rot of wine grapes associated with leaf removal. *Crop Protection*, 30(1), 52-56.
- Laucou, V., Launay, A., Bacilieri, R., Lacombe, T., Adam-Blondon, A. F., Bérard, A., Chauveau A., de Andrés M. T., Hausmann L., Ibáñez J., Le Paslier M-C., Maghradze D., Martinez-Zapater J. M., Maul E., Ponnaiah M., Töpfer R., Péros J-P., & Boursiquot J-

## References

- M. (2018). Extended diversity analysis of cultivated grapevine *Vitis vinifera* with 10K genome-wide SNPs. *PloS one*, 13(2), e0192540.
- Leong, S. L. L., Hocking, A. D., Pitt, J. I., Kazi, B. A., Emmett, R. W., & Scott, E. S. (2006). Australian research on ochratoxigenic fungi and ochratoxin A. *International Journal of Food Microbiology*, 111, S10-S17.
- Li-Mallet, A., Rabot, A., & Geny, L. (2016). Factors controlling inflorescence primordia formation of grapevine: their role in latent bud fruitfulness? A review. *Botany*, 94(3), 147-163.
- Li, Y., Ruperao, P., Batley, J., Edwards, D., Khan, T., Colmer, T. D., Siddique K. H. M. & Sutton, T. (2018). Investigating drought tolerance in chickpea using genome-wide association mapping and genomic selection based on whole-genome resequencing data. *Frontiers in Plant Science*, 9, 190.
- Liu, S., Zhang, Y., Feng, Q., Qin, L., Pan, C., Lamin-Samu, A. T., & Lu, G. (2018). Tomato AUXIN RESPONSE FACTOR 5 regulates fruit set and development via the mediation of auxin and gibberellin signaling. *Scientific reports*, 8(1), 1-16.
- Lodhi, M. A., Ye, G. N., Weeden, N. F., Reisch, B. I., & Daly, M. J. (1995). A molecular marker based linkage map of *Vitis*. *Genome*, 38(4), 786-794.
- Lorenzo M. R., Sabalza F. C., Sarasa A. S., Abad F., Zapater J. M. M., Marcos J. I. (2019). Intra-varietal diversity for agronomic traits in 'Garnacha Blanca'. *VITIS* 58(1):33-35.
- Malooof, J. N. (2003). QTL for plant growth and morphology. *Current opinion in plant biology*, 6(1), 85-90.
- Marguerit, E., Boury, C., Manicki, A., Donnart, M., Butterlin, G., Némorin, A., Wiedemann-Merdinoglu S., Merdinoglu D., Ollat N. & Decroocq, S. (2009). Genetic dissection of sex determinism, inflorescence morphology and downy mildew resistance in grapevine. *Theoretical and Applied Genetics*, 118(7), 1261-1278.
- Marois, J. J., Nelson, J. K., Morrison, J. C., Lile, L. S., & Bledsoe, A. M. (1986). The influence of berry contact within grape clusters on the development of *Botrytis cinerea* and epicuticular wax. *American Journal of Enology and Viticulture*, 37(4), 293-296.
- Matthews, M. A., & Nuzzo, V. (2007). Berry Size and Yield Paradigms on Grapes and Wines Quality. *Acta Horticulturae*, 754(754), 423-436. doi:10.17660/ActaHortic.2007.754.56
- Maul E., Röckel F., Kecke S., Ganesch A. & Töpfer R. (2019). Vitis International Variety Catalogue. www.vivc.de – (08/2020).
- McGovern PE, Mondavi RG (2003) *Ancient Wine: The search for the origins of viniculture*. (pp. 1-14), Princeton. University Press.
- McKey, D., Elias, M., Pujol, B. and Duputié, A. (2010), The evolutionary ecology of clonally propagated domesticated plants. *New Phytologist*, 186: 318-332.
- Migicovsky, Z., & Myles, S. (2017). Exploiting wild relatives for genomics-assisted breeding of perennial crops. *Frontiers in Plant Science*, 8, 460.
- Migicovsky, Z., Sawler, J., Gardner, K. M., Aradhya, M. K., Prins, B. H., Schwaninger, H. R., Bustamante C. D., Buckler E. S., Zhong G-Y., Brown P. J. & Myles, S. (2017). Patterns of genomic and phenomic diversity in wine and table grapes. *Horticulture research*, 4(1), 1-11.
- Mitchell, J. W., Mandava, N., Worley, J. F., Plimmer, J. R., & Smith, M. V. (1970). Brassins—a new family of plant hormones from rape pollen. *Nature*, 225(5237), 1065-1066.
- Molitor, D., Behr, M., Hoffmann, L., & Evers, D. (2012). Research note: Benefits and drawbacks of pre-bloom applications of gibberellic acid (GA3) for stem elongation in Sauvignon blanc. *South African Journal of Enology and Viticulture*, 33(2), 198-202.

## References

- Molitor, D., Junk, J., Evers, D., Hoffmann, L., & Beyer, M. (2014). A high-resolution cumulative degree day-based model to simulate phenological development of grapevine. *American Journal of Enology and Viticulture*, 65(1), 72-80.
- Mosedale, J. R., Abernethy, K. E., Smart, R. E., Wilson, R. J., & Maclean, I. M. (2016). Climate change impacts and adaptive strategies: lessons from the grapevine. *Global change biology*, 22(11), 3814-3828.
- Nair, N. G., & Allen, R. N. (1993). Infection of grape flowers and berries by *Botrytis cinerea* as a function of time and temperature. *Mycological Research*, 97(8), 1012-1014.
- Organisation Internationale de la Vigne et du Vin (2007) OIV descriptor list for grape varieties and *Vitis* species ( Organisation Internationale de la Vigne et du Vin: Paris, France).
- OIV (2015) 2nd edition of the OIV descriptor list for grape varieties and *Vitis* species. Organisation Internationale de la Vigne et du Vin 18 rue d'Aguesseau F-75008 Paris – France [www.oiv.int](http://www.oiv.int)
- OIV (2017) Focus OIV 2017 Distribution of the world's grapevine varieties. OIV - Organisation Internationale de la Vigne et du Vin 18 rue d'Aguesseau F-75008 Paris – France [www.oiv.int](http://www.oiv.int)
- OIV (2019) Statistical report on world vitiviniculture 2019. Statistics Unit of the International Organisation of Vine and Wine International Organisation of Vine and Wine 18 rue d'Aguesseau75008 Paris, France [www.oiv.int](http://www.oiv.int)
- Omidbakhshfard, M. A., Proost, S., Fujikura, U., & Mueller-Roeber, B. (2015). Growth-regulating factors (GRFs): a small transcription factor family with important functions in plant biology. *Molecular plant*, 8(7), 998-1010.
- Palumbo, F., Vannozzi, A., Magon, G., Lucchin, M., & Barcaccia, G. (2019). Genomics of flower identity in grapevine (*Vitis vinifera* L.). *Frontiers in Plant Science*, 10, 316.
- Patel G. I., Olmo H. P. (1955) Cytogenetics of *Vitis*: I. The hybrid *V. Viniferar* X *V. Rotundifolia*. *American Journal of Botany* 42 141-159
- Paulus, S. (2019). Measuring crops in 3D: using geometry for plant phenotyping. *Plant methods*, 15(1), 103.
- R Core Team (2020) R: A language and environment for statistical computing [Computer software manual]. Vienna, Austria. Retrieved from <http://www.R-project.org/>
- Ramos M. J. N., Coito J., Fino J., Cunha J., Silva H., de Almeida P. G., Costa M. M. R., Amancio S., Paulo O. S., Rocheta M. (2017). Deep analysis of wild *Vitis* flower transcriptome reveals unexplored genome regions associated with sex specification. *Plant molecular biology*, 93(1-2), 151-170.
- Reineke, A., & Selim, M. (2019). Elevated atmospheric CO<sub>2</sub> concentrations alter grapevine (*Vitis vinifera*) systemic transcriptional response to European grapevine moth (*Lobesia botrana*) herbivory. *Scientific reports*, 9(1), 1-12.
- Rex, F., Fechter, I., Hausmann, L., & Töpfer, R. (2014). QTL mapping of black rot (*Guignardia bidwellii*) resistance in the grapevine rootstock 'Börner' (*V. riparia* Gm183 × *V. cinerea* Arnold). *Theoretical and Applied Genetics*, 127(7), 1667-1677.
- Riaz S., De Lorenzis G., Velasco D., Koehmstedt A., Maghradze D., Bobokashvili Z., Musayev M., Zdunic G., Laucou V., Andrew Walker M., Failla O., Preece J. E., Aradhya M. & Arroyo-Garcia R. (2018). Genetic diversity analysis of cultivated and wild grapevine (*Vitis vinifera* L.) accessions around the Mediterranean basin and Central Asia. *BMC plant biology*, 18(1), 137.

## References

- Richter, R., Gabriel, D., Rist, F., Töpfer, R., & Zyprian, E. (2019). Identification of co-located QTLs and genomic regions affecting grapevine cluster architecture. *Theoretical and Applied Genetics*, 132(4), 1159-1177.
- Richter, R., Rossmann, S., Gabriel, D., Töpfer, R., Theres, K., & Zyprian, E. (2020). Differential expression of transcription factor- and further growth-related genes correlates with contrasting cluster architecture in *Vitis vinifera* 'Pinot Noir' and *Vitis* spp. genotypes. *Theoretical and Applied Genetics*, 133(12), 3249-3272.
- Richter, R., Rossmann, S., Töpfer, R., Theres, K., & Zyprian, E. (2017). Genetic analysis of loose cluster architecture in grapevine. In *BIO Web of Conferences* (Vol. 9, p. 01016). EDP Sciences.
- Rist, F., Gabriel, D., Mack, J., Steinhage, V., Töpfer, R., & Herzog, K. (2019). Combination of an Automated 3D Field Phenotyping Workflow and Predictive Modelling for High-Throughput and Non-Invasive Phenotyping of Grape Bunches. *Remote Sensing*, 11(24), 2953.
- Rist, F., Herzog, K., Mack, J., Richter, R., Steinhage, V., & Töpfer, R. (2018). High-precision phenotyping of grape bunch architecture using fast 3D sensor and automation. *Sensors*, 18(3), 763.
- Rossmann, S., Richter, R., Sun, H., Schneeberger, K., Töpfer, R., Zyprian, E., & Theres, K. (2020). Mutations in the miR396 binding site of the growth-regulating factor gene *VvGRF4* modulate inflorescence architecture in grapevine. *The Plant Journal*, 101(5), 1234-1248.
- Royo C., Torres-Perez R., Mauri N., Diestro N., Cabezas J. A., Marchal C., Lacombe T., Ibanez J., Tornel M., Carreno J., Martinez-Zapater J. M., Carbonell-Bejerano P. (2018). The major origin of seedless grapes is associated with a missense mutation in the MADS-box gene *VviAGL11*. *Plant physiology*, 177(3), 1234-1253.
- Sablowski, R., & Carnier Dornelas, M. (2014). Interplay between cell growth and cell cycle in plants. *Journal of Experimental Botany*, 65(10), 2703-2714.
- Sapkota, S.D., Chen, L.L., Yang, S., Hyma, K.E., Cadle-Davidson, L.E. and Hwang, C.F. (2019). Quantitative trait locus mapping of downy mildew and *Botrytis* bunch rot resistance in a *Vitis aestivalis*-derived 'Norton'-based population. *Acta Horti*. 1248, 305-312 .
- Schildberger, B., Faltis, C., Arnold, M., & Eder, R. (2011). Effects of prohexadione-calcium on grape cluster structure and susceptibility to bunch rot (*Botrytis cinerea*) in cv. grüner veltliner. *Journal of Plant Pathology*, S33-S37.
- Schmid J., Manty F. & Lindner B. (2019). *Geisenheimer Rebsorten und Klone* (3rd ed. Vol. Bd. 90). Geisenheim: Forschungsanstalt Geisenheim Fachgebiet Rebenzüchtung und Rebenveredelung.
- Schwander, F., Eibach, R., Fechter, I., Hausmann, L., Zyprian, E., & Töpfer, R. (2012). Rpv10: a new locus from the Asian *Vitis* gene pool for pyramiding downy mildew resistance loci in grapevine. *Theoretical and Applied Genetics*, 124(1), 163-176.
- Sharma, B., Joshi, D., Yadav, P. K., Gupta, A. K., & Bhatt, T. K. (2016). Role of ubiquitin-mediated degradation system in plant biology. *Frontiers in plant science*, 7, 806.
- Shavrukov, Y. N., Dry, I. B., & Thomas, M. R. (2004). Inflorescence and bunch architecture development in *Vitis vinifera* L. *Australian journal of grape and wine research*, 10(2), 116-124.

## References

- Shen, Y., Xiang, Y., Xu, E., Ge, X., & Li, Z. (2018). Major co-localized QTL for plant height, branch initiation height, stem diameter, and flowering time in an alien introgression derived *Brassica napus* DH population. *Frontiers in plant science*, 9, 390.
- Shimada, Y., Goda, H., Nakamura, A., Takatsuto, S., Fujioka, S., & Yoshida, S. (2003). Organ-specific expression of brassinosteroid-biosynthetic genes and distribution of endogenous brassinosteroids in *Arabidopsis*. *Plant physiology*, 131(1), 287-297.
- Shiri, Y., Solouki, M., Ebrahimie, E., Emamjomeh, A., & Zahiri, J. (2018). Unraveling the transcriptional complexity of compactness in sistan grape cluster. *Plant Science*, 270, 198-208.
- Smart, R., & Robinson, M. (1991). *Sunlight into wine: a handbook for winegrape canopy management*. Winetitles. Adelaide, S. Australia.
- Spring, O., Gomez-Zeledon, J., Hadziabdic, D., Trigliano, R. N., Thines, M., & Lebeda, A. (2018). Biological characteristics and assessment of virulence diversity in pathosystems of economically important biotrophic oomycetes. *Critical Reviews in Plant Sciences*, 37(6), 439-495.
- Stocker, T. F.; Qin, D.; Plattner, G.-K.; Tignor, M. M. B.; Allen, S. K.; Boschung, J.; Nauels, A.; Xia, Y.; Bex, V.; Midgley, P. M. (Eds.) (2014). *Climate Change 2013: The Physical Science Basis. Contribution of Working Group I to the Fifth Assessment Report of IPCC the Intergovernmental Panel on Climate Change*. Cambridge: Cambridge University Press 10.1017/CBO9781107415324.
- Stone, S. L., & Callis, J. (2007). Ubiquitin ligases mediate growth and development by promoting protein death. *Current opinion in plant biology*, 10(6), 624-632.
- Szklarczyk D., Gable A. L., Lyon D., Junge A., Wyder S., Huerta-Cepas J., Simonovic M., Doncheva N. T., Morris J. H., Bork P., Jensen L. J., v Mering C. (2019) STRING v11: protein-protein association networks with increased coverage, supporting functional discovery in genome-wide experimental datasets. *Nucleic acids research*, 47(D1), D607-D613.
- Tang, Y., Liu, H., Guo, S., Wang, B., Li, Z., Chong, K., & Xu, Y. (2018). OsmiR396d affects gibberellin and brassinosteroid signaling to regulate plant architecture in rice. *Plant physiology*, 176(1), 946-959.
- Tanksley, S. D., Young, N. D., Paterson, A. H., & Bonierbale, M. W. (1989). RFLP mapping in plant breeding: new tools for an old science. *Bio/technology*, 7(3), 257-264.
- Tello, J., Aguirrezábal, R., Hernáiz, S., Larreina, B., Montemayor, M. I., Vaquero, E., & Ibáñez, J. (2015). Multicultivar and multivariate study of the natural variation for grapevine bunch compactness. *Australian journal of grape and wine research*, 21(2), 277-289.
- Tello, J., & Ibáñez Marcos, J. (2014). Evaluation of indexes for the quantitative and objective estimation of grapevine bunch compactness. *VITIS* 53(1), 9-16.
- Tello, J., & Ibáñez, J. (2018). What do we know about grapevine bunch compactness? A state-of-the-art review. *Australian journal of grape and wine research*, 24(1), 6-23.
- Tello, J., Roux, C., Chouiki, H., Laucou, V., Sarah, G., Weber, A., Santoni S., Flutre T., Pons T., This P., Peros J. P. & Doligez A. (2019). A novel high-density grapevine (*Vitis vinifera* L.) integrated linkage map using GBS in a half-diallel population. *Theoretical and Applied Genetics*, 132(8), 2237-2252.
- Tello, J., Torres-Pérez, R., Grimplet, J., & Ibáñez, J. (2016). Association analysis of grapevine bunch traits using a comprehensive approach. *Theoretical and Applied Genetics*, 129(2), 227-242.

## References

- Theiler, R., & Coombe, B. G. (1985). Influence of berry growth and growth regulators on the development of grape peduncles in *Vitis vinifera* L. *VITIS*, 24(1), 1-11.
- Thompson, M. M., & Olmo, H. P. (1963). Cytological studies of cytochimeric and tetraploid grapes. *American Journal of Botany*, 50(9), 901-906.
- Tian, Y., Fan, M., Qin, Z., Lv, H., Wang, M., Zhang, Z., ... & Ding, Z. (2018). Hydrogen peroxide positively regulates brassinosteroid signaling through oxidation of the BRASSINAZOLE-RESISTANT1 transcription factor. *Nature communications*, 9(1), 1-13.
- Töpfer R., Hausmann L. & Eibach R. (2016) Molecular breeding. In: Adam-Blondon, A. F., Martinez-Zapater, J. M., & Kole, C. (Eds.). *Genetics, genomics, and breeding of grapes*. CRC Press, pp 188-213.
- Töpfer R., Hausmann L., Harst M., Maul E. & Zyprian E. (2011) New horizons for grapevine breeding. In: Flachowsky H, Hanke M-V (Eds.) *Methods in Temperate Fruit Breeding*. Global Science Books, Ltd., Ikenobe, Japan, pp 79-100.
- Vail, M. E., & Marois, J. J. (1991). Grape cluster architecture and the susceptibility of berries to *Botrytis cinerea*. *Phytopathology*, 81(2), 188-191.
- Valdés-Gómez, H., Fermaud, M., Roudet, J., Calonnec, A., & Gary, C. (2008). Grey mould incidence is reduced on grapevines with lower vegetative and reproductive growth. *Crop Protection*, 27(8), 1174-1186.
- van Leeuwen C., Destrac-Irvine A., Dubernet M., Duchêne E., Gowdy M., Marguerit E., Pieri P., Parker A., de Rességuier L. & Ollat N. (2019). An update on the impact of climate change in viticulture and potential adaptations. *Agronomy*, 9(9), 514.
- Van Ooijen, J. W. (2009). MapQTL® 6, Software for the mapping of quantitative trait loci in experimental populations of diploid species. *Kyazma BV, Wageningen*, 59.
- Van Ooijen, J., Sandbrink, H., Purimahua, C., Vrieling, R., Verkerk, R., Zabel, P., & Lindhout, P. (1993). *Mapping quantitative genes involved in a trait assessed on an ordinal scale: a case study with bacterial canker in Lycopersicon peruvianum*. Technomic Publishing Co., Inc., Lancaster, PA
- Vezzulli S., Troglio M., Coppola G., Jermakow A., Cartwright D., Zharkikh A., Stefanini M., Grando M. S., Viola R., Adam-Blondon A-F., Thomas M., This P. & Velasco R. (2008). A reference integrated map for cultivated grapevine (*Vitis vinifera* L.) from three crosses, based on 283 SSR and 501 SNP-based markers. *Theoretical and Applied Genetics*, 117(4), 499-511.
- Weeden N., Hemmatt M., Lawson D., Lodhi M., Bell R., Manganaris A., Reischs B., Brown S. & Ye G. (1994) Development and application of molecular marker linkage maps in woody fruit crops. In *Progress in temperate fruit breeding* (pp. 269-273). Springer, Dordrecht.
- Wen J, Lu L, Nie Z-L, Liu X-Q, Zhang N, Ickert-Bond S, Gerrath J, Manchester S, Boggan J, Chen Z (2018) A new phylogenetic tribal classification of the grape family (Vitaceae): Tribal classification of Vitaceae. *Journal of Systematics and Evolution* 56(4):262-272.
- Williams, J. G., Kubelik, A. R., Livak, K. J., Rafalski, J. A., & Tingey, S. V. (1990). DNA polymorphisms amplified by arbitrary primers are useful as genetic markers. *Nucleic acids research*, 18(22), 6531-6535.
- Wong, D. C., Sweetman, C., Drew, D. P., & Ford, C. M. (2013). VTCdb: a gene co-expression database for the crop species *Vitis vinifera* (grapevine). *BMC genomics*, 14(1), 882.
- Yakushiji, H., Kobayashi, S., Goto-Yamamoto, N., Jeong, S. T., Sueta, T., Mitani, N., & Azuma, A. (2006). A skin color mutation of grapevine, from black-skinned Pinot Noir

## References

- to white-skinned Pinot Blanc, is caused by deletion of the functional *VvmybA1* allele. *Bioscience, biotechnology, and biochemistry*, 70(6), 1506-1508.
- Zhang, J., Hausmann, L., Eibach, R., Welter, L. J., Töpfer, R., & Zyprian, E. M. (2009a). A framework map from grapevine V3125 (*Vitis vinifera* 'Schiava grossa' × 'Riesling') × rootstock cultivar 'Börner' (*Vitis riparia* × *Vitis cinerea*) to localize genetic determinants of phylloxera root resistance. *Theoretical and applied genetics*, 119(6), 1039-1051.
- Zhang L. Y., Bai M. Y., Wu J., Zhu J. Y., Wang H., Zhang Z., Wang W., Sun Y., Zhao J., Sun X., Yang H., Xu Y., Kim S. H., Fujioka S., Lin W. H., Chong K., Lu T., Wang Z. Y. (2009b) Antagonistic HLH/bHLH transcription factors mediate brassinosteroid regulation of cell elongation and plant development in rice and *Arabidopsis*. *The Plant Cell*, 21(12), 3767-3780.
- Zhao X, Li W-F, Wang Y, Ma Z-H, Yang S-J, Zhou Q, Mao J, Chen B-H (2019). Elevated CO<sub>2</sub> concentration promotes photosynthesis of grape (*Vitis vinifera* L. cv. 'Pinot noir') plantlet in vitro by regulating RbcS and Rca revealed by proteomic and transcriptomic profiles. *BMC plant biology* 19(1):42.
- Zhao, X., Li, W. F., Wang, Y., Ma, Z. H., Yang, S. J., Zhou, Q., Mao J. & Chen, B. H. (2019). Elevated CO<sub>2</sub> concentration promotes photosynthesis of grape (*Vitis vinifera* L. cv. 'Pinot noir') plantlet in vitro by regulating RbcS and Rca revealed by proteomic and transcriptomic profiles. *BMC plant biology*, 19(1), 42.
- Zini E., Dolzani C., Stefanini M., Gratl V., Bettinelli P., Nicolini D., Betta G, Dorigatti C., Velasco R., Letschka T. & Vezzulli S. (2019). R-loci arrangement versus downy and powdery mildew resistance level: A *Vitis* Hybrid Survey. *International journal of molecular sciences*, 20(14), 3526.
- Zou C, Karn A, Reisch B, Nguyen A, Sun Y, Bao Y, Campbell MS, Church D, Williams S, Xu X, Ledbetter CA, Patel S, Fennell A, Glaubitz JC, Clark M, Ware D, Londo JP, Sun Q, Cadle-Davidson L (2020) Haplotyping the *Vitis* collinear core genome with rhAmpSeq improves marker transferability in a diverse genus. *Nature communications*, 11(1), 1-11.
- Zyprian E., Ochssner I., Schwander F., Simon S., Hausmann L., Bonow-Rex M., Moreno-Sanz P., Grando M. S., Wiedemann-Merdinoglu S., Merdinoglu D., Eibach R. & Töpfer R. (2016). Quantitative trait loci affecting pathogen resistance and ripening of grapevines. *Molecular Genetics and Genomics*, 291(4), 1573-1594.
- Zyprian, E., Richter, R., Rossmann, S., Theres, K., & Töpfer, R. (2018, July). Molecular analysis of bunch architecture in grapevine. In *XII International Conference on Grapevine Breeding and Genetics* 1248 (pp. 327-330).

## 8 - Appendices

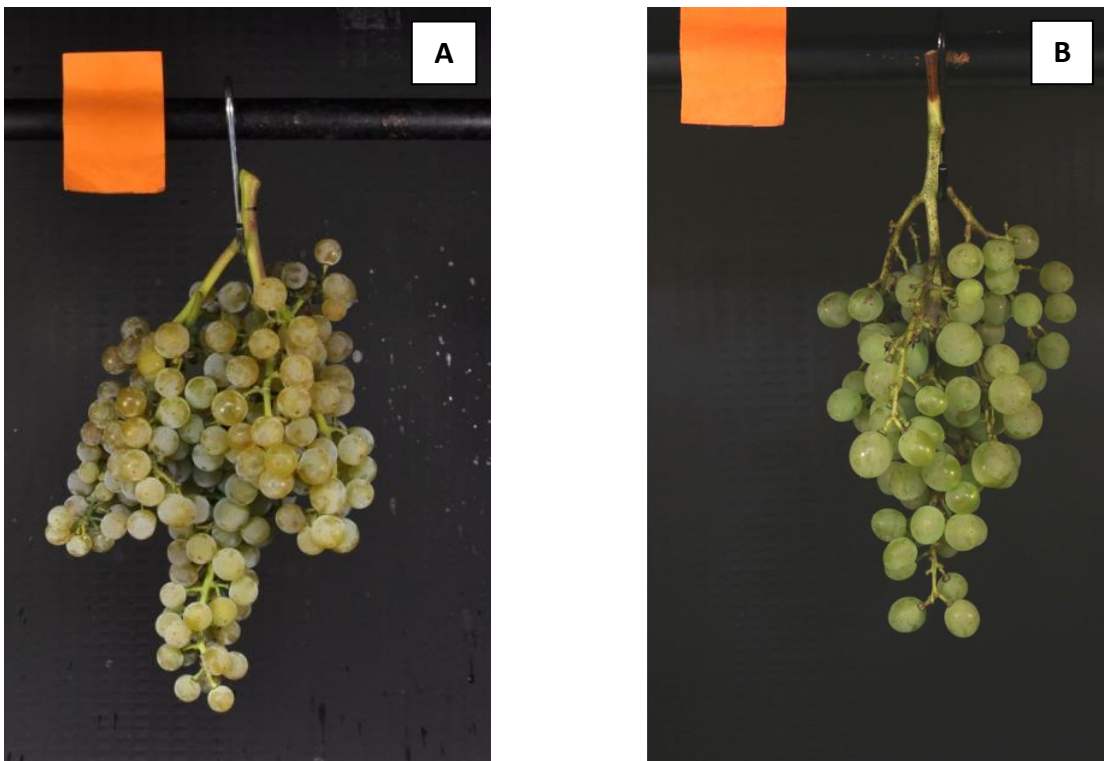
**Appendix I: Electronic supplementary materials from Chapter 2 Richter et al. (2019)**

**Identification of co-located QTLs and genomic regions affecting grapevine cluster architecture**

**Robert Richter, Doreen Gabriel, Florian Rist, Reinhard Töpfer, Eva Zyprian**

**Theoretical and Applied Genetics (2019) 132:1159–1177**

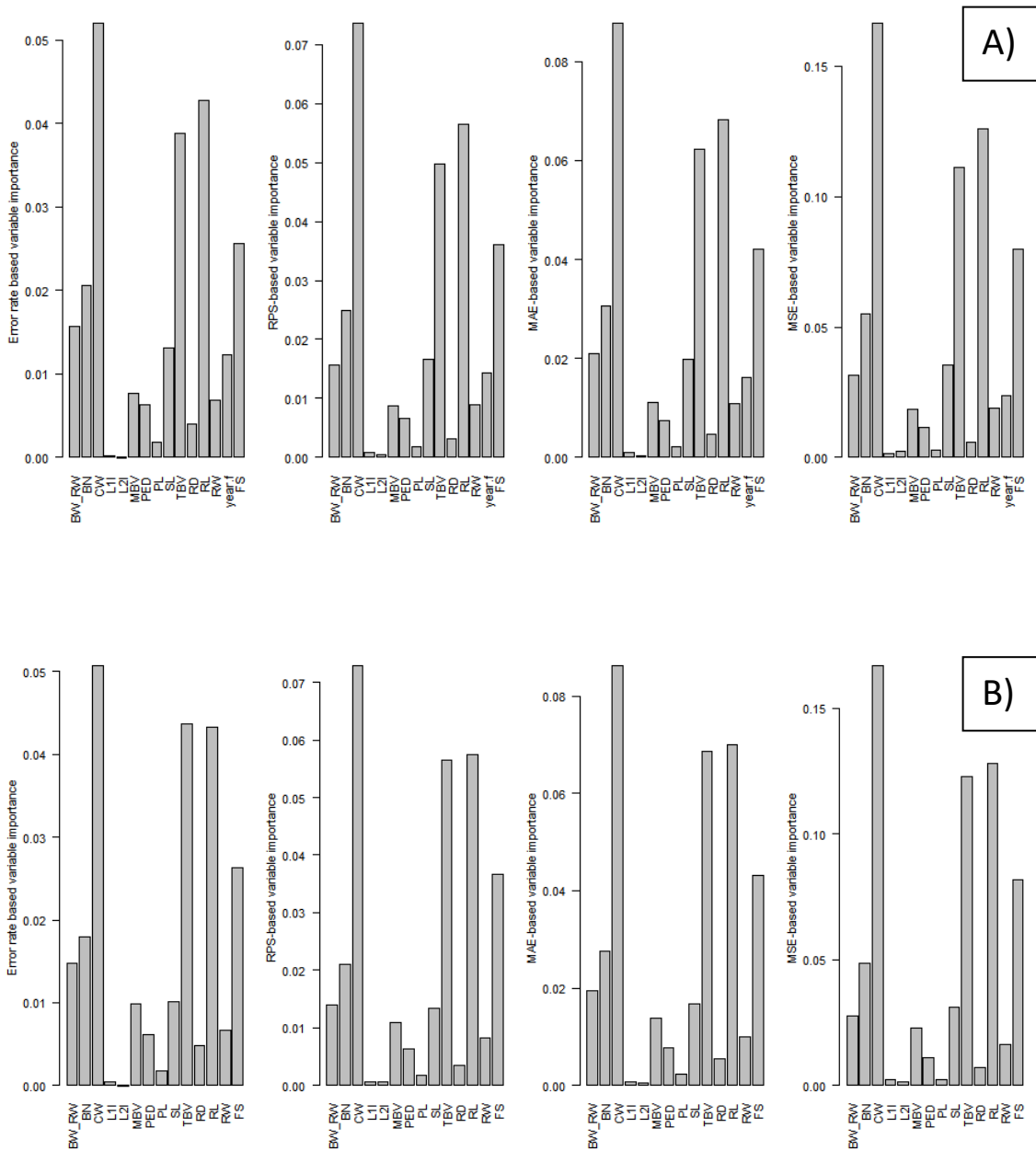
<https://doi.org/10.1007/s00122-018-3269-1>



**Online Resource 1** Pictures of the parental types of the cross GF.GA-47-42 x 'Villard Blanc'. Both varieties showed reduced cluster compactness. A) maternal parent GF.GA-47-42 B) paternal parent 'Villard Blanc'.



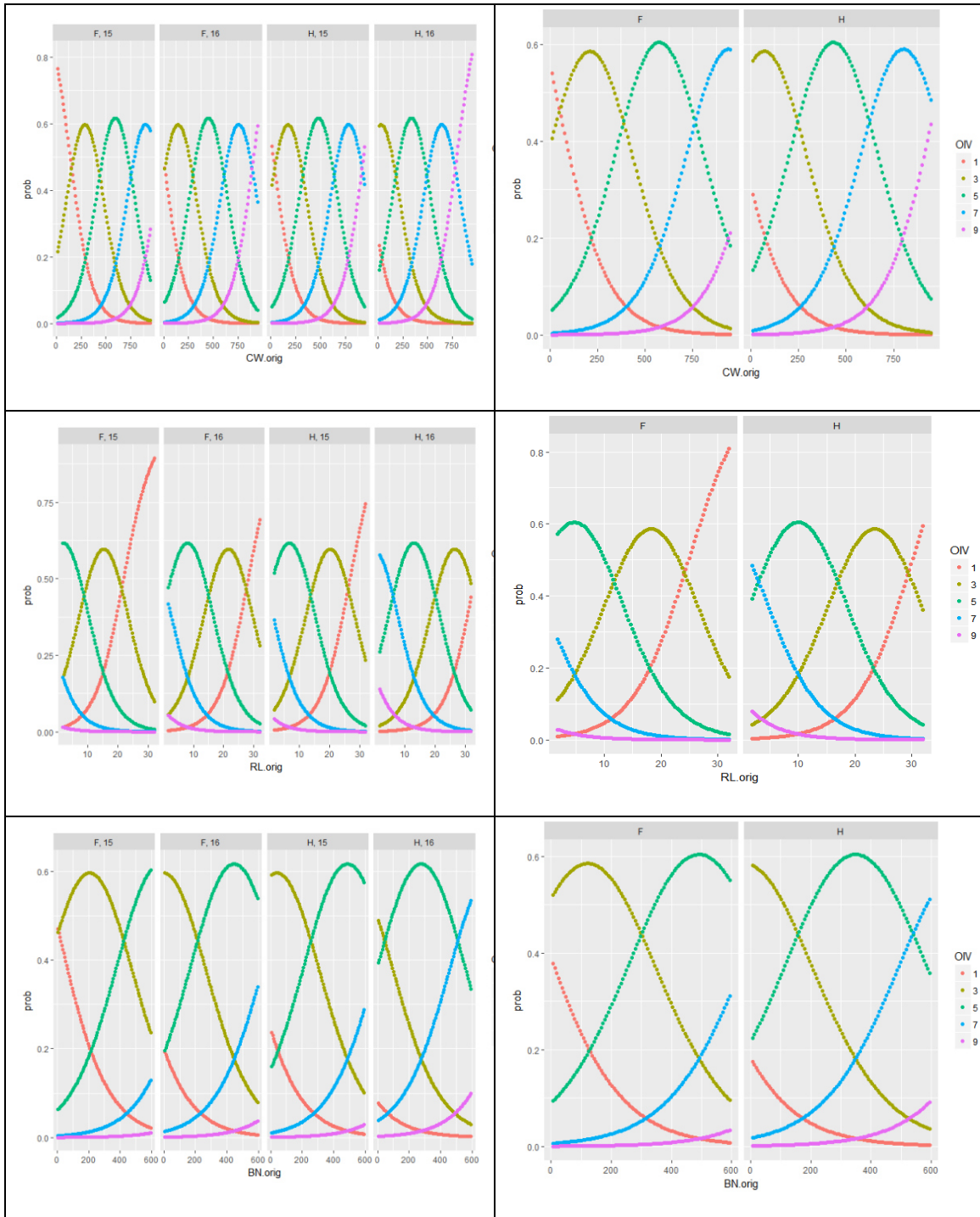
ESM\_3 Overview of the importance of cluster architecture variables



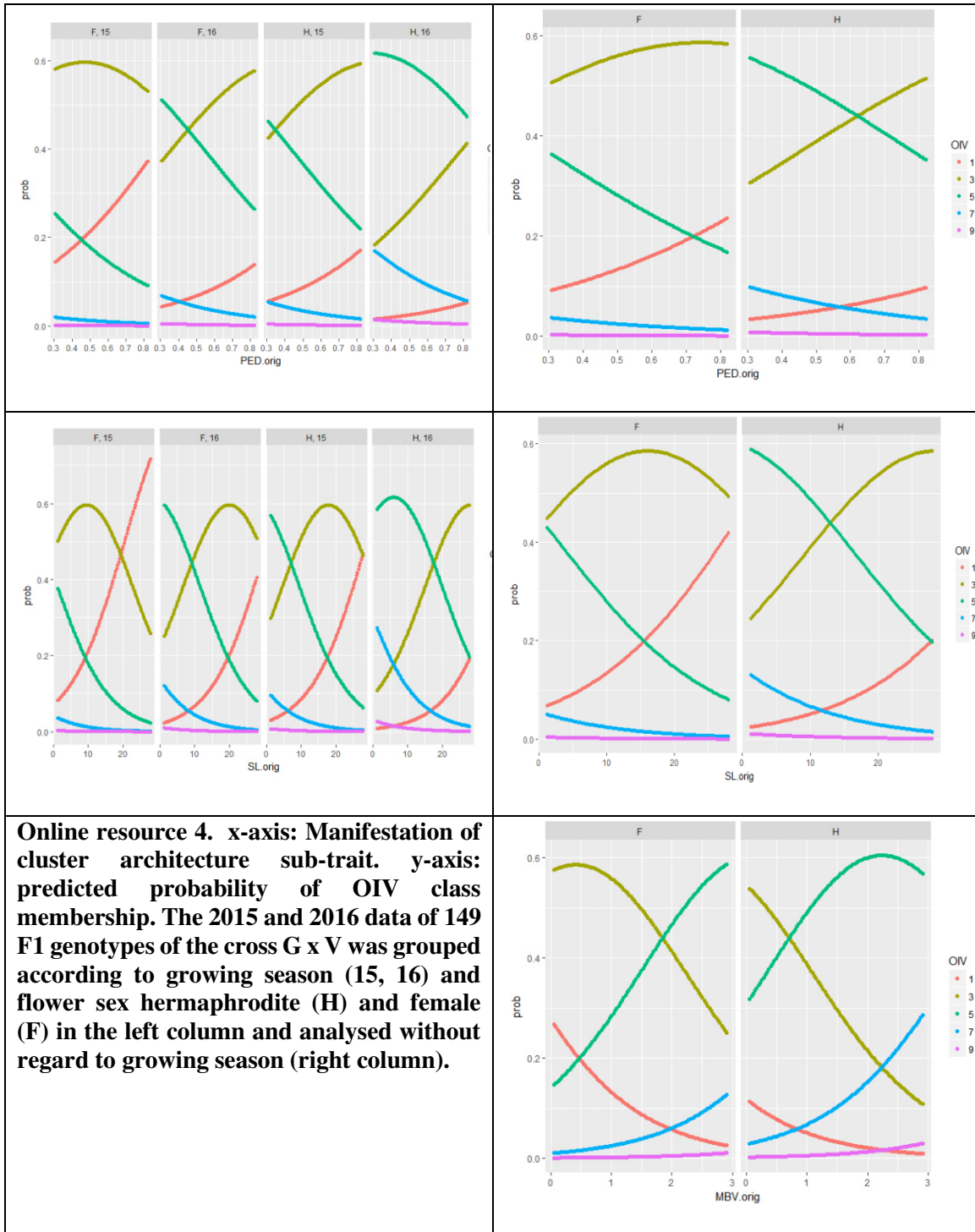
**Online Resource 3** Overview of the importance of cluster architecture variables for the prediction of the OIV204 compactness descriptor using the “cforest” function for random forest calculation with the R-package “party”. The quality of the importance prediction was assessed with error estimates i.e. error rate, ranked probability scores (RPS), mean absolute error (MAE), mean standard error (MSE). The combined 2015 and 2016 dataset was used with season as predictor variable (A) and without season as predictor variable (B).

# Appendix I

## ESM\_4 Probability distribution for the manifestation of main cluster architecture sub-traits



# Appendix I



## Appendix I

### ESM\_5 Error rate (ER) assessment for the prediction accuracy in CLM models OIV204 for classes and flower sex

**Online Resource 5** Error rate (ER) assessment for the prediction accuracy in cumulative link models (CLM) over OIV204 classes and flower sex. For CLM models with the lowest AIC values, (see Table 2) the ER was used to assess the prediction accuracy. OIV204 classes and flower sex members exhibited different error rates. All model variants were assessed with a mixed dataset neglecting the season information (-season) or using season as additional factor variable for modeling (+season)

<b>ER for each OIV204 class</b>					
<b>class</b>	<b>1</b>	<b>3</b>	<b>5</b>	<b>7</b>	<b>9</b>
<b>15/16 - season</b>	0.55	0.39	0.31	0.85	1
<b>15/16 + season</b>	0.51	0.37	0.32	0.75	1
<b>ER for flower sex groups</b>					
<b>Sex</b>	<b>Female</b>	<b>Hermaphrodite</b>			
<b>15/16 - season</b>	0.41	0.45			
<b>15/16 + season</b>	0.39	0.43			

**ESM\_6 Results of QTL analysis Online Resource 6** QTLs related to cluster architecture in 149 F1 individuals of the segregating population of the cross Gf.GA-47-42 x 'Villard Blanc' calculated with interval mapping (IM) and interval mapping with flower sex as cofactor (FS) during four growing seasons. Cluster architecture traits in bold do statistically contribute to a high extent to cluster

		Cluster architecture related QTLs					LODmax associated marker				Closest confidence interval flanking marker		
Cal- culation method	IG	Trait/ Season	LODmax position [cM]	LOD max value	IG- wide thresh.	%Expl	Marker name	Position [cM]	physical position on PN 40024 12X.v2 Cost3	Flanking marker upper limit	Flanking marker lower limit	Position [cM] upper limit	Position [cM] lower limit
IM	1	PL_15	13.822	8.23	3.2	23.3	SNP1025_100FEM	13.822	22.957.941	SNP1157_64CMZ	SNP357_371FEM	3.354	14.864
IM	1	PL_14	16.864	7.14	3.2	20.3	55553gene_1_GF_WRKY	20.486	21.461.191	SNP357_371FEM	VMC2B3	14.864	23.892
IM	1	PL_16	16.864	10.79	3.1	28.4	SNP1025_100FEM	13.822	22.957.941	SNP1021_163FEM	SNP477_239FEM	12.71	18.848
IM	1	OIV_16	30.898	4.37	3.1	12.7	SNP1241_207FEM	30.898	12.608.167	VVIN61	VMC2B3	35.336	23.892
IM	1	OIV_17	30.898	3.67	3.2	10.7	SNP1241_207FEM	30.898	12.608.167	VVIN61	VMC2B3	35.336	23.892
IM	1	PED_14	30.898	3.57	3.3	10.7	SNP1241_207FEM	30.898	12.608.167	SNP269_308FEM	VMC2B3	48.629	23.892
IM	1	PED_15	30.898	3.65	3.2	11.1	SNP1241_207FEM	30.898	12.608.167	VMC3G9	VMC2B3	44.55	23.892
IM	1	PED_13	69.3	3.44	3.3	11.4	GF01_24	69.3	287.042	GF01_50	VVS29	60.816	71.032
IM	1	PED_16	75.547	5.1	3.3	14.6	GF01_24	69.3	287.042	GF01_16_128	VV_1_3844131FEM	68.284	78.016
IM	2	RL_14	12.027	3.07	2.6	12.4	VVIB23_312	12.027	4.807.391	GF02_07	VRZAG93	1.919	20.815
IM	2	RL_15	12.027	4.09	2.6	12.4	VVIB23_312	12.027	4.807.391	GF02_07	VRZAG93	1.919	20.815
IM	2	RL_16	12.027	3.98	2.5	11.6	VVIB23_312	12.027	4.807.391	GF02_07	VMC3B10	1.919	15.689
IM	2	SL_15	12.027	2.64	2.6	8.1	VVIB23_312	12.027	4.807.391	GF02_07	VMC5G7	1.919	25.916
IM	2	SL_16	12.027	2.93	2.5	8.6	VVIB23_312	12.027	4.807.391	GF02_07	VRZAG93	1.919	20.815
IM	2	CW_13	13.003	5.77	2.5	16.7	GF02_12_170	13.003	5.012.979	GF02_07	GF02_42_167	1.919	14.936
IM	2	CW_14	13.003	3.08	2.6	9.2	GF02_12_170	13.003	5.012.979	GF02_07	VRZAG93	1.919	20.815
IM	2	OIV_15	13.003	11.07	2.6	29	GF02_12_170	13.003	5.012.979	VVIB23_312	SNP581_114eCMZ	12.027	14.583
IM	2	OIV_16	13.003	5.32	2.5	15.2	GF02_12_170	13.003	5.012.979	GF02_07	VMC3B10	1.919	15.689
IM	2	OIV_17	13.003	6.65	2.6	18.6	GF02_12_170	13.003	5.012.979	GF02_07	SNP581_114eCMZ	1.919	14.583
IM	2	RL_14	18.689	3.34	2.5	10.1	VRZAG93	20.815	5.632.401	GF02_07	VMC5G7	1.919	25.916

Appendix I

IM+FS	3	PED_13	0	3.36	3	10.6	1044J09FFEM	0	1.900.405	1044J09FFEM	0	GF03_09_285	18.956
IM+FS	3	PED_15	0	2.91	2.9	8.6	1044J09FFEM	0	1.900.405	1044J09FFEM	0	GF03_09_285	18.956
IM+FS	3	PED_16	0	3.21	3.1	9	1044J09FFEM	0	1.900.405	1044J09FFEM	0	GF03_09_285	18.956
IM	3	MBV_13	7	3.2	2.8	10.6	1044J09FFEM	0	1.900.405	1044J09FFEM	0	GF03_09_285	18.956
IM	3	MBV_14	8	3.09	3	12.9	1044J09FFEM	0	1.900.405	1044J09FFEM	0	GF03_09_298	20.134
IM	3	SL_15	73.719	4.52	3	11.3	GF03_07_273	73.719	16.500.873	VCHR03a_196	67.908	GF03_05	79.157
IM	3	RL_15	74.788	4.2	3.2	9.2	GF03_07_236	74.788	16.500.873	VCHR03a_196	67.908	2018J24FFEM	80.683
IM	3	RL_16	74.788	2.96	3.1	9.8	GF03_07_236	74.788	16.500.873	VCHR03a_196	67.908	2018J24FFEM	80.683
IM	3	SL_16	77.788	3.84	3.1	9.5	GF03_07_236	74.788	16.500.873	VCHR03a_196	67.908	2018J24FFEM	80.683
IM	10	CW_14	69.861	2.96	3	8.9	VRZAG7_106	69.861	23.172.655	GF10_07	61.266	VRZAG7_106	69.861
IM	10	CW_15	69.861	5.03	2.8	14.4	VRZAG7_106	69.861	23.172.655	GF10_07	61.266	VRZAG7_106	69.861
	10	CW_16	69.861	4.02	2.9	11.8	VRZAG7_106	69.861	23.172.655	1037C16FFEM	57.779	VRZAG7_106	69.861
IM	10	TBV_14	69.861	3.23	3	9.8	VRZAG7_106	69.861	23.172.655	GF10_07	61.266	VRZAG7_106	69.861
IM	10	TBV_16	69.861	4.57	2.9	13.5	VRZAG7_106	69.861	23.172.655	1037C16FFEM	57.779	VRZAG7_106	69.861
IM+FS	10	BN_14	69.861	3.47	2.9	10.1	VRZAG7_106	69.861	23.172.655	GF10_07	61.266	VRZAG7_106	69.861
IM+FS	10	BN_15	69.861	3.09	2.9	8.9	VRZAG7_106	69.861	23.172.655	VMC8D3_160	47.761	VRZAG7_106	69.861
IM+FS	10	BN_16	69.861	6.27	2.9	17.4	VRZAG7_106	69.861	23.172.655	GF10_07	61.266	VRZAG7_106	69.861
IM+FS	10	BW_15	69.861	6.57	2.9	16.8	VRZAG7_106	69.861	23.172.655	GF10_07	61.266	VRZAG7_106	69.861
IM+FS	10	BW_16	69.861	4.34	2.8	12.5	VRZAG7_106	69.861	23.172.655	GF10_05	55.421	VRZAG7_106	69.861
IM	11	PED_14	0	5.06	2.8	14.8	VMC6C3	0	3.308.426	VMC6C3	0	VVMD25	7.389
IM	11	PED_16	0	5.49	2.8	15.6	VMC6C3	0	3.308.426	VMC6C3	0	VVMD25	7.389
IM	11	PED_13	3	7.64	2.8	23.6	VMC6C3	0	3.308.426	VMC6C3	0	GF11_03_128	9.724
IM	11	PED_15	3	6.57	2.8	19.1	VMC6C3	0	3.308.426	VMC6C3	0	GF11_03_128	9.724
IM	12	CW_15	51.393	3.24	2.9	7.8	GF12_07	51.393	22.414.306	Gf12_17_323	47.705	SNP1119_176CMZ	62.968
IM	12	MBV_13	53.672	3.54	2.9	11.8	GF12_09_87	53.672	23.246.484	GF12_07	51.393	SNP1119_176CMZ	62.968
IM	12	CW_13	59.49	3.04	3	9.4	GF12_09_83	59.49	23.246.484	GF12_09_87	53.672	SNP1119_176CMZ	62.968
IM	12	MBV_14	59.49	3.17	3	9.7	GF12_09_83	59.49	23.246.484	Gf12_17_323	47.705	SNP1119_176CMZ	62.968
IM	12	MBV_16	59.49	4.68	2.8	13.6	GF12_09_83	59.49	23.246.484	GF12_19	54.779	SNP1119_176CMZ	62.968
IM	12	MBV_15	62.968	3.44	1	10.3	SNP1119_176CMZ	62.968	23.795.082	GF12_19	54.779	SNP1119_176CMZ	62.968

Appendix I

IM	14	PL_15	47.031	4.31	3.1	13	SNP1411_565FEM	47.031	23.135.445	GF14_09komb	45.128	VVMD24komb	51.21
IM	14	PL_16	47.031	3.85	3.1	11.3	SNP1411_565FEM	47.031	23.135.445	2019E13FFEM	39.629	GF14_14	70.312
IM+FS	14	Wing_16	67.396	2.69	3	7.3	GF14_20_255	67.396	28.305.705	UDV_025komb	63.444	GF14_14	70.312
IM	14	PL_14	69.692	4.45	3.1	13.2	GF14_19	69.692	28.192.022	VMC6E1komp	65.053	GF14_05	73.527
IM+FS	14	Wing_17	69.692	4.68	3.2	13.3	GF14_19	69.692	28.192.022	GF14_20_264	66.056	GF14_05	73.527
IM	15	OIV_17	0	3.85	2.9	11.2	GF15_08_277	0	2.951.468	GF15_08_277	0	Gf15_06_177	13.745
IM	15	OIV_16	7.773	6.58	2.9	18.5	GMI026FEM	9.353	14.397.063	GF15_08_277	0	GF15_28_375	10.417
IM	15	OIV_15	36.041	3.56	2.8	10.4	Gf15_06_164	35.337	36.728	GF15_05	29.623	VMC8G3.2_291	39.562
IM	17	MBV_15	10.319	7.17	1	20.2	SCU_06	14.405	3.290.363	SNP677_509FEM	0	VRZAG15	27.514
IM	17	MBV_16	18.405	5.35	2.9	15.4	VRZAG15	27.514	6.588.726	SNP677_509FEM	0	EDS1_CF_SNP1837GF	36.609
IM	17	MBV_14	27.514	5.03	3	14.9	VRZAG15	27.514	6.588.726	SNP677_509FEM	0	EDS1_CF_SNP1837GF	36.609
IM	17	CW_15	32.514	3.11	2.7	9.2	VRZAG15	27.514	6.588.726	SCU_06	14.405	EDS1_CF_SNP1520GF	37.061
IM	17	OIV_15	34.514	2.84	2.8	8.4	EDS1_CF_SNP1837GF	36.609	8.686.027	VRZAG15	27.514	UDV_092	40.483
IM	17	OIV_16	36.609	5.3	2.7	15.2	EDS1_CF_SNP1837GF	36.609	8.686.027	VRZAG15	27.514	UDV_092	40.483
IM	17	OIV_17	36.609	5.16	2.8	14.8	EDS1_CF_SNP1837GF	36.609	8.686.027	VRZAG15	27.514	VvEDS1gene_1_GF	36.957
IM+FS	17	BN_15	36.609	3.57	2.8	10.3	EDS1_CF_SNP1837GF	36.609	8.686.027	VRZAG15	27.514	UDV_092	40.483
IM	17	CW_16	36.957	3.69	2.7	10.8	VvEDS1gene_1_GF	36.957	3.930.996	VRZAG15	27.514	GF17_07	53.635
IM+FS	17	BN_16	36.957	4.88	2.7	13.8	VvEDS1gene_1_GF	36.957	3.930.996	EDS1_CF_SNP1837GF	36.609	UDV_092	40.483
IM	17	CW_14	44.483	3.02	2.9	9.1	UDV_092	44.483	9.613.080	EDS1_CF_SNP1520GF	37.061	GF17_07	53.635
IM	18	CW_15	0	2.93	3	8.6	VMC2A3	0	948.244	VMC2A3	0	VV1_1617CMZ	20.861
IM	18	RW_15	6.756	4.99	3	14.3	VMC3E05_117	6.756	321.045	VMC2A3	0	SNP219_172FEM	18.212
IM	18	RW_16	11.612	3.98	3.2	11.6	1082L02FFEM	11.612	3.418.164	VMC2A3	0	SNP219_172FEM	18.212
IM	18	CW_16	15.047	4.93	3.2	14.2	SCU_10	15.047	4.520.661	VMC3E05_110	4.756	VV1_1617CMZ	20.861
IM+FS	18	BN_16	15.047	5.27	3	15.1	SCU_10	15.047	4.520.661	VMC8B5	10.829	SNP219_172FEM	18.212
IM+FS	18	BN_15	21.517	4.27	3	12.1	VV_18_6624520FEM	21.517	6.720.583	SNP355_154FEM	18.266	VV_18_9582805FEM	31.194
IM	18	PED_14	23.776	5.45	3	15.9	VMCNG1B09	23.776	5.645.610	VMC8B5	10.829	VV_18_9582805FEM	31.194
IM	18	PED_15	24.776	6.72	3.1	19.4	VMCNG1B09	24.776	5.645.610	VMC8B5	10.829	VV_18_9582805FEM	31.194
IM	18	PED_16	24.776	5.39	3	15.3	VMCNG1B09	24.776	5.645.610	VMC8B5	10.829	VV_18_9582805FEM	31.194

<sup>a</sup> QTL position on linkage group (LG). <sup>b</sup> Genetic position of the maximum logarithm of the odds value (LOD<sub>max</sub>). <sup>c</sup> Linkage group specific significance level for the detection of a QTL. <sup>d</sup> Percentage of explained phenotypic variance. <sup>e</sup> Genetic position of the LOD<sub>max</sub> marker in centiMorgan (cM) on the consensus map (Zyprian et al. 2016). <sup>f</sup> Physical position of the LOD<sub>max</sub> marker in the reference sequence of the Grapevine genome (Canaguier et al. 2017). <sup>g</sup> Genetic position of confidence interval (LOD<sub>max</sub>-1)-limiting marker. <sup>h</sup> Physical position of the LOD<sub>max</sub>-1)-limiting marker.

## Appendix I

### ESM\_7 QTL comparison

#### Online Resource 7 QTL comparison

Attributes of QTLs reproducibly calculated in the cross population with interval mapping (IM) and with interval mapping applying flower sex as co-variable for interval mapping (IM+FS).

<b>QTLs IM</b>	<b>LOD<sub>max</sub></b>	<b>Explained Variance (%)</b>	<b>Extension of confidence interval [cM]</b>
<b>Median</b>	4.15	12.10	12.87
<b>mean</b>	4.66	13.48	15.05
<b>stdv</b>	1.78	4.72	7.33
<b>min</b>	2.64	7.80	1.65
<b>max</b>	11.07	29.00	36.61
<b>QTLs IM+FS</b>	<b>LODmax</b>	<b>Explained Variance (%)</b>	<b>Extension of confidence interval [cM]</b>
<b>Median</b>	3.92	11.35	8.60
<b>mean</b>	4.18	11.84	11.87
<b>stdv</b>	1.23	3.13	5.79
<b>min</b>	2.69	7.30	3.87
<b>max</b>	6.57	17.40	22.10
<b>T-test p-value</b>	0.35	0.14	0.22

## Appendix I

### ESM\_8 Gene ontology analysis

<b>Online Resource 8</b> Table of Gene ontology (GO) enrichment analysis with genes positioned in confidence intervals of cluster architecture related QTLs. compared to all the genes in the reference genome PN40024 12x.v2					
Linkage group	Gene IDs	GO term*	Enrichment**	Putative Function***	QTL Cluster
1	VIT_200s0225g00170	GO:0051186 GO:0009636 GO:0098754	2.61	peroxidase 3	OIV_20 4 + PED
1	VIT_200s0291g00060	GO:0006820 GO:0006817	2.61	inorganic phosphate transporter 2-1	
1	VIT_201s0010g00390	GO:0051186 GO:0009636 GO:0098754 GO:0009636 GO:0098754	2.99	peroxidase 7-like	
1	VIT_201s0010g00590	GO:0051186	2.61	short-chain dehydrogenase reductase sdr	
1	VIT_201s0010g00720	GO:0009636 GO:0098754	2.99	hypothetical protein	
1	VIT_201s0010g00840	GO:0051186 GO:0042180 GO:1901663 GO:1901661 GO:0042181 GO:0009234 GO:0009233	45.28	menaquinone biosynthesis	
1	VIT_201s0010g00850	GO:0051186 GO:0042180 GO:1901663 GO:1901661 GO:0042181 GO:0009234 GO:0009233	45.28	2-oxoglutarate decarboxylase hydro-lyase magnesium ion binding protein	
1	VIT_201s0010g00870	GO:0051186 GO:0042180 GO:1901663 GO:1901661 GO:0042181 GO:0009234 GO:0009233	45.28	2-oxoglutarate decarboxylase hydro-lyase magnesium ion binding protein	
1	VIT_201s0010g00900	GO:0051186	2.61	isochorismate synthase	
1	VIT_201s0010g00960	GO:0051186 GO:0009636 GO:0098754	2.99	peroxidase 57	

## Appendix I

1	VIT_201s0010g01090	GO:0051186 GO:0009636 GO:0098754	2.99	peroxidase 49 precursor
1	VIT_201s0010g01130	GO:0051186	2.61	6-phosphogluconate dehydrogenase
1	VIT_201s0010g01180	GO:0051186	2.61	cytokine-induced anti-apoptosis inhibitor fe-s biogenesis
1	VIT_201s0026g00830	GO:0051186 GO:0009636 GO:0098754	2.99	peroxidase 65
1	VIT_201s0026g00990	GO:0051186	2.61	pyruvate dehydrogenase e1 alpha subunit
1	VIT_201s0026g01100	GO:0051186	2.61	5-formyltetrahydrofolate cycloligase
1	VIT_201s0026g01330	GO:0051186 GO:0009636 GO:0098754	2.99	glutathione s-transferase
1	VIT_201s0026g01340	GO:0051186 GO:0009636 GO:0098754	2.99	glutathione s-transferase u17
1	VIT_201s0026g01380	GO:0051186 GO:0009636 GO:0098754	2.99	glutathione s-transferase
1	VIT_201s0026g01460	GO:0009636 GO:0098754	2.99	thioredoxin h2
1	VIT_201s0026g02370	GO:0051186 GO:0009636 GO:0098754	2.99	glutathione s-transferase
1	VIT_201s0026g02390	GO:0051186 GO:0009636 GO:0098754	2.99	glutathione s-transferase
1	VIT_201s0026g02400	GO:0051186 GO:0009636 GO:0098754	2.99	glutathione s-transferase
1	VIT_201s0026g02630	GO:0051186	2.61	gtp cyclohydrolase i
1	VIT_201s0127g00150	GO:0051186 GO:0042180 GO:1901663 GO:1901661 GO:0042181	14.3	2-phytyl- -naphtoquinone chloroplastic-like
1	VIT_201s0127g00260	GO:0051186	2.61	atp-citrate lyase a-1
1	VIT_201s0127g00420	GO:0051186 GO:0042180 GO:1901663 GO:1901661 GO:0042181 GO:0009234G O:0009233	45.28	naphthoate synthase

## Appendix I

1	VIT_201s0127g00450	GO:0051186	2.61	iron-sulfur cluster assembly enzyme mitochondrial-like	
1	VIT_201s0127g00490	GO:0051186	2.61	pantothenate kinase 2	
1	VIT_201s0127g00520	GO:0009636 GO:0098754	2.99	probable nucleoredoxin 1-like	
1	VIT_201s0127g00540	GO:0009636 GO:0098754	2.99	probable nucleoredoxin 1-like	
1	VIT_201s0127g00560	GO:0009636 GO:0098754	2.99	probable nucleoredoxin 1-like	
1	VIT_201s0127g00590	GO:0009636 GO:0098754	2.99	probable nucleoredoxin 1-like	
1	VIT_201s0127g00600	GO:0009636 GO:0098754	2.99	probable nucleoredoxin 1-like	
1	VIT_201s0137g00660	GO:0051186 GO:0042180 GO:1901663 GO:1901661 GO:0042181	14.3	hypothetical protein	
1	VIT_201s0182g00060	GO:0006817	13.32	phosphate transporter pho1 homolog 3-like	
1	VIT_201s0182g00130	GO:0006817	13.32	phosphate transporter pho1 homolog 3-like	
1	VIT_201s0182g00140	GO:0006817	13.32	pho1-like protein	
1	VIT_201s0182g00150	GO:0006817	13.32	pho1-like protein	
2(+/-1MB)	VIT_202s0025g04960	GO:0032147 GO:0060236	50.4	cell cycle regulated microtubule associated protein	
2(+/-1MB)	VIT_202s0025g05060	GO:0007018 GO:0032886 GO:0048364	50.4	armadillo repeat-containing kinesin-like protein 2-like	RL + SL + CW + OIV204
2(+/-1MB)	VIT_202s0025g05070	GO:0007018 GO:0032886 GO:0048364	50.4	armadillo repeat-containing kinesin-like protein 2	
2(+/-1MB)	VIT_202s0025g05090	GO:0007018 GO:0032886 GO:0048364	50.4	armadillo repeat-containing kinesin-like protein 2-like	
3.1	VIT_203s0038g00730	GO:0035434	4.28	hypothetical protein	
3.1	VIT_203s0038g00840	GO:0009719	15.69	gaga-binding transcriptional activator	
3.1	VIT_203s0038g00930	GO:0009733	33.54	saur family protein	
3.1	VIT_203s0038g00940	GO:0009733	33.54	saur family protein	
3.1	VIT_203s0038g00950	GO:0009733	33.54	saur family protein	PED + MBV
3.1	VIT_203s0038g01080	GO:0009733	33.54	auxin-induced protein 15a	
3.1	VIT_203s0038g01090	GO:0009733	33.54	hypothetical protein	
3.1	VIT_203s0038g01100	GO:0009733	33.54	auxin-induced protein 15a	

## Appendix I

3.1	VIT_203s0038g01110	GO:0009733	33.54	hypothetical protein
3.1	VIT_203s0038g01120	GO:0009733	33.54	auxin-induced protein 15a
3.1	VIT_203s0038g01130	GO:0009733	33.54	hypothetical protein
3.1	VIT_203s0038g01150	GO:0009733	33.54	hypothetical protein
3.1	VIT_203s0038g01160	GO:0009733	33.54	auxin-induced protein 15a
3.1	VIT_203s0038g01170	GO:0009733	33.54	hypothetical protein
3.1	VIT_203s0038g01180	GO:0009733	33.54	auxin-induced protein 15a
3.1	VIT_203s0038g01190	GO:0009733	33.54	hypothetical protein
3.1	VIT_203s0038g01210	GO:0009733	33.54	hypothetical protein
3.1	VIT_203s0038g01220	GO:0009733	33.54	auxin-induced protein 15a
3.1	VIT_203s0038g01230	GO:0009733	33.54	hypothetical protein
3.1	VIT_203s0038g01250	GO:0009733	33.54	hypothetical protein
3.1	VIT_203s0038g01260	GO:0009733	33.54	auxin-induced protein 15a
3.1	VIT_203s0038g01270	GO:0009733	33.54	hypothetical protein
3.1	VIT_203s0038g01280	GO:0009733	33.54	auxin-induced protein 15a
3.1	VIT_203s0038g01290	GO:0009733	33.54	auxin-induced protein 15a
3.1	VIT_203s0038g01300	GO:0009733	33.54	auxin-induced protein 10a5
3.1	VIT_203s0038g01310	GO:0009733	33.54	saur family protein
3.1	VIT_203s0038g01400	GO:0050896	2.61	probable disease resistance rpp8-like protein 2-like
3.1	VIT_203s0038g01520	GO:0050896	2.61	nbs- <i>lrr</i> resistance protein
3.1	VIT_203s0038g01530	GO:0050896	2.61	nbs- <i>lrr</i> resistance protein
3.1	VIT_203s0038g01540	GO:0006820	4.15	nbs- <i>lrr</i> resistance protein
3.1	VIT_203s0038g01550	GO:0050896	2.61	nbs- <i>lrr</i> resistance protein
3.1	VIT_203s0038g01610	GO:0006820	4.15	nbs- <i>lrr</i> resistance protein
3.1	VIT_203s0038g01620	GO:0050896	2.61	nbs- <i>lrr</i> resistance protein
3.1	VIT_203s0038g01630	GO:0050896	2.61	nbs- <i>lrr</i> resistance protein
3.1	VIT_203s0038g01670	GO:0006820	4.15	nbs- <i>lrr</i> resistance protein
3.1	VIT_203s0038g01750	GO:0050896	2.61	nbs- <i>lrr</i> resistance protein
3.1	VIT_203s0038g01940	GO:0006811	3.84	magnesium transporter nipa2-like
3.1	VIT_203s0038g01970	GO:0006418	14.03	amidase -like
3.1	VIT_203s0038g01990	GO:0006418	14.03	hypothetical protein
3.1	VIT_203s0038g02000	GO:0006418	14.03	amidase -like
3.1	VIT_203s0038g02010	GO:0006418	14.03	hypothetical protein

## Appendix I

3.1	VIT_203s0038g02020	GO:0006418	14.03	low quality protein: amidase -like	
3.1	VIT_203s0038g02030	GO:0006418	14.03	hypothetical protein	
3.1	VIT_203s0038g02040	GO:0006418	14.03	hypothetical protein	
3.1	VIT_203s0038g02140	GO:0006820	4.15	auxin influx carrier component	
3.1	VIT_203s0038g02290	GO:0006820	4.15	amino acid amino acid permease	
3.1	VIT_203s0038g02320	GO:0050896	2.61	l-ascorbate peroxidase	
3.1	VIT_203s0038g02380	GO:0050896	2.61	rac-like gtp-binding protein arac3	
3.1	VIT_203s0038g02400	GO:0050896	2.61	atp binding	
3.2	VIT_203s0110g00300	GO:0035434 GO:0006825	36.29	copper transporter	SL + RL
3.2	VIT_203s0110g00360	GO:0035434 GO:0006825	36.29	copper transporter	
3.2	VIT_203s0110g00370	GO:0035434 GO:0006825	36.29	copper transporter	
3.2	VIT_203s0110g00430	GO:0035434 GO:0006825	36.29	copper transporter	
10	VIT_210s0042g00840	GO:0006732	4.98	stilbene synthase	CW + BN
10	VIT_210s0042g00860	GO:0006732	4.98	stilbene synthase	
10	VIT_210s0042g00870	GO:0006732	4.98	stilbene synthase	
10	VIT_210s0042g00880	GO:0006732	4.98	stilbene synthase	
10	VIT_210s0042g00890	GO:0006732	4.98	stilbene synthase	
10	VIT_210s0042g00910	GO:0006732	4.98	stilbene synthase	
10	VIT_210s0042g00920	GO:0006732	4.98	stilbene synthase	
10	VIT_210s0042g00930	GO:0006732	4.98	stilbene synthase	
10	VIT_210s0042g00950	GO:0006732	4.98	succinyl- ligase	
10	VIT_210s0042g01020	GO:0006732	4.98	isochorismatase hydrolase family protein	
10	VIT_210s0071g00810	GO:0035721 GO:0042073	91.38	uncharacterized protein	
10	VIT_210s0071g00840	GO:0035721 GO:0042073	91.38	uncharacterized protein	
10	VIT_210s0071g00850	GO:0035721 GO:0042073	91.38	uncharacterized protein	
10	VIT_210s0071g01020	GO:0006732	4.98	lipoic acid lipoic acid synthetase	
12	VIT_212s0034g01030	GO:0006952	5.24	disease resistance rpp13-like protein 1-like	MBV + CW
12	VIT_212s0034g01070	GO:0006952	5.24	disease resistance rpp13-like protein 1-like	
12	VIT_212s0034g01440	GO:0050789	3.02	transmembrane emp24 domain-containing protein 10	

## Appendix I

12	VIT_212s0034g01460	GO:0006952	5.24	disease resistance protein at3g14460-like
12	VIT_212s0034g01470	GO:0006952	5.24	disease resistance rpp13-like protein 1-like
12	VIT_212s0034g01480	GO:0006952	5.24	disease resistance rpp13-like protein 1-like
12	VIT_212s0034g01490	GO:0006952	5.24	disease resistance rpp13-like protein 1-like
12	VIT_212s0034g01580	GO:0006811	3.67	disease resistance rpp13-like protein 1-like
12	VIT_212s0034g01660	GO:0006952	5.24	disease resistance rpp13-like protein 1-like
12	VIT_212s0034g01700	GO:0006952	5.24	disease resistance rpp13-like protein 1-like
12	VIT_212s0034g01750	GO:0006952	5.24	disease resistance rpp13-like protein 1-like
12	VIT_212s0034g01850	GO:0050789	3.02	l-type lectin-domain containing receptor
12	VIT_212s0034g02040	GO:0006811	3.67	disease resistance protein at3g14460-like
12	VIT_212s0034g02230	GO:0050789	3.02	udp-glucose:glycoprotein glucosyltransferase
12	VIT_212s0034g02310	GO:0006952	5.24	disease resistance protein at3g14460-like
12	VIT_212s0034g02340	GO:0006811	3.67	disease resistance rpp13-like protein 1-like
12	VIT_212s0034g02400	GO:0006952	5.24	disease resistance protein at3g14460-like
12	VIT_212s0034g02440	GO:0006952	5.24	disease resistance protein at3g14460-like
12	VIT_212s0034g02500	GO:0006952	5.24	disease resistance protein at3g14460-like
12	VIT_212s0034g02530	GO:0006952	5.24	disease resistance protein at3g14460-like
12	VIT_212s0034g02540	GO:0050789	3.02	hypothetical protein
12	VIT_212s0034g02570	GO:0009719	3.06	probable lrr receptor-like serine threonine-protein kinase
12	VIT_212s0034g02580	GO:0009719	3.06	probable leucine-rich repeat receptor-like protein kinase at1g35710-like
12	VIT_212s0034g02600	GO:0009719 GO:0050789	3.06	probable leucine-rich repeat receptor-like protein kinase at1g35710-like
12	VIT_212s0035g00020	GO:0050789 GO:0009719	3.02	probable lrr receptor-like serine threonine-protein kinase at4g08850-like
12	VIT_212s0035g00030	GO:0006378	12.64	cleavage and polyadenylation specificity factor subunit 3-i
12	VIT_212s0035g00070	GO:0050789	3.02	probable lrr receptor-like serine threonine-protein kinase
12	VIT_212s0035g00080	GO:0009719	3.06	probable lrr receptor-like serine threonine-protein kinase
12	VIT_212s0035g00140	GO:0009719	3.06	probable lrr receptor-like serine threonine-protein kinase at4g08850-like
12	VIT_212s0035g00160	GO:0006378	12.64	cleavage and polyadenylation specificity factor subunit 3-i
12	VIT_212s0035g00170	GO:0006378	12.64	cleavage and polyadenylation specificity factor subunit 3-i

## Appendix I

12	VIT_212s0035g00180	GO:0009719	3.06	probable lrr receptor-like serine threonine-protein kinase at4g08850-like	
12	VIT_212s0035g00190	GO:0006378	12.64	cleavage and polyadenylation specificity factor subunit 3-i	
12	VIT_212s0035g00260	GO:0006952	5.24	mlo-like protein 4	
12	VIT_212s0035g00310	GO:0050789	3.02	serine threonine protein kinase	
12	VIT_212s0035g00410	GO:0006811	3.67	disease resistance protein at3g14460-like	
12	VIT_212s0035g00420	GO:0006952	5.24	disease resistance protein at3g14460-like	
12	VIT_212s0035g00680	GO:0050789	3.02	protein kinase chloroplastnon-imprinted in prader-willi angelman syndrome region	
12	VIT_212s0035g00720	GO:0006811	3.67	PREDICTED: magnesium transporter NIPA2	
12	VIT_212s0035g00770	GO:0006952	5.24	nitrogen fixation protein	
12	VIT_212s0035g00900	GO:0009719	3.06	protein tify 3b	
12	VIT_212s0035g00910	GO:0006811	3.67	sodium-bile acid	
12	VIT_212s0035g00990	GO:0009719	3.06	receptor protein kinase clavata 1	
12	VIT_212s0035g01140	GO:0009719	3.06	ras-related protein rab11c	
12	VIT_212s0035g01150	GO:0009719	3.06	ras-related protein rabd1	
12	VIT_212s0035g01210	GO:0006811	3.67	cytochrome c	
12	VIT_212s0035g01230	GO:0050789	3.02	hypothetical protein	
12	VIT_212s0035g01260	GO:0006952	5.24	disease resistance protein at4g27190-like	
12	VIT_212s0035g01280	GO:0006952	5.24	disease resistance protein at4g27190-like	
12	VIT_212s0035g01330	GO:0006952	5.24	disease resistance protein at4g27190-like	
12	VIT_212s0035g01470	GO:0006952	5.24	disease resistance protein at4g27190-like	
12	VIT_212s0035g01490	GO:0050789	3.02	type ii peroxiredoxin	
12	VIT_212s0035g01560	GO:0050789	3.02	hypothetical protein	
12	VIT_212s0035g01630	GO:0006952	5.24	disease resistance protein at4g27190-like	
12	VIT_212s0035g01720	GO:0006811	3.67	chloride channel	
12	VIT_212s0035g01810	GO:0050789	3.02	spindle assembly checkpoint component	
12	VIT_212s0035g01900	GO:0050789	3.02	pectinesterase	
17	VIT_217s0000g03640	GO:0090305	2.28	proline-rich protein proline-rich protein precursor	OIV_20 4 + CW
17	VIT_217s0000g03650	GO:0090305	2.28	hypothetical protein proline-rich protein precursor	
17	VIT_217s0000g04640	GO:0090305	2.28	h aca ribonucleoprotein complex subunit 2	
17	VIT_217s0000g04710	GO:0090305	2.28	pentatricopeptide repeat-containing protein	
17	VIT_217s0000g05090	GO:0090305	2.28	pentatricopeptide repeat-containing protein	

## Appendix I

17	VIT_217s0000g05290	GO:0090305	2.28	pre-mrna cleavage complex ii protein family
17	VIT_217s0000g05300	GO:0090305	2.28	pre-mrna cleavage complex ii protein family
17	VIT_217s0000g05310	GO:0090305	2.28	pre-mrna cleavage complex ii protein family
17	VIT_217s0000g05510	GO:0090305	2.28	pentatricopeptide repeat-containing protein
17	VIT_217s0000g05770	GO:0090305	2.28	nuclear ribonuclease z
17	VIT_217s0000g06090	GO:0090305	2.28	pentatricopeptide repeat-containing protein
17	VIT_217s0000g06100	GO:0090305	2.28	pentatricopeptide repeat-containing protein
17	VIT_217s0000g06170	GO:0090305	2.28	hypothetical protein
17	VIT_217s0000g06260	GO:0090305	2.28	pentatricopeptide repeat-containing protein
17	VIT_217s0000g06320	GO:0090305	2.28	hnh endonuclease
17	VIT_217s0000g06390	GO:0090305	2.28	pentatricopeptide repeat-containing protein
17	VIT_217s0000g06470	GO:0090305	2.28	pentatricopeptide repeat-containing protein
17	VIT_217s0000g06480	GO:0090305	2.28	pentatricopeptide repeat-containing protein
17	VIT_217s0000g06500	GO:0090305	2.28	hypothetical protein
17	VIT_217s0000g06510	GO:0090305	2.28	exonuclease family protein
17	VIT_217s0000g06540	GO:0090305	2.28	uncharacterized protein loc100265514
17	VIT_217s0000g06660	GO:0090305	2.28	hypothetical protein
17	VIT_217s0000g06770	GO:0090305	2.28	pentatricopeptide repeat-containing protein
17	VIT_217s0000g06900	GO:0090305	2.28	zinc finger ran-binding domain-containing protein 3-like
17	VIT_217s0000g07500	GO:0090305	2.28	pentatricopeptide repeat-containing protein chloroplastic-like
17	VIT_217s0000g07620	GO:0090305	2.28	pentatricopeptide repeat-containing protein mitochondrial-like
17	VIT_217s0000g07830	GO:0090305	2.28	hypothetical protein
17	VIT_217s0000g08000	GO:0090305	2.28	nuclear fusion defective 2 protein ribonuclease iii
17	VIT_217s0000g08280	GO:0090305	2.28	hypothetical protein
17	VIT_217s0000g08490	GO:0090305	2.28	exosome complex exonuclease rrp40
17	VIT_217s0000g09040	GO:0090305	2.28	pentatricopeptide repeat-containing protein
17	VIT_217s0000g09300	GO:0090305	2.28	organelle transcript processing partial
17	VIT_217s0000g09320	GO:0090305	2.28	pachytene checkpoint protein 2 homolog
17	VIT_217s0000g09330	GO:0090305	2.28	pentatricopeptide repeat-containing protein
17	VIT_217s0000g09860	GO:0090305	2.28	pentatricopeptide repeat-containing
17	VIT_217s0000g09970	GO:0090305	2.28	dna-(apurinic or apyrimidinic site) lyase

## Appendix I

18	VIT_218s0001g00770	GO:0016042	4.77	phospholipase d delta-like	BN + CW	
18	VIT_218s0001g03430	GO:0051555 GO:0051554 GO:0051553 GO:0051552	36.94	flavonol synthase		
18	VIT_218s0001g03470	GO:0051555 GO:0051554 GO:0051553 GO:0051552	36.94	flavonol synthase		
18	VIT_218s0001g03490	GO:0051555 GO:0051554 GO:0051553 GO:0051552	36.94	flavonol synthase		
18	VIT_218s0001g03510	GO:0051555 GO:0051554 GO:0051553 GO:0051552	36.94	flavonol synthase		
18	VIT_218s0001g10830	GO:0016042	4.77	hypothetical protein patatin t5		
18	VIT_218s0001g10870	GO:0016042	4.77	hypothetical protein		
18	VIT_218s0001g10880	GO:0016042	4.77	patatin group a-3-like		
18	VIT_218s0001g10900	GO:0016042	4.77	patatin-like protein		
18	VIT_218s0001g10910	GO:0016042	4.77	hypothetical protein		
18	VIT_218s0001g10920	GO:0016042	4.77	patatin-like protein		
18	VIT_218s0001g10930	GO:0016042	4.77	patatin t5		
18	VIT_218s0001g10940	GO:0016042	4.77	patatin group a-3-like		
18	VIT_218s0001g10950	GO:0016042	4.77	patatin-like protein		
18	VIT_218s0001g10970	GO:0016042	4.77	patatin group a-3-like		
18	VIT_218s0001g11010	GO:0016042	4.77	patatin-like protein		
*enriched PANTHER GO terms    ** maximum Panther derived GO term enrichment factor    *** CRIBI Fast gene search BLAST						

## Appendix II

### Appendix II: Electronic supplementary materials from Chapter 3 Richter et al. (2020)

Differential expression of transcription factor- and further growth related genes correlates with contrasting cluster architecture in *Vitis vinifera* ‘Pinot Noir’ and *Vitis* spp. genotypes

Robert Richter, Susanne Rossmann, Doreen Gabriel, Reinhard Töpfer, Klaus Theres and Eva Zyprian

Theoretical and Applied Genetics (2020) 133:3249–3272

<https://doi.org/10.1007/s00122-020-03667-0>

**Online resource 1** SSR marker analysis for ‘Pinot Noir’ clones at three locations

	VMC3a9_1	VMC3a9_2	VMC5g7_1	VMC5g7_2	VMC8g6_1	VMC8g6_2	VrZAG79_1	VrZAG79_2	VVS2_1	VVS2_2	VVMD32_1	VVMD32_2
PN Reference JKI	72	78	190	200	147	169	237	243	137	152	242	274
En777_B_1	72	78	190	218	147	169	237	243	137	152	242	274
En777_B_2	72	78	190	218	147	169	237	243	137	152	242	274
En777_H_1	72	78	190	218	147	169	237	242	137	152	242	274
En777_H_2	72	78	190	218	147	169	237	243	137	152	242	274
FkCL_H_1	72	78	190	200	147	169	237	243	137	152	242	274
FkCL_H_2	72	78	190	200	147	169	237	243	137	152	242	274
FkCL_P_1	72	78	190	200	147	169	237	243	137	152	242	274
FkCL_P_2	72	78	190	200	147	169	237	243	137	152	242	274
FkCh_B_1	72	78	190	200	147	169	237	243	137	152	242	274
FkCh_B_2	72	78	190	200	147	169	237	243	137	152	242	274
FkCh_H_1	72	78	190	200	147	169	237	243	137	152	242	274
FkCh_H_2	72	78	190	200	147	169	237	243	137	152	242	274
FkCh_P_1	72	78	190	200	147	169	237	243	137	152	242	274
FkCh_P_2	72	78	190	200	147	169	237	243	137	152	242	274
Fr12L_B_1	72	78	190	200	147	169	237	243	137	152	242	274
Fr12L_B_2	72	78	190	200	147	169	237	243	137	152	242	274
Fr12L_H_1	72	78	190	200	147	169	237	243	137	152	242	274
Fr12L_H_2	72	78	190	200	147	169	237	243	137	152	242	274
Fr13L_B_1	72	78	190	200	147	169	237	243	137	152	242	274
Fr13L_B_2	72	78	190	200	147	169	237	243	137	152	242	274
Fr13L_H_1	72	78	190	200	147	169	237	243	137	152	242	274
Fr13L_H_2	72	78	190	200	147	169	237	243	137	152	242	274
Fr1801_B_1	72	78	190	200	147	169	237	243	137	152	242	274
Fr1801_B_2	72	78	190	200	147	169	237	243	137	152	242	274
Fr1801_H_1	72	78	190	200	147	169	237	243	137	152	242	274
Fr1801_H_2	72	78	190	200	147	169	237	243	137	152	242	274
Gm186_H_1	72	78	190	218	147	169	237	243	137	152	242	274
Gm186_H_2	72	78	190	218	147	169	237	243	137	152	242	274

## Appendix II

Gm1-86 P 1	72	78	190	218	147	169	237	243	137	152	242	274
Gm1-86 P 2	72	78	190	218	147	169	237	243	137	152	242	274
Gm18 H 1	72	78	190	200	147	169	237	243	137	152	242	274
Gm18 H 2	72	78	190	200	147	169	237	243	137	152	242	274
Gm20-13 B 1	72	78	190	200	147	169	237	243	137	152	242	274
Gm20-13 B 2	72	78	190	200	147	169	237	243	137	152	242	274
Gm20-13 H 1	72	78	190	200	147	169	237	243	137	152	242	274
Gm20-13 H 2	72	78	190	200	147	169	237	243	137	152	242	274
Gm20-13 P 1	72	78	190	200	147	169	237	243	137	152	242	274
Gm20-13 P 2	72	78	190	200	147	169	237	243	137	152	242	274
WeM171 P 1	72	78	190	200	147	169	237	243	137	152	242	274
WeM171 P 2	72	78	190	200	147	169	237	243	137	152	242	274
WeM1 H 1	72	78	190	200	147	169	237	243	137	152	242	274
WeM1 H 2	72	78	190	200	147	169	237	243	137	152	242	274
WeM242 H 1	72	78	190	200	147	169	237	243	137	152	242	274
WeM242 H 2	72	78	190	200	147	169	237	243	137	152	242	274

**Online resource 2** Weather recording stations, plant protection schedules, average climate conditions and plant vigor at three trial fields

Average air temperature and precipitation were recorded with the nearest weather stations to the trial field region and at comparable latitude during the period of April to September. Vegetative vigor was estimated with the weight of the pruned wood per vine.

Trial field location (Trial field management)	Weather station (Identifier)	latitude over zero:	Trial field established / vine spacing	Plant protection schedule	Season	Average Air temp. [°C]	Average precipitation Apr.-Sept. [mm/m <sup>2</sup> ]	Pruning wood weight [kg]
Baden 48°07'15.9"N 7°37'06.0"E (integrated)	König-schaffhausen (84)	185 m	1997 2.0m*1.1m	BBCH 17-65 sulphur, synthetic fungicides BBCH 65-81 synthetic fungicides every 10-12 days	2015 2016 2017	12.0 11.2 11.7	47.1 67.9 53.5	1.176 <sup>a</sup> 1.096 <sup>a</sup> -
Hesse 49°37'28.7"N 8°38'54.0"E (integrated)	Hirschberg (135)	100 m	1995 1.8m*1.0m	BBCH 17-65 sulphur, synthetic fungicides BBCH 65-81 synthetic fungicides every 10-12 days	2015 2016 2017	12.0 11.4 11.0	50.5 64.9 73.1	0.720 <sup>b</sup> 0.795 <sup>b</sup> -
Palatinate 49°13'07.8"N 8°02'40.5"E (organic)	Sieboldingen (88)	192 m	2003 2.0m*1.0m	BBCH 17-81 copper, sulphur, BBCH 79-85 copper, carbonates every 7 days	2015 2016 2017	11.7 10.8 11.0	36.0 48.5 53.3	0.408 <sup>c</sup> 0.504 <sup>c</sup> -

Letters given in superscript form indicate significant differences between measurement records according to ANOVA  $\alpha=0.05$

## Appendix II

### Online resource 3 Sampling schedule for gene expression experiments.

Rachis samples (three unrelated biological repeats) were taken twice, at pre bloom (phenological stage BBCH57) and at past bloom (BBCH71; see Figure 3) at the three locations Palatinate (P), Hesse (H) and Baden (B) during the seasons 2015-2017. The sampling dates ranged over up to 16 days due to the targets for cumulated degree day (CDD) sum (400° BBCH57 and 700° BBCH71) for the phenological stages according to Molitor et al. (2014)

Sampling schedule					
Location	BBCH	Season	Day of year	Sampling	°CDD start at BBCH09
P	57	2015	152	01.06.2015	421.2
P	57	2016	161	09.06.2016	415.69
P	57	2017	154	03.06.2017	416.65
H	57	2015	149	29.05.2015	398.27
H	57	2016	157	05.06.2016	447.21
H	57	2017	152	01.06.2017	401.87
B	57	2015	146	31.05.2015	390.33
B	57	2016	159	07.06.2016	422.07
B	57	2017	150	30.05.2017	420.15
P	71	2015	177	26.06.2015	714.83
P	71	2016	186	04.07.2016	708.59
P	71	2017	177	26.06.2017	712.11
H	71	2015	176	25.06.2015	725.96
H	71	2016	178	26.06.2016	703.37
H	71	2017	171	22.06.2017	677.38
B	71	2015	170	19.06.2015	698.01
B	71	2016	182	30.06.2016	712.93
B	71	2017	171	20.06.2017	711.26

## Appendix II

**Online resource 4** Phenotypic measurements recorded during four seasons on selected F1 individuals of the cross population (‘Calardis Musqué’ × ‘Villard Blanc’).

Mean of pedicel lengths and rachis lengths measured at selected F1 individuals recorded over four seasons. The selected genotypes showed distinct short resp. long pedicel- and rachis lengths. n= number of independently sampled clusters per genotype, for each cluster ten pedicels were measured

Pheno-type	Genotype	Pedicel length [cm]				Pheno- type	Genotype	Rachis length [cm]			
		2013 (n=12)	2014 (n=3)	2015 (n=6)	2016 (n=6)			2013 (n=12)	2014 (n=3)	2015 (n=6)	2016 (n=6)
PED max	89-30-212	0.63	0.58	0.73	0.71	RL max	89-30-405	16.6	20.27	22.79	25.11
PED max	89-30-294	0.63	0.53	0.7	0.64	RL max	89-30-484	13.6	18.71	22.13	23.85
PED max	89-30-354	0.67	0.53	0.67	0.74	RL max	89-30-503	*	22.65	22.47	29.25
PED max	89-30-380	0.66	0.64	0.65	0.67	RL max	89-30-059	16.23	23.61	22.45	25.21
PED min	89-30-194	0.49	0.27	0.39	0.49	RL min	89-30-241	*	*	9.63	7.74
PED min	89-30-558	0.48	0.25	0.39	0.4	RL min	89-30-647	9.34	12.21	10.93	9.18
PED min	89-30-594	0.43	0.35	0.4	0.47	RL min	89-30-680	11.24	7.29	12.01	15.06
PED min	89-30-598	0.34	0.29	0.39	0.45	RL min	89-30-052	9.93	14.26	14.15	14.9

T-test results and descriptive values for the measurements of pedicel lengths and rachis lengths of the selected F1 hybrids

PED max = four individuals with extreme long pedicel length, PED min = four individuals with extreme short pedicel length RL max = four individuals with extreme long rachis length RL min = four individuals with extreme short rachis length) SEM = Standard error of the mean

T-test ( <i>p</i> -value)	PED max	PED min	RL max	RL min
	<i>p</i> -value = (5.45E-11) <i>df</i> (27)		<i>p</i> -value = (1.24E-08) <i>df</i> (23)	
Mean	0.64	0.39	21.66	11.27
SEM	0.015	0.019	1.035	0.692
Minimum	0.53	0.25	13.6	7.29
Maximum	0.74	0.49	29.25	15.06

## Appendix II

**Online resource 5** Primers for the quantitative Real Time amplification of candidate genes and reference genes. Primers used for the reference gene amplification are highlighted in grey.

<sup>1</sup> Gene ID V1	Gene ID costV3	Forward sequence 5' →3'	Reverse sequence 5' →3'	<sup>2</sup> Amp [bp]	Bibliography
VIT_00s0313g00070	Vitvi07g01441	AGGTTGAGCAAGG AAGTTGCA	CTCGGCTCAATCC AGCTTCA	127	Jiang et al. 2012
VIT_01s0010g01810	Vitvi01g01457	TCGCCGTTGTCCG AGTTT	ACTTCCACTCCAC CACCT	151	Rossmann et al. 2020
VIT_01s0010g02430	Vitvi01g01534	CAAGATGAGGGTG TTAAATCGT	ACCTCATTTGTTGC CTTGCT	119	Rossmann et al. 2020
VIT_01s0011g06410	Vitvi01g00553	CTCCATGCGGGTC CTTGT	GTGCGTTGGTTTCT GGGATT	108	Jiang et al. 2012
VIT_01s0026g02030	Vitvi01g00964	AAGCCAAAAGCGC AGACA	GCAATAGGCGCTC CGACAA	118	Zhang et al. 2009
VIT_01s0127g00260	Vitvi01g00698	GGCGCGCAAGAAG ATCAGAGA	CCCACGCTTGCCA AATAACAT	199	Rossmann et al. 2020
VIT_01s0127g00710	Vitvi01g00733	CCCACCTCCTTTAT GACCGCTA	CAAGAAAATCCTC CATCAACCGT	232	Rossmann et al. 2020
VIT_01s0127g00870	Vitvi01g00747	AGGCGTCTTTGCTT CGGTATT	CGCATTTTGAGCG GCAAGT	134	Rossmann et al. 2020
VIT_01s0146g00400	Vitvi01g01733	TCCCACTCCGACA CCACCTT	TCTTCCTGGCTTT CTTGCCGTTT	131	Rossmann et al. 2020
VIT_01s0146g00480	Vitvi01g02293	CCGCCATGGAACCT TGATTCT	GCGAACGGCGGAT TATTCT	196	Rossmann et al. 2020
VIT_02s0012g00990	Vitvi02g00666	GCTGCCACACCTT ACTCAT	ATGTACTTACCCC AACAGATGTC	204	Rossmann et al. 2020
VIT_02s0012g01380	Vitvi02g00702	GAGACTCCGGCCA CCAACAA	GCCCAGCCTTCAC CACATTT	128	Rossmann et al. 2020
VIT_02s0012g01400	Vitvi02g00704	CCTCGATTCATTCC GCTTCT	CGGTGCTGATGC TCTT	85	Rossmann et al. 2020
VIT_02s0025g03010	Vitvi02g00276	GGCTGCGAGAGAG TCGTAAA	ACCTTTTCCATCCC CAGATCCA	83	Rossmann et al. 2020
VIT_02s0025g03140	Vitvi02g01375	CCCGGTTTGACAT TTCTCAT	CCTCTTGCACTTCG AATCCT	68	Rossmann et al. 2020
VIT_02s0025g03180	Vitvi02g00287	CAACATGGTCCTT GCAATC	GGTTGGAGATGGA GCTTCTG	190	Rossmann et al. 2020
VIT_02s0025g04340	Vitvi02g01409	CCGAGTGAAATAA GGCATGT	ATAATTGAGGAGG GCTCACA	41	Rossmann et al. 2020
VIT_02s0025g04660	Vitvi02g00429	TTGACTGCTGCTCT TGTGCTT	CCACTCCCAAAAA CAGAACCTT	133	Rossmann et al. 2020
VIT_02s0025g04720	Vitvi02g00435	CCCTGAAGACAAG CGCGATA	GGGTACCATGTTG TGGAGGATGAAG	298	Rossmann et al. 2020
VIT_02s0154g00320	Vitvi02g00532	CCTTCTCCTTGCCC TAAACCT	GGTGGCTTTTTGTG TGGTTTTT	102	Rossmann et al. 2020
VIT_02s0154g00380	Vitvi02g01443	CAGCCTCCTCTAC AACCT	CTGCTGCTGCTTCT TCTT	130	Rossmann et al. 2020
VIT_02s0241g00030	Vitvi02g01424	CTTCAGTCTTACC TACTGTGA	AGAAGCTTCTTTT GATACCGATAG	70	Rossmann et al. 2020
VIT_03s0097g00700	Vitvi03g00860	GGCCTTATGGGGA GAACCTT	TGCCCGAGTGCCT GTAAA	56	Rossmann et al. 2020
VIT_04s0008g00180	Vitvi04g00009	CCCTGGACTGTTTC TGTTGCT	AGGACTGCTGGGG GCAAAA	128	Rossmann et al. 2020
VIT_04s0008g00370	Vitvi04g00029	CAAGCAAGGAGAG CCAGACA	CCCGTCACAAGCT CAAGCAA	133	Rossmann et al. 2020
VIT_04s0008g01100	Vitvi04g00091	CCCCTTGATGGCC AAGTAT	GGAGAGGGGATGC TGAGAT	197	Rossmann et al. 2020
VIT_04s0008g01810	Vitvi04g00155	GCTGCAGATTGAG GTGGTT	GTCTGTTCCGCCCTG GAAT	149	Rossmann et al. 2020
VIT_04s0008g01910	Vitvi04g00164	TCTCCCTCTCCCTC GTCTTC	CATCCTCACCCCC CACTTCA	210	Rossmann et al. 2020
VIT_04s0008g02900	Vitvi04g00256	GGGAGGAATTGAA GGCTATGG	GCACCAATGCGCA GCAAA	162	Rossmann et al. 2020
VIT_04s0008g02920	Vitvi04g00259	GTGGCTCCCAAGT TAGTGAT	ACCACCGACAGT TCTTTTG	145	Rossmann et al. 2020
VIT_04s0008g04050	Vitvi04g00350	CCTCACACTCCCA TGCCAAA	CCCAAACAAAAAG CAGCAGCAGAA	89	Rossmann et al. 2020

## Appendix II

VIT_04s0008g04200	Vitvi04g0 0361	CGAGAGTGCCAA GAGGTT	CGCATGACCCTGG CAGAA	108	Rossmann et al. 2020
VIT_04s0008g05150	Vitvi04g0 1894	TCTCGCCAAGGG GTTTT	CTGAAACACTCCA TCCTGCTT	145	Rossmann et al. 2020
VIT_04s0008g05770	Vitvi04g0 0512	GGCCGGAAAGGGA GGTTAT	CGCCAGCCGACTT CAAGA	88	Rossmann et al. 2020
VIT_04s0008g05830	Vitvi04g0 0517	GTCTCAGATCGCG TCATTGT	TTGTGGACAGCTC CTGCTT	93	Rossmann et al. 2020
VIT_04s0008g06670	Vitvi04g0 0602	CCCAATCCGATTC TCTCAACAA	CCCTCCTCACCTTC AACAC	123	Rossmann et al. 2020
VIT_04s0023g03070	Vitvi04g0 1426	GGACCTAAGCTGG AACAAG	CACCGTTGCAGGA ATCTT	118	Jiang et al. 2012
VIT_04s0069g00790	Vitvi04g0 0736	ATCCCAGCAAAGA CATCAGT	AAACAGAACCAGG CCAAGA	212	Rossmann et al. 2020
VIT_04s0079g00260	Vitvi04g0 0836	ACCACAAGCCTGC AATTTT	GGCTCTGACCTCA AGGTT	112	Rossmann et al. 2020
VIT_07s0031g01850	Vitvi07g0 1861	TGGGCAGCTAGGA GGAAGATT	GTGGGGGATGCAG TTATGGT	75	Jiang et al. 2012
VIT_08s0007g01310	Vitvi08g0 1277	ATGGGAAGAGCTG GTTTGG	AGCGGCTAGTGTT CAAATCC	42	Rossmann et al. 2020
VIT_08s0007g01320	N.A.	GGGGCCGATTCTC AACAGT	ACCACCTCATGGA CCTTCCT	142	Rossmann et al. 2020
VIT_08s0007g01350	Vitvi08g0 2224	CTCCTCCTCCTCAC GACAGA	CACGCCATCACAG CACTT	76	Rossmann et al. 2020
VIT_08s0007g01360	Vitvi08g0 2225	AACGCCAAACCAG GGACTACA	ACTCTGACTCTCG CCTTCACT	60	Rossmann et al. 2020
VIT_08s0007g01370	Vitvi08g0 1281	GGCGGCCAGCGAC AAGA	GGCAGCTTGGGTT CTGGAT	80	Rossmann et al. 2020
VIT_08s0040g00040	Vitvi08g0 0880	GAGGGTCGTCAGG ATTTGGA	GCCCTGCACCTAC CATCTCTA	71	Selim et al. 2012
VIT_08s0040g01710	Vitvi08g0 1022	ACTGGATTTGGTG CGACTT	CGTGTGGCATGAG TCTGTT	117	Rossmann et al. 2020
VIT_08s0058g00930	Vitvi08g0 0816	TCGGACGGGGAAA AGTATGCAA	CCTGGGGCCAACCT CTACAAT	125	Rossmann et al. 2020
VIT_08s0058g00990	Vitvi08g0 0823	TGGGTGCTTCTTTG CTTCGT	CGCCCGCATTCTTT TCACT	111	Rossmann et al. 2020
VIT_09s0070g00470	N.A.	TGCCAAAAGGGAC CTCTGAT	TCGGGAGGAGGAA GAGGAGCTA	113	Jiang et al. 2012
VIT_11s0016g03710	Vitvi11g0 0317	GTCCGAATCGGCT GCTTGAA	TCGGGTTCCATCG CACTT	88	Rossmann et al. 2020
VIT_12s0059g00190	Vitvi12g0 0342	CTCCGGCCAGCTC CAACA	GCCCCTACTCTTGC CCTAAAC	153	Dal Santo et al. 2013
VIT_14s0066g01060	Vitvi14g0 1745	CCACCTACAGAAC TCCCAAAA	TATCCCTCCCTAG ACCTCCAAT	158	Rossmann et al. 2020
VIT_14s0066g01390	Vitvi14g0 1780	ATTTGACTCGGGG AAAGCA	TGGCAGCAAGTGA CTGATG	110	Rossmann et al. 2020
VIT_14s0083g00410	Vitvi14g0 1273	CCTTCCCAACCTCC CTTTC	CCTCTCCAACCCC ATCATCAC	173	Correa et al. 2014
VIT_14s0108g00700	Vitvi14g0 1952	AGTGCAGTGATG AACAGAGA	GGGCTGCTGCGTA TAGTG	184	Rossmann et al. 2020
VIT_14s0108g00740	Vitvi14g0 3084	CGCCATTTCATG CTTCAC	CAAAAACAACACTC GCACACAATC	139	Rossmann et al. 2020
VIT_14s0219g00230	Vitvi14g0 1635	CCGGCTGGTGGAC AGTAT	AGAGATGGTTATG CGGTTGGAT	140	Vargas et al. 2013
VIT_15s0048g01750	Vitvi15g0 0816	CCACCACTCTCTA CCAAACC	CCGACCTTGCCAC CTTTCA	85	Rossmann et al. 2020
VvGRF4	Vitvi16g0 0073	ACCAACCAATCCC AATTCCA	TTCGCCTACCTCG GGTTT	102	Rossmann et al. 2020
VIT_17s0000g02470	Vitvi17g0 0217	GGTCCCTGCTTCTC AGTCT	TTGCCTGCGCCTG GTTGTA	121	Rossmann et al. 2020
VIT_17s0000g03550	Vitvi17g0 0307	GGAGAGAGAAAG GCTCGAGTT	AGCATGGAAAGGC GATCAT	104	Rossmann et al. 2020
VIT_17s0000g03750	Vitvi17g0 1407	ACAGAGAGGGGA GAGCTT	TTGTACCACCTGA GATTTGCT	159	Rossmann et al. 2020
VIT_17s0000g04470	Vitvi17g0 1426	TCCGCCCTGTGTTT TTCT	AACAACCTTCCGA TTCCAGATAC	60	Rossmann et al. 2020
VIT_17s0000g05000	Vitvi17g0 0471	GTCGCCTTCTGCT CAATC	CGGGGCCAAATCC ATTGT	151	Rossmann et al. 2020
VIT_17s0000g05070	Vitvi17g0 0480	TCTCTCTCCATAAC CTCCCTCAAAC	CCATTAGCGGTGG CAGAAC	159	Rossmann et al. 2020
VIT_17s0000g05570	Vitvi17g0 0533	GCAGGCTTCCAC TTCAAA	CGCTCATCTGTCC ACCAT	94	Rossmann et al. 2020
VIT_17s0000g07350	Vitvi17g0 0713	GAGGATGTGCTGA GGATGGA	TGTGGTCGCATAG CCGTTT	118	Rossmann et al. 2020

## Appendix II

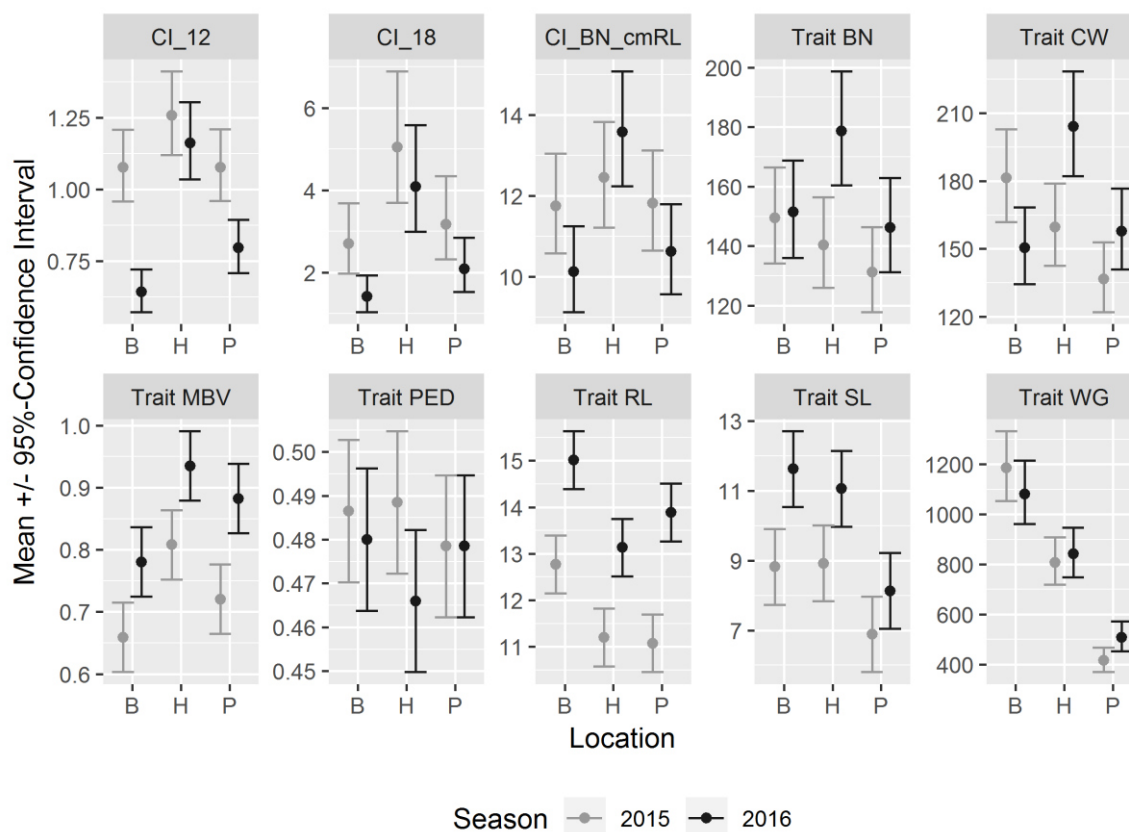
VIT_17s0000g09190	Vitvi17g00906	AGGGTTCCTGCTG TGGAT	ACACAACCTCCCCT AACTTCAC	66	Rossmann et al. 2020
VIT_17s0000g09310	Vitvi17g00919	ACCCCGATGACT ACCTTT	CCCTGTGCTTTTGC TGGAT	169	Rossmann et al. 2020
VIT_17s0000g09470	Vitvi17g00936	AATTGTCACAGCT TCACCCAAAG	CGCGGTCCACTTG GCTTATC	164	Rossmann et al. 2020
VIT_17s0000g09790	Vitvi17g00975	GGGTTGGATGTTT TTGCAAGAT	CCGCCTACTTCGCT TCTTC	97	Rossmann et al. 2020
VIT_17s0000g10430	Vitvi17g01598	TTCTCGTTGAGGG CTATT	CCACAGACTTCAT CGGTGACA	70	Selim et al. 2012
VIT_17s0053g00990	Vitvi17g01251	CTTCTATGGCGGG GGTGAT	GCCACAGCTCAAC CCATT	133	Hoffmann 2015
VIT_18s0001g03160	Vitvi18g00289	CGCCTTTCGCACTT GTTC	GGAAGCCAAGCAC CATTATTTT	84	Rossmann et al. 2020
VIT_18s0001g03540	Vitvi18g00310	GGGCTACCAACAT TCTCTACAC	TCCCCAAAAGCCC AATAAACAG	167	Rossmann et al. 2020
VIT_18s0001g04890	Vitvi18g00363	TGTGCCGGTGCCT TCTTT	CCTTCTACGCTGG GCCTAA	118	Rossmann et al. 2020
VIT_18s0001g04910	Vitvi18g00365	ATCTGCGGCTTGC ATTACAC	AGCTCCACCCATA AAACCAACA	128	Rossmann et al. 2020
VIT_18s0001g05060	Vitvi18g02571	CAAGCCTCAACTG CTCATAC	CACATCAACACAA CCAGTGAAC	165	Rossmann et al. 2020
VIT_18s0001g05800	Vitvi18g00414	GGCATTGACTGGG ACCAAAA	CCACCTCTTCTGCA TCTCT	140	Rossmann et al. 2020
VIT_18s0001g07340	Vitvi18g00510	CCCGTTCAGCTTA TGTTTCAT	AGTGTGGGGGAG AAGGT	104	Rossmann et al. 2020
VIT_18s0001g07460	Vitvi18g00517	GCAGATGAGGGGA GAGGATA	GTGGCGATCTCGG TCATT	129	Jiang et al. 2012
VIT_18s0001g09230	Vitvi18g00675	ACAAGCGATGCCA CTACGAA	GGCAGGTTGAGGT CGAAGT	106	Rossmann et al. 2020
VIT_18s0001g09400	Vitvi18g00687	CGGATTGCTGGTT CGTCAT	GTGGCTCGTTGCGT CCTT	116	Rossmann et al. 2020
VIT_18s0001g09510	Vitvi18g02657	AGGGAGGCAGAA GACGATGA	GTCCAGCCGAGG TATCTGT	132	Rossmann et al. 2020
VIT_18s0001g09910	Vitvi18g00730	CGAAAGAAGCCAA CAGCAT	CACCGTTTCTGGC GCATA	140	Rossmann et al. 2020
VIT_18s0001g10130	Vitvi18g00755	CACCCGTGAAGGC AAGTC	CGCCGTCTTTGTCA TGTT	83	Rossmann et al. 2020
VIT_18s0001g10610	Vitvi18g02683	AAACATGCCTCGT CATTGGAA	CGCCGTTTTGTCA TGGT	119	Rossmann et al. 2020
VIT_18s0001g10640	Vitvi18g02686	CCGTACGTGCCTA GATTAAAGAA	CCAAGCATCCCCA AATGGAA	44	Rossmann et al. 2020
VIT_18s0001g11160	Vitvi18g00842	GTTCGTTTGGGCT GTGTACT	CTCCTCGTCTGAC ATTTGCTT	76	Rossmann et al. 2020
VIT_19s0015g00270	Vitvi19g02058	CGGAGAGTGTGC TGATGAT	GCTTGACTTTTCG GGTTTTCGT	149	Rossmann et al. 2020
VIT_19s0015g00490	Vitvi19g02064	ACGGAACCGGAGA AGACACT	CCCCATCAGAATC GCCATCT	108	Rossmann et al. 2020
VIT_19s0015g01230	Vitvi19g00750	CGTTGTGAAATA GCTGTGGAT	AATGGGTGGTGGT GGATTG	87	Rossmann et al. 2020
VIT_19s0015g01890	Vitvi19g00928	CATTTCATCACCCC CGTCTCT	ATTCCCACATTCCC CAAACCTCA	93	Jiang et al. 2012

<sup>1</sup>Annotation based on RNA-Seq results reported in (Rossmann et al. 2020). The *Vitis* gene annotations for candidate genes based on literature reporting data for rice and tomato were retrieved with their protein sequence from the NCBI Gene Bank (<https://www.ncbi.nlm.nih.gov/nucleotide>). This sequence was then used for an orthologue search restricted to orthologs in *Vitis vinifera* with the ‘hierarchical catalogue of orthologs’ (<https://www.orthodb.org>) (Kriventseva et al. 2019).

<sup>2</sup>Amplicon length of the product based on the reference genome PN40024 assembly version 12x.v2 (Canaguier et al. 2017)

## Appendix II

**Online resource 6a** Effects of trial location and growing season on important cluster architecture sub-traits and compactness indices for the ‘Pinot Noir’ clones Gm20-13 and FkCH, which were the two reference clones that were sampled across all seasons and locations. Means and 95% confidence intervals were estimated with generalized linear models (n = 120).



Estimated marginal means for measurements from 2015 and 2016 at three trial fields located in German wine growing regions. Hesse (H) and Palatinate (P) belong to viticulture area A (cool climate). Baden (B) belongs to viticulture area B (moderate climate). For trait abbreviations see table 3.

## Appendix II

**Online resource 6b** ANOVA results for important cluster architecture sub traits and compactness indices for two ‘Pinot Noir’ clones that were sampled across all seasons and locations. Means and 95% confidence intervals were estimated with generalized linear models. ANOVA results of a reciprocal design (n = 120) for the measurements of the ‘Pinot Noir’ clones Gm20-13 and FkCH at all locations and seasons. P-values for the effects of field location and growing season on cluster architecture sub-traits and compactness indices, obtained from generalized linear models (GLM) with negative binomial (NB) or gamma distribution or ordinary least squares models (OLS) and ANOVA sums of squares type 3 test. For trait abbreviations see table 3.

Trait / Index	Model	Clone	Location	Season	Location: Season
BN	NB GLM	0.000	0.059	0.008	0.130
CW	Gamma GLM	0.000	0.004	0.178	0.002
MBV	OLS	0.000	0.002	0.000	0.868
TBV	NB GLM	0.000	0.000	0.000	0.195
RD	OLS	0.004	0.000	0.133	0.151
RL	OLS	0.019	0.000	0.000	0.436
RW	OLS	0.000	0.006	0.000	0.367
SL	OLS	0.722	0.000	0.000	0.362
PL	OLS	0.125	0.208	0.081	0.101
PED	OLS	0.882	0.746	0.155	0.378
L1I	OLS	0.694	0.168	0.199	0.568
L2I	OLS	0.179	0.274	0.089	0.337
BN_cmRL	Gamma GLM	0.000	0.000	0.188	0.052
CI_12	Gamma GLM	0.000	0.000	0.000	0.000
CI_18	Gamma GLM	0.081	0.000	0.004	0.606
WG	Gamma GLM	0.024	0.000	0.293	0.043

**Online resource 6c** ANOVA results for important cluster architecture sub traits and compactness indices for 12 ‘Pinot Noir’ clones that were sampled across all seasons and locations. Means and 95% confidence intervals were estimated with generalized linear models. ANOVA results for measurements of twelve ‘Pinot Noir’ clones (n = 400). P-values for the effects of field location and growing season on cluster architecture sub-traits and compactness indices, obtained from generalized linear models (GLM) with negative binomial (NB) or gamma distribution or ordinary least squares models (OLS) and ANOVA sums of squares type 3 test. For trait abbreviations, see table 3.

Trait / Index	Model	Clone	Location	Season	Location: Season
BN	NB GLM	0.056	0.000	0.004	0.001
CW	Gamma GLM	0.000	0.000	0.000	0.000
MBV	OLS	0.000	0.009	0.000	0.000
TBV	NB GLM	0.000	0.000	0.009	0.327
RD	OLS	0.000	0.000	0.009	0.327
RL	OLS	0.000	0.000	0.000	0.244
RW	OLS	0.000	0.000	0.000	0.007
SL	OLS	0.000	0.004	0.000	0.527
PL	OLS	0.000	0.008	0.062	0.107
PED	OLS	0.000	0.662	0.000	0.368
L1I	OLS	0.053	0.864	0.235	0.216
L2I	OLS	0.083	0.159	0.225	0.983
BN_cmRL	Gamma GLM	0.000	0.000	0.043	0.041
CI_12	Gamma GLM	0.000	0.000	0.001	0.000
CI_18	Gamma GLM	0.000	0.000	0.021	0.058
WG	Gamma GLM	0.000	0.000	0.007	0.042

**Online resource 7** Relative gene expression  $\log_{(2)} FC (-\Delta\Delta t)$  at BBCH57 and BBCH71 as determined with a linear model:  $\log_{(2)} FC \sim clone * season * location$  for 'Pinot Noir' clones with divergent cluster architecture. Cluster architecture types are indicated in the header as follows: loose (LCC) = blue; compact (CCC) = orange; mixed berried (MBC) = green. Vineyard locations are included in the sample names: B = Baden; H = Hesse; P = Palatinat. Season is indicated as YY. Abbreviations for clone names are given in table 1. The values are relative to clone Gm20-13 (small berries and short rachis features) and the mean of two internal control genes. Genes highlighted in grey show a stable differential expression between clones with different cluster types over multiple seasons

**Time point BBCH57 loosely clustered clones**

Genes/samples	Fr12L.B.16	Fr12L.B.17	Fr12L.H.16	Fr12L.H.17	Fr13L.B.16	Fr13L.B.17	Fr13L.H.16	Fr13L.H.17	Gm1_86.H.15	Gm1_86.H.16	Gm1_86.H.17	Gm1_86.P.15	Gm1_86.P.16	Gm1_86.P.17	WeM1.H.16	WeM1.H.17	WeM171.P.15	WeM171.P.16	WeM171.P.17	WeM242.H.16	WeM242.H.17
VIT_00s0313g00070	-0.03	-0.11	0.55	0.23	0.09	-0.02	0.55	0.15	0.38	0.01	-0.31	0.27	-0.24	0.26	0.33	0.60	0.44	0.18	0.34	0.51	0.52
VIT_01s0010g01810	-0.96	-0.76	0.03	-0.61	0.22	0.09	0.74	0.08	1.85	-0.50	0.16	-0.08	0.10	4.94	0.65	1.06	0.79	-0.31	6.10	0.28	0.37
VIT_01s0010g02430	-0.66	0.00	1.24	-0.59	-0.56	0.02	0.50	-0.59	2.25	0.31	-0.90	0.01	0.47	-0.43	1.02	-0.48	-0.17	-0.12	-0.05	0.49	-0.20
VIT_01s0011g06410	-0.01	0.05	0.42	0.15	-0.11	-0.09	0.57	0.03	0.92	0.47	-0.08	0.03	0.08	0.00	0.36	0.33	0.05	-0.10	0.16	0.46	0.64
VIT_01s0026g02030	0.27	0.10	0.33	0.10	0.22	0.36	-0.29	0.23	0.70	-0.19	0.06	0.02	-0.28	0.30	0.15	-0.17	-0.02	0.05	0.92	0.29	-0.21
VIT_01s0127g00260	-0.12	-0.14	1.35	1.02	-0.34	0.10	1.26	0.41	1.35	0.29	-0.12	0.21	0.50	-0.05	0.71	0.92	-0.04	0.44	0.21	0.99	1.21
VIT_01s0127g00710	11.55	12.02	-0.41	-0.11	11.23	11.86	-0.48	0.30	-2.21	-0.62	-0.81	18.78	11.41	18.32	-0.81	-0.07	17.99	10.68	18.63	-0.34	-0.08
VIT_01s0127g00870	0.07	0.40	2.22	-0.01	0.15	0.43	2.41	-0.13	3.45	1.56	0.12	0.54	0.21	0.62	2.06	0.53	0.29	0.32	1.04	2.11	0.77
VIT_01s0146g00400	-0.55	0.38	0.25	0.11	-0.41	0.29	0.38	-0.19	2.08	0.54	-0.11	0.70	1.07	0.08	0.42	-0.03	0.63	0.70	0.50	0.25	0.40
VIT_01s0146g00480	0.31	0.20	0.45	-0.41	-0.86	-0.27	1.14	-0.56	0.63	0.21	-0.70	1.12	-0.76	-1.49	0.60	-0.20	0.70	0.32	-0.86	1.38	-0.12
VIT_02s0012g00990	11.74	6.59	-0.57	-0.25	11.38	6.36	-0.22	0.19	0.44	-0.34	-0.01	23.50	19.60	12.04	-0.19	0.11	24.06	18.71	12.23	-0.31	-0.04
VIT_02s0012g01380	-0.14	-0.07	-0.40	0.35	0.07	0.01	-0.92	0.24	-2.11	-1.02	-0.01	0.71	-0.24	-0.28	-0.73	0.31	0.58	-0.30	-0.49	-0.51	-0.07
VIT_02s0025g03180	-0.21	0.17	0.13	0.07	-0.33	0.02	0.30	0.27	-0.20	0.09	0.13	-0.68	0.02	0.09	-0.13	0.30	-0.16	-0.27	-0.02	0.10	0.85
VIT_02s0025g04340	0.24	0.62	-0.60	-0.27	0.59	0.63	0.21	-0.13	-1.66	0.37	-0.57	1.18	-1.41	-1.10	-0.12	-0.77	0.89	0.17	-0.71	-0.39	-0.86
VIT_02s0025g04660	0.16	-0.33	-0.28	0.12	0.34	-0.19	0.02	0.05	-1.13	-0.49	-0.40	0.52	-0.43	-0.44	-0.93	0.60	0.44	0.29	-0.16	-0.13	0.22
VIT_02s0025g04720	-0.30	7.05	1.25	0.53	-0.57	6.97	1.07	0.29	3.16	0.39	-0.15	-0.23	1.11	-0.36	0.86	0.77	-0.32	0.15	0.50	0.62	0.83
VIT_02s0154g00320	0.09	0.31	0.34	0.05	-0.18	0.35	0.90	0.50	2.74	0.27	0.15	-1.11	1.16	0.79	0.55	0.26	0.49	0.35	1.08	0.93	0.12
VIT_02s0154g00380	0.90	-0.63	-0.17	0.10	0.21	-0.51	0.01	-0.35	-0.20	0.30	-0.01	2.05	-1.48	-1.00	-0.34	-0.43	3.44	-0.58	0.74	1.15	0.03
VIT_02s0241g00030	-0.25	0.07	1.00	0.07	0.10	0.21	0.70	0.11	0.03	0.36	-0.19	-0.12	-0.19	0.18	0.68	0.54	0.05	-0.03	0.11	0.61	0.51
VIT_03s0097g00700	0.12	0.13	-0.49	0.05	-0.05	1.61	0.09	-0.59	0.51	-0.02	-0.22	3.47	0.04	0.68	-0.31	-0.11	1.76	1.04	1.52	-0.51	-0.67

## Appendix II

VIT_04s0008g00180	-0.48	0.35	0.59	0.42	-0.11	0.27	0.64	0.19	1.17	0.58	-0.10	0.17	0.40	0.20	0.63	0.51	0.09	0.13	0.11	0.52	0.47
VIT_04s0008g00370	0.48	0.30	-0.06	0.57	0.34	0.36	-0.16	0.89	-0.59	-0.25	0.45	-0.18	-0.80	-0.47	0.20	0.66	0.13	0.31	-0.16	0.52	0.75
VIT_04s0008g01100	-0.43	-0.21	-0.75	0.17	-0.53	-0.20	-0.37	-0.15	-1.34	-0.65	-0.87	0.47	-0.69	-0.50	-0.56	-0.51	0.33	-1.14	-0.55	-0.58	-0.18
VIT_04s0008g01810	0.69	1.26	0.52	0.51	0.25	1.05	0.58	0.44	1.50	0.44	0.67	0.40	0.86	0.32	0.74	1.08	0.57	0.33	0.64	0.81	1.00
VIT_04s0008g01910	-0.39	0.16	0.63	0.05	-0.81	0.05	0.54	-0.07	1.72	0.46	-0.23	-0.24	0.57	0.19	0.56	-0.08	0.22	-0.08	0.71	0.42	0.35
VIT_04s0008g02920	-0.42	-0.45	0.78	0.63	-0.75	-0.34	0.44	0.56	0.87	0.30	0.01	0.82	-0.28	0.79	0.73	0.63	0.40	0.08	0.42	0.21	0.51
VIT_04s0008g04050	-0.63	0.08	1.21	1.65	-0.81	-0.52	0.96	1.47	0.57	1.70	2.04	-0.28	0.45	1.20	0.58	1.24	0.33	-0.33	0.38	0.65	1.67
VIT_04s0008g04200	-0.55	0.40	0.81	-0.18	-0.71	0.20	0.85	0.20	1.34	0.87	-0.07	1.21	0.56	-0.27	0.66	-0.01	0.44	-0.83	0.56	0.34	0.85
VIT_04s0008g05150	-0.47	0.20	0.31	-0.18	-0.19	-0.05	0.68	0.14	0.58	0.51	-0.20	0.83	0.70	0.00	0.45	0.38	0.74	-0.63	0.16	0.41	0.64
VIT_04s0008g05770	0.37	-0.53	-1.03	0.55	0.90	-0.31	-0.52	0.27	-1.54	-0.21	0.27	0.20	-0.46	-0.18	-0.48	0.57	0.25	0.09	-0.42	-0.29	0.30
VIT_04s0008g05830	-0.35	0.48	1.03	-0.18	-0.20	0.42	1.20	0.04	2.24	1.02	0.27	0.07	1.09	0.32	1.09	0.26	0.05	0.04	0.62	0.90	0.60
VIT_04s0008g06670	-0.24	0.11	0.69	-0.94	-0.25	0.15	0.51	-0.92	2.07	0.18	-0.91	-0.68	0.39	-0.69	0.80	-0.76	-0.45	-0.17	-0.15	0.40	-0.20
VIT_04s0023g03070	-0.35	-0.29	1.14	0.20	-0.27	0.03	1.40	0.27	1.22	0.55	-0.12	0.41	-0.21	0.30	0.92	0.36	0.12	0.19	0.23	1.12	0.68
VIT_04s0069g00790	3.93	-0.36	0.34	0.43	4.03	-0.13	0.17	0.22	-0.24	-0.81	-0.18	0.01	-0.20	-0.26	0.02	0.61	0.10	0.00	-0.06	0.30	0.45
VIT_04s0079g00260	-0.59	0.36	0.56	-0.21	-0.70	0.13	0.49	-0.07	1.09	-0.22	-0.63	1.25	0.57	-0.09	0.45	0.28	0.61	-0.12	0.52	0.23	0.56
VIT_08s0007g01310	0.47	-0.09	0.70	0.12	0.52	-0.09	0.36	0.35	-0.53	0.26	-0.11	0.14	-0.43	-0.32	0.08	0.33	-0.14	0.44	-0.11	0.22	0.72
VIT_08s0007g01320	0.70	0.19	0.76	0.30	0.86	0.24	0.41	0.34	-0.32	0.20	-0.16	0.38	-0.51	-0.40	-0.05	0.32	0.24	0.47	-0.13	0.24	0.83
VIT_08s0007g01360	0.07	-0.32	-1.15	-0.49	0.29	-0.18	-1.12	-0.18	-2.24	-0.35	-0.44	-0.36	-1.21	0.15	-0.65	-0.90	-0.03	-0.61	-0.47	-0.80	-1.17
VIT_08s0007g01370	-0.98	-0.10	-0.82	-1.40	-0.68	0.08	-0.47	-1.90	-1.02	-0.18	-1.79	-0.63	-0.51	-1.15	0.89	-1.17	-0.30	-0.67	-0.90	-0.93	-1.82
VIT_08s0040g01710	-0.17	-0.17	0.59	0.53	-0.14	-0.15	0.68	0.17	1.46	0.51	-0.04	-0.04	0.70	-0.49	0.26	0.50	-0.14	0.35	0.18	0.46	0.83
VIT_08s0058g00930	-0.30	-0.22	-0.04	-0.02	0.54	0.15	-0.43	-0.28	-1.93	-0.34	-0.51	-0.14	-0.62	0.10	-0.66	-0.22	-0.13	-0.55	-0.18	-0.50	0.08
VIT_08s0058g00990	-0.19	-0.21	0.20	0.04	0.12	0.21	-0.19	-0.09	0.38	0.14	-0.18	0.40	-0.07	-0.12	0.07	0.22	0.87	0.14	-0.21	0.04	0.23
VIT_11s0016g03710	-0.92	0.11	0.50	-0.17	-0.53	-0.17	0.71	-0.15	2.01	0.42	-0.23	0.99	0.98	0.62	0.77	0.34	0.55	0.15	1.00	0.47	0.90
VIT_12s0059g00190	-0.58	-0.22	-0.02	-0.78	-0.01	-0.16	0.40	0.09	2.15	-0.14	-0.32	-0.32	0.67	-0.85	0.27	-0.42	-0.26	0.07	0.04	0.20	0.30
VIT_14s0066g01060	6.76	-0.54	-0.24	1.12	7.40	-1.48	0.31	0.18	1.36	-0.23	0.00	1.81	0.65	1.27	0.27	-0.14	0.25	-0.28	0.08	0.38	2.04
VIT_14s0066g01390	0.11	0.14	-0.10	0.17	0.16	0.02	-0.34	0.22	0.00	-0.11	-0.02	0.42	0.52	-0.27	-0.65	0.42	0.34	0.15	0.06	-0.26	0.30
VIT_14s0083g00410	-0.71	0.09	-0.79	-0.44	-0.53	0.01	-0.73	-0.42	-0.85	-1.18	-0.33	0.88	0.48	-0.07	-0.99	0.45	0.85	0.39	0.01	-0.67	-0.11
VIT_14s0108g00700	0.32	-0.21	1.17	0.56	-0.31	-0.19	1.35	0.29	2.17	0.68	0.37	-0.29	0.41	1.13	0.65	1.32	0.78	0.89	1.32	0.84	1.72
VIT_14s0108g00740	0.44	0.65	0.67	0.17	0.54	0.75	1.00	0.09	1.84	0.78	0.29	-0.42	0.62	0.14	1.09	0.19	0.44	0.04	0.62	0.75	0.50

## Appendix II

VIT_14s0219g00230	-0.27	0.03	1.14	0.78	0.33	-0.41	1.14	-0.05	2.58	1.12	-0.03	0.31	1.75	0.38	1.27	0.46	0.19	0.86	0.37	0.69	1.64
VIT_15s0048g01750	-0.05	0.30	1.01	-0.29	-0.63	0.43	1.09	-0.12	2.63	0.55	-0.08	-0.45	0.68	-0.02	1.04	-0.23	0.18	-0.01	0.53	0.97	0.26
VIT_17s0000g02470	-0.39	0.33	1.51	0.48	-0.25	0.44	1.36	0.12	2.23	0.69	0.04	0.18	0.83	0.80	1.04	0.64	0.21	0.31	0.65	1.24	1.14
VIT_17s0000g03550	-0.47	-0.07	1.19	0.40	-0.61	-0.38	1.07	0.14	1.73	1.05	-0.02	0.44	0.49	0.40	1.34	0.32	0.28	-0.24	0.24	0.78	0.92
VIT_17s0000g03750	-0.39	0.17	0.28	0.81	-0.18	0.36	0.51	0.65	0.97	-0.31	0.18	0.71	0.88	0.30	-0.10	1.15	0.39	0.46	0.34	0.16	1.05
VIT_17s0000g04470	0.34	0.00	0.23	0.61	0.54	0.12	0.24	0.58	-1.62	0.02	0.03	0.14	-0.49	-0.44	0.35	0.66	0.93	-0.19	-0.19	0.46	0.36
VIT_17s0000g05070	-0.10	-0.21	-0.65	0.33	0.29	-0.09	-0.39	0.00	-1.23	-0.22	-0.31	-0.09	-0.40	-0.35	-0.45	-0.17	0.22	-0.27	-0.62	-0.56	-0.11
VIT_17s0000g05570	-0.60	0.25	1.02	-0.08	-0.23	-0.16	0.85	-0.37	2.29	0.94	-0.26	0.18	1.21	0.39	0.63	0.06	0.13	0.16	0.72	0.55	0.19
VIT_17s0000g09190	0.20	-0.76	-0.02	1.07	0.36	-0.29	-0.18	0.45	-1.84	-0.25	0.22	0.14	-0.56	-0.14	0.61	0.92	0.53	-0.18	-0.54	0.07	0.38
VIT_17s0000g09310	-0.36	-0.03	-0.45	0.33	-0.65	-0.19	-0.26	0.12	-1.26	-0.68	-0.23	1.18	-0.33	-0.47	-0.50	0.33	0.87	-1.17	-0.35	-0.17	0.41
VIT_17s0000g09470	-0.04	0.11	-0.36	-0.07	-0.12	0.33	-0.44	-0.26	-0.20	-0.46	-0.23	-0.09	-0.23	0.07	0.21	0.66	0.41	0.23	-0.27	-0.04	0.13
VIT_17s0053g00990	0.14	0.83	0.94	0.27	-0.26	1.05	1.30	0.64	2.09	0.57	0.66	-0.50	1.17	0.15	1.11	1.13	-0.09	0.30	0.68	1.28	0.60
VIT_18s0001g03160	-0.43	-0.46	-1.05	-0.50	0.02	-0.16	-0.77	-0.41	-1.43	-0.32	-0.32	0.08	-0.51	0.05	-0.82	-0.55	-0.05	-0.48	0.17	-0.91	-0.22
VIT_18s0001g03540	0.03	-0.21	-0.29	-0.03	0.28	0.27	-0.30	-0.08	-0.48	-0.33	-0.69	-0.02	-0.80	0.06	-0.85	0.26	0.34	0.11	0.02	-0.25	0.27
VIT_18s0001g04890	-0.43	-0.16	-0.65	-0.83	-0.37	-0.01	-0.75	-0.79	-0.37	-0.74	-0.69	-0.41	-0.17	0.05	-0.32	-0.29	-0.24	-0.22	0.19	-0.57	-0.36
VIT_18s0001g05060	-0.24	-0.17	1.84	0.22	-0.60	-0.31	1.97	0.03	2.05	0.59	-0.38	0.26	0.64	-0.68	1.35	1.36	0.05	0.70	-0.23	1.42	0.86
VIT_18s0001g07340	-1.80	-1.04	1.30	0.38	-1.05	-0.72	1.71	0.37	5.12	0.98	0.00	0.57	1.84	0.56	1.53	0.18	0.30	-0.03	0.62	1.31	1.17
VIT_18s0001g07460	-0.49	0.12	0.61	0.39	0.37	-0.04	0.53	0.27	0.34	0.34	-0.09	-0.37	0.42	0.31	0.71	0.28	0.31	0.09	0.45	0.67	0.29
VIT_18s0001g09230	0.10	-0.26	0.48	-0.08	-0.17	0.10	0.70	-0.18	-0.47	0.15	-0.74	0.15	-0.73	-0.82	1.44	-0.08	0.44	-0.04	-0.82	0.85	-0.06
VIT_18s0001g09400	-0.12	0.62	1.53	0.69	-0.60	0.42	1.17	0.45	3.22	0.51	0.38	0.26	1.01	-0.04	0.96	0.87	0.28	0.27	0.93	0.89	0.56
VIT_18s0001g09510	0.25	-0.05	-0.19	0.28	0.59	-0.19	-0.12	0.08	-1.12	0.19	-0.21	0.08	-0.39	-0.27	0.07	-0.26	0.22	-0.05	-0.35	-0.08	-0.57
VIT_18s0001g09910	-0.29	0.23	0.21	0.61	0.14	0.29	-0.08	0.46	-0.81	-0.35	0.39	-0.53	0.36	-0.52	-0.58	0.56	-0.13	-0.05	-0.44	-0.04	0.15
VIT_18s0001g10130	0.73	-0.53	-0.17	0.61	0.95	-0.21	-0.04	0.37	-4.09	-1.13	-0.73	-0.64	-2.21	-0.17	-0.71	0.27	0.86	-0.42	-0.04	-0.17	0.62
VIT_18s0001g10610	0.40	-0.10	-0.58	-0.17	-0.02	-0.26	-0.33	-0.25	-1.26	-0.40	-0.13	-0.66	-0.17	0.22	-0.22	-0.26	0.13	-0.31	-0.02	-0.15	0.38
VIT_18s0001g10640	0.56	-0.71	-0.45	0.06	0.76	-0.40	-0.33	0.08	-3.87	-0.70	-0.58	-1.03	-2.15	-0.28	-0.71	-0.29	0.08	-0.74	-0.43	-0.37	0.07
VIT_19s0015g00270	-0.13	5.73	-1.48	-0.13	0.02	5.78	-1.43	-0.28	-1.97	-1.15	-0.52	0.80	-0.28	-0.91	-1.25	-0.15	0.22	-0.24	-1.24	-0.93	-0.87
VIT_19s0015g00490	-0.55	-0.10	0.80	-0.56	-0.56	0.10	0.39	-0.77	2.60	0.21	-0.76	-0.21	0.52	-0.73	0.78	-0.81	-0.13	-0.06	-0.19	0.35	-0.37
VIT_19s0015g01230	-0.42	0.08	0.76	-1.15	-0.58	0.05	0.40	-1.02	2.16	0.30	-0.77	-0.25	0.43	-0.22	0.72	-0.65	-0.21	-0.10	0.30	0.36	-0.51
vGRF4	1.72	2.14	1.96	1.70	1.54	2.34	1.84	1.96	2.08	1.41	1.51	1.49	1.93	1.35	1.52	2.19	1.85	0.88	1.77	1.94	1.86

Online resource 7 continued

Time point BBCH57 compactly clustered clones

Genes/Samples	En777.B.15	En777.B.16	En777.B.17	En777.H.15	En777.H.16	En777.H.17	RKCH.B.15	RKCH.B.16	RKCH.B.17	RKCH.H.15	RKCH.H.16	RKCH.H.17	RKCH.P.15	RKCH.P.16	RKCH.P.17	RKCL.H.15	RKCL.H.16	RKCL.H.17	RKCL.P.15	RKCL.P.16	RKCL.P.17
VIT_00s0313g00070	0.10	-0.15	-0.37	0.40	0.38	0.44	0.02	-0.10	-0.02	0.29	0.03	-0.31	0.35	-0.34	0.22	0.18	0.07	-0.15	0.54	0.11	0.55
VIT_01s0010g01810	-0.85	-0.73	-1.13	0.71	0.23	0.33	-1.06	-0.71	-1.00	0.08	-0.13	-0.03	-0.34	0.13	4.33	0.83	0.67	-0.04	-1.06	0.27	5.42
VIT_01s0010g02430	0.16	-0.18	-0.06	1.94	0.82	-0.31	0.03	-0.60	-0.35	0.82	0.58	-1.12	-1.09	0.19	0.27	1.23	0.42	-1.20	-0.08	0.45	-0.06
VIT_01s0011g06410	0.74	-0.07	0.09	0.82	0.35	-0.24	0.66	0.11	-0.15	0.46	0.28	-0.20	-0.01	0.09	0.17	0.57	0.38	-0.10	0.27	0.29	-0.05
VIT_01s0026g02030	-0.07	0.03	-0.45	-0.35	-0.18	-0.04	0.61	-0.18	-0.12	-0.26	-0.57	-0.04	-0.17	-0.47	-0.11	-0.57	-0.35	-0.11	-0.16	0.10	0.69
VIT_01s0127g00260	0.63	-0.32	-0.44	1.20	0.97	0.52	0.71	-0.43	-0.22	0.52	0.51	-0.31	-0.69	0.17	0.05	0.91	0.85	-0.27	0.22	0.51	0.74
VIT_01s0127g00710	7.48	11.99	12.06	-0.37	0.45	-3.86	8.28	11.91	12.04	-0.67	-0.26	0.62	19.12	12.31	18.35	-0.95	-0.11	0.46	18.48	12.62	18.81
VIT_01s0127g00870	1.06	-0.30	-0.09	1.96	1.50	0.47	0.52	-0.14	-0.06	1.42	1.12	-0.66	-0.87	-0.10	0.36	2.01	1.31	-0.16	-0.44	-0.04	0.14
VIT_01s0146g00400	0.24	-0.26	0.36	1.16	0.37	-0.24	0.00	-0.34	0.00	0.99	0.06	-0.59	-0.43	0.32	0.39	1.26	0.11	-0.50	0.32	0.45	0.01
VIT_01s0146g00480	0.22	0.22	-0.20	0.31	0.39	0.57	0.82	-0.04	-0.29	0.34	0.57	0.43	1.12	-0.26	-1.05	-0.24	0.56	-0.01	1.09	0.04	-0.97
VIT_02s0012g00990	0.03	11.84	6.18	0.08	-0.20	0.09	0.21	11.54	5.71	0.14	-0.54	-0.04	23.95	19.73	12.17	0.39	-0.31	0.21	23.85	19.77	12.33
VIT_02s0012g01380	-0.41	0.13	-0.37	-0.45	-0.14	0.36	0.09	0.09	-0.44	-0.50	-0.66	0.35	1.50	0.08	-0.51	-0.99	-0.80	0.02	1.43	0.44	0.19
VIT_02s0025g03180	4.60	-0.04	0.35	-0.16	0.29	-0.15	4.59	-0.10	0.21	0.30	0.38	0.37	0.03	0.04	0.04	0.19	0.48	0.29	0.29	0.19	0.15
VIT_02s0025g04340	-0.70	0.47	0.48	-0.77	-0.87	-0.26	-0.03	0.54	0.91	0.14	-0.48	-0.20	2.24	-0.44	-1.75	-1.55	-0.93	-0.37	0.90	-1.11	-1.83
VIT_02s0025g04660	-0.15	0.32	-0.60	-0.56	-0.09	0.48	0.15	0.15	-0.01	-0.19	-0.42	0.34	1.26	-0.30	-0.02	-0.91	-0.78	0.24	0.88	-0.30	-0.20
VIT_02s0025g04720	0.76	-0.68	5.77	2.12	0.80	-0.06	0.69	-0.69	6.42	1.20	0.60	-0.63	-1.42	0.61	0.65	2.36	1.15	-0.73	-0.56	0.73	1.22
VIT_02s0154g00320	-0.13	0.04	-0.20	0.36	1.13	0.20	-0.46	-0.62	-1.02	1.20	0.24	-1.48	-2.06	0.50	0.16	1.09	0.87	-0.05	-1.35	1.01	-0.03
VIT_02s0154g00380	0.10	-0.19	-1.12	-1.41	-0.04	-0.18	2.04	0.09	-0.11	-0.89	0.16	0.45	3.02	-0.65	-0.32	-0.81	0.47	0.68	2.44	-0.04	0.86
VIT_02s0241g00030	-0.17	-0.10	-0.09	0.39	0.60	0.13	0.26	0.11	0.08	0.16	0.16	-0.18	0.07	0.12	0.22	-0.01	0.41	-0.33	0.25	0.20	0.41
VIT_03s0097g00700	1.20	1.44	0.30	1.35	-0.09	0.39	1.21	0.11	1.46	0.65	-0.36	-0.26	1.93	-0.37	0.48	0.16	-1.29	-0.35	3.10	0.70	0.84
VIT_04s0008g00180	0.58	-0.17	-0.06	0.99	0.63	0.32	0.34	-0.42	-0.30	0.23	-0.09	-0.68	-0.68	-0.04	0.03	0.60	0.36	-0.42	0.14	0.21	0.16
VIT_04s0008g00370	0.17	0.00	-0.28	-0.53	-0.11	0.29	0.22	0.26	-0.05	0.51	0.61	0.99	0.96	-0.20	-0.15	-0.46	0.13	0.34	0.54	0.19	0.15
VIT_04s0008g01100	0.22	0.36	0.03	-0.06	0.07	0.21	0.62	0.09	-0.19	-0.53	-0.36	0.53	1.45	0.39	-0.36	-0.26	0.02	0.46	1.06	0.57	-0.35

## Appendix II

VIT_04s0008g01810	0.32	0.25	0.39	0.87	0.30	0.36	0.13	0.11	0.19	0.94	0.37	-0.12	-0.19	0.47	0.39	0.87	0.53	0.07	0.19	0.32	0.37
VIT_04s0008g01910	0.52	-0.30	0.00	0.73	0.35	-0.16	0.28	-0.31	-0.46	0.34	0.16	-0.72	-0.68	0.28	0.59	1.03	0.71	-0.15	-0.17	0.28	0.25
VIT_04s0008g02920	0.31	-0.79	-0.16	1.82	0.85	0.81	0.49	-0.29	-0.07	0.62	0.01	-0.52	-0.03	0.27	0.45	1.41	0.45	0.24	0.62	0.42	0.71
VIT_04s0008g04050	0.62	-0.11	0.59	1.14	1.52	2.01	0.22	-0.07	-0.22	0.33	0.93	0.96	-0.82	0.32	-0.03	0.71	0.69	0.46	-0.02	0.67	-0.13
VIT_04s0008g04200	3.14	-0.32	0.22	1.28	0.87	0.45	3.02	-0.47	-0.44	0.24	0.39	-0.67	-0.27	0.21	0.19	0.89	0.58	-0.23	0.17	0.28	0.11
VIT_04s0008g05150	0.75	-0.20	0.49	0.61	0.81	0.05	0.91	-0.31	-0.20	-0.39	0.44	-0.48	0.08	0.30	0.15	0.67	0.66	-0.22	0.13	0.68	0.10
VIT_04s0008g05770	-0.01	0.73	-0.19	-0.62	-0.23	0.60	-0.19	0.36	-0.43	-0.11	-0.32	0.68	1.36	-0.40	-0.30	-0.83	-0.35	0.64	0.29	-0.33	-0.20
VIT_04s0008g05830	0.45	-0.21	0.25	1.08	0.66	0.06	0.27	-0.34	-0.13	0.72	0.74	-0.49	-1.11	0.50	0.45	1.35	1.13	-0.33	-0.32	0.29	0.29
VIT_04s0008g06670	0.32	0.05	0.05	1.31	0.44	-0.39	0.15	-0.47	-0.46	0.59	0.76	-0.90	-1.28	0.07	0.22	1.06	0.53	-1.18	-0.46	0.15	-0.25
VIT_04s0023g03070	0.11	-0.18	-0.54	0.75	0.99	0.54	0.30	-0.08	-0.18	0.57	0.43	-0.23	-0.17	-0.13	0.12	0.37	0.58	-0.19	0.24	-0.05	0.66
VIT_04s0069g00790	0.07	4.21	-0.46	-0.16	0.06	0.34	0.67	4.24	-0.16	-0.25	-0.30	0.46	0.51	0.03	-0.33	-0.27	-0.03	0.30	0.55	0.20	0.09
VIT_04s0079g00260	0.11	-0.11	-0.18	0.68	0.60	0.27	0.47	-0.38	-0.22	-0.37	-0.08	-0.58	-0.20	0.04	0.26	0.27	0.12	-0.38	0.71	0.39	0.28
VIT_08s0007g01310	-0.56	-0.25	-0.46	0.11	-0.51	0.48	-0.09	0.58	-0.47	-0.11	-0.34	-0.18	0.16	-0.19	-0.68	-0.43	-0.85	-0.50	-0.08	-0.04	-0.41
VIT_08s0007g01320	0.03	-0.13	-0.39	0.23	-0.54	0.57	0.65	0.56	-0.58	0.17	-0.35	-0.04	0.54	-0.03	-0.69	-0.33	-0.74	-0.33	0.45	0.04	-0.50
VIT_08s0007g01360	-0.68	0.31	0.04	-0.99	-0.28	-0.05	-0.03	0.30	-0.14	-0.20	-0.73	0.12	0.72	-0.55	-0.22	-1.32	-0.72	-0.02	0.12	-0.44	-0.15
VIT_08s0007g01370	-0.33	-0.48	0.55	-0.64	0.66	-0.66	0.40	-0.14	-0.01	0.05	-0.01	-0.75	1.22	0.19	-0.25	-0.08	0.19	-1.10	0.84	0.49	-0.79
VIT_08s0040g01710	0.34	-0.37	-0.21	0.95	0.43	0.07	0.17	-0.38	-0.47	0.76	0.33	-0.19	-0.71	0.24	-0.02	1.01	0.54	-0.12	-0.34	0.29	-0.38
VIT_08s0058g00930	-0.24	0.14	-0.16	-0.84	0.22	0.14	0.28	0.43	0.48	-0.57	-0.58	0.21	0.58	0.00	0.24	-1.12	-0.31	-0.01	0.60	0.39	0.79
VIT_08s0058g00990	0.50	0.07	0.34	0.95	0.48	0.38	0.08	-0.11	0.05	0.24	-0.29	0.37	0.88	0.12	-0.05	-0.04	-0.02	-0.37	1.54	0.42	0.47
VIT_11s0016g03710	0.24	-0.28	-0.20	1.00	0.51	0.35	-0.14	-0.73	-0.30	0.30	-0.32	-0.86	-0.31	0.01	0.66	0.56	0.00	-0.45	0.42	0.40	0.85
VIT_12s0059g00190	0.05	-0.58	-0.55	1.01	0.65	0.10	0.07	-0.52	-1.20	0.73	0.38	-0.34	-0.82	0.76	-0.18	1.31	0.59	-0.34	-0.49	0.75	0.19
VIT_14s0066g01060	3.34	6.72	-1.34	0.27	0.07	-0.04	3.60	6.69	0.21	-0.68	-0.89	-0.29	-0.93	0.15	-0.08	-0.18	0.19	0.00	0.29	0.36	0.95
VIT_14s0066g01390	0.29	0.14	0.09	0.25	-0.14	0.30	0.59	0.08	-0.15	0.23	-0.07	0.34	1.00	0.27	-0.21	-0.07	-0.35	0.12	0.59	0.38	-0.22
VIT_14s0083g00410	-0.65	0.36	-0.20	-0.83	1.56	0.68	0.62	0.46	0.16	-0.45	1.39	0.53	1.35	0.36	-0.40	-0.63	-0.56	-0.22	0.85	0.65	0.44
VIT_14s0108g00700	0.99	-0.20	-0.83	1.56	0.68	0.62	0.46	0.16	-0.45	1.39	0.53	0.17	-0.68	0.24	1.32	2.29	0.36	0.38	-0.21	-0.04	0.80
VIT_14s0108g00740	0.71	0.33	0.50	0.43	0.40	0.00	0.60	0.23	0.30	0.89	0.21	-0.37	-0.43	0.50	0.48	0.93	0.71	-0.11	-0.07	0.46	0.05
VIT_14s0219g00230	1.25	-0.09	-0.10	1.43	0.68	-0.10	-0.16	-0.50	0.07	1.35	0.57	-1.17	-1.21	0.21	0.53	1.56	0.87	-0.27	0.40	1.12	0.33
VIT_15s0048g01750	0.39	-0.04	0.12	1.29	0.56	-0.28	0.20	-0.19	-0.07	0.95	0.79	-0.79	-1.12	0.47	0.42	1.59	0.91	-0.63	-0.41	0.49	0.04
VIT_17s0000g02470	0.39	-0.13	-0.21	1.20	0.95	0.12	0.36	-0.16	-0.14	0.86	0.48	-0.22	-0.55	0.31	0.53	1.39	0.90	-0.43	0.09	0.55	0.62

## Appendix II

VIT_17s0000g03550	0.48	-0.15	0.06	1.08	1.12	0.18	0.17	-0.21	-0.42	0.06	0.22	-1.02	-0.54	0.09	0.36	0.91	0.77	-0.50	0.43	0.33	0.46
VIT_17s0000g03750	0.14	-0.41	-0.27	0.80	0.42	0.70	0.24	-0.39	-0.17	0.10	-0.40	0.02	0.19	0.46	-0.17	0.43	-0.23	0.03	0.46	0.54	0.39
VIT_17s0000g04470	-0.26	0.12	-0.31	-0.53	0.45	0.51	0.16	0.30	-0.22	-0.35	0.22	0.36	1.18	0.02	-0.15	-0.12	0.10	0.07	1.08	0.22	-0.13
VIT_17s0000g05070	0.00	0.26	0.03	-0.23	-0.12	0.35	0.03	0.17	0.01	0.09	-0.49	0.51	1.22	-0.05	-0.35	-0.35	-0.01	0.15	0.59	-0.02	-0.44
VIT_17s0000g05570	0.59	-0.34	0.10	1.34	0.44	-0.44	0.54	-0.52	-0.37	0.80	0.39	-0.92	-0.84	0.48	0.91	1.55	0.52	-0.38	-0.10	0.52	0.20
VIT_17s0000g09190	-0.25	0.11	-0.25	-0.44	-0.06	0.52	0.05	0.41	-0.01	-0.49	-0.51	1.09	1.46	-0.33	-0.62	-0.87	-0.20	0.74	1.08	0.32	0.08
VIT_17s0000g09310	0.20	0.26	-0.27	-0.11	0.12	0.46	1.16	0.01	-0.54	-0.52	-0.59	0.24	1.51	0.09	-0.56	-0.58	-0.04	0.34	1.45	0.60	-0.16
VIT_17s0000g09470	-0.34	0.15	-0.03	-0.24	-0.05	-0.03	-0.05	0.00	-0.02	0.25	-0.42	-0.31	1.26	0.18	-0.25	-0.49	-0.05	-0.41	0.93	0.45	0.02
VIT_17s0053g00990	0.78	0.14	0.23	1.11	0.57	-0.10	0.81	-0.25	0.74	1.20	0.90	0.19	-0.86	0.59	0.49	0.96	1.49	0.04	-0.25	0.29	0.52
VIT_18s0001g03160	-0.35	0.35	0.08	-0.37	-0.22	-0.03	-0.02	0.11	0.08	-0.37	-0.39	0.02	1.50	0.15	0.19	-0.84	-0.41	-0.08	0.64	0.00	0.17
VIT_18s0001g03540	0.32	0.03	-0.41	-0.19	-0.15	-0.27	0.47	0.33	0.11	0.17	-0.39	0.01	0.81	-0.05	0.08	-0.71	-0.55	0.17	0.51	-0.32	0.33
VIT_18s0001g04890	0.06	0.04	-0.10	-0.33	-0.32	-0.60	0.31	-0.01	0.04	0.00	-0.42	-0.13	0.12	0.18	0.23	-0.24	-0.37	-0.46	0.27	0.06	0.21
VIT_18s0001g05060	0.60	-0.32	-0.68	1.40	1.21	0.46	0.49	-0.40	-0.07	0.57	0.55	-0.57	-0.71	0.03	-0.54	1.27	1.32	-0.56	0.11	0.34	0.15
VIT_18s0001g07340	0.26	-0.53	-1.09	3.04	1.51	-0.20	-0.15	-1.23	-0.64	1.32	0.58	-1.28	-2.00	0.79	0.45	3.09	1.16	-0.51	-0.18	1.08	0.47
VIT_18s0001g07460	0.29	0.28	-0.08	0.43	0.59	0.28	0.14	-0.27	-0.26	0.40	0.13	-0.41	-0.22	-0.17	0.39	0.44	0.63	-0.28	0.46	0.39	0.64
VIT_18s0001g09230	-0.34	-0.11	-0.24	-0.12	0.07	-0.08	-0.16	0.31	-0.21	0.03	0.32	-0.08	0.67	-0.56	-1.04	-0.41	0.06	-0.57	0.67	-0.10	-0.73
VIT_18s0001g09400	0.36	-0.57	-0.50	2.44	0.85	0.13	0.14	-0.53	-0.32	1.42	0.76	-0.60	-0.62	0.64	0.97	2.52	1.04	-0.44	0.06	0.75	1.29
VIT_18s0001g09510	0.06	0.39	-0.01	-0.57	-0.09	0.11	0.37	0.31	-0.27	-0.39	-0.20	0.32	0.78	-0.09	-0.54	-0.77	-0.20	0.14	0.54	-0.08	-0.36
VIT_18s0001g09910	0.18	0.20	0.08	-0.24	0.16	0.23	0.40	-0.15	0.67	-0.24	0.13	0.84	0.37	0.35	-0.21	-0.44	0.16	0.39	0.47	0.59	0.12
VIT_18s0001g10130	-0.73	0.19	-0.67	-1.67	-0.03	-0.64	0.66	0.97	0.28	-0.39	-0.13	0.59	2.35	-0.92	-0.15	-1.78	0.05	0.21	1.26	-0.28	0.47
VIT_18s0001g10610	0.11	0.50	0.10	-0.69	-0.11	-0.35	0.00	0.46	-0.10	-0.10	-0.08	0.12	0.66	0.00	0.13	-0.57	-0.13	0.07	0.48	0.04	-0.34
VIT_19s0015g00270	-3.63	0.38	-0.53	-1.76	0.08	-0.34	0.20	0.96	0.42	-0.82	-0.08	0.28	1.31	-1.14	-0.01	-2.00	-0.49	-0.19	0.29	-0.67	0.22
VIT_19s0015g00490	-0.77	0.20	6.02	-0.70	-0.51	0.32	0.15	-0.02	5.86	-0.17	-0.81	0.55	1.82	-0.08	-1.13	-1.09	-0.97	0.18	0.69	0.16	-0.36
VIT_19s0015g01230	0.23	-0.09	-0.07	1.83	0.50	-0.54	-0.18	-0.52	-0.68	1.14	0.59	-0.95	-1.13	0.36	0.23	1.42	0.40	-1.14	-0.27	0.53	-0.60
VIT_19s0015g01230	0.24	0.10	0.14	1.45	0.43	-0.64	0.12	-0.36	-0.54	0.75	0.56	-1.09	-1.01	0.21	0.70	1.10	0.49	-1.23	-0.49	0.17	-0.09
VvGRF4	0.31	-0.10	0.17	0.05	0.06	-0.05	0.55	-0.23	0.26	0.40	0.18	0.06	0.56	0.37	0.27	0.29	0.05	-0.36	0.97	0.54	0.32

## Appendix II

### Online resource 7 continued

#### Time point BBCH57 mixed berry clones

Genes/Samples	Fr1801.B.15	Fr1801.B.16	Fr1801.B.17	Fr1801.H.16	Fr1801.H.17
<i>VIT_00s0313g00070</i>	-0.08	0.00	-0.09	0.40	0.25
<i>VIT_01s0010g01810</i>	-0.88	-1.05	-2.17	0.34	0.09
<i>VIT_01s0010g02430</i>	0.50	-0.43	0.12	1.24	-0.98
<i>VIT_01s0011g06410</i>	0.53	-0.17	0.44	0.68	-0.11
<i>VIT_01s0026g02030</i>	0.36	0.06	0.20	-0.06	-0.04
<i>VIT_01s0127g00260</i>	1.00	-0.40	-0.06	1.12	0.01
<i>VIT_01s0127g00710</i>	7.75	11.94	12.47	-0.11	0.57
<i>VIT_01s0127g00870</i>	1.04	0.01	0.32	1.74	-0.22
<i>VIT_01s0146g00400</i>	0.41	-0.43	0.09	0.59	-0.30
<i>VIT_01s0146g00480</i>	0.50	0.03	0.16	0.66	0.12
<i>VIT_02s0012g00990</i>	0.22	11.70	6.33	-0.36	0.12
<i>VIT_02s0012g01380</i>	-0.10	0.07	-0.38	-0.61	0.46
<i>VIT_02s0025g03180</i>	4.32	-0.41	0.42	0.01	-0.25
<i>VIT_02s0025g04340</i>	-0.83	0.13	0.60	-0.15	1.34
<i>VIT_02s0025g04660</i>	0.04	0.23	-0.13	-0.80	0.45
<i>VIT_02s0025g04720</i>	1.14	-0.65	6.79	0.82	-0.98
<i>VIT_02s0154g00320</i>	1.18	-0.02	-0.13	1.34	-0.05
<i>VIT_02s0154g00380</i>	0.65	0.67	-0.72	0.50	-0.31
<i>VIT_02s0241g00030</i>	0.05	-0.11	0.35	0.52	0.29
<i>VIT_03s0097g00700</i>	0.95	0.36	0.44	0.03	0.54
<i>VIT_04s0008g00180</i>	0.36	-0.54	0.10	0.96	-0.32
<i>VIT_04s0008g00370</i>	0.37	-0.45	-0.26	0.32	1.06
<i>VIT_04s0008g01100</i>	0.53	0.06	0.08	0.13	-0.01
<i>VIT_04s0008g01810</i>	0.26	0.10	0.43	-0.14	0.04
<i>VIT_04s0008g01910</i>	0.23	-0.47	0.11	0.96	-0.39
<i>VIT_04s0008g02920</i>	0.66	0.17	-0.20	1.08	0.44
<i>VIT_04s0008g04050</i>	-0.25	0.22	0.76	2.08	1.06
<i>VIT_04s0008g04200</i>	3.20	-0.19	0.11	1.38	-0.08
<i>VIT_04s0008g05150</i>	0.99	0.02	0.40	0.85	-0.39
<i>VIT_04s0008g05770</i>	-0.34	0.12	-0.08	-0.17	1.00
<i>VIT_04s0008g05830</i>	0.40	-0.57	0.16	1.05	-0.29
<i>VIT_04s0008g06670</i>	0.66	-0.25	0.18	1.24	-0.92
<i>VIT_04s0023g03070</i>	0.19	-0.22	-0.15	1.08	0.42
<i>VIT_04s0069g00790</i>	0.11	3.94	-0.22	0.02	0.08
<i>VIT_04s0079g00260</i>	0.49	-0.25	0.00	0.76	0.20
<i>VIT_08s0007g01310</i>	-1.31	-0.01	0.00	-0.18	0.65
<i>VIT_08s0007g01320</i>	-0.56	0.08	0.13	-0.11	0.71
<i>VIT_08s0007g01360</i>	-0.18	0.39	-0.09	-0.56	0.19
<i>VIT_08s0007g01370</i>	0.49	-0.48	0.61	0.30	-0.79

## Appendix II

<i>VIT_08s0040g01710</i>	0.15	-0.63	-0.16	0.71	-0.16
<i>VIT_08s0058g00930</i>	0.09	0.31	0.26	-0.37	0.15
<i>VIT_08s0058g00990</i>	0.85	-0.04	0.30	0.49	0.88
<i>VIT_11s0016g03710</i>	0.34	-0.07	-0.03	0.92	-0.02
<i>VIT_12s0059g00190</i>	0.44	-0.46	-0.40	0.72	-0.23
<i>VIT_14s0066g01060</i>	3.33	6.85	-1.37	0.24	0.04
<i>VIT_14s0066g01390</i>	0.35	-0.11	0.59	-0.32	0.26
<i>VIT_14s0083g00410</i>	-0.06	-0.32	-0.09	-1.08	0.05
<i>VIT_14s0108g00700</i>	0.44	0.08	-0.07	0.77	-0.14
<i>VIT_14s0108g00740</i>	0.53	-0.07	0.21	1.07	-0.10
<i>VIT_14s0219g00230</i>	0.66	-0.96	-0.64	2.16	-0.36
<i>VIT_15s0048g01750</i>	0.33	-0.27	0.27	1.00	-0.71
<i>VIT_17s0000g02470</i>	0.42	-0.52	-0.24	0.98	-0.26
<i>VIT_17s0000g03550</i>	0.27	-0.21	-0.04	1.85	0.12
<i>VIT_17s0000g03750</i>	0.46	-0.22	0.21	-0.09	0.37
<i>VIT_17s0000g04470</i>	-0.57	-0.29	0.08	-0.24	0.29
<i>VIT_17s0000g05070</i>	0.00	0.15	-0.01	-0.45	0.69
<i>VIT_17s0000g05570</i>	0.85	-0.51	-0.27	1.21	-1.44
<i>VIT_17s0000g09190</i>	-0.13	-0.22	-0.60	-0.22	0.50
<i>VIT_17s0000g09310</i>	0.43	-0.46	-0.06	-0.39	0.47
<i>VIT_17s0000g09470</i>	0.20	-0.02	0.11	-0.21	-0.06
<i>VIT_17s0053g00990</i>	0.75	-0.25	0.54	0.63	-0.25
<i>VIT_18s0001g03160</i>	-0.19	0.02	0.09	-0.98	0.29
<i>VIT_18s0001g03540</i>	0.44	0.37	0.41	-0.49	0.81
<i>VIT_18s0001g04890</i>	0.11	-0.21	0.27	-0.70	-0.30
<i>VIT_18s0001g05060</i>	0.44	-0.47	-0.42	1.29	-0.50
<i>VIT_18s0001g07340</i>	0.48	-1.13	-0.62	2.39	-0.59
<i>VIT_18s0001g07460</i>	0.59	-0.43	-0.04	0.81	0.22
<i>VIT_18s0001g09230</i>	-0.20	-0.03	-0.16	0.64	0.33
<i>VIT_18s0001g09400</i>	0.70	-0.47	0.20	0.71	-1.13
<i>VIT_18s0001g09510</i>	0.18	0.01	-0.05	-0.08	0.32
<i>VIT_18s0001g09910</i>	0.16	-0.49	0.46	-0.37	0.04
<i>VIT_18s0001g10130</i>	-0.04	0.19	0.09	-0.65	0.47
<i>VIT_18s0001g10610</i>	-0.24	-0.06	0.06	-0.49	0.05
<i>VIT_18s0001g10640</i>	-0.20	0.75	-0.07	0.03	0.64
<i>VIT_19s0015g00270</i>	0.24	0.16	6.37	-0.90	0.64
<i>VIT_19s0015g00490</i>	0.41	-0.51	0.18	1.09	-0.90
<i>VIT_19s0015g01230</i>	0.47	-0.20	0.20	0.92	-1.46
<i>VvGRF4</i>	0.38	-0.29	0.54	-0.32	-0.33

## Appendix II

### Online resource 7 continued

#### Time point BBCH57 significance level for differential expression

Genes/samples	average expression level	F-value	p-value	adjusted p-value
VIT_00s0313g00070	5.52	0.933	6.00E-01	7.67E-01
VIT_01s0010g01810	9.87	0.097	1.00E+00	1.00E+00
VIT_01s0010g02430	7.99	2.144	8.26E-05	2.80E-04
VIT_01s0011g06410	7.70	0.986	5.04E-01	6.78E-01
VIT_01s0026g02030	9.06	0.964	5.43E-01	7.18E-01
VIT_01s0127g00260	6.86	1.976	4.17E-04	1.30E-03
VIT_01s0127g00710	7.63	0.293	1.00E+00	1.00E+00
VIT_01s0127g00870	5.20	3.303	4.41E-10	4.92E-09
VIT_01s0146g00400	5.74	1.346	7.66E-02	1.33E-01
VIT_01s0146g00480	5.29	0.934	5.98E-01	7.67E-01
VIT_02s0012g00990	8.15	0.623	9.74E-01	1.00E+00
VIT_02s0012g01380	5.48	2.505	2.14E-06	1.04E-05
VIT_02s0025g03180	5.25	0.080	1.00E+00	1.00E+00
VIT_02s0025g04340	5.54	1.224	1.65E-01	2.47E-01
VIT_02s0025g04660	5.32	1.266	1.28E-01	1.96E-01
VIT_02s0025g04720	3.15	0.158	1.00E+00	1.00E+00
VIT_02s0154g00320	2.86	1.831	1.59E-03	4.15E-03
VIT_02s0154g00380	3.80	1.435	4.14E-02	8.17E-02
VIT_02s0241g00030	3.31	0.517	9.96E-01	1.00E+00
VIT_03s0097g00700	4.71	2.588	8.95E-07	5.37E-06
VIT_04s0008g00180	6.02	2.541	1.47E-06	8.19E-06
VIT_04s0008g00370	4.44	1.407	5.06E-02	9.62E-02
VIT_04s0008g01100	5.57	1.762	2.96E-03	7.21E-03
VIT_04s0008g01810	2.63	1.377	6.24E-02	1.11E-01
VIT_04s0008g01910	5.82	1.143	2.55E-01	3.76E-01
VIT_04s0008g02920	4.35	1.591	1.25E-02	2.63E-02
VIT_04s0008g04050	3.60	4.265	1.49E-14	3.87E-13
VIT_04s0008g04200	8.90	0.171	1.00E+00	1.00E+00
VIT_04s0008g05150	7.46	0.896	6.67E-01	8.39E-01
VIT_04s0008g05770	5.98	2.276	2.22E-05	8.67E-05
VIT_04s0008g05830	4.73	2.730	2.03E-07	1.44E-06
VIT_04s0008g06670	2.60	1.308	9.85E-02	1.63E-01
VIT_04s0023g03070	5.57	1.711	4.60E-03	1.09E-02
VIT_04s0069g00790	4.26	0.069	1.00E+00	1.00E+00
VIT_04s0079g00260	7.86	0.992	4.94E-01	6.75E-01
VIT_08s0007g01310	5.79	1.297	1.06E-01	1.71E-01
VIT_08s0007g01320	2.61	1.792	2.25E-03	5.67E-03
VIT_08s0007g01360	7.00	4.174	3.89E-14	7.59E-13
VIT_08s0007g01370	7.50	3.866	1.04E-12	1.62E-11
VIT_08s0040g01710	4.39	1.376	6.27E-02	1.11E-01
VIT_08s0058g00930	1.91	2.159	7.14E-05	2.53E-04

## Appendix II

VIT_08s0058g00990	3.75	1.953	5.21E-04	1.50E-03
VIT_11s0016g03710	6.54	3.139	2.57E-09	2.51E-08
VIT_12s0059g00190	7.06	0.484	9.98E-01	1.00E+00
VIT_14s0066g01060	9.41	0.569	9.89E-01	1.00E+00
VIT_14s0066g01390	4.81	1.861	1.21E-03	3.25E-03
VIT_14s0083g00410	7.25	0.638	9.68E-01	1.00E+00
VIT_14s0108g00700	6.43	1.936	6.09E-04	1.70E-03
VIT_14s0108g00740	8.73	0.439	9.99E-01	1.00E+00
VIT_14s0219g00230	6.51	2.132	9.27E-05	3.01E-04
VIT_15s0048g01750	2.72	2.509	2.05E-06	1.04E-05
VIT_17s0000g02470	2.91	2.489	2.52E-06	1.16E-05
VIT_17s0000g03550	4.98	2.439	4.21E-06	1.73E-05
VIT_17s0000g03750	6.69	1.294	1.07E-01	1.71E-01
VIT_17s0000g04470	6.70	1.558	1.63E-02	3.34E-02
VIT_17s0000g05070	4.27	0.751	8.82E-01	1.00E+00
VIT_17s0000g05570	3.41	2.478	2.83E-06	1.23E-05
VIT_17s0000g09190	8.78	2.708	2.54E-07	1.65E-06
VIT_17s0000g09310	4.22	1.034	4.20E-01	5.85E-01
VIT_17s0000g09470	6.52	0.368	1.00E+00	1.00E+00
VIT_17s0053g00990	2.39	2.925	2.54E-08	1.98E-07
VIT_18s0001g03160	1.96	3.567	2.57E-11	3.34E-10
VIT_18s0001g03540	2.05	2.261	2.57E-05	9.54E-05
VIT_18s0001g04890	4.77	1.331	8.48E-02	1.44E-01
VIT_18s0001g05060	6.51	1.959	4.92E-04	1.48E-03
VIT_18s0001g07340	6.09	1.390	5.70E-02	1.06E-01
VIT_18s0001g07460	6.63	1.053	3.88E-01	5.50E-01
VIT_18s0001g09230	3.87	1.290	1.10E-01	1.72E-01
VIT_18s0001g09400	3.41	3.064	5.76E-09	4.99E-08
VIT_18s0001g09510	8.57	1.433	4.19E-02	8.17E-02
VIT_18s0001g09910	1.47	1.075	3.53E-01	5.09E-01
VIT_18s0001g10130	4.80	5.684	7.00E-21	2.73E-19
VIT_18s0001g10610	7.66	1.594	1.22E-02	2.63E-02
VIT_18s0001g10640	7.87	0.265	1.00E+00	1.00E+00
VIT_19s0015g00270	5.08	0.128	1.00E+00	1.00E+00
VIT_19s0015g00490	4.70	1.661	7.00E-03	1.61E-02
VIT_19s0015g01230	1.96	1.598	1.18E-02	2.63E-02
VvGRF4	5.83	9.702	2.05E-36	1.60E-34

Online resource 7 continued Time point BBCH71 loosely clustered clones

Genes/Samples	Fr12L.B.16	Fr12L.B.17	Fr12L.H.16	Fr12L.H.17	Fr13L.B.16	Fr13L.B.17	Fr13L.H.16	Fr13L.H.17	Gm1_86.H.15	Gm1_86.H.16	Gm1_86.H.17	Gm1_86.P.15	Gm1_86.P.16	Gm1_86.P.17	WeM1.H.16	WeM1.H.17	WeM171.P.15	WeM171.P.16	WeM171.P.17	WeM242.H.16	WeM242.H.17
VIT_01s0010g01810	1.32	2.75	1.42	0.71	1.04	2.60	0.48	0.61	1.39	1.28	1.05	-0.41	-0.20	0.01	0.64	1.26	-0.41	0.15	-0.89	0.73	0.55
VIT_01s0010g02430	1.15	0.90	0.77	1.04	1.11	1.14	0.56	1.12	1.38	1.19	0.96	0.21	0.95	0.71	0.72	1.28	0.27	0.79	0.36	0.99	0.73
VIT_01s0011g06410	0.06	0.45	0.33	0.37	-0.09	0.59	0.16	0.37	0.62	0.06	0.27	-0.11	-0.08	0.63	0.46	0.37	0.05	-0.29	0.25	0.44	0.22
VIT_01s0025g02030	1.19	2.21	2.73	1.27	1.20	2.28	2.74	1.14	1.59	2.19	1.00	1.18	0.76	1.13	2.00	1.84	1.49	0.49	1.09	2.75	1.51
VIT_01s0127g00260	0.93	1.01	1.29	1.41	0.89	1.27	1.12	0.98	1.76	0.90	0.99	0.25	0.27	0.72	1.21	1.25	0.35	0.41	0.27	1.04	0.71
VIT_01s0127g00710	7.16	5.82	3.43	-0.56	7.06	5.95	3.45	-0.59	-1.49	3.08	-1.15	3.45	6.87	2.45	3.54	-0.47	3.66	7.78	3.79	3.36	-0.46
VIT_01s0127g00870	1.85	1.92	1.23	1.27	2.02	1.90	1.22	1.52	2.30	1.66	1.77	1.07	1.51	1.83	1.03	2.01	0.89	0.95	1.20	1.28	1.92
VIT_01s0146g00400	0.94	0.68	0.44	-0.07	0.81	0.87	0.13	-0.17	1.45	0.24	0.14	0.31	0.28	0.79	0.31	-0.10	0.00	0.09	0.57	0.34	-0.03
VIT_01s0146g00480	1.02	1.65	0.42	0.10	0.61	1.41	0.12	-0.29	0.65	-0.22	-0.54	-0.72	-0.08	0.35	0.48	0.28	-0.07	0.12	0.04	0.14	0.18
VIT_02s0012g00990	0.10	3.66	4.03	4.22	-0.12	3.99	3.77	3.81	-0.66	3.83	4.38	7.64	4.64	7.36	4.13	3.47	7.66	4.40	7.63	3.77	3.93
VIT_02s0012g01380	-0.13	-0.93	-0.49	-0.09	-0.35	-0.90	-0.73	-0.66	-1.21	-1.49	-0.96	-0.80	-0.79	-1.18	-0.48	-0.62	-0.40	0.04	-0.66	-0.99	-0.54
VIT_02s0012g01400	-0.20	-0.54	-0.49	0.02	-0.28	-0.84	-0.37	-0.41	-1.11	-1.07	-0.68	-0.43	-0.63	-0.44	-0.20	-0.10	-0.09	-0.09	-0.27	-0.53	-0.06
VIT_02s0025g03010	-0.01	-0.25	0.39	0.18	-0.28	-0.28	0.35	-0.02	-0.59	0.01	-0.49	0.31	-0.19	-0.38	0.60	-0.21	0.18	0.21	-0.24	0.33	-0.41
VIT_02s0025g03180	0.57	0.15	0.90	0.25	0.35	0.20	0.86	0.20	0.09	0.60	-0.70	0.27	0.07	0.04	1.05	0.31	0.26	0.34	0.42	1.16	0.07
VIT_02s0025g04340	-0.73	1.12	-1.61	-1.25	-1.10	0.74	-1.75	-0.68	-2.32	-3.23	-0.61	-2.01	-1.68	-0.66	-0.47	-0.63	-1.25	-0.73	-0.65	-1.53	-1.19
VIT_02s0025g04660	0.37	-0.16	-0.36	-0.71	0.32	-0.31	-0.26	-0.80	-0.44	-1.18	-1.17	-0.79	-0.18	-0.86	-0.55	-0.94	-0.54	0.43	-0.83	-0.83	-0.72
VIT_02s0025g04720	1.79	1.92	1.44	0.99	1.73	2.11	1.27	1.33	2.20	1.20	1.29	0.34	0.73	1.26	1.10	1.51	0.33	0.86	0.37	1.14	0.37
VIT_02s0154g00320	0.40	1.69	0.51	1.04	0.67	1.55	0.29	0.43	0.21	1.01	0.78	-1.14	0.03	0.81	-0.47	1.20	-0.82	-0.43	0.34	0.42	1.47
VIT_02s0154g00380	9.03	2.80	5.99	4.50	9.36	2.85	5.65	3.67	12.23	3.82	2.65	3.78	3.79	1.62	4.85	4.39	4.56	4.06	2.29	5.79	4.35
VIT_03s0097g00700	2.41	1.98	-0.28	-0.86	0.94	1.46	-0.07	0.09	0.12	-1.20	-0.59	-1.52	-0.69	0.72	0.49	0.15	-1.16	1.11	0.38	-0.92	0.21
VIT_04s0008g00370	0.61	1.55	1.67	1.13	0.27	1.25	1.97	0.91	0.32	1.07	0.56	0.30	-1.70	0.66	1.47	1.39	0.70	-0.33	1.24	1.99	1.06
VIT_04s0008g01100	-0.57	-1.83	-0.43	-0.59	-0.84	-1.56	-0.48	-1.41	-1.39	-1.25	-1.19	-0.42	0.01	-1.01	-0.40	-1.72	0.01	0.37	-0.54	-0.47	-0.97
VIT_04s0008g01810	0.97	1.06	0.83	0.90	0.99	0.92	0.73	0.82	1.45	0.89	0.77	0.60	0.59	0.48	0.89	0.62	0.38	0.20	0.19	0.92	0.68

## Appendix II

VIT_04s0008g01910	0.77	0.74	0.52	0.80	0.94	1.02	0.38	0.64	1.25	0.69	0.74	0.46	0.73	0.91	0.51	0.80	0.35	0.42	0.47	0.74	0.53
VIT_04s0008g02900	-0.10	-0.73	0.04	0.16	-0.17	-0.75	-0.13	-0.34	-0.95	-0.52	-0.52	-0.13	-0.50	-0.34	0.40	-0.13	-0.23	-0.03	-0.35	-0.14	-0.20
VIT_04s0008g02920	0.49	0.62	0.21	0.32	0.32	0.42	-0.12	0.36	0.33	-0.27	0.35	-1.10	0.14	0.20	-0.01	-0.08	-0.65	0.64	-0.14	-0.27	0.17
VIT_04s0008g04050	-0.56	-0.76	0.07	-0.76	-0.21	-0.72	-0.06	-0.33	0.33	0.64	0.03	-0.20	0.72	1.16	0.42	0.06	-0.74	0.74	-0.20	0.26	-0.10
VIT_04s0008g04200	1.09	0.40	0.67	-0.07	1.34	0.66	0.84	0.66	1.96	1.04	0.77	0.71	1.51	0.43	0.45	0.63	0.50	1.50	1.21	0.83	0.68
VIT_04s0008g05150	0.88	0.66	0.83	0.20	0.90	0.54	0.69	0.59	1.51	0.86	0.60	0.76	1.38	0.34	0.85	0.51	0.56	1.14	0.61	0.81	0.86
VIT_04s0008g05830	0.86	1.30	0.38	0.23	1.21	1.39	0.45	0.83	2.01	1.05	0.90	0.72	1.10	0.80	0.15	0.67	0.60	0.57	0.57	0.61	0.78
VIT_04s0008g06670	1.48	1.37	0.75	0.83	1.40	1.39	0.45	0.85	1.75	1.12	0.81	0.11	0.98	0.95	0.45	1.13	0.14	0.96	0.49	0.89	0.77
VIT_04s0023g03070	0.33	0.65	0.82	0.36	0.44	0.70	0.66	0.62	0.75	1.07	0.35	0.01	0.62	0.50	0.48	0.60	0.19	0.37	0.50	1.00	0.52
VIT_04s0069g00790	0.38	0.30	0.95	0.72	0.26	0.19	0.78	0.51	0.19	0.13	0.24	0.07	-0.26	0.50	0.99	0.83	0.25	-0.06	0.80	0.95	0.70
VIT_04s0079g00260	0.88	0.54	0.50	0.81	1.00	0.88	0.36	0.93	1.23	0.52	0.79	-0.08	1.00	0.39	0.14	1.05	-0.21	0.85	0.39	0.47	1.08
VIT_08s0007g01310	-0.89	-1.54	-0.79	0.10	-1.25	-2.23	-1.08	-0.03	-1.74	-1.44	-0.42	-0.94	-0.86	-0.35	-0.53	0.19	-0.72	-1.33	-0.20	-1.32	0.82
VIT_08s0007g01320	-0.73	-1.50	-0.61	0.20	-1.11	-2.15	-1.11	-0.25	-1.65	-1.38	-0.46	-0.85	-0.90	-0.25	-0.53	0.10	-0.59	-1.32	-0.18	-1.13	0.89
VIT_08s0007g01360	-1.13	-0.97	-1.07	-0.71	-1.19	-1.25	-1.70	-1.45	-2.36	-0.84	-1.12	-0.72	-0.70	-1.20	-0.90	-1.61	-0.41	-0.82	-0.92	-1.25	-0.97
VIT_08s0007g01370	-0.96	-0.47	-1.16	-0.75	-1.78	-0.04	-1.08	-0.82	-1.07	-1.00	-0.74	-0.92	-1.89	-1.08	-0.71	-0.95	-0.70	-1.27	-0.33	-0.69	-0.67
VIT_08s0040g01710	1.05	1.30	0.73	-0.08	1.20	1.39	0.88	0.47	1.75	0.75	0.26	-0.08	0.22	1.02	0.45	0.54	-0.19	0.19	0.57	0.59	0.27
VIT_08s0058g00930	-0.13	-1.34	-0.35	-0.89	-0.28	-1.32	-0.40	-1.20	-1.03	-1.17	-1.51	-0.68	-0.06	-1.08	-0.22	-1.08	-0.25	0.19	-0.36	-0.87	-0.81
VIT_08s0058g00990	-0.16	0.17	-0.19	-0.57	-0.43	-0.13	-0.47	-1.65	-0.60	-0.70	-1.85	-1.06	-0.46	-0.80	-0.50	-1.33	-1.01	-0.04	-0.25	-0.22	-0.34
VIT_09s0070g00470	0.11	0.43	0.23	0.49	-0.04	0.41	0.19	0.26	0.24	0.32	0.05	0.18	0.06	0.19	0.09	0.42	0.32	0.21	-0.04	0.42	0.34
VIT_11s0016g03710	0.95	0.48	0.69	1.19	1.26	0.67	0.38	1.44	1.82	0.67	0.90	0.31	0.72	-0.42	0.70	0.40	0.21	0.41	-0.24	0.20	1.02
VIT_12s0059g00190	0.40	1.66	0.91	1.64	0.92	1.45	0.63	1.51	1.88	0.93	1.95	0.83	0.79	0.55	0.30	1.89	0.95	0.56	0.35	0.76	1.93
VIT_14s0066g01060	2.57	0.32	-0.25	-0.26	1.68	0.60	-0.30	0.36	1.42	-1.44	0.37	-1.08	-0.04	0.56	0.60	0.29	-0.51	0.97	1.28	-1.27	0.03
VIT_14s0083g00410	0.37	-0.23	-0.80	0.37	0.05	-0.44	-1.11	-0.38	-1.24	-1.79	-0.32	-0.69	-0.06	-0.13	-0.22	-0.24	-0.22	0.35	-0.72	-1.50	-0.64
VIT_14s0108g00700	1.73	0.40	1.16	2.16	2.01	0.53	1.14	2.11	1.46	1.49	2.40	1.03	0.56	0.43	1.20	2.20	0.69	0.83	0.48	1.34	2.30
VIT_14s0108g00740	0.90	0.94	1.24	0.47	0.98	1.23	1.05	0.19	2.00	1.25	0.72	0.49	1.21	1.20	1.25	0.44	0.59	0.43	0.34	1.62	0.54
VIT_14s0219g00230	1.94	1.24	1.19	0.09	1.84	1.38	1.15	0.31	1.62	0.94	0.34	0.21	0.41	1.51	0.96	0.47	0.07	0.45	1.33	1.38	0.51
VIT_15s0048g01750	1.07	1.16	0.58	0.81	1.32	1.21	0.49	1.03	1.73	1.28	1.11	0.22	0.93	0.98	0.47	1.18	0.46	0.67	0.38	0.85	0.89
VIT_17s0000g02470	0.63	1.17	0.53	1.10	0.65	1.51	0.45	0.79	1.75	1.06	0.98	1.00	0.88	1.10	0.38	1.46	0.90	0.81	0.56	0.96	1.20
VIT_17s0000g03550	0.68	0.20	0.15	0.55	0.54	0.17	-0.24	0.78	1.25	-0.10	0.80	0.04	0.68	0.25	0.42	0.62	-0.17	0.42	0.46	0.23	0.92

## Appendix II

VIT_17s0000g03750	0.84	1.22	0.99	1.12	1.07	1.29	0.85	1.78	1.69	0.98	1.00	0.48	0.68	0.36	0.82	1.22	0.43	0.20	0.10	0.79	1.16
VIT_17s0000g04470	-0.10	-0.68	-0.13	0.38	-0.03	-0.56	-0.25	0.18	-0.72	-0.21	-0.56	-0.45	-0.54	-1.17	0.08	-0.28	0.00	0.07	-0.75	0.11	-0.04
VIT_17s0000g05000	1.05	0.65	1.17	0.68	0.97	0.68	1.09	0.38	0.57	0.35	0.12	0.41	0.63	0.49	1.00	0.42	0.59	0.69	0.84	1.06	0.61
VIT_17s0000g05070	0.07	-0.21	-0.19	-0.06	-0.28	-0.51	-0.44	-0.37	0.02	-0.34	-0.23	-0.34	-0.47	-0.45	-0.38	-0.60	-0.29	-0.04	-0.38	-0.25	-0.31
VIT_17s0000g05570	1.32	0.67	0.75	0.46	1.34	0.67	0.76	0.55	1.48	1.01	0.82	0.24	0.91	1.01	0.73	0.77	0.18	0.66	0.80	0.87	0.73
VIT_17s0000g09190	-0.54	-0.64	-0.66	0.21	-0.69	-0.73	-0.76	-0.14	-1.44	-1.10	-0.25	-0.20	-0.95	-0.72	-0.53	0.07	-0.02	-0.18	-0.61	-0.91	-0.15
VIT_17s0000g09310	0.29	-0.05	1.08	0.11	0.17	-0.02	1.03	-0.34	-0.15	0.44	-0.40	-0.03	1.04	0.33	0.87	0.19	0.31	1.84	0.57	0.93	-0.39
VIT_17s0000g09470	-0.59	-0.38	0.02	0.05	-0.66	-0.46	0.05	-0.60	-1.37	-0.66	-0.73	0.00	-0.79	0.16	-0.11	-0.19	0.01	-0.66	0.08	0.20	-0.29
VIT_17s0000g09790	-0.72	-0.35	-0.40	0.18	-0.77	-0.49	-0.37	0.03	-1.49	-1.03	-0.35	0.19	-0.02	-0.65	-0.42	-0.25	0.54	0.15	-0.46	-0.68	-0.63
VIT_17s0053g00990	1.34	1.65	0.77	0.76	1.29	1.84	0.82	1.09	2.47	0.16	1.17	0.64	1.38	1.27	0.91	1.20	0.91	1.18	0.68	0.89	0.64
VIT_18s0001g03160	-0.78	-1.80	-1.58	-1.06	-0.67	-2.14	-1.73	-1.62	-2.20	-1.76	-1.15	-0.62	-0.49	-1.22	-1.54	-1.48	-0.23	-0.72	-1.14	-2.19	-1.00
VIT_18s0001g03540	0.89	0.79	0.84	0.34	0.59	0.38	0.60	-0.24	0.38	-0.09	-0.24	0.39	0.18	0.53	0.65	0.57	0.89	-0.02	0.82	0.60	1.16
VIT_18s0001g04890	-0.28	-0.56	-0.87	-1.06	-0.65	-0.67	-1.48	-1.37	-1.33	-1.28	-1.43	-1.40	-1.10	-0.76	-0.49	-0.85	-0.96	-0.62	-0.36	-1.20	-0.79
VIT_18s0001g04910	0.63	0.36	-0.04	-0.42	0.32	0.68	-0.19	-0.23	-0.34	-0.57	-0.42	-0.85	-0.25	0.14	0.08	0.04	-0.57	0.23	0.31	-0.02	-0.50
VIT_18s0001g05060	1.27	1.75	1.33	1.18	1.14	1.77	1.33	1.23	2.22	1.00	0.97	0.25	0.01	1.25	1.23	1.92	0.28	0.31	0.34	1.10	0.30
VIT_18s0001g07340	1.96	1.71	0.98	1.51	1.72	1.73	0.20	1.52	2.19	0.91	1.91	-0.10	1.19	1.06	0.65	1.90	0.05	1.02	0.32	0.54	1.38
VIT_18s0001g07460	0.82	0.03	0.63	0.10	0.54	-0.05	1.03	-0.36	0.35	0.72	-0.09	0.58	-0.25	0.19	0.54	0.22	0.47	0.14	0.43	1.06	-0.52
VIT_18s0001g09230	0.12	0.53	-0.18	-0.70	-0.09	0.15	0.40	-0.94	-1.00	-0.41	-0.60	-0.50	-0.60	0.05	0.56	-0.22	-0.01	-0.08	0.14	-0.20	-0.15
VIT_18s0001g09400	1.31	2.04	0.97	1.48	1.33	2.13	0.78	1.72	2.23	1.27	1.51	0.36	0.65	0.88	0.50	1.71	0.35	0.69	-0.04	1.08	0.78
VIT_18s0001g09510	-0.80	-0.69	-0.26	-0.22	-0.83	-0.81	-0.55	-0.50	-1.48	-0.02	-0.40	0.07	-0.41	-0.87	-0.30	-0.71	0.13	-0.18	-0.68	-0.31	-0.52
VIT_18s0001g09910	0.56	0.59	0.59	0.08	0.53	0.49	0.63	0.50	0.45	0.03	0.03	0.30	-0.07	0.54	0.15	0.59	0.23	0.14	0.50	0.46	0.15
VIT_18s0001g10130	-0.39	-0.75	0.31	-0.54	-0.73	-1.16	0.58	-1.57	-3.64	-1.39	-3.54	-1.63	-1.49	-1.73	-0.07	-0.11	-0.45	-0.02	0.22	0.54	-0.43
VIT_18s0001g10610	0.55	0.32	0.96	-0.03	0.18	0.24	1.37	-0.83	-0.84	0.79	-1.38	0.17	-0.28	0.81	0.92	0.25	0.25	0.16	0.79	1.51	0.06
VIT_18s0001g10640	-0.53	-0.85	0.19	-1.58	-0.38	-1.64	0.42	-2.09	-2.68	-1.55	-4.03	-1.38	-1.08	-1.86	-0.38	-1.55	-0.67	-0.44	-0.09	-0.13	-1.32
VIT_18s0001g11160	1.01	0.49	0.70	0.88	0.65	0.37	0.63	0.65	0.48	0.31	0.82	0.31	0.32	0.15	0.68	0.68	0.51	0.33	0.25	0.68	0.94
VIT_19s00015g00270	-0.09	-0.67	-0.78	0.56	-0.45	-0.89	-1.23	-0.23	-1.04	-1.33	0.26	-0.28	-0.34	-0.53	-0.62	0.02	0.05	0.08	-0.35	-1.61	-0.07
VIT_19s00015g00490	1.21	1.53	0.50	0.96	1.10	1.50	0.08	0.78	1.85	1.20	1.11	0.04	0.87	1.34	0.10	1.32	0.35	0.91	0.47	0.56	0.59
VIT_19s00015g01230	1.02	1.05	0.38	1.01	0.95	1.62	0.28	1.07	1.77	1.22	0.82	0.15	1.00	0.44	0.28	1.04	0.27	0.85	0.02	0.73	0.79
VvGRF4	2.74	2.83	2.94	3.11	2.58	2.99	2.93	3.28	3.47	2.95	2.78	2.74	2.64	2.35	2.78	3.51	2.93	2.54	2.31	3.04	3.00

Online resource 7 continued Time point BBCH71 compactly clustered clones

Genes/Samples	En777.B.15	En777.B.16	En777.B.17	En777.H.15	En777.H.16	En777.H.17	RKCH.B.15	RKCH.B.16	RKCH.B.17	RKCH.H.15	RKCH.H.16	RKCH.H.17	RKCH.P.15	RKCH.P.16	RKCH.P.17	RKCL.H.15	RKCL.H.16	RKCL.H.17	RKCL.P.15	RKCL.P.16	RKCL.P.17
VIT_01s0010g01810	1.24	0.52	2.22	-0.65	0.47	0.28	0.65	0.75	0.52	0.43	-0.01	0.50	0.91	-0.41	0.16	0.51	0.51	-0.74	-0.18	-0.74	-0.27
VIT_01s0010g02430	0.37	0.33	0.61	1.10	1.04	0.97	-0.20	0.55	0.05	0.46	0.34	0.58	-0.07	0.25	0.21	0.36	0.81	-0.02	-0.44	0.22	-0.19
VIT_01s0011g06410	0.13	-0.19	0.37	0.42	0.54	0.11	-0.37	-0.26	0.50	0.49	0.49	0.12	0.08	-0.02	0.57	0.30	0.34	0.02	0.08	-0.24	0.65
VIT_01s0026g02030	0.13	0.33	0.38	-0.28	1.22	0.45	0.23	0.16	0.52	-0.27	1.11	0.34	-0.01	0.18	1.36	-0.02	1.32	-0.18	0.25	0.19	0.40
VIT_01s0127g00260	0.18	0.27	0.45	1.62	1.30	0.95	-0.21	0.50	0.12	1.48	0.46	0.73	0.05	-0.41	0.23	1.34	0.72	0.43	-0.26	0.04	0.02
VIT_01s0127g00710	7.00	7.43	7.22	-0.12	4.92	0.69	7.66	7.83	7.52	-0.65	4.95	0.05	3.20	7.58	2.69	-0.35	3.93	0.28	4.92	7.11	3.61
VIT_01s0127g00870	0.98	0.51	1.04	1.59	0.99	0.77	-0.26	0.64	0.79	0.89	0.35	0.86	0.11	0.32	0.69	1.18	0.93	0.09	-0.30	0.29	-0.04
VIT_01s0146g00400	0.68	0.02	0.37	0.91	0.59	0.11	0.17	0.25	0.40	0.52	0.67	-0.20	0.24	-0.11	0.62	1.14	0.29	-0.32	0.01	0.19	0.42
VIT_01s0146g00480	0.39	0.83	0.13	0.77	0.90	-0.65	0.18	0.55	0.36	0.61	1.10	-0.05	-1.12	-0.09	-0.18	1.38	0.02	-0.72	-0.72	-0.17	-0.34
VIT_02s0012g00990	-0.19	-0.17	3.78	-0.64	4.16	4.25	0.21	0.00	3.92	-0.48	4.15	4.22	7.20	4.56	7.64	-0.36	3.72	4.16	7.90	4.09	7.43
VIT_02s0012g01380	-0.21	-0.35	-0.66	0.21	-0.10	-0.24	0.29	-0.04	-0.18	0.08	0.00	-0.62	-0.54	-0.29	-1.04	0.05	-0.64	-0.15	-0.16	-0.13	-0.30
VIT_02s0012g01400	-0.44	-0.19	-0.57	-0.02	0.26	-0.05	-0.14	0.00	-0.21	-0.48	0.24	-0.50	-0.73	-0.30	-0.74	-0.21	-0.61	-0.20	-0.46	-0.13	-0.20
VIT_02s0025g03010	-0.74	-0.19	-0.17	-0.19	0.70	-0.17	-0.74	-0.18	0.13	-0.38	0.28	-0.44	-0.44	-0.03	-0.46	-0.16	0.14	-0.10	-0.17	0.07	0.04
VIT_02s0025g03180	0.17	0.07	0.13	0.15	1.18	-0.02	0.04	0.25	-0.16	0.24	1.48	0.18	0.11	-0.13	0.22	0.09	0.78	-0.32	0.21	0.23	0.29
VIT_02s0025g04340	-1.35	-0.80	-0.12	-1.82	-1.01	-0.47	-0.28	-0.07	-0.48	-1.98	-0.87	-0.80	-1.80	-1.01	-1.37	0.25	-2.25	-1.02	-1.51	-0.14	-0.81
VIT_02s0025g04660	-0.01	-0.07	-0.51	0.01	-0.56	-0.53	0.26	0.22	-0.27	0.58	-0.11	-0.75	-0.39	-0.67	-0.94	0.83	-0.62	-0.58	-0.48	0.18	-0.55
VIT_02s0025g04720	0.64	0.59	0.98	1.47	1.06	0.74	0.01	0.70	0.46	1.70	0.60	1.01	0.26	0.21	0.62	1.40	0.78	0.27	-0.04	0.18	0.00
VIT_02s0154g00320	-1.53	0.50	1.42	0.76	1.39	0.48	-1.02	0.37	1.19	0.61	0.36	0.64	0.21	0.55	0.79	0.42	0.68	0.17	-0.31	-0.44	0.34
VIT_02s0154g00380	4.08	3.41	-3.87	5.98	1.93	-0.08	1.93	6.98	-3.65	5.22	4.01	2.66	-0.75	2.93	1.21	9.83	3.56	-5.86	2.19	2.18	-0.33
VIT_03s0097g00700	0.07	0.33	-0.48	0.60	-0.59	-1.27	1.01	0.81	0.09	0.71	-0.04	-0.11	-1.14	-1.24	-0.08	2.59	-0.90	-1.18	-1.17	1.19	-0.33
VIT_04s0008g00370	0.98	-0.33	0.20	0.91	1.48	0.04	0.18	0.58	0.29	1.07	1.78	0.21	0.27	-1.51	0.62	1.03	1.27	-0.10	0.54	-0.12	0.25
VIT_04s0008g01100	-0.28	-0.21	-0.70	-0.30	0.64	0.06	0.01	-0.11	-0.49	-0.59	0.92	-0.37	-0.26	0.90	-0.62	-0.39	0.11	-0.02	0.87	0.17	-0.07
VIT_04s0008g01810	0.30	0.21	0.57	0.98	0.60	0.44	0.07	0.22	-0.11	0.85	0.30	0.43	-0.58	0.14	0.08	1.00	0.28	0.07	-0.14	-0.21	-0.31

## Appendix II

VIT_04s0008g01910	0.52	0.38	0.58	0.87	0.82	0.24	-0.26	0.09	0.24	0.58	0.64	0.41	0.33	0.33	0.43	0.64	0.63	0.26	0.20	0.04	0.17
VIT_04s0008g02900	-0.46	0.06	-0.53	-0.12	0.63	0.01	-0.14	0.04	-0.29	-0.51	0.52	-0.32	-0.33	-0.30	-0.54	-0.32	-0.12	-0.15	-0.27	0.07	-0.10
VIT_04s0008g02920	-0.22	0.23	0.29	1.38	0.48	0.24	-0.02	0.39	0.50	0.71	-0.11	-0.07	-0.59	0.44	0.44	0.55	0.01	0.12	-0.35	0.20	0.35
VIT_04s0008g04050	0.29	0.24	0.29	0.87	0.72	0.44	-0.53	-0.34	-0.05	0.28	0.93	-0.30	-0.14	0.01	-0.05	0.24	0.59	-0.07	-0.37	0.48	0.51
VIT_04s0008g04200	0.55	0.52	0.31	1.60	1.03	0.78	0.20	0.62	0.14	0.97	0.52	0.51	0.26	0.41	0.33	1.27	0.85	0.29	1.25	0.24	0.08
VIT_04s0008g05150	0.44	-0.02	0.31	0.83	0.62	0.39	-0.41	0.18	-0.26	0.10	0.43	0.57	-0.46	0.65	-0.06	0.33	0.53	-0.09	0.47	0.16	-0.45
VIT_04s0008g05830	1.17	0.47	1.01	0.85	0.32	0.57	0.14	0.34	0.20	0.74	-0.04	0.83	0.47	0.33	0.68	1.18	0.32	0.02	0.12	0.10	0.00
VIT_04s0008g06670	0.69	0.44	0.98	0.97	0.76	0.51	0.10	0.73	0.48	0.94	0.56	0.51	-0.01	0.79	0.60	0.49	0.86	-0.20	-0.16	0.41	0.10
VIT_04s0023g03070	-0.19	0.11	0.43	0.95	1.05	0.50	-0.48	0.13	0.10	0.55	0.34	0.20	-0.25	0.25	0.21	0.63	0.69	-0.15	-0.09	0.55	0.22
VIT_04s0069g00790	0.03	-0.13	-0.38	0.50	0.74	-0.01	0.06	0.04	-0.09	0.34	0.96	0.24	-0.17	-0.13	0.13	0.33	0.56	0.05	0.00	0.36	0.39
VIT_04s0079g00260	0.13	0.04	0.65	1.31	0.80	1.26	-0.33	0.24	0.34	0.77	0.13	0.75	-0.55	0.42	0.29	1.02	0.21	0.39	-0.47	0.37	0.48
VIT_08s0007g01310	-1.24	-0.78	-1.03	-0.47	-0.94	0.25	-1.32	-1.05	-1.67	-0.88	-0.44	-0.65	-1.19	-0.32	-1.25	-1.26	-1.47	-0.83	-1.21	-0.40	-0.51
VIT_08s0007g01320	-1.42	-0.70	-1.10	-0.28	-0.82	0.12	-1.39	-1.05	-1.78	-0.72	-0.18	-0.70	-1.23	-0.28	-1.14	-1.05	-1.35	-0.75	-1.07	-0.27	-0.34
VIT_08s0007g01360	-0.63	-0.24	-0.52	-1.42	-0.33	0.04	-0.11	-0.35	-0.55	-1.86	-0.15	-0.71	-0.67	0.10	-1.06	-1.57	-0.97	-0.43	-0.62	-0.21	-0.81
VIT_08s0007g01370	-0.32	-0.67	0.62	0.22	-0.21	0.29	-0.09	-1.02	0.90	-0.02	-0.06	0.07	0.40	-0.28	-0.04	0.83	-0.75	0.20	0.17	0.07	0.31
VIT_08s0040g01710	0.89	0.27	0.83	1.51	0.04	0.01	0.31	0.88	0.53	1.39	0.24	0.31	0.07	0.26	0.45	1.36	0.37	-0.01	-0.32	-0.02	0.14
VIT_08s0058g00930	0.29	-0.10	-0.76	0.21	-0.12	-0.36	0.60	-0.17	-0.24	0.16	0.04	-0.71	0.12	-0.01	-0.95	-0.02	-0.66	-0.33	0.46	0.84	-0.33
VIT_08s0058g00990	-0.66	-0.08	0.13	0.11	-0.24	-0.81	-0.03	0.04	-0.13	-0.07	-0.17	-1.43	-0.64	-0.46	-0.82	0.33	-0.68	-1.38	-0.61	0.52	-0.34
VIT_09s0070g00470	-0.03	-0.17	0.21	0.30	0.59	0.03	0.02	-0.08	0.25	0.25	0.58	-0.03	-0.12	0.02	0.01	0.20	0.26	0.00	0.11	0.27	0.28
VIT_11s0016g03710	-0.08	0.60	0.50	1.10	0.83	1.38	-0.18	0.43	-0.01	0.83	-0.07	1.12	-0.01	0.21	0.10	1.03	0.29	0.49	-0.51	0.22	0.02
VIT_12s0059g00190	0.44	0.37	1.09	0.56	1.40	1.78	0.43	-0.27	-0.17	0.86	0.22	2.33	0.47	-0.47	1.04	1.37	1.08	1.11	0.41	-0.59	0.07
VIT_14s0066g01060	0.44	0.56	0.04	1.39	0.46	1.27	-0.11	1.09	0.88	2.20	0.08	0.49	-0.45	0.34	1.75	2.34	-0.25	0.69	-0.43	1.04	2.08
VIT_14s0083g00410	0.18	0.21	0.08	-0.78	0.28	0.05	0.35	0.64	0.28	-0.38	-0.06	-0.46	-0.52	-0.02	-0.59	-0.41	-0.80	0.08	-0.29	-0.12	0.00
VIT_14s0108g00700	1.26	1.03	0.32	1.40	1.33	1.32	0.54	0.48	-0.28	1.00	1.17	2.39	0.36	0.24	0.41	1.02	1.07	1.49	-0.22	0.65	-0.03
VIT_14s0108g00740	0.20	0.63	0.59	0.96	1.08	0.34	0.03	0.06	0.28	1.10	0.91	0.11	-0.18	-0.13	0.81	1.06	0.81	-0.17	-0.36	0.39	0.18
VIT_14s0219g00230	0.43	0.28	0.84	1.65	1.12	0.00	0.10	0.80	0.88	1.56	1.17	-0.16	0.34	-0.56	0.74	1.40	1.15	-0.65	0.41	0.10	0.67
VIT_15s0048g01750	0.86	0.56	0.92	0.80	0.87	0.36	0.00	0.38	0.35	0.49	0.38	0.62	0.19	0.73	0.50	0.55	0.61	0.18	-0.19	0.49	-0.12
VIT_17s0000g02470	0.30	0.21	0.92	1.14	1.37	0.48	-0.08	-0.02	0.28	1.07	0.48	0.60	0.42	0.25	0.23	1.08	0.94	0.01	0.06	0.46	0.24
VIT_17s0000g03550	0.09	0.48	0.04	1.78	0.47	1.45	-0.39	0.49	-0.21	0.98	0.06	0.82	-0.44	0.33	0.35	1.30	-0.09	0.40	-0.51	0.59	0.57

## Appendix II

VIT_17s0000g03750	0.15	0.86	0.89	1.00	1.15	1.38	-0.09	0.29	-0.24	0.56	0.13	1.11	0.17	-0.04	0.12	0.81	0.32	0.35	-0.20	0.14	-0.20
VIT_17s0000g04470	-0.26	-0.64	-0.45	0.53	0.08	0.47	-0.11	0.14	-0.43	0.18	0.41	0.25	-0.45	-0.67	-1.00	0.33	-0.11	0.16	-0.45	-0.04	-0.28
VIT_17s0000g05000	0.43	0.45	-0.11	0.31	0.53	0.28	0.30	0.62	0.46	0.39	0.85	0.26	0.21	0.28	0.34	0.43	0.62	0.14	0.42	0.52	0.36
VIT_17s0000g05070	0.12	0.02	-0.14	0.75	0.37	0.26	0.12	-0.03	-0.45	0.43	0.49	-0.01	0.04	-0.29	-0.21	0.66	0.13	0.03	-0.15	0.09	0.02
VIT_17s0000g05570	1.04	0.36	0.50	1.21	0.69	0.39	0.25	0.65	0.42	1.08	0.73	0.33	0.18	0.23	0.58	0.99	0.84	-0.17	0.13	0.36	0.24
VIT_17s0000g09190	-0.66	-0.02	-0.53	-0.31	0.19	0.30	-0.09	-0.06	-0.03	-0.55	0.20	-0.13	-0.13	-0.55	-0.81	-0.14	-0.78	0.30	-0.57	-0.28	-0.09
VIT_17s0000g09310	0.05	0.17	0.10	0.37	1.75	0.00	-0.23	-0.20	-0.07	0.04	1.06	-0.24	-1.40	1.30	-0.04	0.23	1.01	-0.07	0.48	1.33	0.43
VIT_17s0000g09470	-0.30	-0.45	-0.16	-0.70	0.77	-0.67	0.19	-0.54	0.02	-0.41	0.23	-1.06	-0.03	-0.25	-0.60	-0.87	-0.11	-0.54	-0.11	-0.26	-0.11
VIT_17s0000g09790	-1.02	-0.52	-0.72	-1.10	-0.42	-0.21	-0.12	-0.52	-0.14	-1.17	-0.29	-0.23	-0.35	0.30	-0.79	-1.04	-0.74	0.16	-0.02	-0.48	-0.17
VIT_17s0053g00990	0.59	0.29	0.83	0.90	-0.21	0.40	0.33	0.18	0.21	1.94	-0.45	0.66	0.28	-0.12	0.80	1.39	0.21	0.13	0.41	-0.19	0.29
VIT_18s0001g03160	-0.51	0.46	-0.53	-0.99	-0.23	0.66	0.07	0.32	-0.70	-0.89	-0.26	-0.32	-0.27	0.03	-1.36	-0.87	-0.96	-0.27	-0.03	-0.25	-0.30
VIT_18s0001g03540	-0.43	-0.02	-0.56	-0.54	-0.29	-0.59	-0.16	-0.06	-0.69	-0.30	0.29	-0.15	-0.25	-0.11	0.01	-0.44	-0.12	-0.83	0.03	0.20	-0.02
VIT_18s0001g04890	-0.04	-0.41	-0.23	-0.65	-0.49	-0.21	0.14	-0.48	-0.32	-0.39	-0.14	-0.56	-0.47	0.04	-0.56	-0.42	-0.45	-0.86	-0.04	-0.21	-0.36
VIT_18s0001g04910	0.40	0.11	0.31	-0.13	0.19	-0.19	0.23	0.32	0.44	0.29	0.61	-0.15	-0.24	0.07	0.41	0.20	0.16	-0.27	-0.05	0.34	0.29
VIT_18s0001g05060	0.40	0.54	0.67	1.50	1.16	0.51	-0.05	0.60	0.35	1.82	0.50	0.62	0.18	-0.35	0.23	1.56	0.72	0.19	-0.36	-0.14	0.10
VIT_18s0001g07340	-0.41	0.63	1.04	2.00	0.79	1.78	-1.90	0.88	0.68	1.67	0.45	0.83	-0.27	1.16	0.87	1.85	0.54	0.91	-0.68	0.80	0.65
VIT_18s0001g07460	0.21	0.15	-0.56	0.21	0.97	-0.30	0.23	0.68	-0.55	0.03	0.93	0.05	0.37	-0.65	-0.15	0.43	0.68	-0.24	0.52	0.03	0.21
VIT_18s0001g09230	-0.30	0.02	-0.59	0.12	0.29	-0.68	0.08	0.31	0.22	-0.23	0.41	-0.88	-0.50	-0.14	-0.88	0.07	-0.55	-0.97	-1.23	-0.02	-0.47
VIT_18s0001g09400	0.53	0.54	1.25	1.44	0.93	0.78	-0.16	0.64	0.55	1.50	0.40	1.07	0.42	0.29	0.58	1.45	0.59	0.71	0.08	0.19	-0.01
VIT_18s0001g09510	-0.63	-0.18	-0.20	-0.99	0.02	-0.08	-0.20	-0.33	0.03	-1.34	0.07	-0.38	-0.28	0.10	-0.70	-1.15	-0.38	-0.06	0.02	0.11	-0.30
VIT_18s0001g09910	0.65	0.33	0.06	0.64	0.07	0.06	0.28	0.49	0.29	0.84	0.66	0.25	0.42	-0.12	0.20	0.73	0.19	-0.02	0.41	0.44	0.36
VIT_18s0001g10130	-2.22	-1.31	-0.93	-1.46	0.12	-1.74	-0.51	-0.13	-0.62	-0.77	1.06	-0.70	0.07	-0.82	-1.50	-0.85	0.13	-1.50	0.41	0.01	0.08
VIT_18s0001g10610	-0.32	0.10	0.42	-0.23	1.62	-1.17	-0.19	-0.10	0.45	-0.25	1.45	-0.62	0.32	-0.31	-0.17	-0.31	0.87	-1.11	0.08	0.46	0.38
VIT_18s0001g10640	-1.76	-1.03	-1.03	-1.35	-0.27	-1.96	-0.21	0.17	-0.44	-0.67	0.38	-1.05	-0.28	-0.86	-1.35	-0.75	-0.10	-1.98	-0.09	0.14	-0.15
VIT_18s0001g11160	-0.37	-0.05	-0.38	0.37	0.25	0.16	-0.05	0.42	0.18	0.37	0.39	0.09	-0.36	-0.14	0.13	0.29	-0.13	-0.06	-0.20	0.12	-0.13
VIT_19s00015g00270	0.48	-0.22	-0.66	-0.26	-0.37	0.47	0.73	0.80	-0.27	0.29	-0.15	0.09	-0.97	0.02	-0.82	0.23	-0.95	0.61	-0.66	-0.01	-0.53
VIT_19s00015g00490	0.37	0.30	1.00	1.05	0.89	0.61	-0.08	0.42	0.56	0.89	0.43	0.46	0.11	0.82	0.67	0.61	0.73	-0.01	-0.31	0.31	0.11
VIT_19s00015g01230	0.45	0.26	0.90	0.89	0.51	0.68	-0.09	0.59	0.26	0.91	0.43	0.58	-0.01	0.40	0.37	0.57	0.72	-0.23	-0.28	0.24	-0.25
VvGRF4	0.17	-0.30	-0.06	0.63	0.70	0.18	0.07	0.28	-0.44	0.49	0.96	0.48	-0.09	0.40	-0.20	0.64	0.88	-0.19	0.31	0.52	-0.45

## Appendix II

### Online resource 7 continued

#### Time point BBCH71 mixed berry clones

Genes/Samples	Fr1801.B.15	Fr1801.B.16	Fr1801.B.17	Fr1801.H.16	Fr1801.H.17
<i>VIT_01s0010g01810</i>	1.25	1.79	3.51	-0.34	0.04
<i>VIT_01s0010g02430</i>	-1.33	0.78	1.26	-0.43	0.48
<i>VIT_01s0011g06410</i>	0.03	0.23	0.56	-0.08	0.01
<i>VIT_01s0026g02030</i>	-0.07	-0.05	0.74	-3.93	1.27
<i>VIT_01s0127g00260</i>	-0.92	0.11	0.75	0.02	0.26
<i>VIT_01s0127g00710</i>	7.42	7.34	7.00	4.27	0.68
<i>VIT_01s0127g00870</i>	-0.94	0.98	1.33	-0.83	1.03
<i>VIT_01s0146g00400</i>	-0.59	-0.03	0.43	-0.84	0.08
<i>VIT_01s0146g00480</i>	-0.22	-0.85	0.47	-0.21	0.90
<i>VIT_02s0012g00990</i>	0.22	-0.75	4.02	4.12	4.09
<i>VIT_02s0012g01380</i>	-0.08	0.01	-0.50	0.29	-0.23
<i>VIT_02s0012g01400</i>	0.20	-0.03	-0.60	0.17	0.12
<i>VIT_02s0025g03010</i>	0.06	-0.28	-0.62	0.41	-0.37
<i>VIT_02s0025g03180</i>	-0.31	0.32	-0.21	0.03	-0.46
<i>VIT_02s0025g04340</i>	1.08	-0.15	1.56	1.00	1.67
<i>VIT_02s0025g04660</i>	0.18	-0.19	0.13	-0.19	-0.69
<i>VIT_02s0025g04720</i>	-0.82	0.04	1.43	-0.78	0.04
<i>VIT_02s0154g00320</i>	-1.45	0.58	2.06	0.00	1.01
<i>VIT_02s0154g00380</i>	5.34	2.57	-0.24	-3.03	3.04
<i>VIT_03s0097g00700</i>	0.06	0.66	0.68	-0.72	0.68
<i>VIT_04s0008g00370</i>	0.46	-0.58	-0.08	0.87	0.31
<i>VIT_04s0008g01100</i>	-0.22	-0.26	-0.94	0.69	-0.13
<i>VIT_04s0008g01810</i>	-0.32	0.50	0.74	-0.16	0.44
<i>VIT_04s0008g01910</i>	-0.47	0.02	0.76	-0.60	0.14
<i>VIT_04s0008g02900</i>	0.11	0.08	-0.25	0.56	0.10
<i>VIT_04s0008g02920</i>	-0.44	0.04	0.66	0.30	0.29
<i>VIT_04s0008g04050</i>	-0.13	0.21	-0.07	0.69	0.54
<i>VIT_04s0008g04200</i>	-1.22	0.69	0.42	-0.51	0.64
<i>VIT_04s0008g05150</i>	-0.14	0.86	0.33	-0.28	0.90
<i>VIT_04s0008g05830</i>	-0.51	0.67	1.18	-0.98	0.32
<i>VIT_04s0008g06670</i>	-1.07	1.04	1.25	-0.57	0.28
<i>VIT_04s0023g03070</i>	-0.77	0.28	0.58	0.24	0.21
<i>VIT_04s0069g00790</i>	-0.04	-0.21	-0.12	0.28	0.43
<i>VIT_04s0079g00260</i>	-1.38	0.31	1.06	-0.70	1.22
<i>VIT_08s0007g01310</i>	0.54	0.09	-0.55	0.43	0.90
<i>VIT_08s0007g01320</i>	0.34	-0.03	-0.61	0.49	0.93
<i>VIT_08s0007g01360</i>	0.34	-0.06	-0.47	0.29	-0.01

## Appendix II

VIT_08s0007g01370	-0.15	-0.63	0.13	-0.11	-0.01
VIT_08s0040g01710	0.15	0.61	0.62	-0.81	-0.17
VIT_08s0058g00930	0.22	-0.02	-0.91	0.18	-0.04
VIT_08s0058g00990	-0.47	0.02	0.25	0.15	-0.23
VIT_09s0070g00470	-0.15	-0.18	0.34	-0.11	0.07
VIT_11s0016g03710	-1.12	0.57	0.99	-0.78	0.82
VIT_12s0059g00190	-0.62	0.41	2.01	-0.46	1.59
VIT_14s0066g01060	-0.82	0.82	-0.26	-2.63	0.60
VIT_14s0083g00410	0.20	0.41	0.08	-0.58	0.09
VIT_14s0108g00700	0.09	0.47	0.30	-0.49	1.84
VIT_14s0108g00740	-0.76	-0.59	0.71	-0.39	-0.07
VIT_14s0219g00230	-1.51	0.85	0.65	-0.88	0.12
VIT_15s0048g01750	-0.51	0.73	1.11	-0.63	0.24
VIT_17s0000g02470	-0.94	0.44	1.35	-0.44	0.25
VIT_17s0000g03550	-0.88	0.50	-0.07	-0.14	1.06
VIT_17s0000g03750	-0.06	0.47	1.07	-0.27	0.30
VIT_17s0000g04470	0.10	0.27	-0.80	0.32	-0.13
VIT_17s0000g05000	-0.29	0.10	-0.38	0.21	0.02
VIT_17s0000g05070	0.43	-0.18	0.05	0.12	-0.24
VIT_17s0000g05570	-0.91	0.76	0.74	-0.74	0.19
VIT_17s0000g09190	0.32	-0.49	-1.11	0.05	-0.51
VIT_17s0000g09310	-0.23	-0.69	-0.27	0.64	-0.29
VIT_17s0000g09470	0.27	-0.64	0.30	0.89	0.01
VIT_17s0000g09790	0.86	-0.54	-0.78	0.41	-0.56
VIT_17s0053g00990	-1.10	0.62	1.15	-0.89	0.39
VIT_18s0001g03160	0.01	0.14	-0.86	-0.03	0.21
VIT_18s0001g03540	0.62	0.29	0.01	-0.11	0.36
VIT_18s0001g04890	0.07	-0.12	-0.16	-0.45	-0.11
VIT_18s0001g04910	-0.45	-0.35	0.12	-0.30	-0.54
VIT_18s0001g05060	-0.94	-0.08	1.21	-0.59	-0.04
VIT_18s0001g07340	-2.72	0.95	1.45	-1.65	1.83
VIT_18s0001g07460	0.28	0.51	-1.26	0.25	-0.74
VIT_18s0001g09230	0.21	-0.30	0.01	0.21	0.27
VIT_18s0001g09400	-0.93	0.62	1.78	-0.77	0.42
VIT_18s0001g09510	0.39	0.02	-0.17	0.71	-0.43
VIT_18s0001g09910	-0.19	0.01	-0.24	0.02	-0.12
VIT_18s0001g10130	0.44	0.02	-0.31	0.61	-0.41
VIT_18s0001g10610	0.40	0.00	0.15	0.67	-0.53
VIT_18s0001g10640	0.93	0.39	-0.30	0.83	-0.86
VIT_18s0001g11160	-0.30	0.20	0.01	-0.28	0.59
VIT_19s0015g00270	0.22	0.60	-0.47	-0.92	0.56
VIT_19s0015g00490	-1.16	0.87	1.62	-0.91	0.27
VIT_19s0015g01230	-1.10	0.78	1.05	-1.01	0.17
VvGRF4	-0.36	0.23	0.33	-0.10	0.13

## Appendix II

### Online resource 7 continued

#### Time point BBCH71 significance level for differential expression

Genes/samples	average expression level	F-value	p-value	adjusted p-value
VIT_01s0010g01810	9.18	500.576	2.01E-249	1.63E-247
VIT_01s0010g02430	5.47	10.961	1.40E-41	1.45E-41
VIT_01s0011g06410	7.97	12.413	2.88E-46	3.07E-46
VIT_01s0026g02030	6.12	89.270	1.72E-145	4.65E-144
VIT_01s0127g00260	3.10	46.096	2.29E-108	7.72E-108
VIT_01s0127g00710	7.66	14.128	2.10E-51	2.33E-51
VIT_01s0127g00870	4.79	95.015	4.13E-149	1.67E-147
VIT_01s0146g00400	5.62	30.336	1.81E-86	2.87E-86
VIT_01s0146g00480	8.91	16.623	3.21E-58	3.77E-58
VIT_02s0012g00990	7.86	3.847	8.56E-13	8.78E-13
VIT_02s0012g01380	2.56	13.104	2.19E-48	2.40E-48
VIT_02s0012g01400	2.43	66.159	2.37E-128	2.13E-127
VIT_02s0025g03010	4.18	25.754	2.35E-78	3.28E-78
VIT_02s0025g03180	5.20	18.575	4.32E-63	5.22E-63
VIT_02s0025g04340	5.12	27.587	9.95E-82	1.49E-81
VIT_02s0025g04660	4.77	23.789	1.58E-74	2.13E-74
VIT_02s0025g04720	2.08	34.490	5.08E-93	9.34E-93
VIT_02s0154g00320	2.56	3.222	8.07E-10	8.07E-10
VIT_02s0154g00380	12.11	56.010	4.90E-119	2.65E-118
VIT_03s0097g00700	7.70	39.804	1.63E-100	4.00E-100
VIT_04s0008g00370	4.36	36.792	2.24E-96	4.90E-96
VIT_04s0008g01100	5.84	36.118	2.06E-95	4.07E-95
VIT_04s0008g01810	5.98	34.222	1.28E-92	2.26E-92
VIT_04s0008g01910	5.92	36.324	1.04E-95	2.11E-95
VIT_04s0008g02900	4.65	49.061	9.42E-112	3.63E-111
VIT_04s0008g02920	3.51	58.562	1.64E-121	1.11E-120
VIT_04s0008g04050	6.16	26.021	7.37E-79	1.08E-78
VIT_04s0008g04200	7.57	15.282	1.20E-54	1.37E-54
VIT_04s0008g05150	7.09	39.023	1.81E-99	4.32E-99
VIT_04s0008g05830	4.04	56.419	1.94E-119	1.12E-118
VIT_04s0008g06670	4.57	55.815	7.64E-119	3.87E-118
VIT_04s0023g03070	4.95	45.449	1.33E-107	3.98E-107
VIT_04s0069g00790	4.74	20.944	1.52E-68	1.90E-68
VIT_04s0079g00260	6.29	49.061	9.42E-112	3.63E-111
VIT_08s0007g01310	5.38	20.783	3.46E-68	4.25E-68
VIT_08s0007g01320	4.30	3.304	3.26E-10	3.30E-10
VIT_08s0007g01360	4.56	48.552	3.49E-111	1.23E-110
VIT_08s0007g01370	6.56	45.642	7.85E-108	2.45E-107
VIT_08s0040g01710	2.31	44.882	6.32E-107	1.83E-106
VIT_08s0058g00930	2.12	18.078	6.94E-62	8.27E-62

## Appendix II

VIT_08s0058g00990	5.55	25.920	1.14E-78	1.63E-78
VIT_09s0070g00470	5.84	22.093	4.98E-71	6.51E-71
VIT_11s0016g03710	5.22	32.033	3.14E-89	5.09E-89
VIT_12s0059g00190	6.68	13.097	2.31E-48	2.49E-48
VIT_14s0066g01060	6.22	29.741	1.79E-85	2.74E-85
VIT_14s0083g00410	6.71	52.341	2.70E-115	1.21E-114
VIT_14s0108g00700	8.80	36.409	7.86E-96	1.63E-95
VIT_14s0108g00740	9.36	16.546	5.07E-58	5.87E-58
VIT_14s0219g00230	5.20	12.249	9.44E-46	9.93E-46
VIT_15s0048g01750	2.70	74.065	9.33E-135	1.26E-133
VIT_17s0000g02470	2.47	22.079	5.32E-71	6.84E-71
VIT_17s0000g03550	3.85	25.133	3.59E-77	4.92E-77
VIT_17s0000g03750	6.62	48.634	2.82E-111	1.04E-110
VIT_17s0000g04470	7.25	40.874	6.39E-102	1.62E-101
VIT_17s0000g05000	3.01	41.298	1.81E-102	4.72E-102
VIT_17s0000g05070	3.87	15.054	5.09E-54	5.73E-54
VIT_17s0000g05570	4.35	75.271	1.12E-135	1.81E-134
VIT_17s0000g09190	4.36	35.612	1.12E-94	2.15E-94
VIT_17s0000g09310	4.34	42.781	2.37E-104	6.40E-104
VIT_17s0000g09470	6.72	43.461	3.38E-105	9.45E-105
VIT_17s0000g09790	3.94	32.591	4.13E-90	6.83E-90
VIT_17s0053g00990	2.82	82.776	3.96E-141	8.02E-140
VIT_18s0001g03160	3.73	71.365	1.21E-132	1.40E-131
VIT_18s0001g03540	3.94	66.986	4.71E-129	4.77E-128
VIT_18s0001g04890	3.08	61.222	5.42E-124	4.39E-123
VIT_18s0001g04910	2.65	21.398	1.54E-69	1.96E-69
VIT_18s0001g05060	5.63	55.211	3.06E-118	1.46E-117
VIT_18s0001g07340	3.45	45.775	5.47E-108	1.77E-107
VIT_18s0001g07460	7.50	25.920	1.14E-78	1.63E-78
VIT_18s0001g09230	5.11	30.044	5.53E-86	8.62E-86
VIT_18s0001g09400	2.48	51.586	1.69E-114	7.21E-114
VIT_18s0001g09510	3.88	37.516	2.13E-97	4.80E-97
VIT_18s0001g09910	1.15	22.094	4.96E-71	6.51E-71
VIT_18s0001g10130	5.47	34.118	1.84E-92	3.17E-92
VIT_18s0001g10610	2.90	38.127	3.04E-98	7.03E-98
VIT_18s0001g10640	8.25	34.966	9.93E-94	1.87E-93
VIT_18s0001g11160	3.62	34.271	1.08E-92	1.95E-92
VIT_19s0015g00270	4.90	58.983	6.54E-122	4.81E-121
VIT_19s0015g00490	3.73	57.270	2.85E-120	1.78E-119
VIT_19s0015g01230	7.06	33.190	4.82E-91	8.13E-91
VvGRF4	6.83	36.507	5.69E-96	1.21E-95

## Appendix II

**Online resource 8** Variance partition analysis of experimental, biological and technical factors to reveal their fractions of explained variance in relative candidate gene expression  $\log(2)$  ( $\Delta C_t$ ).

Factors of variance are: cluster type (loose, mixed berried, compact), bio replicates, (biological variance), season, batch (technical variance), location, gene pool (selection background) and clone (11 'Pinot Noir' clones). <sup>1</sup>Median of the fraction of variance explained by an individual factor.

### BBCH57

Gene ID	Batch	Bio Replicates	Clone	Cluster Type	Clone Pool	Location	Season	Residuals
<i>VIT_04s0008g01100</i>	0.170	0.178	0.000	0.154	0.018	0.215	0.042	0.223
<i>VvGRF4</i>	0.008	0.083	0.017	0.584	0.000	0.002	0.181	0.125
<i>VIT_18s0001g03160</i>	0.000	0.044	0.011	0.134	0.000	0.163	0.260	0.388
<sup>1</sup> Median	0.008	0.083	0.011	0.154	0.000	0.163	0.181	0.223

### BBCH71

Gene ID	Batch	Bio Replicates	Clone	Cluster Type	Clone Pool	Location	Season	Residuals
<i>VIT_01s0010g02430</i>	0.014	0.317	0.000	0.229	0.021	0.013	0.096	0.310
<i>VIT_01s0026g02030</i>	0.012	0.329	0.000	0.325	0.000	0.014	0.010	0.310
<i>VIT_01s0127g00870</i>	0.015	0.282	0.000	0.423	0.000	0.010	0.100	0.169
<i>VIT_02s0025g04720</i>	0.134	0.159	0.000	0.264	0.000	0.011	0.069	0.363
<i>VIT_04s0008g01100</i>	0.049	0.136	0.000	0.272	0.000	0.061	0.167	0.315
<i>VIT_08s0007g01370</i>	0.000	0.079	0.000	0.279	0.000	0.000	0.243	0.399
<i>VvGRF4</i>	0.008	0.067	0.000	0.835	0.000	0.000	0.026	0.064
<i>VIT_17s0000g03750</i>	0.060	0.196	0.000	0.255	0.104	0.059	0.019	0.307
<i>VIT_17s0000g05000</i>	0.035	0.000	0.000	0.271	0.030	0.061	0.262	0.342
<i>VIT_17s0053g00990</i>	0.028	0.198	0.000	0.318	0.000	0.016	0.270	0.170
<i>VIT_18s0001g03160</i>	0.151	0.120	0.000	0.365	0.018	0.082	0.000	0.263
<i>VIT_18s0001g03540</i>	0.005	0.070	0.000	0.136	0.054	0.220	0.384	0.132
<i>VIT_18s0001g04890</i>	0.340	0.142	0.000	0.229	0.007	0.000	0.128	0.154
<i>VIT_18s0001g05060</i>	0.126	0.213	0.000	0.232	0.000	0.070	0.160	0.200
<i>VIT_18s0001g11160</i>	0.000	0.287	0.000	0.331	0.018	0.000	0.112	0.252
Median	0.028	0.159	0.000	0.272	0.000	0.014	0.112	0.263

## Appendix II

**Online resource 9** Spearman correlation coefficients between the relative expression of selected genes and key sub-traits of cluster architecture, vegetative vigor (wood gain, WG) and coefficients of correlation between two given genes.

The gene expression relative to *GAPDH* and *UBIc* as  $\log_2$  of the fold change was measured just before flowering (BBCH57) and just after flowering (BBCH71). The measurement results for cluster architecture sub traits of ‘Pinot Noir’ clones were recorded at ripe grape clusters (BBCH89). Wood gain was recorded after leaves had fallen (BBCH97). Spearman correlation (*r*) is significant with \**p* < 0.05, \*\**p* < 0.01, \*\*\**p* < 0.001 and \*\*\*\**p* < 0.0001. For trait abbreviations see Table 3. For gene functions see Table 4. Significant, coherent correlations over two seasons are labeled in color. For information regarding the expression clusters c1 to c5 see Figure 5. Candidate genes with putative transcription factor function are labeled in bold.

### Sampling BBCH57

Season	Gene ID	<i>VIT_04s0008g01100</i> <b>VvGRF4</b>	BN	CW	<i>VIT_18s0001g03160</i> gene expression cluster	MBV	PED	RL	SL	WG	c1	c2	c1	
2015	<i>VIT_04s0008g01100</i>	0.72*	0.60		-0.94****	-0.82**	-0.49	-0.10	0.50			-0.83**	0.79**	c1
2016	<i>VIT_04s0008g01100</i>	0.40	-0.48		-0.78**	-0.93***	-0.59	0.31	0.77**			-0.90***	0.95****	c1
2015	<b>VvGRF4</b>	-0.37	-0.21		0.87**	0.92***	0.50	-0.07	-0.78**	-0.83**			-0.98****	c2
2016	<b>VvGRF4</b>	-0.33	0.67*		0.90***	0.89***	0.41	-0.56	-0.93***	-0.90***			-0.95****	c2
2015	<i>VIT_18s0001g03160</i>	0.37	0.21		-0.83**	-0.83**	-0.38	0.16	0.83**	0.79**		-0.98****		c1
2016	<i>VIT_18s0001g03160</i>	0.31	-0.64*		-0.88***	-0.84**	-0.45	0.42	0.88***	0.95****		-0.95****		c1

## Appendix II

### Online resource 9 continued

#### Sampling BBCH71 Spearman correlation between genes and CA sub-traits

Season	Gene ID	BN	CW	MBV	PED	RL	SL	WG
2015	<i>VIT_01s0010g02430</i>	-0.75****	-0.68***	0.90****	0.63**	-0.45*	-0.81****	-0.97****
2016	<i>VIT_01s0010g02430</i>	0.61**	0.70***	0.82****	0.63**	0.16	-0.62**	-0.54*
2015	<b><i>VIT_01s0026g02030</i></b>	-0.70***	-0.60**	0.85****	0.72***	-0.24	-0.71***	-0.89****
2016	<b><i>VIT_01s0026g02030</i></b>	0.81****	0.87****	0.77****	0.48*	-0.01	-0.52*	-0.61**
2015	<i>VIT_01s0127g00870</i>	-0.71***	-0.64**	0.88****	0.65**	-0.44*	-0.81****	-0.96****
2016	<i>VIT_01s0127g00870</i>	0.52*	0.69***	0.92****	0.74****	0.23	-0.69***	-0.70***
2015	<i>VIT_02s0025g04720</i>	-0.62**	-0.54*	0.81****	0.61**	-0.44*	-0.80****	-0.94****
2016	<i>VIT_02s0025g04720</i>	0.77****	0.81****	0.76****	0.51*	0.00	-0.57**	-0.59**
2015	<i>VIT_04s0008g01100</i>	0.77****	0.68***	-0.87****	-0.66***	0.39	0.73***	0.94****
2016	<i>VIT_04s0008g01100</i>	-0.31	-0.56**	-0.88****	-0.79****	-0.21	0.75****	0.87****
2015	<i>VIT_08s0007g01370</i>	0.77****	0.66***	-0.86****	-0.69***	0.30	0.67***	0.91****
2016	<i>VIT_08s0007g01370</i>	-0.44*	-0.64**	-0.88****	-0.70***	-0.31	0.55**	0.53*
2015	<b><i>VvGRF4</i></b>	-0.64**	-0.55**	0.83****	0.72***	-0.31	-0.76****	-0.90****
2016	<b><i>VvGRF4</i></b>	0.62**	0.72***	0.84****	0.66***	0.18	-0.58**	-0.55**
2015	<i>VIT_17s0000g03750</i>	-0.58**	-0.49*	0.78****	0.70***	-0.37	-0.76****	-0.90****
2016	<i>VIT_17s0000g03750</i>	0.77****	0.73***	0.56**	0.24	-0.17	-0.44*	-0.30
2015	<b><i>VIT_17s0000g05000</i></b>	-0.32	-0.22	0.59**	0.48*	-0.22	-0.69***	-0.71***
2016	<b><i>VIT_17s0000g05000</i></b>	0.85****	0.88****	0.63**	0.23	-0.10	-0.38	-0.48*
2015	<i>VIT_17s0053g00990</i>	-0.63**	-0.54**	0.81****	0.65***	-0.40	-0.77****	-0.93****
2016	<i>VIT_17s0053g00990</i>	0.54**	0.68***	0.88****	0.70***	0.16	-0.66***	-0.65***
2015	<i>VIT_18s0001g03160</i>	0.65**	0.58**	-0.82****	-0.61**	0.46*	0.81****	0.96****
2016	<i>VIT_18s0001g03160</i>	-0.64**	-0.81****	-0.89****	-0.61**	-0.06	0.70***	0.80****
2015	<i>VIT_18s0001g03540</i>	0.21	0.40	-0.28	0.26	0.88****	0.78****	0.51*
2016	<i>VIT_18s0001g03540</i>	-0.26	-0.52*	-0.79****	-0.65***	-0.10	0.75****	0.96****
2015	<i>VIT_18s0001g04890</i>	0.76****	0.69***	-0.90****	-0.61**	0.46*	0.80****	0.98****
2016	<i>VIT_18s0001g04890</i>	-0.27	-0.54**	-0.88****	-0.82****	-0.30	0.72***	0.86****
2015	<i>VIT_18s0001g05060</i>	-0.72***	-0.64**	0.88****	0.61**	-0.47*	-0.81****	-0.98****
2016	<i>VIT_18s0001g05060</i>	0.75****	0.80****	0.76****	0.51*	-0.02	-0.61**	-0.63**
2015	<i>VIT_18s0001g11160</i>	-0.77****	-0.70***	0.92****	0.63**	-0.43*	-0.79****	-0.98****
2016	<i>VIT_18s0001g11160</i>	0.75****	0.76****	0.66***	0.33	-0.02	-0.39	-0.35

Online resource 9 continued

Sampling BBCH71 Spearman correlation between differential expressed genes

Season	Gene ID	c5	c4	c5	c5	c1	c1	c2	c5	c3	c5	c3	c1	c1	c5	c3	c1	c5	c3	gene expression cluster
2015	VIT_01s0010g02430		0.92****	0.99****	0.95****	-0.97****	-0.93****	0.93****	0.93****	0.70****	0.95****	-0.45*	-0.99****	-0.97****	0.95****	-0.45*	0.98****	0.99****	0.98****	c5
2016	VIT_01s0010g02430		0.86****	0.96****	0.92****	-0.74****	-0.87****	0.97****	0.83****	0.72****	0.95****	-0.57**	-0.73****	-0.88****	0.92****	-0.57**	0.82****	0.92****	0.82****	c5
2015	VIT_01s0026g02030	0.92****		0.92****	0.88****	-0.90****	-0.90****	0.97****	0.89****	0.79****	0.90****	-0.25	-0.91****	-0.89****	0.90****	-0.25	0.92****	0.90****	0.92****	c4
2016	VIT_01s0026g02030	0.86****		0.82****	0.98****	-0.67****	-0.72****	0.87****	0.89****	0.89****	0.86****	-0.56**	-0.62**	-0.91****	0.97****	-0.56**	0.89****	0.97****	0.89****	c4
2015	VIT_01s0127g00870	0.99****	0.92****		0.96****	-0.96****	-0.91****	0.95****	0.95****	0.73****	0.95****	-0.45*	-0.98****	-0.98****	0.99****	-0.45*	0.97****	0.99****	0.97****	c5
2016	VIT_01s0127g00870	0.96****	0.82****		0.87****	-0.86****	-0.89****	0.96****	0.71****	0.66****	0.97****	-0.74****	-0.85****	-0.92****	0.88****	-0.74****	0.73****	0.88****	0.73****	c5
2015	VIT_02s0025g04720	0.95****	0.88****	0.96****		-0.93****	-0.88****	0.92****	0.98****	0.79****	0.98****	-0.47*	-0.95****	-0.99****	0.97****	-0.47*	0.93****	0.97****	0.93****	c5
2016	VIT_02s0025g04720	0.92****	0.98****	0.87****		-0.71****	-0.73****	0.92****	0.91****	0.83****	0.91****	-0.57**	-0.64**	-0.93****	0.98****	-0.57**	0.87****	0.98****	0.87****	c5
2015	VIT_04s0008g01100	-0.97****	-0.90****				0.98****	-0.87****	-0.89****	-0.60**	-0.95****	0.34	0.98****	0.95****	-0.95****	0.34	-0.97****	-0.97****	-0.95****	c1
2016	VIT_04s0008g01100	-0.74****	-0.67****				0.70****	-0.74****	-0.45*	-0.42*	-0.83****	0.92****	0.97****	0.88****	-0.74****	0.92****	-0.74****	-0.74****	-0.46*	c1
2015	VIT_08s0007g01370	-0.93****	-0.90****				0.98****	-0.86****	-0.83****	-0.56**	-0.92****	0.21	0.93****	0.91****	-0.92****	0.21	-0.92****	-0.92****	-0.92****	c1
2016	VIT_08s0007g01370	-0.87****	-0.72****				0.70****	-0.88****	-0.63**	-0.64**	-0.88****	0.54**	0.76****	0.73****	-0.73**	0.54**	-0.73**	-0.73**	-0.73**	c1
2015	VvGRF4	0.93****	0.97****	0.95****	0.92****	-0.87****	-0.86****		0.94****	0.85****	0.92****	-0.35	-0.91****	-0.92****	0.92****	-0.35	0.92****	0.92****	0.92****	c2
2016	VvGRF4	0.97****	0.87****	0.96****	0.92****	-0.74****	-0.88****		0.83****	0.74****	0.97****	-0.57**	-0.72****	-0.89****	0.89****	-0.57**	0.86****	0.89****	0.86****	c2
2015	VIT_17s0000g03750	0.93****	0.89****	0.95****	0.98****	-0.89****	-0.83****	0.94****	0.81****	0.81****	0.96****	-0.42	-0.92****	-0.96****	0.94****	-0.42	0.90****	0.94****	0.90****	c5
2016	VIT_17s0000g03750	0.83****	0.89****	0.71****	0.91****	-0.63**	-0.63**	0.83****	0.84****	0.84****	0.76****	-0.27	-0.37	-0.76****	0.88****	-0.27	0.91****	0.88****	0.91****	c5
2015	VIT_17s0000g05000	0.70****	0.79****	0.73****	0.79****	-0.60**	-0.56**	0.85****	0.81****		0.75****	-0.39	-0.68**	-0.74****	0.71****	-0.39	0.69****	0.71****	0.69****	c3
2016	VIT_17s0000g05000	0.72****	0.89****	0.66****	0.83****	-0.42*	-0.64**	0.74****	0.84****		0.68****	-0.38	-0.42	-0.74****	0.81****	-0.38	0.89****	0.81****	0.89****	c3

## Online resource 9 continued

2015	VIT_17s0053g00990	0.95****	0.90****	0.95****	0.98****	-0.95****	-0.92****	0.92****	0.96****	0.75****	-0.98****	-0.40	-0.95****	0.96****	0.92****	c5
2016	VIT_17s0053g00990	0.95****	0.86****	0.97****	0.91****	-0.83****	-0.88****	0.97****	0.76****	0.68****	-0.92****	-0.67**	-0.80****	0.90****	0.79****	c5
2015	VIT_18s0001g03160	-0.97****	-0.89****	-0.98****	-0.99****	0.95****	0.91****	-0.92****	-0.96****	-0.74****	-0.98****	0.48*	0.97****	-0.99****	-0.94****	c1
2016	VIT_18s0001g03160	-0.88****	-0.91****	-0.92****	-0.93****	0.88****	0.73***	-0.89****	-0.76****	-0.74****	-0.92****	0.79****	0.80****	-0.93****	-0.75****	c1
2015	VIT_18s0001g03540	-0.45*	-0.25	-0.45*	-0.47*	0.34	0.21	-0.35	-0.42	-0.39	-0.40	0.48*	0.45*	-0.47*	-0.43*	c3
2016	VIT_18s0001g03540	-0.57**	-0.56**	-0.74****	-0.57**	0.92****	0.54**	-0.57**	-0.27	-0.38	-0.67****	0.79****	0.92****	-0.62**	-0.29	c3
2015	VIT_18s0001g04890	-0.99****	-0.91****	-0.98****	-0.95****	0.98****	0.93****	-0.91****	-0.92****	-0.68****	-0.95****	0.45*	0.97****	-0.99****	-0.98****	c1
2016	VIT_18s0001g04890	-0.73***	-0.62**	-0.85****	-0.64**	0.97****	0.76****	-0.72**	-0.37	-0.42	-0.80****	0.92****	0.92****	-0.68****	-0.42	c1
2015	VIT_18s0001g05060	0.90****	0.90****	0.99****	0.97****	-0.97****	-0.92****	0.92****	0.94****	0.71***	0.96****	-0.47*	-0.99****	0.97****	0.97****	c5
2016	VIT_18s0001g05060	0.92****	0.97****	0.88****	0.98****	-0.74****	-0.73****	0.89****	0.88****	0.81****	0.90****	-0.62**	-0.68****	0.84****	0.84****	c5
2015	VIT_18s0001g11160	0.98****	0.92****	0.97****	0.93****	-0.95****	-0.92****	0.92****	0.90****	0.69****	0.92****	-0.43*	-0.98****	0.97****	0.97****	c3
2016	VIT_18s0001g11160	0.82****	0.89****	0.73***	0.87****	-0.46*	-0.73***	0.86****	0.91****	0.89****	0.79****	-0.29	-0.42	0.84****	0.84****	c3

## Appendix II

**Online resource 10** Relative gene expression  $\log_{(2)} FC - \Delta\Delta ct$  at BBCH71 as calculated with a linear model:  $\log_{(2)} FC \sim \text{genotype} * \text{season} * \text{biological replicate}$  for three biological and two technical replicates of F1 siblings of the cross population and reference cultivars with divergent cluster architecture (in the seasons 2016 and 2017). Abbreviations for genotype names are presented in Table 2b. The gene expression is relative to the mean of *GAPDH* and *UBIc*. For standardization of the F1 individuals, the value relative to the mean of four individuals with short pedicels and rachises was used (Table 2b). For standardization of loosely clustered OIV reference varieties, a contrast to the mean of the compactly clustered PN clones Gm20-13 and Frank Charisma was calculated.

Gene	F1 RL max-min	F1 PED max-min	PN loose-PN compact	OIV204 loose-PN compact	F-value	p-value	adjusted p-value
<i>VvGRF4</i>	-0.45	0.34	2.5	-0.55	29.863	1.45E-20	3.12E-19
<i>VIT_01s0127g00870</i>	-0.85	1.78	1.07	0.98	27.203	5.71E-19	8.18E-18
<i>VIT_18s0001g03160</i>	-2	-1.85	-0.38	-0.52	11.107	2.36E-08	1.07E-07
<i>VIT_08s0007g01370</i>	-0.08	-0.84	-1.15	-1.65	9.686	2.47E-07	9.67E-07
<i>VIT_17s0053g00990</i>	-3.05	1.22	0.77	0.69	8.803	1.08E-06	4.01E-06
<i>VIT_18s0001g11160</i>	0.13	-0.61	0.41	0.52	5.471	3.00E-04	8.06E-04
<i>VIT_01s0026g02030</i>	-0.59	1.14	0.66	0.79	3.339	1.09E-02	2.40E-02
<i>VIT_04s0008g01100</i>	0.98	-1.02	-0.43	0.62	3.281	1.20E-02	2.51E-02

## Appendix III: Supplementary materials from Chapter 4

## Supplementary materials from Chapter 4.2

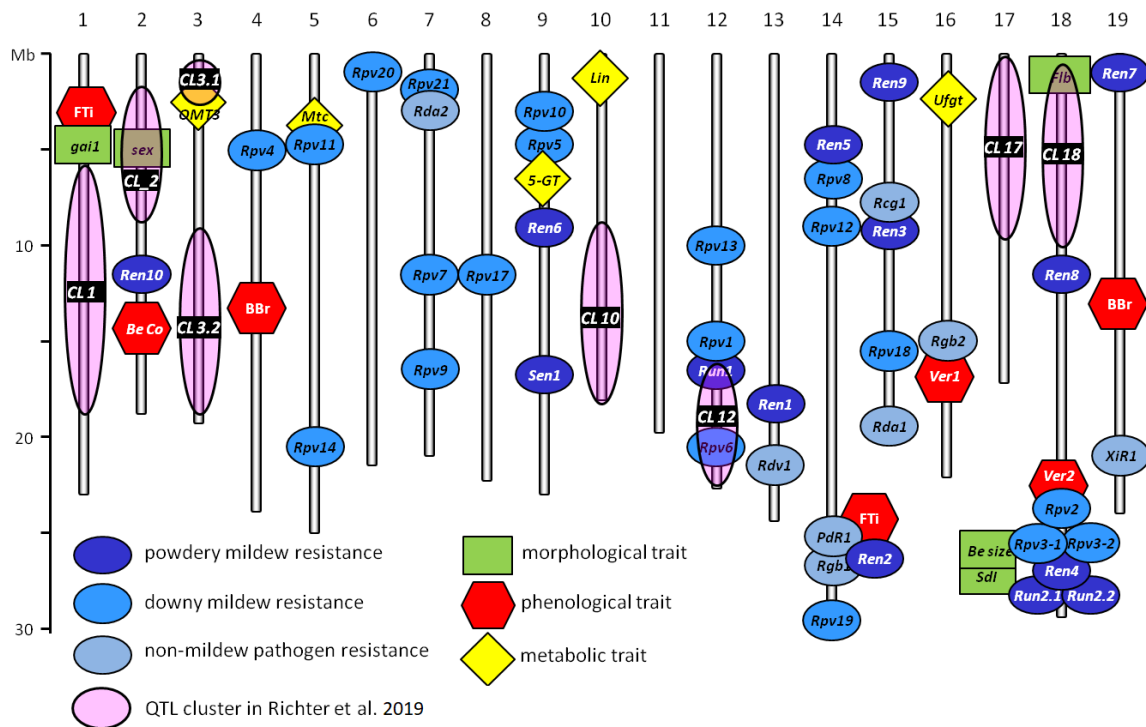


**Figure 1** Schematic overview of the genomic positions of mapped grapevine trait loci reprinted from Figure 7.6 in (Delrot et al. 2020). Numbering and scale of the 19 chromosomes are according to the 12X reference genome sequence of PN40024 and amended with genetic regions of co localized QTLs for cluster architecture sub-traits as reported in Richter et al. (2019). QTLs for cluster architecture (pink) do co localized with QTLs for flower sex (Chr. 2). On Chr.12 the resistance loci for *E. necator* and *P. viticola* does co-localize with the loci for berry volume and cluster weight. A mutation causing impaired mesocarp development (fleshless berries) co-localizes with pedicel length berry number and cluster weight (Chr. 18). Notably the QTL OMT3 for methoxypyrazine synthesis is in close (~300 Kbp) distance to the CA associated QTLs for berry volume and pedicel length (Chr. 3). Information about the overlapping loci are derived from VIVC database ([www.vivc.de/loci](http://www.vivc.de/loci)) and references there in.

## Appendix III

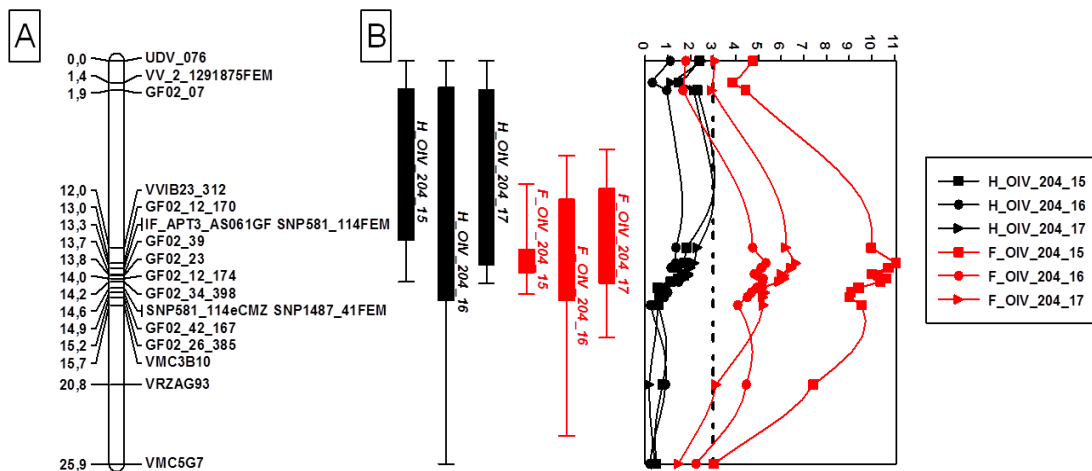


**Figure 2**

Genetic maps for linkage group 2 of the cross (‘Calardis Musqué’ x ‘Villard Blanc’) and QTLs for cluster density (OIV204 scoring).

A) Genetic consensus map for linkage group 2 Depicted at the left hand, side of the chromosome the marker positions in [cM] on the right as reported in Zyprian et al. (2016).

B) QTLs for cluster density (OIV204 scoring) derived with interval mapping and their confidence intervals LOD<sub>max</sub>-1 (bars) LOD<sub>max</sub>-2 (lines). The x-axis of the point diagram depicts the LOD value for each marker and the y-axis represents the position of the marker on the LG [cM]. The dashed line indicates the LOD = 3 level as reasonable threshold of probability for the recognition as a QTL. Notably, for the 103 individuals of the population with hermaphroditic flowers (in black) no QTL was calculated. For the entire population including 49 individuals with female flowers (in red) a QTL for cluster density could be consecutively calculated in the seasons from 2015 to 2017.

For the marker GF02-12 two alleles with amplicates of 170 bp and 174 bp were detected in the offspring of the cross ‘Calardis Musqué’ x ‘Villard Blanc’ (Zyprian et al. 2016). Marker data available in the Institute of Grapevine Breeding, Geilweilerhof show that ‘Bacchus’, the maternal parent of ‘Calardis Musqué’, introduces the 170 bp allele. The second allele, with 174 bp, was observed in ‘Calardis Musqué’ and ‘Villard Blanc’ with the latter most probably being homozygous for this allele. The 170 bp allele was evaluated with a lm<sub>xll</sub> segregation type where (m) represents the 170 bp allele that segregates in the maternal parent only. Comparing the cluster density of individuals with (lm) genotype to (ll) genotypes revealed a moderate but significant lower compactness for the (lm) genotypes having the 174/170 bp allele combination. In addition, the evaluation of the 174 bp allele of the marker Gf02-12 with a hk x hk segregation type (174 bp/170 bp) x (174 bp/0 bp) accounts for the possibility of the absence of the 174 bp allele i.e. 170 bp/0bp (kk) if the paternal parent is not homozygous for the 174 bp allele. Comparing the cluster density of individuals with the 174 bp/174 bp, 174 bp/170 bp or 174/0 bp (h-) genotype to the 170 bp/0bp (kk) genotypes and reveals a significant lower compactness

## Appendix III

for the genotypes that show no 174 bp allele (kk). Regarding FS determination, all 46 F1 individuals with a female flower type also lack the 174 bp SSR amplification product at this locus (kk). Whereas, 102 hermaphrodite F1 individuals had a heterozygous or homozygous 174 bp amplification product at this locus (ll, lm, h-). The F1 genotype Gf.1989-30-0361 in the cross population recombines a hermaphrodite flower type with the absence of the 174 bp amplification product (kk) at this locus. This recombination uncouples the in general unwanted female flower type from the desired loose cluster architecture (Figure 3).

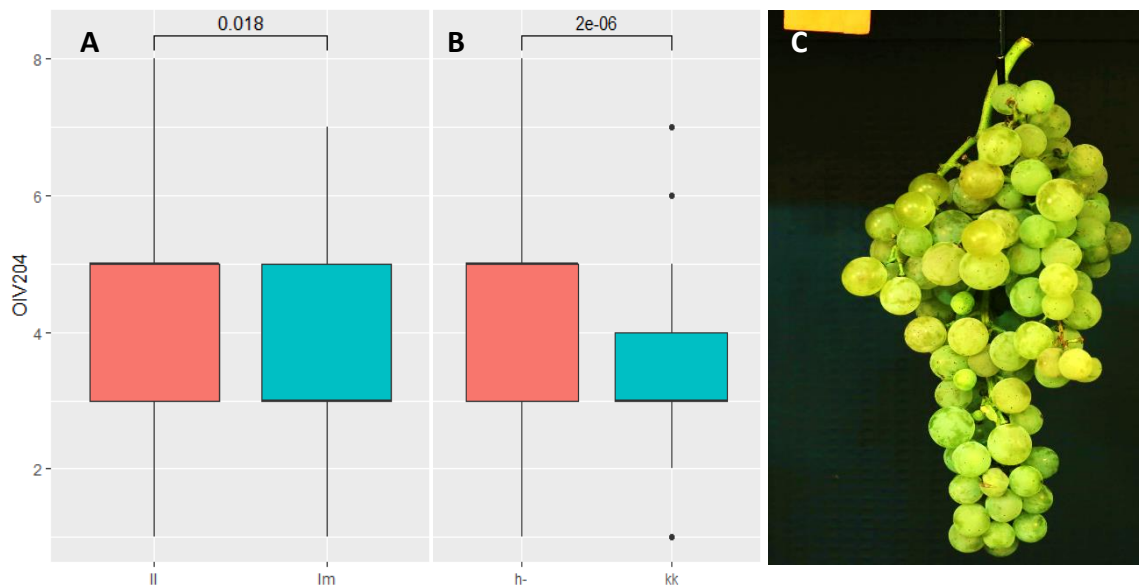


**Figure 3**

**A)** Distribution of the phenotypic median dataset grouped by genotypes. x-axis: The median of cluster compactness (OIV descriptor 204) recorded in 149 F1 individuals of the cross ('Calardis Musqué' x 'Villard Blanc') during the seasons 2015 to 2017. y-axis: genotypes having different GF02-12\_170 marker alleles **ll** = 174bp/174 bp, **lm** = 174/170 bp. *p*- value: Kruskal Wallis test.

**B)** Distribution of the phenotypic median dataset grouped by genotypes. x-axis: The median of cluster compactness (OIV descriptor 204) recorded in 149 F1 individuals of the cross ('Calardis Musqué' x 'Villard Blanc') during the seasons 2015 to 2017. y-axis: genotypes having different GF02-12\_174 marker alleles **h-** = 174 bp/174 bp, 174 bp/170 bp and 174 bp/0 bp, **kk**= 170 bp/0 bp. *p*- value: Kruskal Wallis.

**C)** Cluster of the F1 genotype Gf.1989-30-0361 at BBCH89 showing very loose cluster architecture during the seasons 2015-2017 (Median for OIV descriptor 204 = 1) The size standard in orange indicates 3cm. This is the only recombinant genotype in the cross population with a (kk) allele (linked to loose cluster architecture) at the GF02-12-174 marker but hermaphrodite flowers.

### Supplementary materials from Chapter 4.3

#### Plant material and phenotypic data

The cross population ('Calardis Musqué' x 'Villard Blanc') described in (Richter et al. 2019) shows considerable variation for several cluster architecture sub-traits. Phenotypic records presented in the study of Richter et al., 2019) were used **I)** to build the median value for cluster compactness over four seasons (2013 and 2015-2017) according the descriptor OIV204 (OIV 2015). **II)** Mean values for the cluster architecture sub-traits berry number (BN), cluster weight (CW), mean berry volume (MBV), pedicel length (PED), rachis length (RL), and shoulder length (SL) were calculated with the data of several seasons as stated in Richter et al., 2019). **III)** Records taken in 2013 and 2016 for the length of the 1<sup>st</sup> to 3<sup>rd</sup> laterals of the rachis were summed up to the "total lateral length" (TLL). Here also the mean value for TLL was calculated over both seasons. The cumulated multi seasonal phenotypic records for important features of cluster architecture were used as phenotype dataset to infer the genetic effect of markers on cluster architecture in the genetic background of the cross population.

#### Genotypic data

The statistic software MapQTL 6 was used as stated in the manual (van Ooijen 2009) for the identification of genotypes (marker alleles) causing significant different mean values in the phenotypic data i.e. show significant different loose or compact cluster compactness as estimated with the descriptor OIV204 (cluster compactness) (OIV 2015). All 546 molecular markers contributing to the genetic map described in (Zyprian et al. 2016) have been used for a non-parametric mapping based on rank sums i.e. a Kruskal-Wallis test was calculated as described by (van Ooijen et al. 1993). A marker showing significant ( $p < 0.005$ ) genotypic variance for OIV204 compactness during two or more seasons was subsequently further scrutinized to infer which sub-trait is involved in the loose cluster appearance. The mean values for cluster architecture sub-traits were compared with the genotypic variants of 38 Markers in the cross population

## Appendix III

using genotype wise box plots and a Kruskal-Wallis test. To this end, the statistic software R version 3.5.3 (R Core Team 2020) was used to analyze the data with the command “stat\_compare\_means” of the package “ggpubr” (Kassambara 2018).

### Results

For a cross population, this study revealed 38 markers with the capacity to divide the genotypes with significantly different phenotypic values for cluster compactness (OIV204) during two or more seasons (Table 1). These markers were further scrutinized whether they could discriminate loose and compact clustered individuals not only in certain seasons but also with the average values for cluster architecture traits recorded between 2013 and 2017. With the exception of “VMC6C3” and “VRZAG7\_106”, 36 markers could repeat their significantly different genotypic results in the cumulated cluster compactness records (Table 1). The detailed assessment of cluster architecture sub-traits per genotype revealed that the divergence of compactness was based on specific cluster architecture sub-traits. In 11 cases, the markers revealed impact only on berry related sub-traits; nine markers grouped the genotypes according to phenotypic differences in rachis related sub-traits and 15 markers showed impact on both classes of sub-traits (Table 1).





## Supplementary materials from Chapter 4.5

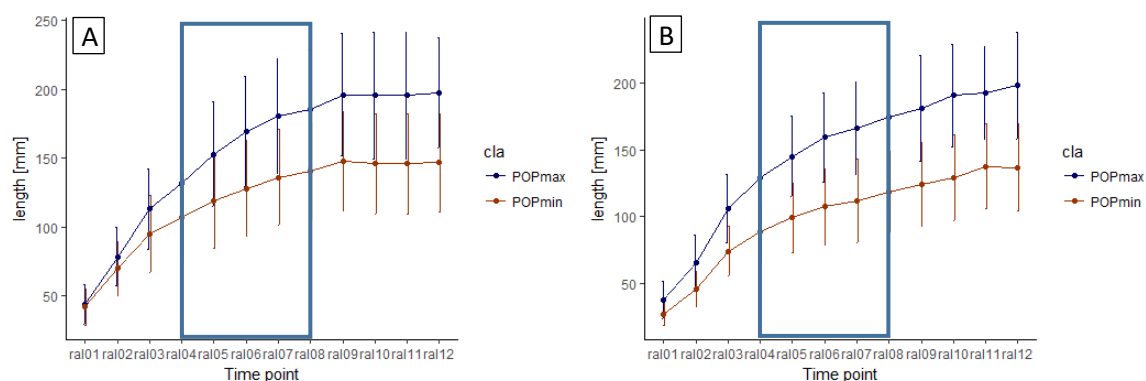


**Figure 4** Time series starting at BBCH15 for weekly mean values of rachis length of extreme long and short genotypes of the population ('Calardis Musqué' x 'Villard Blanc'). POPmax = selection of the twenty genotypes having the longest rachis length based on the preliminary measurements recorded in 2014. POPmin = selection of the twenty genotypes having the shortest rachis length based on the preliminary measurements recorded in 2014. A) Measurement records of eight repeatedly measured bunches inserted at eight independent vines during the season 2015. B) Measurement records of eight repeatedly measured bunches inserted at eight independent vines during the season 2016. The error bars indicate the standard deviation from the mean of eight replicates. The cube marks the period between BBCH57 and BBCH71

Table 2: Results obtained with the 'Search Tool for the Retrieval of Interacting Genes/Proteins' (STRING) <https://string-db.org> for interaction between candidate genes in the first shell and evidence based interaction with non-candidate genes in the second shell. Evidence based scores are: EDI = experimentally determined interaction, AT= automated text mining bitscore = Index, based on similarity of protein sequences to query protein as measure of homology

Selected STRING database results for 15 differentially expressed candidate genes for cluster architecture of Chapter 3 (Richter et al. 2020)					
Setting: 1 <sup>st</sup> shell: minimum combined score 0.5 2 <sup>nd</sup> Shell: no additional interaction					
Node 1	Node 2	Connected by means of		combined score	Notes
VIT_18s0001g03540.t01	VIT_18s0001g03160.t01	EDI	AT	0.584	Two Interacting pairs among the 15 candidate genes that are mentioned in Richter et al. (2020)
VIT_17s0053g00990.t01 (EXP8)	VIT_04s0008g01100.t01 (DWF4)	AT		0.531	
Selected STRING database results for PRE 6					
Setting: 1 <sup>st</sup> shell: minimum combined score 0.5 2 <sup>nd</sup> Shell: 50 proteins with scores higher than 0.6					
VIT_15s0021g02140.t01	VIT_01s0026g02030.t01 (PRE6)	EDI		0.634	2 <sup>nd</sup> shell is enriched with proteins related to Ubiquitin mediated proteolysis when compared to the whole genome
VIT_17s0000g01560.t01	VIT_01s0026g02030.t01 (PRE6)	EDI		0.634	2 <sup>nd</sup> shell is enriched with proteins related to protein transport when compared to the whole genome
STRING database results for GRF4 Protein homologues in <i>V. vinifera</i>					
VIT_00s0494g00010		bitscore		239	Protein Homologs for GRF4 in <i>V. vinifera</i> . As a rule-of-thumb, bitscores below 60 may indicate spurious hits.
VIT_02s0025g02680		bitscore		229	

Table 2: continued

VIT_02s0025g04910	bitscore	172	
VIT_08s0007g03760	bitscore	163	
VIT_09s0002g01350	bitscore	145	
VIT_11s0016g01250	bitscore	143	
VIT_15s0048g01740		141	
VIT_16s0098g01080		140	
VIT_18s0001g08650		115	

## List of Abbreviations

BBCH	Biologische Bundesanstalt für Land- und Forstwirtschaft, Bundessortenamt und Chemische Industrie
BC1	Back cross one
BN	Berry number
BÖLN	Bundesprogramm ökologischer Landbau und andere Formen der nachhaltiger Landwirtschaft
bp	base pairs
BR	Brassinosteroid
<i>BRI1</i>	<i>BRASSINOSTERIOD INSENSITIVE 1</i>
<i>BZR1</i>	<i>BRASSINAZOLE-RESISTANT1</i>
CA	Cluster architecture
Chr	Chromosome
cM	centi Morgan
CRISPR/cas	Clustered Regularly Interspaced Short Palindromic Repeats/ CRISPR-associated
CW	Cluster weight
DNA	Deoxyribonucleic acid
<i>DWF4</i>	<i>Dwarf 4</i>
<i>EXP</i>	<i>Expansin</i>
F1	first filial generation
F2	second filial generation
FAO	Food and Agriculture Organization of the United Nations
Flb	Fleshless berries
Fr	Freiburg
FS	Flower sex
FTi	Flowering time

## List of Abbreviations

GBS	Genotyping by sequencing
GF.GA-47-42	breeding line (Variety name 'Calardis Musqué')
Gm	Geisenheim
GRF	Growth regulation factor
ha	hectare
HT-q-PCR	High through put quantitative polymerase chain reaction
<i>IL11</i>	<i>INCREASED LEAF INCLINATION 1</i>
IPCC	Intergovernmental Panel on Climate Change
KASP	Kompetitive allele specific PCR
Kbp	Kilo base pairs
L1	Outer layer in the shoot apical meristem (tunica)
L2	Inner layer in the shoot apical meristem (corpus)
LG	Linkage group
LOD <sub>max</sub>	Maximum recorded logarithmic odds ratio
MAS	Marker-assisted selection
Mbp	Mega base pairs
MBV	Mean berry volume
MBV	Mean berry volume
miRNA	Micro Ribonucleic acid
MPIPZ	Max Planck Institute for Plant Breeding Research
NGS	Next generation sequencing
NIL	Near isogenic inbred line
OIV	International Organisation of Vine and Wine
<i>OMT3</i>	O-methyl transferase/isobutyl-methoxy pyrazine formation <sup>3</sup>
PCA	Principal component analysis
PED	Pediceal length
PN	Pinot Noir

## List of Abbreviations

PP2A	PP2A serine/threonine protein phosphatase 2A
PRE6	Transcription factor PACLOBUTRAZOLE-RESISTANCE 6
QTL	Quantitative trait locus
RAD	Restriction site associated DNA
RAPD	Randomly amplified polymorphic DNA
RAD Seq	Restriction site associated sequencing
RIL	Recombinant inbred line
RING	Really interesting new gene
RL	Rachis length
RNA	Ribonucleic acid
RT-q-PCR	Reverse transcription-quantitative polymerase chain reaction
SEP1	Transcription factor SEPALLATA 1
SL	Shoulder length
SNP	Single nucleotide polymorphism
SSR	Simple sequence repeat
TCP	TEOSINTE-BRANCHED/CYCLOIDEA/PROLIFERATING CELL FACTORS
TLL	Total lateral length
USD	US-Dollar
<i>VvPI</i>	<i>PISTILLATA-like</i> MADS-box gene
We	Weinsberg

## Declaration

I declare that the dissertation here submitted is entirely my own work, written without any illegitimate help by any third party and solely with materials as indicated in the dissertation. I have indicated in the text where I have used texts from already published sources, either word for word or in substance, and where I have made statements based on oral information given to me. At all times during the investigations carried out by me and described in the dissertation, I have followed the principles of good scientific practice as defined in the “Statutes of the Justus Liebig University Gießen for the Safeguarding of Good Scientific Practice

# Acknowledgments

I am very grateful to my supervisors Prof. Dr. R. Töpfer and Prof. Dr. R. Snowdon for their joint supervision of this scientific work. I would like to thank Prof. Dr. E. Zyprian and Prof. Dr. R. Töpfer for the on-site advices, suggestions, and support during this thesis work.

Sincere thanks to Dr. D. P. Zandler for many discussions, his support in proofreading and his potential to empower and motivate me whenever it was needed.

Many thanks to Dr. A. Schwandner for her advice in the field of genetic mapping.

Many thanks to Dr. D. Gabriel, F. Rist, Dr. R. Töpfer, Dr. E. Zyprian, Dr. S. Rossmann and Dr. K. Theres for being co-authors for the publications and all unmentioned project partners for the excellent cooperation.

Many thanks to Dr. L. Hausmann, Dr. F. Schwander, Dr. A. Kircherer, Dr. O. Trapp, Dr. E. Maul for being always willing to listen and respond when things came up in their area of expertise.

Thanks to S. Elser, M. Schneider, S. Schatt for their help with my experiments.

I would like to thank Dr. W. Köglmeier, H. Heupel, N. Adam and R. Donadel for being a great assistance in bibliographic concerns.

Big thanks to the permanent and associated members of the K-G-D making vine, wine and everyday life enjoyable and working days fun.

Most sincere thanks to my family and friends, who supported me throughout the years by a broad range of individual support or necessary distraction.

A special thanks to Katrin for being incredible patient with me!

The project is was supported by funds of the Federal Ministry of Food and Agriculture (BMEL) based on a decision of the parliament of the Federal Republic of Germany via the Federal Office for Agriculture and Food (BLE) under the Federal Programme for Ecological Farming and Other Forms of Sustainable Agriculture.





